

**SUPPORTED IMIDAZOLIUM-BASED IONIC LIQUID  
MEMBRANES AS A CONTACTOR FOR THE SELECTIVE  
ABSORPTION OF CO<sub>2</sub> BY AQUEOUS  
MONOETHANOLAMINE**

**NURUL AIN BINTI RAMLI**

**FACULTY OF ENGINEERING  
UNIVERSITY OF MALAYA  
KUALA LUMPUR**

**2019**

**SUPPORTED IMIDAZOLIUM-BASED IONIC LIQUID  
MEMBRANES AS A CONTACTOR FOR THE  
SELECTIVE ABSORPTION OF CO<sub>2</sub> BY AQUEOUS  
MONOETHANOLAMINE**

**NURUL AIN BINTI RAMLI**

**THESIS SUBMITTED IN FULFILMENT OF THE  
REQUIREMENTS FOR THE DEGREE OF DOCTOR OF  
PHILOSOPHY**

**FACULTY OF ENGINEERING  
UNIVERSITY OF MALAYA  
KUALA LUMPUR**

**2019**

**UNIVERSITY OF MALAYA**  
**ORIGINAL LITERARY WORK DECLARATION**

Name of Candidate: **NURUL AIN BINTI RAMLI**

Registration/Matric No: **KHA 130052**

Name of Degree: **DOCTOR OF PHILOSOPHY (CHEMICAL ENGINEERING)**

Title of Project Paper/Research Report/Dissertation/Thesis ("this Work"):

**SUPPORTED IMIDAZOLIUM-BASED IONIC LIQUID MEMBRANES AS  
A CONTACTOR FOR THE SELECTIVE ABSORPTION OF CO<sub>2</sub> BY  
AQUEOUS MONOETHANOLAMINE**

Field of Study: **PURIFICATION AND SEPARATION PROCESSES**

I do solemnly and sincerely declare that:

- (1) I am the sole author/writer of this Work;
- (2) This Work is original;
- (3) Any use of any work in which copyright exists was done by way of fair dealing and for permitted purposes and any excerpt or extract from, or reference to or reproduction of any copyright work has been disclosed expressly and sufficiently and the title of the Work and its authorship have been acknowledged in this Work;
- (4) I do not have any actual knowledge nor do I ought reasonably to know that the making of this work constitutes an infringement of any copyright work;
- (5) I hereby assign all and every rights in the copyright to this Work to the University of Malaya ("UM"), who henceforth shall be owner of the copyright in this Work and that any reproduction or use in any form or by any means whatsoever is prohibited without the written consent of UM having been first had and obtained;
- (6) I am fully aware that if in the course of making this Work I have infringed any copyright whether intentionally or otherwise, I may be subject to legal action or any other action as may be determined by UM.

Candidate's Signature

Date:

Subscribed and solemnly declared before,

Witness's Signature

Date:

Name:

Designation:

# **SUPPORTED IMIDAZOLIUM-BASED IONIC LIQUID MEMBRANES AS A CONTACTOR FOR THE SELECTIVE ABSORPTION OF CO<sub>2</sub> BY AQUEOUS MONOETHANOLAMINE**

## **ABSTRACT**

Carbon dioxide (CO<sub>2</sub>) capture using supported ionic liquid membranes has been receiving a lot of attention in the past few years. The use of supported ionic liquid membranes and solvents that possesses good selectivity of capturing CO<sub>2</sub> from flue gases has the potential to replace conventional absorption method. However, common good solvents for CO<sub>2</sub> capture will extensively undergo degradation due to the presence of oxygen. Therefore in this work, novel technology of supported ionic liquids membranes (SILMs) is therefore used as contactor for the selective absorption of CO<sub>2</sub> by aqueous monoethanolamine (MEA). First, a series of ILs were screened using COSMO-RS. For this purpose, CO<sub>2</sub> absorption capacity and CO<sub>2</sub>/O<sub>2</sub> selectivity of some selected ILs was predicted using this molecular modelling system. Results from the analysis revealed that [emim] [NTf<sub>2</sub>] IL was a good candidate for further absorption process, due to its good characteristics in its moderate hydrophobicity and CO<sub>2</sub>/O<sub>2</sub> selectivity. Next, the role of viscosity in preparation of a new supported ionic liquid membrane (SILM) and its chemical stability were investigated. The maximum amount of ionic liquid immobilized within the membranes was acquired at [emim] [NTf<sub>2</sub>] IL: acetone; (80:20) composition. At this composition, the IL was also found to be homogeneously distributed. Based on the above results, the SILMs were found to be more stable in aqueous solution of MEA. This stability was corresponding with results of the ionic liquid losses obtained by mass balance. Subsequently, the CO<sub>2</sub> absorption performance and CO<sub>2</sub>/O<sub>2</sub> selectivity of the SILM and its performance with that of the blank membrane; were evaluated and compared at different temperatures (303 to 348 K) and gas velocities ( $4.63 \times 10^{-6}$  to  $3.70 \times 10^{-5}$  m s<sup>-1</sup>). At pseudo-steady-state and long-

term operation conditions, results showed that the efficiency of the CO<sub>2</sub> absorption process of SILMs had almost doubled with an average selectivity factor of CO<sub>2</sub>/O<sub>2</sub> around 5 times, as compared to the blank contactor system. In addition, the mass transfer coefficient using SILMs was found to be 3.3 times higher as compared to the blank system. Finally, the effect of important operating conditions on CO<sub>2</sub> absorption performance and CO<sub>2</sub>/O<sub>2</sub> selectivity of the supported ionic liquid membrane (SILM) were investigated. Higher value of the overall mass transfer coefficient of  $3.83 \times 10^{-5} \text{ ms}^{-1}$  was obtained at optimal operating conditions, with a measured CO<sub>2</sub>/O<sub>2</sub> selectivity of 140. In conclusion, results in this work ultimately suggests the promising potentials of [emim] [NTf<sub>2</sub>]-SILMs for further evaluation work; especially for the prevention of oxidative degradation of the amine solvents in membrane contactors applications for CO<sub>2</sub> capture.

**Keywords:** Carbon dioxide (CO<sub>2</sub>) capture, COSMO-RS, supported ionic liquids membranes (SILMs), monoethanolamine (MEA), CO<sub>2</sub>/O<sub>2</sub> selectivity

# **MEMBRAN SOKONGAN BERASASKAN CECAIR IONIK IMIDAZOLIUM SEBAGAI KONTAKTOR UNTUK PENYERAPAN SELEKTIF CO<sub>2</sub> OLEH LARUTAN AKUEUS AMINA**

## **ABSTRAK**

Pemerangkapan karbon dioksida (CO<sub>2</sub>) menggunakan membran sokongan cecair ionik telah mendapat perhatian pada tahun-tahun kebelakangan ini. Kombinasi penggunaan membran sokongan cecair ionik dan pelarut yang mempunyai sifat selektif yang baik untuk memerangkap karbon dioksida daripada gas serombong berpotensi untuk menggantikan kaedah penyerapan konvensional. Walau bagaimanapun, pelarut terbaik yang biasa digunakan untuk memerangkap karbon dioksida akan mengalami kemerosotan dengan kehadiran oksigen. Oleh itu, dalam kajian ini, teknologi novel membran sokongan cecair ionik (SILMs) sebagai kontaktor akan digunakan untuk penyerapan selektif CO<sub>2</sub> oleh larutan akueus amina (MEA). Pertama sekali, beberapa siri cecair ionik akan diimbaskan dengan menggunakan COSMO-RS. Bagi tujuan ini, keupayaan beberapa cecair ionik yang terpilih untuk memerangkap CO<sub>2</sub> dan kadar selektivitinya terhadap CO<sub>2</sub>/O<sub>2</sub> telah diramalkan dengan menggunakan sistem pemodelan molekul ini. Hasil daripada analisis mendedahkan bahawa [emim] [NTf<sub>2</sub>] IL adalah cecair ionik terbaik untuk proses penyerapan terhadap CO<sub>2</sub> kerana mempunyai ciri hidrofobik yang baik dan sangat selektif terhadap CO<sub>2</sub>/O<sub>2</sub>. Kemudian, peranan kelikatan dalam penyediaan membran sokongan cecair ionik (SILM) yang baru dan kestabilan kimianya telah dikenalpasti. Jumlah maksimum cecair ionik dalam membran telah diperolehi melalui komposisi [emim] [NTf<sub>2</sub>] IL: aseton; (80:20). Pada komposisi ini, cecair ionik juga didapati diedarkan secara homogen. Berdasarkan kajian tersebut, SILMs didapati lebih stabil di dalam larutan akueus amina (MEA). Kenyataan ini berpadanan dengan kadar kehilangan cecair ionik, seperti yang ditentukan oleh keseimbangan jisim. Penyiasatan lanjut untuk membandingkan prestasi modul membran

yang tidak diubah suai dan SILMs telah dilaksanakan pada suhu (303 hingga 348 K) dan halaju gas ( $4.63 \times 10^{-6}$  to  $3.70 \times 10^{-5} \text{ m s}^{-1}$ ) yang berbeza. Pada keadaan separa mantap dan operasi jangka masa panjang, keputusan menunjukkan bahawa kecekapan proses penyerapan  $\text{CO}_2$  bagi SILMs adalah dua kali ganda dengan purata faktor selektiviti  $\text{CO}_2/\text{O}_2$  sekitar 5 kali ganda lebih baik berbanding dengan sistem kontaktor yang tidak diubah suai. Selain itu, keputusan juga menunjukkan bahawa nilai keseluruhan pekali pemindahan jisim bagi SILMs adalah 3.3 kali ganda lebih baik berbanding sistem kontaktor yang tidak diubah suai. Akhir sekali, kesan keadaan operasi penting terhadap prestasi penyerapan  $\text{CO}_2$  dan selektiviti  $\text{CO}_2/\text{O}_2$  dengan menggunakan membran sokongan cecair ionik (SILM) telah disiasat. Nilai keseluruhan yang lebih tinggi daripada pekali pemindahan jisim sebanyak  $3.83 \times 10^{-5} \text{ m s}^{-1}$  telah diperolehi pada keadaan operasi optimum dengan faktor selektiviti  $\text{CO}_2/\text{O}_2$  ialah 140. Kesimpulannya, sistem kontaktor membran yang telah diubah suai ini telah menunjukkan potensi yang besar untuk digunakan dalam proses penangkapan  $\text{CO}_2$  bagi sektor industri dan berupaya untuk menghalang proses pengoksidaan larutan amina (MEA) yang sering berlaku dalam sistem kontaktor membran gas-cecair.

**Kata kunci:** Pemerangkapan karbon dioksida ( $\text{CO}_2$ ), COSMO-RS, membran sokongan cecair ionik (SILMs), larutan amina (MEA), selektiviti  $\text{CO}_2/\text{O}_2$

## ACKNOWLEDGEMENTS

Assalamualaikum Wrth. Wbth.

Alhamdulillah, all praises to Allah for the strengths and His blessing in completing this thesis. This dissertation would not have been possible without the guidance and the help of several individuals who in one way or another contributed and extended their valuable assistance in the preparation and completion of this study.

Special appreciation goes to my supervisor, Dr. Nur Awanis Hashim, for her patience, motivation, enthusiasm, and immense knowledge. Her invaluable help of constructive comments and suggestions throughout the experimental and thesis works have contributed to the success of this research. Not forgotten, my appreciation to my co-supervisor Prof. Dr. Mohamed Kheireddine Taieb Aroua, for his support and knowledge regarding this topic.

I would like to express my appreciation to the Dean, Faculty of Engineering, University of Malaya and also to the Deputy Dean (Research) for their support and help towards my postgraduate affairs. I would also like to record my appreciation to the Ministry of Education and University for providing the financial means and laboratory facilities. My acknowledgement also goes to all the technicians and office staffs of Department of Chemical Engineering, University of Malaya for their cooperation.

Sincere thanks to all my friends especially Fatin, Hawaiah, Fariha, Ogy, Hassimah, Azlan and others for their kindness and moral support during my study. Thanks for the friendship and memories.



Last but not least, my deepest gratitude goes to my beloved parents; Mr. Ramli Ibrahim and Mrs. Norihan Kamarudin and also to my lovely siblings, sister in-law, childrens and Mohd Haizal Mohd Husin for their endless love, care, prayers and encouragement. To those who indirectly contributed in this research, your kindness means a lot to me. Thank you very much.

University of Malaya

## TABLE OF CONTENTS

<b>Abstract.....</b>	<b>iii</b>
<b>Abstrak.....</b>	<b>v</b>
<b>Acknowledgements.....</b>	<b>vii</b>
<b>Table of Contents.....</b>	<b>viii</b>
<b>List of Figures.....</b>	<b>xiii</b>
<b>List of Tables.....</b>	<b>xix</b>
<b>List of Abbreviations and Symbols.....</b>	<b>xx</b>

### CHAPTER 1: INTRODUCTION

1.1	Background.....	1
1.2	Problem statement.....	4
1.3	Research scope and objectives.....	4
1.4	Outlines of thesis.....	6

### CHAPTER 2: LITERATURE REVIEW

2.1	Membrane contactor.....	7
2.2	Membrane contactors for CO <sub>2</sub> absorption.....	8
2.2.1	Mass transfer fundamentals.....	8
2.3	Major challenges for membranes as contactor.....	13
2.3.1	Membrane wetting.....	13
2.3.1.1	Fundamental of membrane wetting .....	13
2.3.1.2	Mechanisms of wetting.....	15
2.3.2	Membrane fouling.....	16
2.3.3	Membrane degradation.....	17
2.4	Membranes in membrane contactors.....	18

2.5	Surface modification of membranes .....	18
2.6	Absorbent selection.....	19
2.6.1	Absorbent selection criteria.....	19
2.6.2	CO <sub>2</sub> absorbents in membrane contactors.....	21
2.7	Module design.....	22
2.7.1	Longitudinal flow module.....	24
2.7.2	Cross-flow module.....	25
2.8	Ionic liquid membranes (ILMs).....	27
2.8.1	Preparation methods of ILMs .....	30
2.8.2	Supported ionic liquid membranes (SILMs).....	31
2.8.3	Stability of ILMs.....	33
2.8.3.1	Stability of SILMs.....	33
2.8.4	Application of ILM for gas separation.....	35
2.8.5	Transport mechanisms through ILMs .....	42
2.8.5.1	Transport mechanism of gases through membranes.....	42
2.9	COSMO-RS for ionic liquids (ILs) screening.....	44
2.10	Physical versus chemical absorption .....	45
2.11	Summary.....	46

### **CHAPTER 3: MATERIALS AND METHODS**

3.1	Screening of ionic liquids (ILs) using COSMO-RS analysis .....	49
3.2	Preparation of supported ionic liquid membranes (SILMs) .....	53
3.2.1	Materials.....	53
3.2.2	Supported ionic liquid membranes (SILMs) preparation.....	54
3.3	SILMs characterization and stability.....	55
3.4	CO <sub>2</sub> absorption study in a gas-liquid membrane contactor system .....	55

3.5	Performances and selectivity of CO <sub>2</sub> /O <sub>2</sub> using blank and supported ionic liquid membranes (SILMs) contactor system.....	57
3.5.1	Determination of CO <sub>2</sub> loading.....	58
3.5.1	Mass transfer calculations.....	60

## CHAPTER 4: RESULTS AND DISCUSSION

4.1	COSMO-RS analysis.....	64
4.1.1	Prediction and calculation of Henry's Law constants (H) of CO <sub>2</sub> , N <sub>2</sub> , and O <sub>2</sub> were made at different temperatures.....	64
4.1.2	Sigma profiles/ molecular interaction .....	71
4.1.3	Activity coefficient at infinite dilution.....	77
4.1.4	Conclusion (Section 4.1).....	81
4.2	Preparation of supported ionic liquid membranes (SILMs) .....	82
4.2.1	Physical properties of binary mixtures.....	82
4.2.2	Supported ionic liquid membranes (SILMs).....	83
4.2.3	SILM stability .....	90
4.2.4	Summary (Section 4.2).....	95
4.3	Comparison of performances between blank and supported ionic liquid membranes (SILMs) contactor system (Parallel mode).....	96
4.3.1	Selectivity of the SILM contactor in parallel flow mode.....	102
4.3.2	Mass transfer calculations.....	106
4.3.3	Long-term performances of SILM contactor in parallel flow mode....	107
4.3.4	Summary (Section 4.3).....	110
4.4	CO <sub>2</sub> absorption study under different operating conditions (Cross-flow mode).....	112
4.4.1	Effects of MEA concentration.....	112
4.4.2	Effects of absorbent temperature.....	113

4.4.3	Effects of liquid flow rate.....	115
4.4.4	Effects of gas inlet composition.....	116
4.4.5	Effects of gas flow rate.....	117
4.4.6	Selective absorption of CO <sub>2</sub> by aqueous monoethanolamine (MEA).....	118
4.4.7	Summary (Section 4.4).....	127

## **CHAPTER 4: CONCLUSION AND RECOMMENDATIONS**

5.1	Conclusion.....	129
5.2	Recommendations for future work.....	132
	<b>References.....</b>	<b>133</b>
	<b>List of Publications and Papers Presented.....</b>	<b>158</b>

University of Malaya

## LIST OF FIGURES

<b>Figure 1.1:</b> Recent trend in monthly mean carbon dioxide that was globally averaged over marine surface sites. (-♦-: monthly mean values, -■-: after correction for the average seasonal cycle) (Dlugokencky & Tans, 2017).....	1
<b>Figure 2.1:</b> Mass transfer mechanism through a porous membrane in (a) non-wetted mode (with gas-filled pores); (b) wetted mode (with liquid-filled pores); (c) through a hollow fiber (gas on the shell side and liquid on the tube side).....	9
<b>Figure 2.2:</b> (a) Parallel flow module (countercurrent flow); (b) Liqui-Cel Extra-Flow membrane contactor (Liqui-Cel).....	25
<b>Figure 2.3:</b> Cross-flow membrane contactor modules developed by (a) Aker Kvaerner (Hoff, 2003); (b) the Netherlands Organization for Applied Scientific Research (TNO) (Cui and deMontigny, 2013).....	26
<b>Figure 2.4:</b> Frequently used cations of ionic liquids.....	28
<b>Figure 2.5:</b> Frequently used anions of ionic liquids.....	28
<b>Figure 2.6:</b> Two major approaches for utilizing ILs as membrane material.....	30
<b>Figure 3.1:</b> Summary of research methodology.....	48
<b>Figure 3.2:</b> Flowchart of property calculation with the COSMOthermX (Adapted from COSMOthermX, 2013).....	50
<b>Figure 3.3:</b> Molecular structures of [emim] [NTf <sub>2</sub> ] IL, acetone and monoethanolamine (MEA).....	54
<b>Figure 3.4:</b> Experimental setup for CO <sub>2</sub> absorption.....	56
<b>Figure 3.5:</b> a) Parallel flow Liqui-Cel and b) Cross-flow Liqui-Cel gas-liquid membrane contactor.....	58
<b>Figure 4.1:</b> Henry's law constant for CO <sub>2</sub> in different types of imidazolium-based ILs where ( ◊ ) [bmim] [DCA], ( ● ) [bmim] [BF <sub>4</sub> ], ( ▼ ) [bmim] [TFA], ( ■ ) [emim] [TFO], ( □ ) [emim] [FAP] and ( ▲ ) [emim] [NTf <sub>2</sub> ].....	65
<b>Figure 4.2:</b> Henry's law constant for N <sub>2</sub> in different types of imidazolium-based ILs where ( ◊ ) [bmim] [DCA], ( ● ) [bmim] [BF <sub>4</sub> ], ( ▼ ) [bmim] [TFA], ( ■ ) [emim] [TFO], ( □ ) [emim] [FAP] and ( ▲ ) [emim] [NTf <sub>2</sub> ].....	65
<b>Figure 4.3:</b> Henry's law constant for O <sub>2</sub> in different types of imidazolium-based ILs where ( ◊ ) [bmim] [DCA], ( ● ) [bmim] [BF <sub>4</sub> ], ( ▼ ) [bmim] [TFA], ( ■ ) [emim] [TFO], ( □ ) [emim] [FAP] and ( ▲ ) [emim] [NTf <sub>2</sub> ].....	66

**Figure 4.4:** Selectivity of CO<sub>2</sub>/N<sub>2</sub> in different types of imidazolium-based ILs where ( ◊ ) [bmim] [DCA], ( ● ) [bmim] [BF<sub>4</sub>], ( ▼ ) [bmim] [TFA], ( ■ ) [emim] [TFO], ( □ ) [emim] [FAP] and ( ▲ ) [emim] [NTf<sub>2</sub>].....68

**Figure 4.5:** Selectivity of CO<sub>2</sub>/O<sub>2</sub> in different types of imidazolium-based ILs where ( ◊ ) [bmim] [DCA], ( ● ) [bmim] [BF<sub>4</sub>], ( ▼ ) [bmim] [TFA], ( ■ ) [emim] [TFO], ( □ ) [emim] [FAP] and ( ▲ ) [emim] [NTf<sub>2</sub>].....69

**Figure 4.6:** Sigma profile of several imidazolium-based ILs with a CO<sub>2</sub> where ( - ) [bmim] [DCA], ( - ) [bmim] [BF<sub>4</sub>], ( - ) [bmim] [TFA], ( - ) [emim] [TFO], ( - ) [emim] [FAP], ( - ) [emim] [NTf<sub>2</sub>] and ( ... ) gas.....74

**Figure 4.7:** Sigma profile of several imidazolium-based ILs with a N<sub>2</sub> where ( - ) [bmim] [DCA], ( - ) [bmim] [BF<sub>4</sub>], ( - ) [bmim] [TFA], ( - ) [emim] [TFO], ( - ) [emim] [FAP], ( - ) [emim] [NTf<sub>2</sub>] and ( ... ) gas.....75

**Figure 4.8:** Sigma profile of several imidazolium-based ILs with a O<sub>2</sub> where ( - ) [bmim] [DCA], ( - ) [bmim] [BF<sub>4</sub>], ( - ) [bmim] [TFA], ( - ) [emim] [TFO], ( - ) [emim] [FAP], ( - ) [emim] [NTf<sub>2</sub>] and ( ... ) gas.....76

**Figure 4.9:** Screening charge density  $\sigma$  of the conformer of anions, cations, CO<sub>2</sub>, N<sub>2</sub> and O<sub>2</sub>.....77

**Figure 4.10:** Activity coefficients data of water in imidazolium-based ionic liquids (ILs) between 298.15 and 348.15 K where ( ◊ ) [bmim] [DCA], ( ● ) [bmim] [BF<sub>4</sub>], ( ▼ ) [bmim] [TFA], ( ■ ) [emim] [TFO], ( □ ) [emim] [FAP] and ( ▲ ) [emim] [NTf<sub>2</sub>].....80

**Figure 4.11:** Activity coefficients data of MEA in imidazolium-based ionic liquids (ILs) at 298.15 to 348.15 K where ( ◊ ) [bmim] [DCA], ( ● ) [bmim] [BF<sub>4</sub>], ( ▼ ) [bmim] [TFA], ( ■ ) [emim] [TFO], ( □ ) [emim] [FAP] and ( ▲ ) [emim] [NTf<sub>2</sub>].....80

**Figure 4.12:** Viscosity ( ● ) and RI ( ◊ ) value of binary mixtures at various [emim] [NTf<sub>2</sub>] IL: acetone compositions.....83

**Figure 4.13:** Effect of [emim] [NTf<sub>2</sub>] IL: acetone composition (v/v) on the amount of immobilized IL of SILMs preparation.....84

**Figure 4.14:** Micrographs of scanning electron of blank PP and prepared SILMs membranes (outer layer) at different magnifications (Secondary Electron).....87

**Figure 4.15:** EDX spectra of a) PP, b) S1, c) S3 and d) S10 membranes .....88



**Figure 4.16:** Micrographs of scanning electron (interior side) of a) S10 at 1000X, b) S10 at 5000X, c) S3 at 1000X and d) S3 membranes at 5000X magnification (Backscattered).....89

**Figure 4.17:** Micrographs of scanning electron of blank PP and S3 membranes before and after immersion in MEA solution for 14 days at 70°C .....92

**Figure 4.18:** EDX spectra of PP membranes before and after immersion with MEA solution for 14 days at 70°C where (-) blank PP, (-) PP - pure MEA and (-) PP - 2M MEA.....94

**Figure 4.19:** EDX spectra of S3 membranes before and after immersion with MEA solution for 14 days at 70°C where (-) S3 – 2M MEA, (-) S3 - pure MEA and (-) S3.....94

**Figure 4.20:** CO<sub>2</sub> outlet concentration (dimensionless) versus experimental time (time required to achieve steady-state) of blank membrane contactor system at different temperatures (Operating conditions: absorbent concentration = 2M MEA; absorbent temperatures = 303 to 348 K; gas velocity =  $4.63 \times 10^{-6} \text{ m s}^{-1}$ ; liquid velocity =  $9.26 \times 10^{-6} \text{ m s}^{-1}$ ; gas inlet composition (v/v %) = 10% of CO<sub>2</sub>: 10% of O<sub>2</sub> and N<sub>2</sub> balances).....99

**Figure 4.21:** CO<sub>2</sub> outlet concentration (dimensionless) versus experimental time (time required to achieve steady-state) of supported ionic liquid membrane contactor system at different temperatures (Operating conditions: absorbent concentration = 2M MEA; absorbent temperatures = 303 to 348 K; gas velocity =  $4.63 \times 10^{-6} \text{ m s}^{-1}$ ; liquid velocity =  $9.26 \times 10^{-6} \text{ m s}^{-1}$ ; gas inlet composition (v/v %) = 10% of CO<sub>2</sub>: 10% of O<sub>2</sub> and N<sub>2</sub> balances).....99

**Figure 4.22:** CO<sub>2</sub> outlet concentration (dimensionless) versus experimental time (time required to achieve steady-state) of blank membrane contactor system at different gas velocities (Operating conditions: absorbent concentration = 2M MEA; absorbent temperature = 303 K; gas velocities =  $4.63 \times 10^{-6}$  to  $3.70 \times 10^{-5} \text{ m s}^{-1}$ ; liquid velocity =  $9.26 \times 10^{-6} \text{ m s}^{-1}$ ; gas inlet composition (v/v %) = 10% of CO<sub>2</sub>: 10% of O<sub>2</sub> and N<sub>2</sub> balances).....100

**Figure 4.23:** CO<sub>2</sub> outlet concentration (dimensionless) versus experimental time (time required to achieve steady-state) of supported ionic liquid membrane contactor system at different gas velocities (Operating conditions: absorbent concentration = 2M MEA; absorbent temperature = 303 K; gas velocities =  $4.63 \times 10^{-6}$  to  $3.70 \times 10^{-5} \text{ m s}^{-1}$ ; liquid velocity =  $9.26 \times 10^{-6} \text{ m s}^{-1}$ ; gas inlet composition (v/v %) = 10% of CO<sub>2</sub>: 10% of O<sub>2</sub> and N<sub>2</sub> balances).....100

**Figure 4.24:** CO<sub>2</sub> absorption performances of both membrane contactor systems at different temperatures where (●) Efficiency – Blank, (◊) Efficiency – SILMs, (▲) Flux – Blank and (△) Flux – SILMs (Operating conditions: absorbent concentration = 2M MEA; absorbent temperatures = 303 to 348 K; gas velocity =  $4.63 \times 10^{-6} \text{ m s}^{-1}$ ; liquid velocity =  $9.26 \times 10^{-6} \text{ m s}^{-1}$ ; gas inlet composition (v/v %) = 10% of CO<sub>2</sub>: 10% of O<sub>2</sub> and N<sub>2</sub> balances).....101

**Figure 4.25:** CO<sub>2</sub> absorption performances of both membrane contactor systems at different gas flow velocities where (●) Efficiency – Blank, (○) Efficiency – SILMs, (▲) Flux – Blank and (△) Flux – SILMs (Operating conditions: absorbent concentration = 2M MEA; absorbent temperature = 303 K; gas velocities =  $4.63 \times 10^{-6}$  to  $3.70 \times 10^{-5} \text{ m s}^{-1}$ ; liquid velocity =  $9.26 \times 10^{-6} \text{ m s}^{-1}$ ; gas inlet composition (v/v %) = 10% of CO<sub>2</sub>: 10% of O<sub>2</sub> and N<sub>2</sub> balances).....101

**Figure 4.26:** Loading of CO<sub>2</sub> and O<sub>2</sub> for both membranes contactor systems at different temperatures where (△) CO<sub>2</sub> loading – SILMs, (▲) CO<sub>2</sub> loading – PP, (○) O<sub>2</sub> loading – SILMs and (●) O<sub>2</sub> loading – PP (Operating conditions: absorbent concentration = 2M MEA; absorbent temperatures = 303 to 348 K; gas velocity =  $4.63 \times 10^{-6} \text{ m s}^{-1}$ ; liquid velocity =  $9.26 \times 10^{-6} \text{ m s}^{-1}$ ; gas inlet composition (v/v %) = 10% of CO<sub>2</sub>: 10% of O<sub>2</sub> and N<sub>2</sub> balances).....104

**Figure 4.27:** Selectivity of CO<sub>2</sub>/O<sub>2</sub> for blank and supported ionic liquid membranes contactor systems at different temperatures (Operating conditions: absorbent concentration = 2M MEA; absorbent temperatures = 303 to 348 K; gas velocity =  $4.63 \times 10^{-6} \text{ m s}^{-1}$ ; liquid velocity =  $9.26 \times 10^{-6} \text{ m s}^{-1}$ ; gas inlet composition (v/v %) = 10% of CO<sub>2</sub>: 10% of O<sub>2</sub> and N<sub>2</sub> balances).....104

**Figure 4.28:** Loading of CO<sub>2</sub> and O<sub>2</sub> for both membranes contactor systems at different gas velocities where (△) CO<sub>2</sub> loading – SILMs, (▲) CO<sub>2</sub> loading – PP, (○) O<sub>2</sub> loading – SILMs and (●) O<sub>2</sub> loading – PP (Operating conditions: absorbent concentration = 2M MEA; absorbent temperature = 303 K; gas velocities =  $4.63 \times 10^{-6}$  to  $3.70 \times 10^{-5} \text{ m s}^{-1}$ ; liquid velocity =  $9.26 \times 10^{-6} \text{ m s}^{-1}$ ; gas inlet composition (v/v %) = 10% of CO<sub>2</sub>: 10% of O<sub>2</sub> and N<sub>2</sub> balances).....105

**Figure 4.29:** Selectivity of CO<sub>2</sub>/O<sub>2</sub> for blank and supported ionic liquid membranes contactor systems at different gas velocities (Operating conditions: absorbent concentration = 2M MEA; absorbent temperature = 303 K; gas velocities =  $4.63 \times 10^{-6}$  to  $3.70 \times 10^{-5} \text{ m s}^{-1}$ ; liquid velocity =  $9.26 \times 10^{-6} \text{ m s}^{-1}$ ; gas inlet composition (v/v %) = 10% of CO<sub>2</sub>: 10% of O<sub>2</sub> and N<sub>2</sub> balances).....105

**Figure 4.30:** CO<sub>2</sub> absorption efficiency of both membrane contactor systems for long-term operation where (▲) Efficiency – SILMs (Cycle 1), (▲) Efficiency SILMs (Cycle 2), (▲) Efficiency – SILMs (Cycle 3), (●) Efficiency -Blank (Cycle 1), (●) Efficiency – Blank (Cycle 2), (●) Efficiency – Blank (Cycle 3) (Operating conditions: absorbent concentration = 2M MEA; absorbent temperature = 303 K; gas velocity =  $4.63 \times 10^{-6} \text{ m s}^{-1}$ ; liquid velocity =  $9.26 \times 10^{-6} \text{ m s}^{-1}$ ; gas inlet composition (v/v %) = 10% of CO<sub>2</sub>: 10% of O<sub>2</sub> and N<sub>2</sub> balances).....109

**Figure 4.31:** CO<sub>2</sub> absorption flux of both membrane contactor systems for long-term operation where (▲) Flux – SILMs (Cycle 1), (▲) Flux – SILMs (Cycle 2), (▲) Flux – SILMs (Cycle 3), (●) Flux – Blank (Cycle 1), (●) Flux – Blank (Cycle 2), (●) Flux – Blank (Cycle 3) (Operating conditions: absorbent concentration = 2M MEA; absorbent temperature = 303 K; gas velocity =  $4.63 \times 10^{-6} \text{ m s}^{-1}$ ; liquid velocity =  $9.26 \times 10^{-6} \text{ m s}^{-1}$ ; gas inlet composition (v/v %) = 10% of CO<sub>2</sub>: 10% of O<sub>2</sub> and N<sub>2</sub> balances).....109

**Figure 4.32:** Selectivity of CO<sub>2</sub>/O<sub>2</sub> for blank and supported ionic liquid membranes contactor systems for long-term operation (▲) Selectivity – SILMs (Cycle 1), (▲) Selectivity – SILMs (Cycle 2), (▲) Selectivity – SILMs (Cycle 3), (●) Selectivity – Blank (Cycle 1), (●) Selectivity – Blank (Cycle 2), (●) Selectivity – Blank (Cycle 3) (Operating conditions: absorbent concentration = 2M MEA; absorbent temperature = 303 K; gas velocity =  $4.63 \times 10^{-6} \text{ m s}^{-1}$ ; liquid velocity =  $9.26 \times 10^{-6} \text{ m s}^{-1}$ ; gas inlet composition (v/v %) = 10% of CO<sub>2</sub>: 10% of O<sub>2</sub> and N<sub>2</sub> balances).....110

**Figure 4.33:** Effects of MEA concentration on (●) CO<sub>2</sub> absorption efficiency (%) and (○) flux (Operating conditions: absorbent concentrations = 0.5 to 4M MEA; absorbent temperature = 303 K; gas flow rate = 100 ml min<sup>-1</sup>; liquid flow rate = 500 ml min<sup>-1</sup>; gas inlet composition (v/v %) = 30% of CO<sub>2</sub>: 10% of O<sub>2</sub> and N<sub>2</sub> balances).....113

**Figure 4.34:** Effects of absorbent temperature on (●) CO<sub>2</sub> absorption efficiency (%) and (○) flux (Operating conditions: absorbent concentration = 2M MEA; absorbent temperatures = 303 to 348 K; gas flow rate = 100 ml min<sup>-1</sup>; liquid flow rate = 500 ml min<sup>-1</sup>; gas inlet composition (v/v %) = 30% of CO<sub>2</sub>: 10% of O<sub>2</sub> and N<sub>2</sub> balances).....114

**Figure 4.35:** Effects of liquid flow rate on (●) CO<sub>2</sub> absorption efficiency (%) and (○) flux (Operating conditions: absorbent concentration = 2M MEA; absorbent temperature = 303 K; gas flow rate = 100 ml min<sup>-1</sup>; liquid flow rates = 100 to 500 ml min<sup>-1</sup>; gas inlet composition (v/v %) = 30% of CO<sub>2</sub>: 10% of O<sub>2</sub> and N<sub>2</sub> balances).....115

**Figure 4.36:** Effects of gas inlet composition on (●) CO<sub>2</sub> absorption efficiency (%) and (○) flux (Operating conditions: absorbent concentration = 2M MEA; absorbent temperature = 303 K; gas flow rate = 50 ml min<sup>-1</sup>; liquid flow rate = 500 ml min<sup>-1</sup>; gas inlet compositions (v/v %) = 10 to 30% of CO<sub>2</sub>: 10% of O<sub>2</sub> and N<sub>2</sub> balances).....117

**Figure 4.37:** Effects of gas flow rate on (●) CO<sub>2</sub> absorption efficiency (%) and (○) flux (Operating conditions: absorbent concentration = 2M MEA; absorbent temperature = 303 K; gas flow rates = 50 to 400 ml min<sup>-1</sup>; liquid flow rate = 500 ml min<sup>-1</sup>; gas inlet composition (v/v %) = 30% of CO<sub>2</sub>: 10% of O<sub>2</sub> and N<sub>2</sub> balances).....118

**Figure 4.38:** Loading of CO<sub>2</sub> and O<sub>2</sub> for supported ionic liquid membranes contactor at different MEA concentrations where (●) CO<sub>2</sub> loading and (○) O<sub>2</sub> loading (Operating conditions: absorbent concentrations = 0.5 to 4M MEA; absorbent temperature = 303 K; gas flow rate = 100 ml min<sup>-1</sup>; liquid flow rate = 500 ml min<sup>-1</sup>; gas inlet composition (v/v %) = 30% of CO<sub>2</sub>: 10% of O<sub>2</sub> and N<sub>2</sub> balances).....119

**Figure 4.39:** Selectivity of CO<sub>2</sub>/O<sub>2</sub> for supported ionic liquid membranes contactor system at different MEA concentrations (Operating conditions: absorbent concentrations = 0.5 to 4M MEA; absorbent temperature = 303 K; gas flow rate = 100 ml min<sup>-1</sup>; liquid flow rate = 500 ml min<sup>-1</sup>; gas inlet composition (v/v %) = 30% of CO<sub>2</sub>: 10% of O<sub>2</sub> and N<sub>2</sub> balances).....120

**Figure 4.40:** Loading of CO<sub>2</sub> and O<sub>2</sub> for supported ionic liquid membranes contactor at different temperatures where (●) CO<sub>2</sub> loading and (○) O<sub>2</sub> loading (Operating conditions: absorbent concentration = 2M MEA; absorbent temperatures = 303 to 348 K; gas flow rate = 100 ml min<sup>-1</sup>; liquid flow rate = 500 ml min<sup>-1</sup>; gas inlet composition (v/v %) = 30% of CO<sub>2</sub>: 10% of O<sub>2</sub> and N<sub>2</sub> balances).....121

**Figure 4.41:** Selectivity of CO<sub>2</sub>/O<sub>2</sub> for supported ionic liquid membranes contactor system at different temperatures (Operating conditions: absorbent concentration = 2M MEA; absorbent temperatures = 303 to 348 K; gas velocities = 100 ml min<sup>-1</sup>; liquid velocity = 500 ml min<sup>-1</sup>; gas inlet composition (v/v %) = 30% of CO<sub>2</sub>: 10% of O<sub>2</sub> and N<sub>2</sub> balances).....121

**Figure 4.42:** Loading of CO<sub>2</sub> and O<sub>2</sub> for supported ionic liquid membranes contactor at different liquid flow rates where (●) CO<sub>2</sub> loading and (○) O<sub>2</sub> loading (Operating conditions: absorbent concentration = 2M MEA; absorbent temperature = 303 K; gas flow rate = 100 ml min<sup>-1</sup>; liquid flow rates = 100 to 500 ml min<sup>-1</sup>; gas inlet composition (v/v %) = 30% of CO<sub>2</sub>: 10% of O<sub>2</sub> and N<sub>2</sub> balances).....122

**Figure 4.43:** Selectivity of CO<sub>2</sub>/O<sub>2</sub> for supported ionic liquid membranes contactor system at different liquid flow rates (Operating conditions: absorbent concentration = 2M MEA; absorbent temperature = 303 K; gas flow rate = 100 ml min<sup>-1</sup>; liquid flow rates = 100 to 500 ml min<sup>-1</sup>; gas inlet composition (v/v %) = 30% of CO<sub>2</sub>: 10% of O<sub>2</sub> and N<sub>2</sub> balances).....123

**Figure 4.44:** Loading of CO<sub>2</sub> and O<sub>2</sub> for supported ionic liquid membranes contactor at different gas inlets where (●) CO<sub>2</sub> loading and (○) O<sub>2</sub> loading (Operating conditions: absorbent concentration = 2M MEA; absorbent temperature = 303 K; gas flow rate = 50 ml min<sup>-1</sup>; liquid flow rate = 500 ml min<sup>-1</sup>; gas inlet compositions (v/v %) = 10 to 30% of CO<sub>2</sub>: 10% of O<sub>2</sub> and N<sub>2</sub> balances).....124

**Figure 4.45:** Selectivity of CO<sub>2</sub>/O<sub>2</sub> for supported ionic liquid membranes contactor system at different gas inlets (Operating conditions: absorbent concentration = 2M MEA; absorbent temperature = 303 K; gas flow rate = 50 ml min<sup>-1</sup>; liquid flow rate = 500 ml min<sup>-1</sup>; gas inlet compositions (v/v %) = 10 to 30% of CO<sub>2</sub>: 10% of O<sub>2</sub> and N<sub>2</sub> balances).....124

**Figure 4.46:** Loading of CO<sub>2</sub> and O<sub>2</sub> for supported ionic liquid membranes contactor at different gas flow rates where (●) CO<sub>2</sub> loading and (○) O<sub>2</sub> loading (Operating conditions: absorbent concentration = 2M MEA; absorbent temperature = 303 K; gas flow rates = 50 to 400 ml min<sup>-1</sup>; liquid flow rate = 500 ml min<sup>-1</sup>; gas inlet composition (v/v %) = 30% of CO<sub>2</sub>: 10% of O<sub>2</sub> and N<sub>2</sub> balances).....125

**Figure 4.47:** Selectivity of CO<sub>2</sub>/O<sub>2</sub> for supported ionic liquid membranes contactor system at different gas flow rates (Operating conditions: absorbent concentration = 2M MEA; absorbent temperature = 303 K; gas flow rates = 50 to 400 ml min<sup>-1</sup>; liquid flow rate = 500 ml min<sup>-1</sup>; gas inlet composition (v/v %) = 30% of CO<sub>2</sub>: 10% of O<sub>2</sub> and N<sub>2</sub> balances).....125

## LIST OF TABLES

<b>Table 2.1:</b> The glass transition temperature ( $T_g$ ) and melting temperature ( $T_m$ ) of polymers used as membrane materials in membrane contactors (Schouten & Vander Vegt (1981) and Chanda & Roy (2006)).....	18
<b>Table 2.2:</b> Use of ILMs in separation of gases.....	36
<b>Table 3.1:</b> The sample provenance table for the compounds system.....	51
<b>Table 3.2:</b> Specifications of the [emim] [NTf <sub>2</sub> ] IL (hydrophobic).....	53
<b>Table 3.3:</b> Characteristics of hydrophobic PP hollow fiber membrane.....	53
<b>Table 3.4:</b> Hollow fiber membrane contactor characteristics for parallel and cross-Liqui Cel type.....	57
<b>Table 4.1:</b> Predicted results of CO <sub>2</sub> , N <sub>2</sub> and O <sub>2</sub> in imidazolium-based ILs using COSMOthermX program.....	70
<b>Table 4.2:</b> Polarizability ( $\alpha$ ); dipole moment ( $\mu$ ); and quadrupole moment (Q) for CO <sub>2</sub> , N <sub>2</sub> , and O <sub>2</sub> Copyright 1999, Prentice Hall PTR and Copyright 1966, Taylor and Francis Group.....	71
<b>Table 4.3:</b> Viscosity, RI, and the amount of immobilized IL at various [emim] [NTf <sub>2</sub> ] IL: acetone composition.....	84
<b>Table 4.4:</b> Mean sizes of membrane pores before and after immersion with MEA solutions for 14 days at 70°C.....	91
<b>Table 4.5:</b> Amount of immobilized IL in S3 membranes before and after immersion in MEA solution for 14 days at 70°C.....	91
<b>Table 4.6:</b> Experimental $K_{overall}$ for a) blank and b) SILMs contactor system at different temperatures and gas flow rates.....	106

## LIST OF SYMBOLS AND ABBREVIATIONS

$\Delta p_{g,i}$	:	pressure difference across the membrane
$(a_{ij})$	:	ideal selectivity
$(y_{CO_2,in})$	:	concentration in the inlet
$(y_{CO_2,out})$	:	concentration in the outlet
$A_i$	:	inner surface of the hollow fiber membranes (m <sup>2</sup> )
$C_{g,i}$	:	concentration of the dissolved gas in IL phase
$D_{CO_2,l}$	:	diffusion coefficient of carbon dioxide in the liquid
$D_i$	:	diffusion coefficient
$H_d$	:	dimensionless Henry constant
$J_{CO_2}$	:	CO <sub>2</sub> absorption flux (mol m <sup>-2</sup> s <sup>-1</sup> )
$J_{g,i}$	:	steady-state flux of gas $i$ through the membrane
$K_g$	:	overall mass transfer coefficient based on the gas phase
$K_l$	:	overall mass transfer coefficient based on the liquid phase
$K_{overall}$	:	overall mass transfer coefficient
$L_p$	:	distance between the adjacent pores
$M_W$	:	pure IL molecular weight
$P_T$	:	total pressure
$P_{g,i}$	:	gas permeability
$Q_g$	:	gas flow rate (m <sup>3</sup> s <sup>-1</sup> )
$Q_l$	:	liquid flow rate (m <sup>3</sup> s <sup>-1</sup> )
$S_i$	:	solubility coefficient
$T_g$	:	glass transition temperature
$T_m$	:	melting temperature

$V_{CO_2}$	:	molar volume of carbon dioxide
$V_{HCl}$	:	volume of HCl needed to neutralized the basic species
$V_{Sample}$	:	volume of sample taken for analysis
$d_{max}$	:	maximum pore diameter of the membrane
$d_o, d_i$ and $d_{lm}$	:	outside, inside and log mean diameters in (m)
$d_o, d_i$ , and $d_{ln}$	:	outer, inner and logarithmic mean diameters of the membrane, respectively
$g_b, g_m, l_m$ and $l_b$	:	gas bulk, gas-membrane interface, liquid-membrane interface and liquid bulk, respectively.
$k_g, k_m$ and $k_l$	:	individual mass transfer coefficients for gas, membrane and liquid, respectively
$k_g, k_{mg}, k_l,$	:	mass transfer coefficients of the gas, membrane and liquid
$k_l$	:	mass transfer coefficient in the liquid phase
$l$	:	membrane thickness
$p_{IL}$	:	pure IL density
$x_i$	:	mole fraction of dissolved gas in IL phase
$y^*$ and $x_l^*$	:	molar fractions in the gas and liquid phases respectively
$\delta_L$	:	boundary layer thickness for CO <sub>2</sub> diffusion
$\mu_{MEA}$	:	viscosity of solvent in cP
$[Al_2Cl_7]^-$	:	heptachlorodialuminate ion
$Al_2O_3$	:	aluminium oxide
$BaCl_2$	:	barium chloride
$BaCO_3$	:	white crystalline solid residue of barium carbonate
$CF_4$	:	tetrafluoromethane
$CH_4$	:	methane gas
CNTs	:	carbon nanotubes

CO <sub>2</sub>	:	carbon dioxide gas
COSMO-RS	:	conductor-like screening model for real solvents
DEA	:	diethanolamine
DEEA	:	2-(diethylamino) ethanol
d <sub>h</sub>	:	hydraulic diameter
DMPEG	:	dimethyl ethers of polyethyleneglycol
EDX	:	energy dispersive X-ray analysis
ESB	:	backscattered electrons (ESB) imaging mode
F	:	fluorine
FESEM	:	field emission scanning electron microscope
FTIR	:	fourier-transform infrared spectroscopy
<sup>1</sup> H NMR	:	proton nuclear magnetic resonance
H <sub>2</sub>	:	hydrogen gas
H <sub>2</sub> S	:	hydrogen sulfide gas
HCl	:	hydrochloric acid
He	:	helium gas
ILM	:	ionic liquid membrane
ILs	:	ionic liquids
L	:	fiber length
LEP	:	breakthrough pressure
LMOG	:	low molecular weight organic gelators
MAPA	:	3-(methylamino)propylamine
MD	:	molecular dynamics
MEA	:	monoethanolamine
MEK	:	methylethylketone
N	:	nitrogen



N <sub>2</sub>	:	nitrogen gas
NaHCO <sub>3</sub>	:	sodium bicarbonate
NaOH	:	sodium hydroxide
NH <sub>3</sub>	:	ammonia
O	:	oxygen
p(VDF-HFP)	:	poly(vinylidene fluoride-co-hexafluoropropylene)
PCC	:	post-combustion capture
PE	:	polyethylene
PEEK	:	polyether ether ketone
PEG	:	polyethyleneglycol
PMSQ	:	polymethylsilsesquioxane
PP	:	polypropylene
PTFE	:	polytetrafluoroethylene
PVDF	:	polyvinylidene fluoride
Q	:	quadrupole moment
QSILM	:	quasi-solidified ionic liquid membrane
RI	:	refractive index
RTILs	:	room temperature ionic liquids
S	:	sulphur
SILMs	:	supported ionic liquid membrane
SLMs	:	supported liquid membrane
SO <sub>2</sub>	:	sulfur dioxide gas
TNO	:	Netherlands Organization for Applied Scientific Research
VOCs	:	volatile organic compounds
A	:	polarizability
$\gamma$	:	liquid surface tension

$\mu$	:	dipole moment
$A$	:	membrane area ( $\text{m}^2$ )
$B$	:	pore geometry coefficient
$C$	:	liquid concentration
$E$	:	enhancement factor
$H$	:	Henry's Law constant
$N$	:	gas flux
$P$	:	gas partial pressure
$\alpha$	:	$\text{CO}_2$ loading in mol of $\text{CO}_2$ per mol of amine

#### Cations

[APmim]	:	1-(3-aminopropyl)-3-methylimidazolium
[Aliquat]	:	tri-C8-C10-alkylmethylammonium
[bbim]	:	benzyl-3-butylimidazolium
[bim]	:	1-butylimidazolium
[bmim]	:	1-butyl-3-methylimidazolium
[BMP]	:	1-butyl-3-methylpyrrolidinium
[BMPYR]	:	1-butyl-1-methylpyrrolidinium
[BTNH]	:	butyltrimethylammonium
[C <sub>2</sub> dmim]	:	1-ethyl-2,3-dimethylimidazolium
[C <sub>3</sub> mim]	:	1-propyl-3-methylimidazolium
[C <sub>3</sub> NH <sub>2</sub> mim]	:	N-aminopropyl-3-methylimidazolium
[C <sub>10</sub> mim]	:	1-decyl-3-methylimidazolium
[eeim]	:	1-ethenyl-3-ethyl-imidazolium
[eemim]	:	1-ethenyl-3-ethyl-imidazolium
[emim]	:	1-ethyl-3-methylimidazolium
h[mim] <sub>2</sub>	:	1,6-di(3-methylimidazolium)hexane

[hmim]	:	1-hexyl-3-methylimidazolium
[mim]	:	1-methylimidazolium
[MP Pyrrolidinium]	:	N-methyl-N-propylpyrrolidinium
[MP Piperidinium]	:	N-methyl-N-propylpiperidinium
[N <sub>3333</sub> ]	:	tetrapropylammonium
[N <sub>2224</sub> ]	:	triethylbutylammonium
[N <sub>8881</sub> ]	:	trioctylmethylammonium
[OMA]	:	trioctylmethylammonium
[omim]	:	1-octyl-3-methylimidazolium
pr[mim] <sub>2</sub>	:	1,3-di(3-methyl-imidazolium)propane
[P <sub>4444</sub> ]	:	tetrabutylphosphonium
[Ph <sub>3</sub> t]	:	trihexyl(tetradecyl)phosphonium
[smmim]	:	1-methyl-3-(1-trimethoxysilylmethyl)imidazolium
[TBP]	:	tetrabutylphosphonium
[THTDP]	:	trihexyltetradecylphosphonium
[Vbtma]	:	vinylbenzyltrimethylammonium

#### Anions

[AC]	:	acetate
[B(CN) <sub>4</sub> ]	:	tetracyanoborate
[BETI]	:	bis(perfluoroethyl(sulfonyl))imide
[BF <sub>4</sub> ]	:	tetrafluoroborate
[Br]	:	bromide
BTA	:	butyltrimethylammonium
BTMPP	:	bis(2,4,4-trimethylpentyl)phosphinate
[C(CN) <sub>3</sub> ]	:	tricyanomethane
[CF <sub>3</sub> SO <sub>3</sub> ]	:	trifluoromethanesulfone

[Cl]	:	chloride
[DCA]	:	dicyanamide
[dimalonate]	:	dimalonate
[diglutarate]	:	diglutarate
[dimaleate]	:	dimaleate
[ESO <sub>4</sub> ]	:	ethylsulfate
[FAP]	:	tris(perfluoroalkyl)trifluorophosphate
[Gly]	:	glycine
[Lac]	:	lactate
[malonate]	:	malonate
[maleate]	:	maleate
[MeSO <sub>4</sub> ]	:	methylsulfate
[NTf <sub>2</sub> ]	:	bis(trifluoromethylsulfonyl)imide
[TFO]	:	trifluoromethanesulfonate
[PF <sub>6</sub> ]	:	hexafluorophosphate
[Pro]	:	proline
[SCN]	:	thiocyanate
[TCB]	:	tetracyanoborate
[TCM]	:	tricyanomethanide
[TFA]	:	trifluoroacetate
[TFSI]	:	bis(trifluoromethylsulfonyl)
[TMG]	:	tetramethylguanidinium
[TMG]L	:	1,1,3,3-tetramethylguanidinium lactate
[(TMS) <sub>2</sub> N]	:	bis(trifluoromethanesulfonyl)imide

## CHAPTER 1: INTRODUCTION

### 1.1 Background

CO<sub>2</sub> emissions have been acknowledged to have a negative effect to the environment, which then promotes collaborative work between several nations to find a solution to lesser the extent of emissions (Wang et al., 2004; Zhang et al., 2013). Over the past five years, we have been experiencing constant increase in global atmospheric CO<sub>2</sub> concentration as presented in Figure 1.1. Figure 1.1 displays the monthly mean of global CO<sub>2</sub> concentration over the marine's surface site as reported by the Global Monitory Division of National Oceanic and Atmospheric (NOA)/Earth System Research Laboratory. The data provided in 2016 is a preliminary data that is subject to recalibration to standard emission gas and quality control (Dlugokencky & Tans, 2017). In any case, the increasing trend is worrying and reflects on the severity in the increase of CO<sub>2</sub> global concentration.

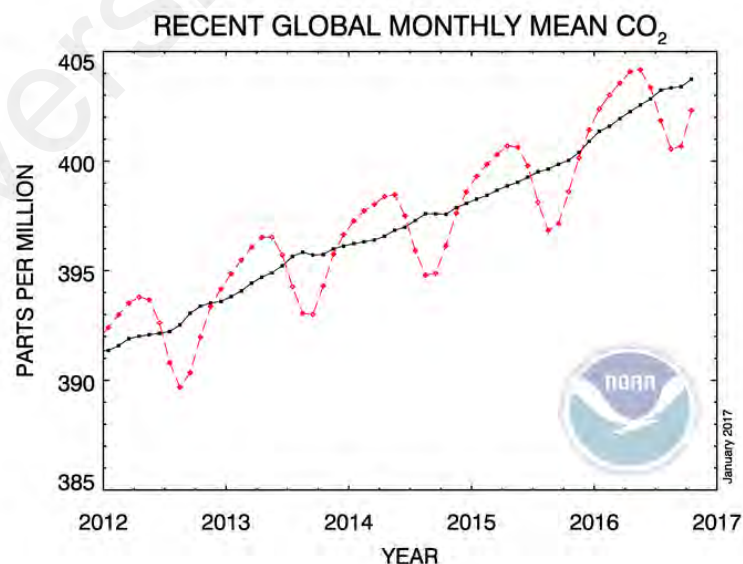


**Figure 1.1:** Recent trend in monthly mean carbon dioxide that was globally averaged over marine surface sites. (-♦-: monthly mean values, -■-: after correction for the average seasonal cycle) (Dlugokencky & Tans, 2017)

Post-combustion capture is the most straightforward schema for capturing CO<sub>2</sub>, although it is also one of the most challenging approaches as well. This is because of the diluted concentration of CO<sub>2</sub> and its low pressure in the flue gas: 12–15 mol % (in a post-combustion flue gas from a coal-fired power plant) (Bara, 2012) and, the poor value of the recovered compound (carbon in the highest oxidation level: CO<sub>2</sub>) (Luis & Van der Bruggen, 2013). In this case, the CO<sub>2</sub> can be removed in a chemical or physical absorption process. Up until today, an effective post-combustion CO<sub>2</sub> capture method is to eliminate CO<sub>2</sub> by chemical absorption using various aqueous amine solutions and is already in the commercial stage (St  phenne, 2014). Various alkanoamines can be applied for the CO<sub>2</sub> post-combustion capture. Monoethanolamine (MEA) is currently the benchmark solvent, because of its good properties towards CO<sub>2</sub> absorption. It exhibits a high rate of absorption of CO<sub>2</sub>, an CO<sub>2</sub> absorption capacity of 1:2 mole of CO<sub>2</sub> per mole of solvent ratio, relatively low solvent cost, low molecular weight, special ease of reclamation and reasonable volatility (da Silva et al., 2012; McCrellis et al., 2016; Ma etl., 2015; Ye et al., 2013). However, amines tend to oxidatively degrade and can cause a reduction of CO<sub>2</sub> absorption capacity (Kohl & Nielsen, 1997). Oxidative degradation due to dissolved O<sub>2</sub> is found to be more dominant than thermal degradation (Lepaumier et al., 2011; Vevelstad, 2013), and has been studied by various researchers previously (Sexton & Rochelle, 2009; Vevelstad et al., 2013; Voice & Rochelle, 2013).

Membrane technology using gas-liquid membrane contactor is a favorable separation technique that overwhelms the shortcomings of this conventional method and is primarily implemented in post-combustion capture. The use of gas-liquid contactors has enabled for a flexible and effective operation that involves a simple process design and scaling up, as well as modular builds (Ismail & Mansourizadeh, 2010; Khaisri et al., 2009; Rezaei et al., 2014). In this membrane based absorption, amine solutions are

extensively used as the solvent (Albo & Irabien, 2012; Albo et al., 2010). However, as stated earlier, oxidative degradation of the solvent tends to arise due to the existence of O<sub>2</sub> as a contaminant in the flue gas stream (Voice & Rochelle, 2013).

Therefore, the need for a membrane with very high selectivity characteristics to extract a relatively low concentration of CO<sub>2</sub> (Powell & Qiao, 2006) and O<sub>2</sub> (Li et al., 1998; Park et al., 2008) from flue gases for post-combustion CO<sub>2</sub> is important (Favre, 2007). Until now, the most prominent way to gain excellent selectivity is the incorporation of ionic liquids (ILs) into polymers membranes, which yields to supported ionic liquid membranes (SILMs) (Krull et al., 2008). Numerous studies have been done in the past, where SILMs were considered for possible applications in gas separations (Abdelrahim et al., 2017; Dai et al., 2017; Gan et al., 2011; Iarikov et al., 2011; Kim et al., 2011; L. Gomez-Coma et al., 2016). Ionic liquids (ILs) can offer attractive transport properties due to its low resistance to diffusion (Dai et al., 2016); while the selectivity can be tuned by choosing appropriate functional groups (Luis & Van der Bruggen, 2013). It is thought that the use of ILs will work to control the rigid challenges faced by the system, (Gorji and Kaghazchi, 2008) compared to other solvents (Bara et al., 2009b; Chen et al., 1999; Chen et al., 2001; Davis and Sandall, 1993; Donaldson and Nguyen, 1980; Francisco et al., 2010; Matsumiya et al., 2005; Park et al., 2000; Saha and Chakma, 1995; Teramoto et al., 1996; Yamaguchi et al., 1996) due to their distinctive characteristics. For example, it has a broad liquidus range, stable thermal properties, insignificant vapour pressure, tuneable physicochemical attributes, and very practicable CO<sub>2</sub> solubility (Hasib-ur-Rahman et al., 2012).

## 1.2 Problem statement

Supported ionic liquid membranes (SILMs) are emerging contactor technologies for CO<sub>2</sub> absorption by aqueous alkanolamines such as MEA. The ideal ionic liquid for such application should be hydrophobic to avoid loss of IL in the aqueous solution and should be characterized by high CO<sub>2</sub> absorption capacity. When applying such technology to remove CO<sub>2</sub> from combustion gas or air, the presence of O<sub>2</sub> can be detrimental to the alkanolamine due to the oxidative degradation of the amine. To address this amine degradation problem, it is important that the ionic liquid should be selective to CO<sub>2</sub> as compared to O<sub>2</sub> in order to reduce the contact of O<sub>2</sub> with the alkanolamine. As such developing a SILM contactor with high CO<sub>2</sub>/O<sub>2</sub> absorption selectivity can be considered as a significant improvement to the technology. In addition, the experimental screening of ILs to choose the best one in terms of hydrophobicity, CO<sub>2</sub> absorption capacity and CO<sub>2</sub>/O<sub>2</sub> selectivity is a very tedious and time consuming process. Using molecular modelling tools such as COSMO-RS can save a lot of time and permit a rigorous screening of various ILs.

## 1.3 Research scope and objectives

The aim of the current project is to evaluate a novel SILM as a contactor for selective absorption of CO<sub>2</sub> by aqueous monoethanolamine (MEA). Imidazolium-containing IL has been utilised in this study as it has low viscosity, is stable across a wide range of liquid temperature, and lacks the halogen atoms that can cause chemical reactions. Furthermore, it is regarded that the information obtained from the COSMO-RS predictions is highly valuable to identify the selectivity of CO<sub>2</sub>/O<sub>2</sub> in a gas-liquid membrane contactor system for selected ionic liquids.



In the recent experiment, preparation will be made on the SILMs from a different composition of 1-ethyl-3-methylimidazolium bis (trifluoromethylsulfonyl) imide: acetone as carriers. This is to obtain a better understanding on the effect's of the preparation method of supported liquid membranes on the stability of the SILM. ILs containing bis(trifluoro-methylsulfonyl)imide ( $[\text{NTf}_2]^-$ ) anion are selected due to their good hydrophobicity and selectivity of  $\text{CO}_2/\text{O}_2$  (COSMO-RS analysis). Meanwhile, PP has been selected as the membrane support in this work. This is because of its excellent characteristics that it possesses: low cost, good thermal stability, and robust mechanical traits. Further investigations toward absorption performances and selectivity of  $\text{CO}_2/\text{O}_2$  of the new supported ionic liquid membrane were conducted, by varying the effect of important operating conditions using parallel and cross-flow type of Liqui-Cel membrane modules. Therefore, the objectives of this work are as follows:

- i. To predict  $\text{CO}_2$  absorption capacity and  $\text{CO}_2/\text{O}_2$  selectivity of some selected ILs, by using the COSMO-RS molecular modelling system.
- ii. To investigate the role of viscosity in preparation of a new supported ionic liquid membrane (SILM) and its chemical stability.
- iii. To evaluate the  $\text{CO}_2$  absorption performance and  $\text{CO}_2/\text{O}_2$  selectivity of the supported ionic liquid membrane and compare its performance with that of the blank membrane.
- iv. To investigate the effects of important operating conditions on  $\text{CO}_2$  absorption performance and  $\text{CO}_2/\text{O}_2$  selectivity of the supported ionic liquid membrane (SILM).

## 1.4 Outline of thesis

This thesis is made up of the following main chapters:

### Chapter One: General Introduction

- This chapter includes a brief introduction to the research and objectives of the study.

### Chapter Two: Literature Review

- This chapter gives a comprehensive literature survey for the state of the art of gas-liquid membrane contactor and supported ionic liquid membranes (SILMs) for CO<sub>2</sub> capture.

### Chapter Three: Methodology

- This chapter describes the experimental procedure which includes the screening process for ILs selection, the preparation of new supported ionic liquid membranes (SILMs) and CO<sub>2</sub> absorption study by using SILMs in a gas-liquid membrane contactor system.

### Chapter Four: Results and Discussion

- This chapter contains the results and discussions of the experiments that were performed.

### Chapter Five: Conclusion

- In the last chapter, the results and findings of this study will be summarized and recommendations for future works have been suggested.



## CHAPTER 2: LITERATURE REVIEW

### 2.1 Membrane contactor

There has been a huge amount of interest on membrane contactors since the 1980s, with Qi and Cussler becoming the earliest to be using hollow fiber membrane contactors for CO<sub>2</sub> absorption (Zhang & Cussler, 1985). There were many successes which involves the commercialization of gas–liquid applications on the membrane contactors. Some of them are CO<sub>2</sub> capture (Park et al., 2008; Li et al., 1998; Poddar et al., 1996), the manufacture of ultrapure water in the semiconductor sector, and membrane distillation (Mavroudi et al., 2003). Membrane contactors are known to be non-dispersive contacting systems, with the membranes are found not to afford selectivity for separation. They act as barriers to separate the two phases instead, and to enhance the effective contact area for mass transfer. The key advantage of membrane contactors is with its very high area of interfacial. It has reduced the equipment size by a lot, which leads to intensification of the process (deMontigny et al., 2005; Falk-Pedersen et al., 2005; Li & Chen, 2005; Zhang & Cussler, 1985). Membrane contactors are able to provide up to 30 times more interfacial area than by using the usual gas absorbers (Gabelman & Hwang, 1999), and the absorber size can also be reduced by 10-times (Feron & Jansen, 1995; Klaassen et al., 2008). Alternatively, there were a few advantages that were quantified by using the membrane contactors in some processes (Falk-Pedersen et al., 2005).

Membrane contactors benefits are due to the integration of the benefits of both membrane separation (modularity and compactness) and liquid absorption (high selectivity) (Feron et al., 1992; Gabelman & Hwang, 1999). In the meantime, membrane contactors major disadvantage is on mass transfer resistance's increase, especially when

the membranes are wetted. Yet, the mass transfer coefficients reduction can be compensated by several advantages (for example a significantly increased interfacial area) and this causes the membrane contactor to be better in the CO<sub>2</sub> capture than traditional systems (Cui & deMontigny, 2013; Li & Chen, 2005; Mansourizadeh & Ismail, 2009; Mavroudi et al., 2003).

## **2.2 Membrane contactors for CO<sub>2</sub> absorption**

Currently, the focus of study has been on the use of membrane contactors for CO<sub>2</sub> absorption (Favre, 2011). The studies that were performed can be divided into several groups: mass transfer, major challenges for membranes, membrane development, absorbent selection, and module design.

### **2.2.1 Mass transfer fundamentals**

By using a membrane contactor setup, the liquid and gas phases are disjointed by porous membranes. Figure 2.1 shows mass transfer through the porous membrane. Universally, there are three successive steps as follows: (i) dispersion from the bulk gas to the gas-membrane interface, (ii) dispersion from the gas-membrane interface to the liquid membrane interface through the membrane pores, and (iii) transfer from the liquid-membrane interface to the bulk liquid followed by physical and/or chemical absorption. It is also commonly called the resistance-in-series model (Figure 2.1).

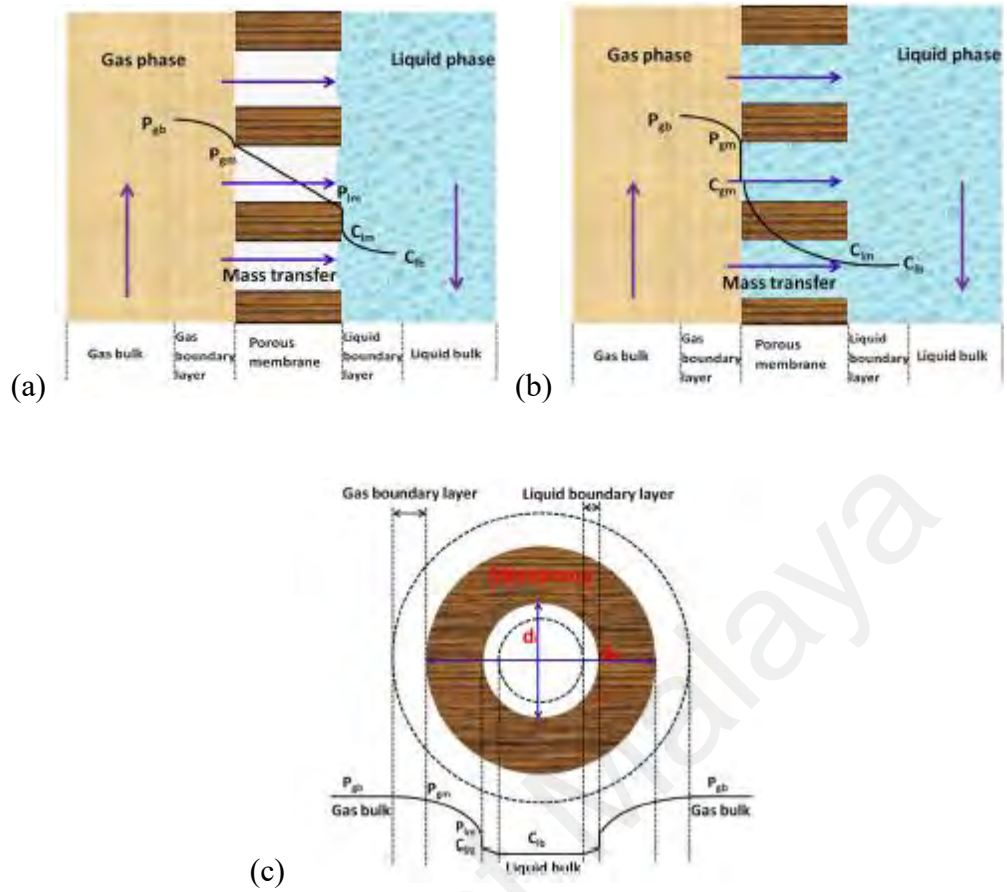


**Figure 2.1:** Mass transfer mechanism through a porous membrane in (a) non-wetted mode (with gas-filled pores); (b) wetted mode (with liquid-filled pores); (c) through a hollow fiber (gas on the shell side and liquid on the tube side).  $P$  and  $C$  are the gas partial pressure and liquid concentration, respectively. The subscripts  $g_b$ ,  $g_m$ ,  $l_m$  and  $l_b$  represent gas bulk, gas membrane interface, liquid-membrane interface and liquid bulk, respectively.

Figure 2.1a displays the mass transfer through a porous membrane in non-wetted mode, that is favored and studied more compared to the wetted mode. Gas flux ( $N$ ) for all three regions (i.e., gas, membrane and liquid) can be articulated by:

$$N = k_g(P_{gb} - P_{gm}) = k_m(P_{gm} - P_{lm}) = k_l(C_{lm} - C_{lb}) \quad (2.1)$$

where  $k_g$ ,  $k_m$  and  $k_l$  are the individual mass transfer coefficients for gas, membrane and liquid, respectively.  $P$  and  $C$  are the gas partial pressure and liquid concentration, respectively. The subscripts  $g_b$ ,  $g_m$ ,  $l_m$  and  $l_b$  represent gas bulk, gas-membrane interface, liquid-membrane interface and liquid bulk, respectively. Henry's Law states

that, the gas partial pressure above the liquid is at equilibrium; and is related to the gas concentration dissolved in the liquid (Wiesler, 1996):

$$P_{lm} = HC_{lm} \quad (2.2)$$

with  $H$  being the Henry's Law constant. The overall mass transfer coefficient  $K_g$  is based on the gas phase, while  $K_l$  is based on the liquid phase, and can be expressed by:

$$N = K_g(P_{gb} - P^*) = K_l(C^* - C_{lb}) \quad (2.3)$$

where

$$P^* = HC_{lb} \text{ and } P_{gb} = HC^* \quad (2.4)$$

based on Equation (2.1)–(2.4), we discover that:

$$\frac{1}{K_g} = \frac{1}{k_g} + \frac{1}{k_m} + \frac{H}{k_l} \quad (2.5A)$$

$$\frac{1}{K_l} = \frac{1}{HK_g} = \frac{1}{Hk_g} + \frac{1}{Hk_m} + \frac{1}{k_l} \quad (2.5B)$$

In most situations, a membrane contactor module is normally made up of a number of small hollow fibers where the tube wall's thickness cannot be disregarded in general. Figure 2.1 shows the mass transfer through a hollow fiber membrane. By taking the membrane wall's thickness into attention, we find that:

$$N = k_g(P_{gb} - P_{gm})(\pi d_o L) = k_m(P_{gm} - P_{lm})(\pi d_{ln} L) = k_l(C_{lm} - C_{lb})(\pi d_i L) \quad (2.6)$$

$$N = K_g(P_{gb} - P^*)(\pi d_o L) = K_l(C^* - C_{lb})(\pi d_i L) \quad (2.7)$$

where  $d_o$ ,  $d_i$ , and  $d_{ln}$  are the outer, inner and logarithmic mean diameters of the membrane, respectively. The overall mass transfer coefficient  $K_g$  is based on the gas phase, and  $K_l$  is based on the liquid phase; that can be articulated respectively as:

$$\frac{1}{K_g} = \frac{1}{k_g} + \frac{d_o}{k_m d_{ln}} + \frac{H d_o}{k_l d_i} \quad (2.8A)$$

$$\frac{1}{K_l} = \frac{d_i}{H d_o K_g} = \frac{d_i}{H d_o k_g} + \frac{d_i}{H d_{ln} k_m} + \frac{1}{k_l} \quad (2.8B)$$

Bearing in mind the enhancement factor ( $E$ ) due to chemical reaction, we discover that:

$$\frac{1}{K_g} = \frac{1}{k_g} + \frac{d_o}{k_m d_{ln}} + \frac{H d_o}{E k_l d_i} \quad (\text{Liquid on the tube side}) \quad (2.9A)$$

$$\frac{1}{K_l} = \frac{d_i}{H d_o K_g} = \frac{d_i}{H d_o k_g} + \frac{d_i}{H d_{ln} k_m} + \frac{1}{E k_l} \quad (\text{Liquid on the tube side}) \quad (2.9B)$$

The above equations are valid when the liquid phase is on the tube side without wetting (i.e. gas phase is on the shell side). If the liquid phase flows onto the shell side (i.e. gas phase is on the tube side), then it applies the following equation:

$$\frac{1}{K_g} = \frac{1}{d_i k_g} + \frac{1}{d_{ln} k_m} + \frac{H}{E d_o k_l} \quad (\text{Gas on the tube side}) \quad (2.10A)$$

$$\frac{1}{K_l} = \frac{d_o}{H d_i K_g} = \frac{d_o}{H d_{i2} k_g} + \frac{d_o}{H d_{ln} d_i k_m} + \frac{1}{E d_i k_l} \quad (\text{Gas on the tube side}) \quad (2.10B)$$



Some researchers (Ho & Sirkar, 1992) are taking different interpretation of Henry's Law in membrane processes, i.e.,  $C_{lm} = HP_{lm}$ , by obtaining the below:

$$\frac{1}{K_g} = \frac{1}{k_g} + \frac{d_o}{d_{ln}k_m} + \frac{d_o}{EHd_i k_l} \quad (\text{Liquid on the tube side}) \quad (2.11A)$$

$$\frac{1}{K_l} = \frac{Hd_i}{d_o K_g} = \frac{Hd_i}{d_o k_g} + \frac{Hd_i}{d_{ln}k_m} + \frac{1}{Ek_l} \quad (\text{Liquid on the tube side}) \quad (2.11-B)$$

$$\frac{1}{K_g} = \frac{1}{k_g} + \frac{d_i}{d_{ln}k_m} + \frac{d_i}{EHd_o k_l} \quad (\text{Gas on the tube side}) \quad (2.12A)$$

$$\frac{1}{K_l} = \frac{Hd_o}{d_i K_g} = \frac{Hd_o}{d_i k_g} + \frac{Hd_o}{d_{ln}k_m} + \frac{1}{Ek_l} \quad (\text{Gas on the tube side}) \quad (2.12B)$$

The fundamental for mass transfer in membrane contactors can be described and well-defined with the equations above. Several studies have used the above Eqn. (2.9)–(2.12) or their derivative formulae (Atchariyawut et al., 2006; Mavroudi et al., 2006; Khaisri et al., 2009; Lin et al., 2009a; Mansourizadeh et al., 2010;). Nevertheless, because of the orientation of the membrane-fluid that was not clear in the literature, or the Henry's Law format that was applied; the equations have sometimes caused confusion. Eqn. (2.9)–(2.12) explains that the overall mass transfer in membrane contactors is using dissimilar flow directions.

## 2.3 Major challenges for membranes as contactor

Membrane wetting, fouling, and degradation are the key issues that were faced when membrane contactors are used. These issues are debated in further details as follows:

### 2.3.1 Membrane wetting

Wetting in membrane contactors is the major matter that desires to be highlighted. This is because the mass transfer resistance can increase considerably, thereby causing a huge drop in absorption performance (Kreulen et al., 1993; Rangwala, 1996; Lu et al., 2005; Zhang et al., 2008a; Mosadegh-Sedghi et al., 2014). The membrane's resistance can be as high as 60% of the total mass transfer resistance and up to six times higher in terms of efficiency in non-wetted mode when compared to using the wetted mode (Rangwala (1996); Wang et al. (2005)).

#### 2.3.1.1 Fundamental of membrane wetting

For a liquid absorbent, the wettability of a membrane is usually assessed through the liquid's entry pressure (LEP is also known as breakthrough pressure) (McGuire et al., 1995; Zhao et al., 2015). LEP is determined by the minimum pressure that is applied on the liquid for it to enter the membrane pores. This can be assessed by the Laplace-Young equation (Franken et al., 1987; Kumar et al., 2002;).

$$LEP = - \frac{4B \gamma \cos \theta}{d_{max}} \quad (2.13)$$

Where  $B$  is the coefficient for the pore's geometry ( $B=1$  for perfectly cylindrical pores;  $0 < B < 1$  for non-cylindrical pores),  $\gamma$  is the surface tension for the liquid,  $\theta$  is the

angle of contact between the liquid absorbent and the membrane's surface, and  $d_{max}$  is the membrane's maximum pore diameter.

The phenomena of wetting were carefully studied by Mosadegh-Sedghi et al. (2014) recently. There are three modes of wetting in membrane contactors that was discussed (Lu et al., 2008; Mansourizadeh & Ismail, 2009; Mosadegh-Sedghi et al., 2014): (a) non-wetting mode, (b) complete-wetting mode and (c) partial-wetting mode. A membrane contactor with greatly hydrophobic hollow fibers, might experience each and every of the three wetting patterns over the entire process. During the first several hours, the membrane module could be non-wetted (Figure 2.1a), consequently it has a high efficiency in absorption. After several days, it can become steadily wetted (i.e., partially wetted), with the effectiveness of absorption decreases radically. After the operation had lasted several months or years, the membrane pores might be completely packed with the liquid absorbent (i.e., completely wetted, Figure 2.1b). Under actual circumstances, the pores of the membrane are very likely to be partially filled with liquid absorbents (i.e., in partial-wetting mode) (Yu et al., 2015). In summary, the wetting is considerably influenced by numerous factors such as:

- i. the characteristics of the membrane (e.g., surface roughness, porosity, tortuosity, and pore diameter)
- ii. the properties of the solvent (e.g., surface tension)
- iii. the interaction between the membrane and the solvent (e.g., the contact angle of the liquid)
- iv. operating conditions (e.g., pressure on the liquid side).

### 2.3.1.2 Mechanisms of wetting

The membrane wetting can be described via numerous dissimilar mechanisms. It is generally acknowledged that the reaction of the chemicals between the membrane and the absorbent in a membrane contactor will cause the degradation of the membrane and subsequently it become wet. Wang et al. (2005) have observed that the morphology of the membrane is changed by the aqueous diethanolamine (DEA) solution, which shows that membrane degradation is due to the chemical reaction between the membrane and DEA. Lv et al. (2010) observed major alterations in morphology of the membrane's surface, hydrophobicity after wetting and surface roughness; then claims that the wetting of the membrane is the outcome from the mechanism of absorption swelling. Rangwala (1996) has reported that trace impurities and ionic species in the absorbent is able to modify the surface of the membrane and permits the penetration of liquid into the pores caused by the necking phenomenon. The enlargement of the pore is also thought to be the key reason for the wetting of the membrane in chemical absorption (Mansourizadeh et al., 2010). Centered on these clarifications for membrane wetting, we predict the following wetting process in most laboratory studies:

- i. Liquid absorbents come into contact with the membrane's surface at an angle of above  $90^\circ$  (i.e., non-wetted).
- ii. Liquid absorbents are able to physically and/or chemically change the properties of the membrane's surface (e.g., hydrophobicity, morphology, roughness and chemical compositions).
- iii. Liquid absorbents are able to penetrate the pores and therefore changing the properties of the pore which will cause the wetting.

Wetting can be triggered by capillary condensation of water vapor in the pores of the membrane (Atchariyawut et al., 2006), together with direct water and/or absorbent penetration into the pores. The condensation of capillary could be a key problem in desorption of the membrane, once there is a substantial flow of water vapor into the fiber's colder section. Li & Chen (2005), Scholes et al. (2014) and Mosadegh-Sedghi et al. (2014) summarized several measures that are in preventing wetting as follows:

- i. with the use of hydrophobic membranes, or hydrophobic modification (i.e., large  $\cos \theta$ )
- ii. with the use of composite membranes with dense skin layers (i.e., small  $d_{max}$ )
- iii. with the use of liquids with high surface tension (i.e., large  $\gamma$ )
- iv. with the increase in compatibility between membranes and absorbents (i.e., avoiding membrane degradation)
- v. with the optimization of operating environments

### **2.3.2 Membrane fouling**

Fouling (e.g., pore plugging) in membrane contactors is getting lesser consideration as compared to wetting. This could be due to the non-commercialization of this technology for CO<sub>2</sub> elimination from flue gas. Almost entire research works that are relevant is done at pilot or bench scales, with the flue gas being mostly manufactured deprived of impurities (e.g., dusts or particles). A new research was conducted by presenting impurities in flue gas, and it shows that the contaminants managed to decrease the efficiency of the process (Zhang et al., 2015). In the real-world CO<sub>2</sub> elimination from flue gas, fouling (which includes pore plugging) occurrences might be a serious unease; since the fine particles found in flue gas is able to considerably increase the resistance of mass transfer (Wang et al., 2014; Zhang et al., 2015). This

results to the need of pre-treatment stages to eliminate the contaminants and to evade this situation. More research on membrane fouling in membrane contactors are crucial and needs to be further studied.

### **2.3.3 Membrane degradation**

Preferably, the membranes applied in contactors must be sufficiently in terms of thermally and chemically stable for maintaining realistic proficiency. Though, the membranes are supplementary favored to be attaching itself to the chemical solvents (Barbe et al., 2000). The liquid absorbents are usually more corrosive after the absorption of CO<sub>2</sub> (Kladkaew et al., 2011; Saiwan et al., 2011), and is found to have bigger affinities to change the chemical structures, membrane morphology and hydrophobicity. This causes the wetting and degradation of the membrane, mainly in absorbent concentrations that are higher.

The degradation of solvents products can cause more destruction to the membrane too. Further to chemical degradation, the degradation of thermal can also become an additional issue. Not all membranes that are being applied in this process have great thermal stabilities. Their dimensional stabilities are influenced by the glass transition temperature ( $T_g$ ) or the melting temperature ( $T_m$ ) (Table 2.1). To avoid the degradation of thermal, polymers that are robust with reasonably high ( $T_g$ ) and ( $T_m$ ), would be chosen for usage in this system. Be reminded that the degradation of the glues that is being applied as the potting medium could be an additional issue once the degradation of membrane happens.

**Table 2.1:** The glass transition temperature ( $T_g$ ) and melting temperature ( $T_m$ ) of polymers used as membrane materials in membrane contactors (Schouten & Vander Vegt (1981) and Chanda & Roy (2006))

Polymer	Type	$T_g(^{\circ}\text{C})$	$T_m(^{\circ}\text{C})$
Polytetrafluoroethylene (PTFE)	Semi-crystalline	127	327
Polypropylene (PP)	Semi-crystalline	-20	176
Polyvinylidene fluoride (PVDF)	Semi-crystalline	$\sim -30$	$\sim 170$
Polyethylene (PE)	Semi-crystalline	-115	137
Polyether ether ketone (PEEK)	Semi-crystalline	145	335

## 2.4 Membranes in membrane contactors

Membranes play a vital part in absorption proficiency; granting which they are not selective to  $\text{CO}_2$  due to it acting as non-dispersive barrier. Usually membranes in membrane contactors are hollow fibers that are primed with the selective skin layer on its outside. Consequently, to avoid the wetting of the membrane; the solvent must be on the shell side, and gas has to flow on the lumen side. This arrangement is able to help in minimizing flow resistance of the solvent, mainly for absorbent with great viscosity. The following properties need to be available in membranes in the membrane contactors:

- i. decent thermal resistance to degradation at increased temperature
- ii. great chemical stability to the absorbent
- iii. great hydrophobicity (i.e. low wetting tendency)
- iv. great porosity to reduce the mass transfer resistance

## 2.5 Surface modification of membranes

Several techniques for surface modification have been considered to advance the performance of the membrane, such as mass transfer coefficient, long-term stability, and

wetting resistance (Lin et al., 2014; Yu et al., 2015). PP membranes are oftenly used in surface modification. This is due to its their relatively great thermal and chemical stabilities, well-controlled porosity and pore size, good availability, and low cost (Lin et al., 2009a; Franco et al., 2011; Lv et al., 2012). Lin et al. (2009a) uses  $\text{CF}_4$  plasma to modify the PP hollow fibers, and it shows that mass transfer coefficient of the treated membrane, membrane durability and absorption flux; is considerably enhanced. Franco et al. (2011) spluttered PTFE onto the surface of the PP membrane using the plasma procedure, and it produces an ultrathin fluorinated hydrophobic layer. It is also able to attain better absorption efficiency in short period ( $\sim 45$  h) owing to the improved resistance to amine absorbent degradation and wetting condition after the surface modification. On the other hand, the better performance did not last long. Lv et al. (2012) put a rough PP layer onto the surface of the PP membrane, using a mixture of methylethylketone (MEK) and cyclohexanone as the non-solvent. The modified surface demonstrated superhydrophobicity (up to  $158^\circ$  of contact angle) and long-term stability. As membrane contactors are estimated to operate for a couple of months (if possible years) in practical  $\text{CO}_2$  absorption, it is really important that it has long-term performance stability in adopting these techniques for surface modification.

## **2.6 Absorbent selection**

### **2.6.1 Absorbent selection criteria**

Technically, any absorbent that is applied in the conventional absorption process can also be utilized in membrane contactors. Nevertheless, some absorbents are more appropriate when we consider their physical and/or chemical properties. According to Dindore et al. (2004), the ideal  $\text{CO}_2$  absorbent ought to have the below features:

- i. substantial absorption capacity (i.e.,  $\text{CO}_2$  loading)



- ii. fast reaction rate
- iii. low heat of reaction if possible
- iv. chemically stable
- v. insignificant thermal and oxidative degradation

The CO<sub>2</sub> solubility is an important factor in the selection of potential solvents. A solvent with great capacity of CO<sub>2</sub> absorption can efficiently lessen the solvent volume and the required surface area, and ultimately the operating cost. Another important element is high reactivity, which leads to high mass fluxes and high absorption rate. This results in a decrease of the liquid phase resistance, which is commonly the primary reason that contributes to the total resistance in a membrane contactor. From the perspective of environment, the absorbents and its degradation compounds ought to be non-toxic to avoid discharge that is harmful. Good thermal stability and low vapor pressure or volatility, should be able to reduce the loss of solvent and thermal degradation throughout the operation. Lastly, the absorbent should be affordable and commercially available. Key factors in choosing the absorbents for membrane contactors are the interactions between the membrane materials and absorbents, in addition to its configurations. A significant requirement is the liquid absorbents should not harm the membrane either physically or chemically, and decent compatibility with the membrane materials that was used. If absorbents attack the chemical structure of membrane materials or swell the membrane materials, then the surface/pore morphology of the membranes will be altered. If a porous membrane is used, an absorbent ought to have high surface tension to provide a highly critical LEP. This will develop the membrane's pore wetting resistance. Absorbents with low viscosity are favored, in order to decrease the overall mass transfer resistance. High viscosity is able to increase the pressure drop of the absorbent, as well as to reduce the mass transfer rate

through the membrane contactor. When running at reduced temperatures or a hollow fiber module is used, high viscosity will cause high energy consumption for absorbent circulation. The absorbents and their degradation compounds must not precipitate during absorption, since the solids formed may block the membrane's pores, or even completely block the path of the liquid. If this were to happen, it would cause a total loss of efficiency. Currently, there are no absorbent that fulfills all these requirements. Some properties need to be chosen while others are to be given up.

### **2.6.2 CO<sub>2</sub> absorbents in membrane contactors**

Both physical and chemical absorbents have been extensively researched for CO<sub>2</sub> removal (Versteeg et al., 1996). Up to now, chemical absorption of CO<sub>2</sub> (particularly using aqueous amine absorbents) is the key post-combustion capture (PCC) technology that is widely used in the industry. Other than amines, chemical absorbents such as ammonia, amino acid salts, alkali, carbonates and some types of ILs have also been examined (Luis et al., 2009a; Jie et al., 2013; Chabanon et al., 2014; Arshad et al., 2014; Jonassen et al., 2014; Deng, 2015; Ansaloni et al., 2015; Im et al., 2015; Chabanon et al., 2015; Dai et al., 2016). Although all of these absorbents are still in the demonstration or development stage that has to be commissioned before it can be applied on scale that is larger.

Amines and its combinations are the utmost examined chemical absorbents for CO<sub>2</sub> removal (Mansourizadeh & Ismail, 2009; Chabanon et al., 2011; Favre & Svendsen, 2012). Monoethanolamine (MEA) is the leading aqueous alkanolamine solution that is being applied in most industrial processes. While this process is able to efficiently remove CO<sub>2</sub>, it does have severe environmental and economic drawbacks:

(1) corrosion to the equipment, (2) solvent loss through evaporation, (3) oxidative and thermal degradation in the course of the absorption-desorption cycle and (4) high energy cost of solvent regeneration (Gao et al., 2013). The main issue being related with chemical absorption using MEA, is the solvent's degradation via irreversible side reactions with CO<sub>2</sub> and other gases in the gas streams. During these procedures, MEA is subject to two main types of degradation, oxidative and thermal degradation. Oxidative degradation happens in the existence of oxygen which results in fragmentation of the amine solvent (Goff and Rochelle, 2004). Meanwhile for thermal degradation, it is also known as carbamate polymerization which occurs at stripper conditions (around 120°C for MEA) in the presence of CO<sub>2</sub>. The degradation of amine then causes the performance of the amine in the absorption process to worsen. Apart from the reduction in absorption capacity, foaming and corrosion are also induced because of the presence of degradation products (Strazisar et al., 2003).

## **2.7 Module design**

In deciding the performance of membrane contactors, the membrane module configuration has an important role to play. In a gas-liquid membrane contactor, the membrane module ought to deliver an efficient gas-liquid interface devoid of the convective flow of fluid through the membrane (i.e., non-dispersive gas-liquid contact). Both tubular and flat sheet membrane modules can be used in a gas-liquid membrane contactor. For membrane contactor applications, a flat sheet membrane module can be attached in a plate-and-frame configuration. Because of the membrane area in a flat sheet membrane module is much lower than that in a hollow fiber module, several researches have described the use of flat sheet membrane contactors for CO<sub>2</sub> separation applications (Dindore et al., 2004; Lin et al., 2009b; Ahmad et al., 2010; Bougie et al.,

2015). Easy module assembly and membrane fabrication are two major benefits over hollow fiber membrane contactors. A tubular membrane module usually talks about the hollow fiber membrane module (inner diameter  $< 1.0\text{mm}$ ) (Mulder, 2003). Hollow fiber membrane contactors have been extensively scrutinized for  $\text{CO}_2$  capture with a wide variety of absorbents. In some situations, tubular membranes with an inner diameter ( $> 5\text{ mm}$ ) that is larger than that of a hollow fiber membrane are used to reduce the pressure drop in PCC; for both inorganic and polymeric membranes.

A hollow fiber module normally means a package of fibers that are packed parallel in a shell, akin to the configuration of a shell and tube heat exchanger. With a lot of hollow fiber membranes with its skin layer on the outside, the liquid phase in a hollow fiber membrane contactor is typically to be on the shell side as to reduce the wetting of the membrane. In the meantime, gas flows on the lumen side that helps in reducing the pressure drop along the membrane. Even though there are a lot of membrane module configurations that has been established, hollow fiber membrane modules with the cross-flow or longitudinal flows are the most widely considered for  $\text{CO}_2$  capture. Yang & Cussler (1986) investigated both cross-flow and longitudinal hollow fibers for gas liquid contact, and establish the fact that cross-flow membrane contactors demonstrate an enhanced performance in absorption. However, most researches that were done are using the longitudinal module design because of its simplicity (Yang & Cussler, 1986).

### **2.7.1 Longitudinal flow module**

Longitudinal flow is also widely recognized as parallel flow. In this arrangement, both fluids (liquid and gas) flows parallel to each other on the opposite sides of a

membrane; either in a counter-current or co-current flow (Figure 2.2) (Li & Chen, 2005; Cui & deMontigny, 2013). A lot of lab-scale researches was conducted by using longitudinal design membrane contactors because it is easy to prepare, has an easy approach towards mass transfer calculations and distinct fluid dynamics (deMontigny et al., 2006). Longitudinal module provides limited efficiency when compared with a cross-flow module (Mansourizadeh & Ismail, 2009). Bypassing and channeling of fluid on the shell side and high shell-side pressure drop, would disturb the overall system performance. The small internal diameter and non-uniform packing of hollow fibers restricts the flow of fluid, which then bounds mass transfer and provides reasonably low mass transfer coefficients (Wickramasinghe et al., 1992). These are the key obstacles in using this sort of module in industrial applications (Bhaumik et al., 1998; Dindore & Versteeg, 2005; Liu et al., 2005a).

Adjustments to longitudinal modules was done in order improve mass transfer and to combine the benefits of cross-flow in the module. A famous commercial example is the Liqui Cell Extra-Flow module presented by CELGARD LLC (Charlotte, NC; formerly Hoechst Celanese) (Liqui-Cel). A diagram of this gas-liquid hollow fiber membrane contactor module is presented in Figure 2.2. A crucial baffle in the shell side of the membrane contactor decreases shell side by providing and passing velocity towards the surface of the membrane, that features a higher mass transfer coefficient than that of a strictly parallel flow (Figure 2.2a) (Wang & Cussler, 1993).

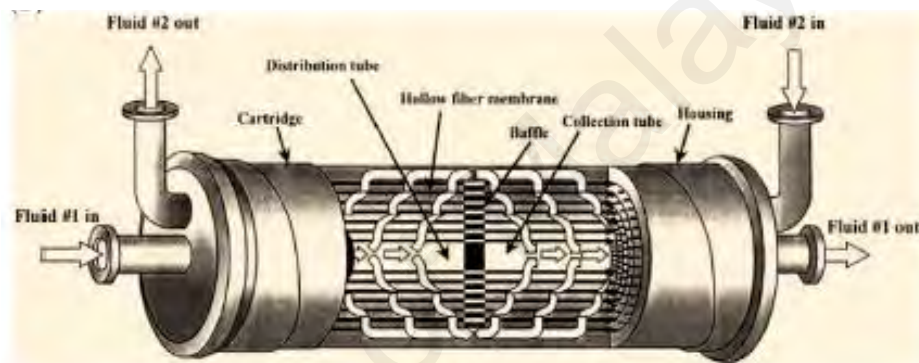
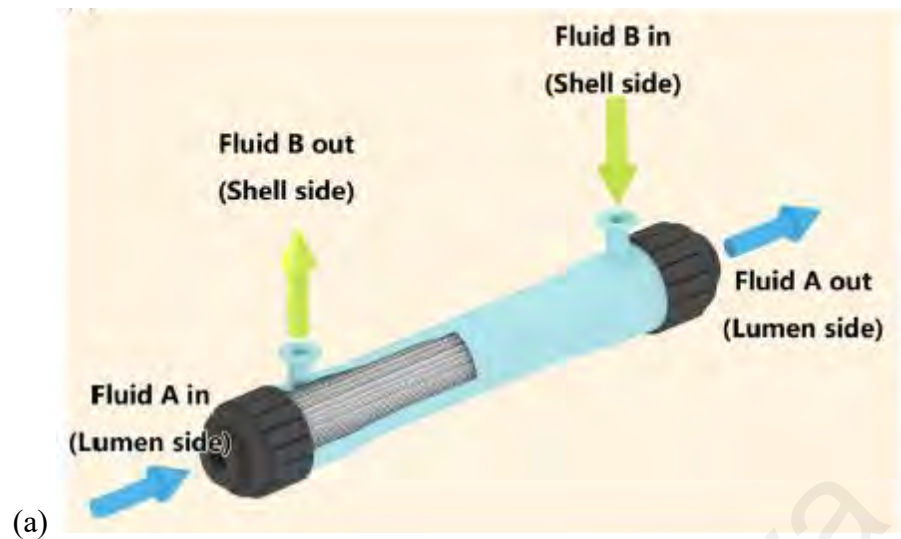


**Figure 2.2:** (a) Parallel flow module (countercurrent flow); (b) Liqui-Cel Extra-Flow membrane contactor (Liqui-Cel)

### 2.7.2 Cross-flow module

Although longitudinal flow modules are the ones that are most investigated, the cross-flow module is actually more effective. To research the special effects of different operating parameters (e.g., solute concentration in the feed stream and gas and liquid flow rates) on the general performance of the system, experiments done using rectangular cross-flow membrane contactor for physical absorption of gas (Dindore & Versteeg, 2005).

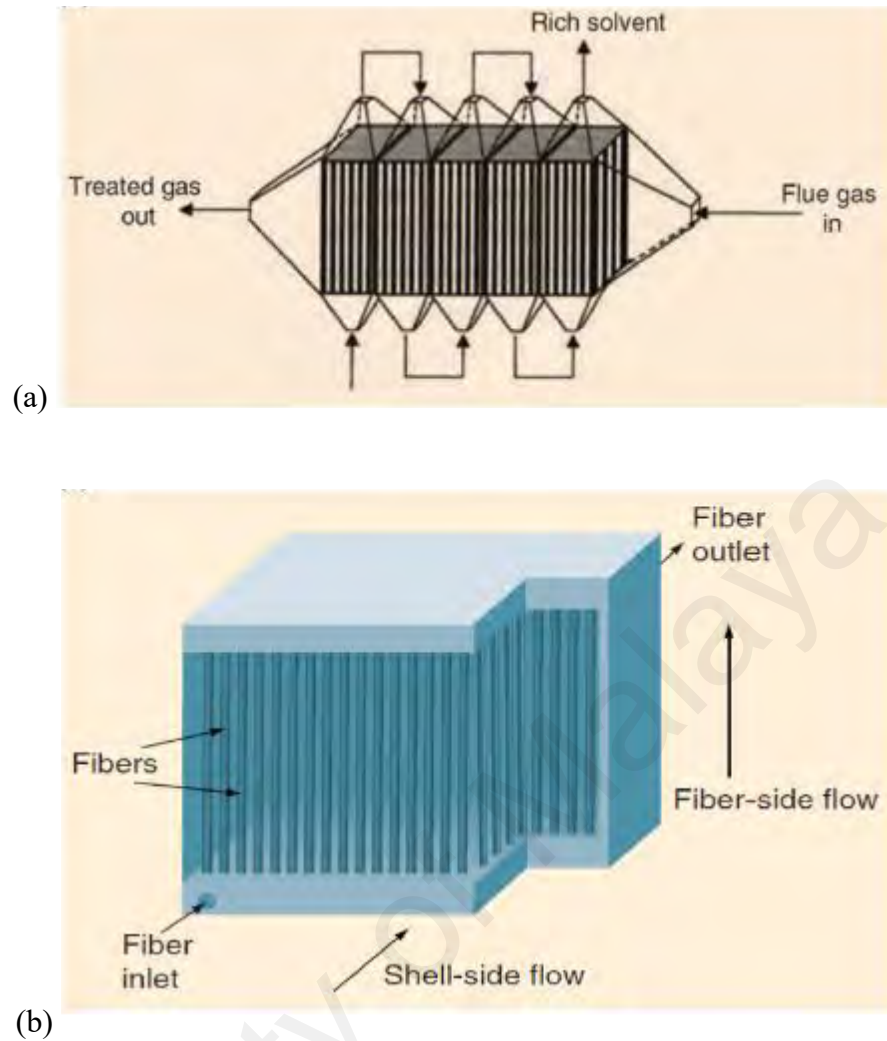


**Figure 2.3:** Cross-flow membrane contactor modules developed by (a) Aker Kvaerner (Hoff, 2003); (b) the Netherlands Organization for Applied Scientific Research (TNO) (Cui & deMontigny, 2013)

The performance of the cross-flow and longitudinal membrane contactors was compared based on the equal module volume and flow per membrane area (Wickramasinghe et al., 1992). It was established that counter-current cross-flow membrane contactors were more proficient. Two instances of cross-flow membrane contactors independently patented by Aker Kvaerner (Norway) and TNO (the Netherlands), are respectively shown in Figure 2.3a (Hoff, 2003) and Figure 2.3b (Feron & Jansen, 1995; Dindore & Versteeg, 2005; Cui & deMontigny, 2013).

## 2.8 Ionic Liquid Membranes (ILMs)

Room temperature ionic liquids (RTILs) which is a type of molten electrolyte ( $T_{melting} < 373$  K), displays numerous exciting properties such as wide electrochemical window, solubility of a widespread sort of organic and inorganic compounds, a liquid range of up to at least 300°C, great thermal stability, non-flammability and negligible vapor pressure; in comparison to the orthodox molecular solvents (Brennecke & Gurkan, 2010; Seddon et al., 2000, 2002). Furthermore, their physicochemical properties are able to be personalized to fulfill precise chemical tasks with the suitable choice of cation, anion, and substituents on the cationic constituent. The arrangements of several frequently used anions and cations of ILs are presented in Figure 2.4 and 2.5, respectively, where the R1, R2, R3 and R4 groups are alkyl groups. As a result, some promising outcomes have been accomplished in terms of its application as a benign medium or solvent in many applications; for example extractions (Chun et al., 2001; Wei et al., 2003; Zhao et al., 2005; Poole & Poole, 2010; Wang et al., 2010b), chemical reactions (de los Ríos et al., 2007; Toral et al., 2007; Plechkova & Seddon, 2008; Fehér et al., 2008; Lozano, 2010), and the separation of various compounds (Rao & Rubin, 2002; Kawanami et al., 2003; Jessop et al., 2003; Wang & Li, 2013).



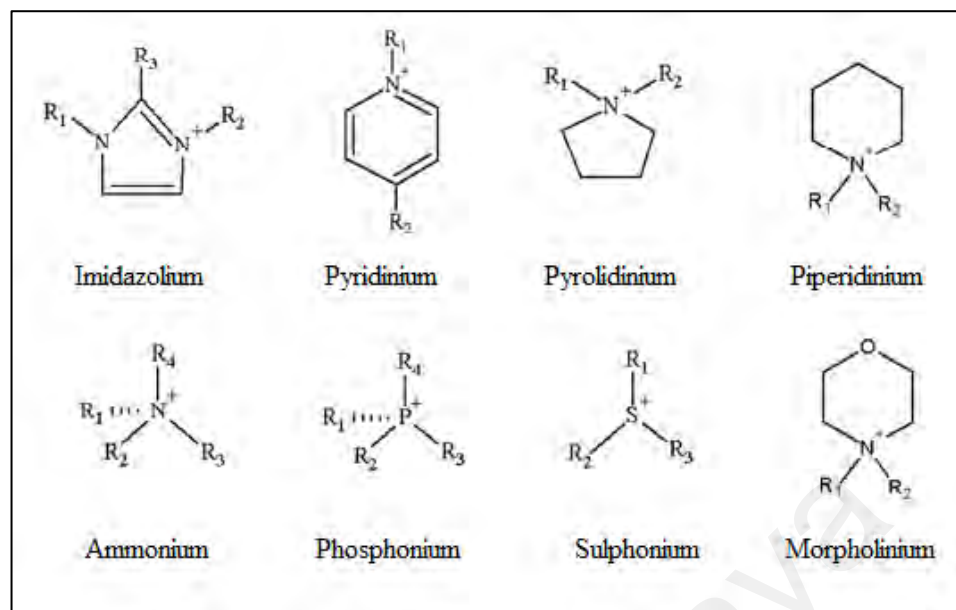


**Figure 2.4:** Frequently used cations of ionic liquids

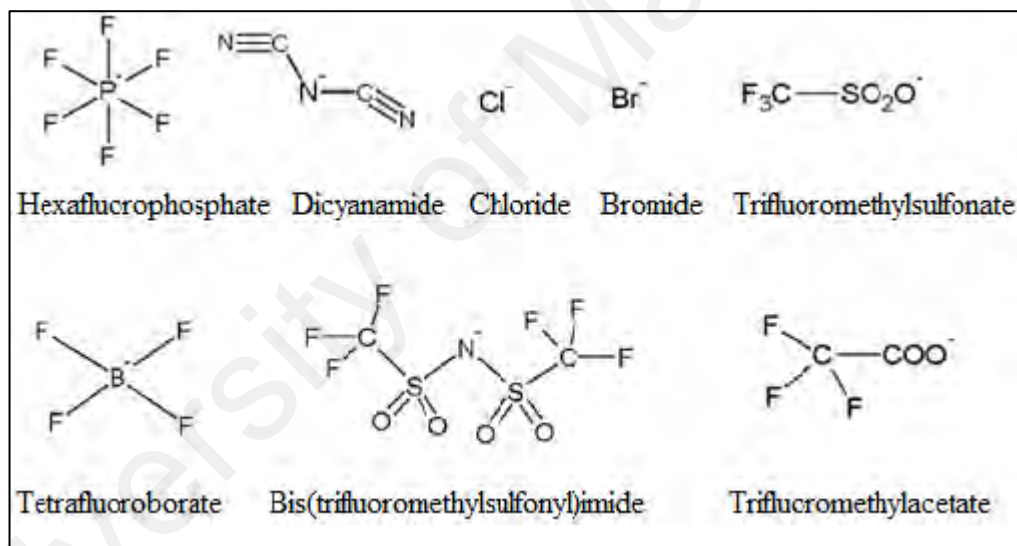


**Figure 2.5:** Frequently used anions of ionic liquids

But there are several limits of IL, for example the high energy requirement for recycling and high price for synthesis; that can affect the commercial feasibilities in a few possible processes. These disadvantages can be overcome by using ionic liquid membrane (ILM) technology. It is made up of permeates and feed parts detached by the membrane comprising IL, that allows stripping and simultaneous extraction at individual side of the ILM. IL can become stable by either quasi-solidification it to

endow material with decent mechanical strength or infusing it into the pores of the membrane. ILM techniques need considerably a less amount of IL as carrier and do not involve extra stages for IL's recovering. As a result, ILMs have various benefits, such as low investment and operational costs, low energy requirements, easy fabrication of compact and flexible devices, etc. Moreover, because of the unique properties of IL, for example its high viscosity and negligible vapor pressure; ILMs are steadier in contrast with traditional SLMs based on organic solvents (Teramoto et al., 2000; Ito et al., 2001; Happel et al., 2003; Yang et al., 2003; Al Marzouqi et al., 2005; Néouze et al., 2006; Poliwoda et al., 2007; Kocherginsky et al., 2007; Schmidt et al., 2008; Krull et al., 2008; Che et al., 2008; Tan et al., 2009; Ebner & Ritter, 2009; Luis et al., 2012). For that reason, ILMs illustrate encouraging application prospective. For the last ten years, several researchers have described that ILMs were employed to execute the split-up of different compounds (e.g. aromatic hydrocarbons (Miyako et al., 2003a; Basheer et al., 2008), esters (de los Ríos et al., 2007; Li et al., 2009), alcohols (Branco et al., 2002a; Fortunato et al., 2005a; Izak et al., 2008; Izák et al., 2009; Heitmann et al., 2012), organic acid (Marták & Schlosser, 2006; Fontanals et al., 2009; Kouki et al., 2010; Blahušiak et al., 2011), and gases (Cserjesi et al., 2009; Yoo et al., 2010; Adibi et al., 2011; Lemus et al., 2011; Kim et al., 2011; Iarikov et al., 2011; Gonzalez-Miquel et al., 2011; Gan et al., 2011a; Gupta et al., 2012; Ren et al., 2012; Kasahara et al., 2012a; Gupta et al., 2013; Chai et al., 2014), to formulate progressive electrochemical devices (e.g. lithium batteries (Shin et al., 2005; Fernicola et al., 2009), solar cells (Kato et al., 2006; Kato & Hayase, 2007) and fuel cells (Lee et al., 2010a; Lee et al., 2010b) to facilitate catalytic reactions (Liu et al., 2005b), etc.

Amid all these applications, numerous publications which relates to the split-up of numerous compounds shows that investigation in this area is rising intensely. The

growth in gas separation studies, exclusively the CO<sub>2</sub> separation have been highlighted in much detail. For instance, Dai et al. (2016) shows the latest development in CO<sub>2</sub> separation membranes based on ILs. Moreover, Lozano et al. (2011) have also provided fresh developments in SILMs. To get better separation of mixtures through ILMs, two vital necessities come up: the establishment of stable ILMs and a decent choice of the carrier that can endure the long-term process. This evaluation is mostly devoted to the current progress in ILM technology, which includes transport mechanisms, application of ILMs, stability and preparation methods. The compatibility between IL and support membrane/gel, preparation methods of ILMs, etc. on the stability of ILMs were emphasized and very detailed. New progress of ILMs in the separation of dissimilar chemical species such as mixed gases was deliberated as well.

### 2.8.1 Preparation methods of ILMs

By using the method of immobilization in IL, ILM can be largely separated into the subsequent types, i.e. supported ionic liquid membrane (SILM) and quasi-solidified ionic liquid membrane (QSILM). Figure 2.6 displays the two major techniques for employing ILs as membrane supporting agents.

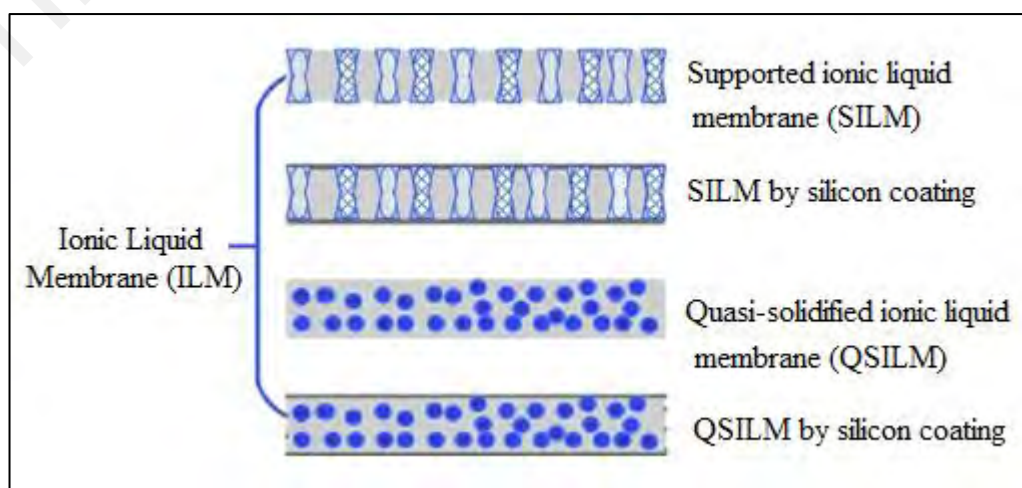


**Figure 2.6:** Two major approaches for utilizing ILs as membrane materials

### 2.8.2 Supported ionic liquid membranes (SILMs)

SILM is one of the three-phase liquid membrane systems whereby capillary forces embrace the IL in the pores of support material. The support material largely includes inorganic and polymeric membranes. As a whole, the preparation of SILM has three methods, i.e. direct immersion, vacuum and pressure that show a crucial part on the operating performance of SILM because of its rather high viscosity of IL.

With the method of direct immersion, IL's impregnation happens by soaking the membrane in the IL by using ambient pressure. Next, the leftover IL is then eliminated from the surface of the material either by wiping it softly with a tissue or leaving it to drip overnight. This is the easiest method as compared to the other two methods. This method has been used to prepare several SILMs (Miyako et al., 2003b; Matsumoto et al., 2005; Nosrati et al., 2011; Panigrahi et al., 2013). For example, Miyako et al. (2003b) have stated that a SILM was acquired by dipping a hydrophobic PP film into [bmim] [PF<sub>6</sub>]. Several SILMs were obtained by soaking a hydrophilic PVDF membrane in six phosphonium based ILs; (Matsumoto et al., 2005). Nosrati et al. (2011) revealed that SILMs were primed by infusing a pure ILs, i.e. eight imidazolium-, one ammonium and one phosphonium-based ILs into the pores of the different membranes (i.e. Mitex, Durapore, Fluoropore). In the case of organic compounds, the SILMs that was prepared with this technique are usually appropriate for transport experimentations (Miyako et al., 2003b; Matsumoto et al., 2005; Nosrati et al., 2011; Panigrahi et al., 2013).

For the method using vacuum, the SILMs can be attained by using these steps. First, the support material is positioned inside a tight vacuum chamber for duration of period to eliminate air from the material's pores. Then, while keeping vacuum in the chamber; IL is spread out at the membrane's surface. Lastly, the IL's excess on membrane's

surface ought to be removed. Using this method, some ceramic nanofiltration (NF) and polymeric membranes have been utilized as support materials to restrain IL (Coelho et al., 2000; Branco et al., 2002a, b; Fortunato et al., 2004; Fortunato et al., 2005b; Izak et al., 2006; Kulkarni et al., 2012). Case in point, Fortunato et al. (2004) have arranged SILMs using four hydrophilic membranes with identical nominal pore size, i.e. PES, nylon, PVDF and PP as support membranes and two ILs, i.e. [omim] [PF<sub>6</sub>] and [bmim] [PF<sub>6</sub>] as liquid phases. They all establish that the quantity of impregnated IL declined with an upsurge in IL's viscosity. This is due to the reduction of capillary force. For organic mixtures' separation, the SILMs that were arranged via this technique can be applied for the pervaporation experiments under lesser pressure.

Meanwhile on the pressure technique, the IL's impregnation is done as per follows: (1) putting the material in an ultrafiltration unit, (2) adding a quantity of IL in the unit, (3) putting on a certain nitrogen pressure to force the IL to flow into the material's pores, (4) discharging the pressure as soon as a thin layer of IL is can be seen on the membrane's surface, and (5) getting rid of the IL's surplus on the surface of the membrane with the similar approach as the final stage of direct immersion technique. The quantity of IL that was infused by using this technique is expected to be related to the IL. For instance, SILMs with [bmim] [NTf<sub>2</sub>], [bmim] [BF<sub>4</sub>] or [bmim] [Cl] supported in Nylon organic membrane was primed using pressure technique (Hernández-Fernández et al., 2007), and the resultant SILMs have established that the support material's pores was entirely occupied with apiece of the ILs. The SILMs prepared via this technique could then be applied for the pervaporation experiments even in pressures that are higher (Fortunato et al., 2005a; Gan et al., 2006; de los Rios et al., 2007; Hernández-Fernández et al., 2009a).

### 2.8.3 Stability of ILMs

ILs has several good features, such as tunability of properties, higher viscosity and negligible vapor pressure, through the alteration of cation and anion. As a result, ILM shows huge prospective as a substitute to the traditional SLM in separation processes since ILM technique allows the benefits of negligible loss of IL and high selectivity as liquid phase under a cross-membrane pressure gradient (Takeuchi et al., 1987; Peng et al., 2007; Izák et al., 2008; Hanioka et al., 2008; Bara et al., 2008; Scovazzo et al., 2009; Raeissi & Peters, 2009; Neves et al., 2009; Bara et al., 2009a; Bara et al., 2009b; Han & Row, 2010).

#### 2.8.3.1 Stability of SILMs

For SILM's situation, its stability is mostly influenced by the interfacial tension between the aqueous and membrane, compatibility between IL and support membrane, preparation method of SILM, along with support membrane and IL's properties, etc. (Chiarizia, 1991; Zha et al., 1995; Yang & Fane, 1997). The support membrane's properties such as porosity, pore size or type; have a crucial factor in the SILMs stability. For the support membrane's type, a minor increase of [bmim] [PF<sub>6</sub>] concentration in the aqueous phase was observed for the SILM with nylon membrane (Ropel et al., 2005). However, the concentration of [bmim] [PF<sub>6</sub>] is persistent for the SILMs with PES, PVDF or PP. SILMs with a hydrophobic membrane are more established compared to hydrophilic membrane due to a likely fragile contact between the hydrophobic IL and hydrophilic support membrane (Ropel et al., 2005; Neves et al., 2010). Besides, the IL loss of SILMs can be largely credited to IL migration from the large pores and membrane compression (Zhao et al., 2012). Consequently, the SILMs system can put up with a reasonably high transmembrane pressure by selecting a,

appropriate support membrane's pore size (Close et al., 2012). For support membrane's porosity, high porosity is usually encouraging due to it can holding up the IL under hydrostatic pressure that causes an increase in stability. Excessive transport effectiveness can also be done by having more surface area. The IL's properties can be tailor-made to a detailed use by altering either the anion or the cation in IL. As a result, the appropriate choice of ILs can significantly upsurge SILMs stability. Other than surface tension and hydrophobicity, the viscosity of IL shows an essential role in SILM's stability. ILs with great viscosity is not able to be removed that easy from the pores under a cross-membrane pressure difference, as they are restrained by large Van der Waals forces (S. Kislik, 2010; Matsumoto et al., 2010). However, ILs with low viscosity was easier to be detached from the support's pores. One of the major issues for the stability of the membrane is the preparation method of SILM. Hernandez Fernandez and coworker (2009), discovered that the losses of ILs normally enlarged by an increase in viscosity of IL immobilized inside the support membrane's pores with vacuum method. The central issue is because lesser ILs are impregnating in the support material's inner layers, because of greater capillary force for more viscous ILs. This can be largely be credited on ILs with high viscosity that is generally immobilized on the furthestmost support membrane's external layer using the vacuum method, and therefore are simply moved into the aqueous phase during this process. Though, the highest stability of SILMs can be achieved by the pressure method; and a slight loss of IL was seen even after an operation that lasts for 7 days. Besides, the extent of IL was perhaps liberated of the IL when impregnation was being done under pressure (Hernandez-Fernandez et al., 2009). Subsequently, the methods of vacuum and direct immersion are proper for the low-viscosity ILs; in order for all the support's pores are filled with ILs to achieve the stable SILMs. Meanwhile for the high-viscosity ILs, pressure method is favored. Also, the compatibility between support membrane and IL has an effect on the

states of the ILs in the support pores. The electrostatic contact between the charged functional group on the support membrane's surface and organic cations in ILs affects the SILMs stable performance (Fortunato et al., 2004). This is primarily caused by the organic cations in ILs have distinctive charge distribution, polarity and molecular structure throughout the imidazolium ring. Additionally, the interfacial strain that is present between membrane and aqueous phase; the water microenvironments inside the IL phase of SILM which establishes a non-selective environment for solute transport, could be shaped during the aqueous solution's transport due to the IL's water solubility (Fortunato et al., 2005a; Matsumoto et al., 2007). The outcome is the deteriorating performance of SILM and also a loss of IL from SILM because of the reduction in viscosity.

#### **2.8.4 Application of ILMs for gas separation**

The separations of CO<sub>2</sub> from industrial gas mixtures have garnered attention all over the world, because of the problem of global warming. This is because of the contact between the electrical charge of IL and quadrupole moment of CO<sub>2</sub> delivers an improvement in the solubility over other gases (Bara et al., 2009c; Bara et al., 2010), ILMs have demonstrated as a good option for the selective separation of CO<sub>2</sub> from gas mixtures; such as He, H<sub>2</sub>, CH<sub>4</sub> and N<sub>2</sub>. A few investigators have expansively explored several causes that affects the CO<sub>2</sub> separation performance of ILMs such as pressure, temperature, nature of the support membrane, plasticization behavior and water content (Scovazzo et al., 2002; Scovazzo et al., 2004a; Scovazzo et al., 2004b; Baltus et al., 2005; Bounaceur et al., 2006; Ilconich et al., 2007; Ho et al., 2008; Hanioka et al., 2008; Myers et al., 2008; Scovazzo et al., 2009; Raeissi & Peters, 2009; Bara et al., 2009b; Zhao et al., 2010; Shi & Sorescu, 2010; Neves et al., 2010; Cserjési et al., 2010; Simons



et al., 2010; Barghi et al., 2010; Kreiter et al., 2011; Jansen et al., 2011; Jindaratsamee et al., 2012; Friess et al., 2012; Close et al., 2012; Kasahara et al., 2012b; Labropoulos et al., 2013; Banu et al., 2013; Tome et al., 2013; Cichowska-Kopczy et al., 2013; Wickramanayake et al., 2014; Tome et al., 2014; Shimoyama et al., 2014), confinement (Shi & Sorescu, 2010), alkyl chain lengths (Neves et al., 2010), anions (Scovazzo et al., 2004b; Scovazzo et al., 2002), cation structure Cichowska-Kopczy et al., 2013), ILs content (Jansen et al., 2011). Table 2.2 displays frequently used support membrane/gel and its resultant IL together with the application of ILM in the separation of gases.

**Table 2.2:** Use of ILMs in separation of gases

Application	IL	Support Membrane	Reference
Separation of CO <sub>2</sub> from N <sub>2</sub>	[APmim][NTf <sub>2</sub> ]	Tubular Al <sub>2</sub> O <sub>3</sub>	Kreiter et al., 2011
	[emim][Ac]	Porous Al <sub>2</sub> O <sub>3</sub> /TiO <sub>2</sub> tubes	Barghi et al., 2010
	[emim][Ac]	PVDF	Santos et al., 2014a
	[emim][B(CN) <sub>4</sub> ]	PTEE	Tome et al., 2014
	[emim][BF <sub>4</sub> ]	PVDF	Jindaratsamee et al., 2011
	[emim][C(CN) <sub>3</sub> ]	PTEE	Tome et al., 2014
	[emim][DCA]	PTEE	Tome et al., 2014
	[emim][ESO <sub>4</sub> ]	PTEE	Shahkaramipour et al., 2014
	[emim][Gly]	PTEE	Kasahara et al., 2012a
	[emim][MeSO <sub>4</sub> ]	PTEE	Tome et al., 2014
	[emim][NTf <sub>2</sub> ]	PES	Scovazzo et al., 2009
	[emim][NTf <sub>2</sub> ]	Al <sub>2</sub> O <sub>3</sub> -Anodisc	Close et al., 2012
	[emim][NTf <sub>2</sub> ]	PTEE	Kasahara et al., 2012b
	[emim][SCN]	PTEE	Tome et al., 2014
	[emim][TCM]	Silica nanoporous ceramic	Labropoulos et al., 2013
	[emim][TFA]	Al <sub>2</sub> O <sub>3</sub> -anodisc	Close et al., 2012

**Table 2.2:** Use of ILMs in separation of gases ‘Table 2.2, continued’

<b>Application</b>	<b>IL</b>	<b>Support Membrane</b>	<b>Reference</b>
Separation of CO <sub>2</sub> from N <sub>2</sub>	[bmim] [Ac]	PVDF	Santos et al., 2014a
	[bmim] [Ac]	Al <sub>2</sub> O <sub>3</sub> -anodisc	Close et al., 2012
	[bmim] [BETI]	PES	Scovazzo, 2009
	[bmim] [BF <sub>4</sub> ]	PVDF	Neves et al., 2010; Neves et al., 2009
	[bmim] [BF <sub>4</sub> ]	PES	Zhao et al., 2010
	[bmim] [DCA]	PVDF	Neves et al., 2009
	[bmim][NTf <sub>2</sub> ]	PTEE	Shimoyama et al., 2014
	[bmim][NTf <sub>2</sub> ]	PVDF	Neves et al., 2009
	[bmim][NTf <sub>2</sub> ]	Al <sub>2</sub> O <sub>3</sub> -anodisc	Close et al., 2012
	[bmim] [TFO]	PVDF	Neves et al., 2009
	[bmim] [PF <sub>6</sub> ]	PTEE	Shimoyama et al., 2014
	[bmim] [PF <sub>6</sub> ]	PVDF	Neves et al., 2009
	[bmim] [TCM]	Silica nanoporous ceramic	Labropoulos et al., 2013
	[hmim] [NTf <sub>2</sub> ]	Al <sub>2</sub> O <sub>3</sub> -anodisc	Close et al., 2012
	[omim] [PF <sub>6</sub> ]	PVDF	Neves et al., 2010
	[C <sub>8</sub> F <sub>13</sub> mim] [NTf <sub>2</sub> ]	Al <sub>2</sub> O <sub>3</sub> -anodisc	Baltus et al., 2005
	[C <sub>10</sub> mim] [BF <sub>4</sub> ]	PVDF	Neves et al., 2010
	[P <sub>4444</sub> ] [Gly]	PTEE	Kasahara et al., 2012a
	[Vbtma] [Ac]	PVDF	Santos et al., 2014a
	[C <sub>3</sub> mim] [NTf <sub>2</sub> ]	PTEE	Kasahara et al., 2012b

**Table 2.2:** Use of ILMs in separation of gases ‘Table 2.2, continued’

<b>Application</b>	<b>IL</b>	<b>Support Membrane</b>	<b>Reference</b>
Separation of CO <sub>2</sub> from CH <sub>4</sub>	[emim] [B(CN) <sub>4</sub> ]	PTEE	Tome et al., 2014
	[emim] [BF <sub>4</sub> ]	PES	Scovazzo et al., 2009
	[emim] [C(CN) <sub>3</sub> ]	PTEE	Tome et al., 2014
	[emim] [CF <sub>3</sub> SO <sub>3</sub> ]	PES	Scovazzo et al., 2009
	[emim] [CF <sub>3</sub> SO <sub>3</sub> ]	PVDF	Scovazzo et al., 2009
	[emim] [DCA]	PES	Scovazzo et al., 2009
	[emim] [DCA]	PTEE	Tome et al., 2014
	[emim] [MeSO <sub>4</sub> ]	PTEE	Tome et al., 2014
	[emim] [NTf <sub>2</sub> ]	PES	Cichowska-Kopczy et al., 2013; Scovazzo et al., 2009
	[emim] [NTf <sub>2</sub> ]	PVDF	Cichowska-Kopczy et al., 2013
	[emim] [NTf <sub>2</sub> ]	PA	Cichowska-Kopczy et al., 2013
	[emim] [NTf <sub>2</sub> ]	PP	Cichowska-Kopczy et al., 2013
	[emim] [NTf <sub>2</sub> ]	PVDF	Baltus et al., 2005
	[emim] [NTf <sub>2</sub> ]	PA	Cichowska-Kopczy et al., 2013
	[emim] [NTf <sub>2</sub> ]	PP	Cichowska-Kopczy et al., 2013
	[emim] [NTf <sub>2</sub> ]	PVDF	Cichowska-Kopczy et al., 2013
	[emim] [SCN]	PTEE	Hanioka et al., 2008

**Table 2.2:** Use of ILMs in separation of gases ‘Table 2.2, continued’

<b>Application</b>	<b>IL</b>	<b>Support Membrane</b>	<b>Reference</b>
Separation of CO <sub>2</sub> from CH <sub>4</sub>	[C <sub>3</sub> NH <sub>2</sub> mim] [NTf <sub>2</sub> ]	PTEE	Hanioka et al., 2008
	[C <sub>3</sub> NH <sub>2</sub> mim] [CF <sub>3</sub> SO <sub>3</sub> ]	PTEE	Hanioka et al., 2008
	[bmim] [BF <sub>4</sub> ]	PVDF	Hanioka et al., 2008
	[bmim] [NTf <sub>2</sub> ]	PTEE	Hanioka et al., 2008
	[bmim] [NTf <sub>2</sub> ]	PVDF	Neves et al., 2010
	[bmim] [NTf <sub>2</sub> ]	PES	Cichowska-Kopczy et al., 2013
	[bmim] [NTf <sub>2</sub> ]	PVDF	Cichowska-Kopczy et al., 2013
	[bmim] [NTf <sub>2</sub> ]	PA	Cichowska-Kopczy et al., 2013
	[bmim] [NTf <sub>2</sub> ]	PP	Cichowska-Kopczy et al., 2013
	[bmim] [PF <sub>6</sub> ]	Al <sub>2</sub> O <sub>3</sub> -anodisc	Barghi et al., 2010
	[bmim] [PF <sub>6</sub> ]	PVDF	Neves et al., 2010
	[bmim] [TFO]	PES	Cichowska-Kopczy et al., 2013
	[bmim] [TFO]	PVDF	Cichowska-Kopczy et al., 2013
	[bmim] [TFO]	PA	Cichowska-Kopczy et al., 2013
	[bmim] [TFO]	PP	Cichowska-Kopczy et al., 2013
	[hmim] [NTf <sub>2</sub> ]	PES	Jindaratamee et al., 2012
	[omim] [PF <sub>6</sub> ]	PVDF	Neves et al., 2010

**Table 2.2:** Use of ILMs in separation of gases ‘Table 2.2, continued’

Application	IL	Support Membrane	Reference
	[C <sub>10</sub> mim] [BF <sub>4</sub> ]	PVDF	Neves et al., 2010
	h[mim] <sub>2</sub> [NTf <sub>2</sub> ] <sub>2</sub>	Alumina NF	Shahkaramipour et al., 2014
	pr[mim] <sub>2</sub> [NTf <sub>2</sub> ] <sub>2</sub>	Alumina NF	Shahkaramipour et al., 2014
	Styrene-based IL	PES	Simons et al., 2010
Separation of biohydrogen from CO <sub>2</sub> and N <sub>2</sub>	[C <sub>3</sub> NH <sub>2</sub> mim] [CF <sub>3</sub> SO <sub>3</sub> ]	PVDF	Neves et al., 2009
Separation of CO <sub>2</sub> from He	[hmim] [NTf <sub>2</sub> ]	PS	Ilconich et al., 2007
Separation of CO <sub>2</sub> from CO	[simmim] [PF <sub>6</sub> ]	g-alumina NF	Vangeli et al., 2010
Separation of CO <sub>2</sub> from CH <sub>4</sub> , N <sub>2</sub> and H <sub>2</sub>	[emim] [TFSI]	P(VDF-HFP)	Friess et al., 2012; Jansen et al., 2013
Separation of CO <sub>2</sub> from CH <sub>4</sub> and N <sub>2</sub>	[emim] [Ac]	PVDF	Tome et al., 2013
Separation of CO <sub>2</sub> from gaseous mixtures of CH <sub>4</sub> , O <sub>2</sub> and N <sub>2</sub>	[emim] [DCA]	PVDF	Tome et al., 2013
	[emim] [Lac]	PVDF	Tome et al., 2013
	[emim] [NTf <sub>2</sub> ]	PVDF	Tome et al., 2013
	[emim] [SCN]	PVDF	Tome et al., 2013
	[hmim] [NTf <sub>2</sub> ]	PES	Bara et al., 2009b
	[omim] [NTf <sub>2</sub> ]	PES	Bara et al., 2009b
Separation of SO <sub>2</sub> from air	[mim] [Ac]	PVDF	Luis et al., 2009b
	[bim] [Ac]	PVDF	Luis et al., 2009b

**Table 2.2:** Use of ILMs in separation of gases ‘Table 2.2, continued’

<b>Application</b>	<b>IL</b>	<b>Support Membrane</b>	<b>Reference</b>
Separation of SO <sub>2</sub> from N <sub>2</sub>	[N <sub>2224</sub> ] [acetate]	PES	Huang et al., 2014
	[N <sub>2224</sub> ] [diglutarate]	PES	Huang et al., 2014
	[N <sub>2224</sub> ] <sub>2</sub> [dimalate]	PES	Huang et al., 2014
	[N <sub>2224</sub> ] [dimalonate]	PES	Huang et al., 2014
	[N <sub>2224</sub> ] <sub>2</sub> [maleate]	PES	Huang et al., 2014
	[N <sub>2224</sub> ] <sub>2</sub> [malonate]	PES	Huang et al., 2014
	[N <sub>2224</sub> ] [NTf <sub>2</sub> ]	PES	Huang et al., 2014
	[N <sub>2224</sub> ] [propionate]	PES	Huang et al., 2014
Separation of SO <sub>2</sub> from CH <sub>4</sub>	[emim] [BF <sub>4</sub> ]	PES	Jiang et al., 2007
	[bmim] [BF <sub>4</sub> ]	PES	Jiang et al., 2007
	[bmim] [PF <sub>6</sub> ]	PES	Jiang et al., 2007
	[bmim] [NTf <sub>2</sub> ]	PES	Jiang et al., 2007
	[N <sub>2224</sub> ] [acetate]	PES	Huang et al., 2014
	[N <sub>2224</sub> ] [dimalonate]	PES	Huang et al., 2014
	[N <sub>2224</sub> ] <sub>2</sub> [dimalate]	PES	Huang et al., 2014
	[N <sub>2224</sub> ] <sub>2</sub> [maleate]	PES	Huang et al., 2014
	[N <sub>2224</sub> ] <sub>2</sub> [malonate]	PES	Huang et al., 2014
	[N <sub>2224</sub> ] [NTf <sub>2</sub> ]	PES	Huang et al., 2014
	[N <sub>2224</sub> ] [propionate]	PES	Huang et al., 2014
Separation of H <sub>2</sub> S from CH <sub>4</sub>	[bmim] [BF <sub>4</sub> ]	PVDF	Park et al., 2009

## 2.8.5 Transport mechanisms through ILMs

### 2.8.5.1 Transport mechanism of gases through membranes

The mechanism of transport of gases through ILMs is tremendously vital and was researched by several groups for the past several years (Gan et al., 2006; Hanioka et al., 2008; Barghi et al., 2010; Santos et al., 2014b). It is thought that the transport of gas through a dense liquid membrane happens as per the mass transfer mechanism of solution-diffusion. Normally, a gas molecule is transported across an ILM with these steps: (1) absorption in the ILM's upstream surface, (2) diffusion across the matrix of the ILM, and (3) desorption in the ILM's downstream face.

The difference in pressure between the permeate side and the feed side, is the main force of a gas molecule going across the membrane. The steady-state flux of gas  $i$  through the membrane ( $J_{g,i}$ ) can be determined by the pressure difference across the membrane ( $\Delta p_{g,i}$ ) the membrane's thickness ( $l$ ) and the gas permeability ( $P_{g,i}$ ), as per the equation below:

$$J_{g,i} = \frac{P_{g,i} \Delta p_{g,i}}{l} \quad (2.14)$$

The best gas permeability through an ILM is linked to the diffusivity data and gas solubility of the ILs:

$$P_{g,i} = S_i D_i \quad (2.15)$$

Consequently, the selectivity ( $a_{ij}$ ) which is ideal is considered by taking the ratio of the ideal gas permeabilities for a given gas pair ( $i$  and  $j$ ):

$$a_{i,j} = \frac{P_{g,i}}{P_{g,j}} = \frac{S_i D_i}{S_j D_j} \quad (2.16)$$

The selectivities which are ideal in Eqn. (2.16) are caused by the variances in the physical solubility of the gases in the IL. The calculation for solubility coefficient of gas in IL phase is using Eqn. (2.17):

$$S_i = \frac{C_{g,i}}{p_{g,i}} \quad (2.17)$$

At low pressures,  $C_{g,i}$  can be calculated using pure IL molecular weight  $M_W$  and pure IL density  $p_{IL}$ :

$$C_{g,i} = x_i \frac{p_{IL}}{M_W} \quad (2.18)$$

where  $x_i$  is mole fraction of dissolved gas in IL phase. Because of the low gas solubility in ILs at low pressures, the mole fraction of dissolved gas in IL is roughly equal to zero.

As a result, Henry's law can be described as per below:

$$H_i = \lim_{x_i \rightarrow 0} \frac{\hat{f}_i}{x_i} \quad (2.19)$$

Substitution Eqns. (2.17)-(2.18) into Eqn. (2.15) yields Eqn. (2.20):

$$P_{g,i} = \frac{D_i p_{IL}}{H_i M_W} \quad (2.20)$$



## 2.9 COSMO-RS for ionic liquids (ILs) screening

The technique being used as contributed by the group, several researchers have made numerous efforts to predict and model CO<sub>2</sub> solubility in a particular number of ILs (Kim et al., 2005); together with the theory of regular solution (Scovazzo et al., 2004a; Kilaru et al., 2008; Finotello et al., 2008), Monte Carlo (Shah & Maginn, 2005) simulations, Molecular Dynamics (MD) (Shi & Maginn, 2008; Kerle et al., 2009;) Conductor-like Screening Model for Real Solvents (COSMO-RS) method (Marsh et al., 2004), equation of state (Kroon et al., 2006) and Quantitative Structure Property Relationship (QSPR) method (Eike et al., 2004).

COSMO-RS has been thought to be appropriate for fast screening of multiple novel solvents, based on all the methods mentioned. This is due to its having no requirements for any group-specific or compound interaction parameters. Moreover, it was discovered to be valuable in predicting gases solubilities qualitatively by numerous researches (Zhang et al., 2008b; Miller et al., 2009; Maiti, 2009; Ab Manan et al., 2009; Palomar et al., 2011; Gonzalez-Miquel et al., 2011). This is as a result of comparing Henry's Law constants for CO<sub>2</sub> in different ILs with values that are experimental (Marsh et al., 2004; Zhang et al., 2008b; Ab Manan et al., 2009; Palomar et al., 2011; Gonzalez-Miquel et al., 2011). Whereas, ILs screening for CO<sub>2</sub> capture was completed by using a pool of 224 ILs by (Gonzalez-Miquel et al., 2011), 170 ILs by (Palomar et al., 2011) and 408 ILs by (Zhang et al., 2008b), respectively. These processes were done as per COSMO-RS prediction of Henry's Law constants of CO<sub>2</sub> (Palomar et al., 2011; Zhang et al., 2008b) and N<sub>2</sub> (Gonzalez-Miquel et al., 2011), at 298.15 K. When joined, the equation of state and COSMO-RS approaches was positively established (Maiti, 2009) their accuracy for CO<sub>2</sub> screening and solubility prediction at T, from 293.15 to

333.15 K, and arriving at its critical pressure. Besides, anions having bromine (Palomar et al., 2011) and fluorine (Zhang et al., 2008b; Maiti, 2009; Palomar et al., 2011); together with phosphonium and guanidinium-based cations (Maiti, 2009) have shown highly CO<sub>2</sub> absorptive capacities. This feature can be associated on a molecular level with potent vdW interaction with IL (Palomar et al., 2011), and higher exothermicity afterwards. Additionally, ILs with thiocyanate anions have shown selectivity as vdW interactions are improved, better selectivity for CO<sub>2</sub>/N<sub>2</sub>, that prefers CO<sub>2</sub> while displaying nearly zero affinity for N<sub>2</sub> (Gonzalez-Miquel et al., 2011). In addition, (Shimoyama & Ito, 2010) have used the COSMO-SAC model (Lin & Sandler, 2002) to predict CO<sub>2</sub> permeabilities, selectivities and solubilities, more precisely in ILs having imidazolium cations.

## **2.10 Physical versus chemical absorption**

The theory of solution-diffusion, describes that the most effective ILs dissolve the biggest amount of CO<sub>2</sub>, but it bind gas molecules weakly. By heating or applying a vacuum to it, the absorbed gas molecules can be readily desorbed from the ILs. This permits the ILs to be used again a number of times for consecutive absorption/desorption cycles without loss of capability.

This put forward the benefit of physisorption over chemisorption (Mahurin et al., 2012). Chemical absorption occurs in ILs that comprise a considerably basic group, such as a carboxylate anion (Gurau et al., 2011), a superbasic moiety (Wang et al., 2010a) or an amino group (Bates et al., 2002). Even though these ILs are efficient in CO<sub>2</sub> capture, only several instances of SILMs made with such ILs are recognized

(Myers et al., 2008; Hanioka et al., 2008). This is due to the difficulty in releasing gas. Inter alia is the center of physical dissolution, the interactions of various polar moieties with the gas molecules of the ILs. From previous works, there are three dissimilar thoughts as to what sort of process the absorption of gas molecules into ionic liquid. These thoughts are:

- i. Chemical process (e.g. [bmim] [BTA], [bmim] [BF<sub>4</sub>], [bmim] [BF<sub>4</sub>], [TMG] [BF<sub>4</sub>], [TMG] [BTA]) (Shiflett & Yokozeki, 2010)
- ii. Combination of a physical and chemical process (e.g. [TMG] L and [MEA] L) (Ren et al., 2010)
- iii. Physical process ([bmim] [Ac] and [bmim] [SO<sub>4</sub>]) (Huang et al., 2006; Ren et al., 2010)

## 2.11 Summary

A lot of attention and publications was provided by the engineering communities that relates to the use of ILs in SILMs for CO<sub>2</sub> gas separations. This shows that research in this field has developed tremendously over the past ten years. For that reason, it is thought that the use of SILMs and solvents that have good selectivity on capturing CO<sub>2</sub> from flue gases would have countless potential to substitute traditional absorption method. In spite of the speedy expansion of SILMs in the last few years, there are still areas that can be improved further. This is true, especially in its application for the CO<sub>2</sub> absorption process in membrane contactor system with solvent that uses MEA. On the other hand, this usually good solvent for carbon dioxide capture needs to go through degradation because of the presence of oxygen. Therefore, studies must be conducted to overcome the challenges related to the tendency of SILMs for selective CO<sub>2</sub> absorption. The prevention of MEA oxidation degradation is the result of it, and to find a method that would display great CO<sub>2</sub> performances and an improved CO<sub>2</sub>/O<sub>2</sub> selectivity. In

addition, researches needs to done at the role of viscosity in the preparation of SILMs, its chemical resistance in interaction with the surrounding phases, stability of the liquid inside the membrane's and long-term operation of the membrane.

University of Malaya

## CHAPTER 3: MATERIALS AND METHODS

Supported imidazolium-based ionic liquids membranes as a contactor for the selective absorption of CO<sub>2</sub> by aqueous monoethanolamine

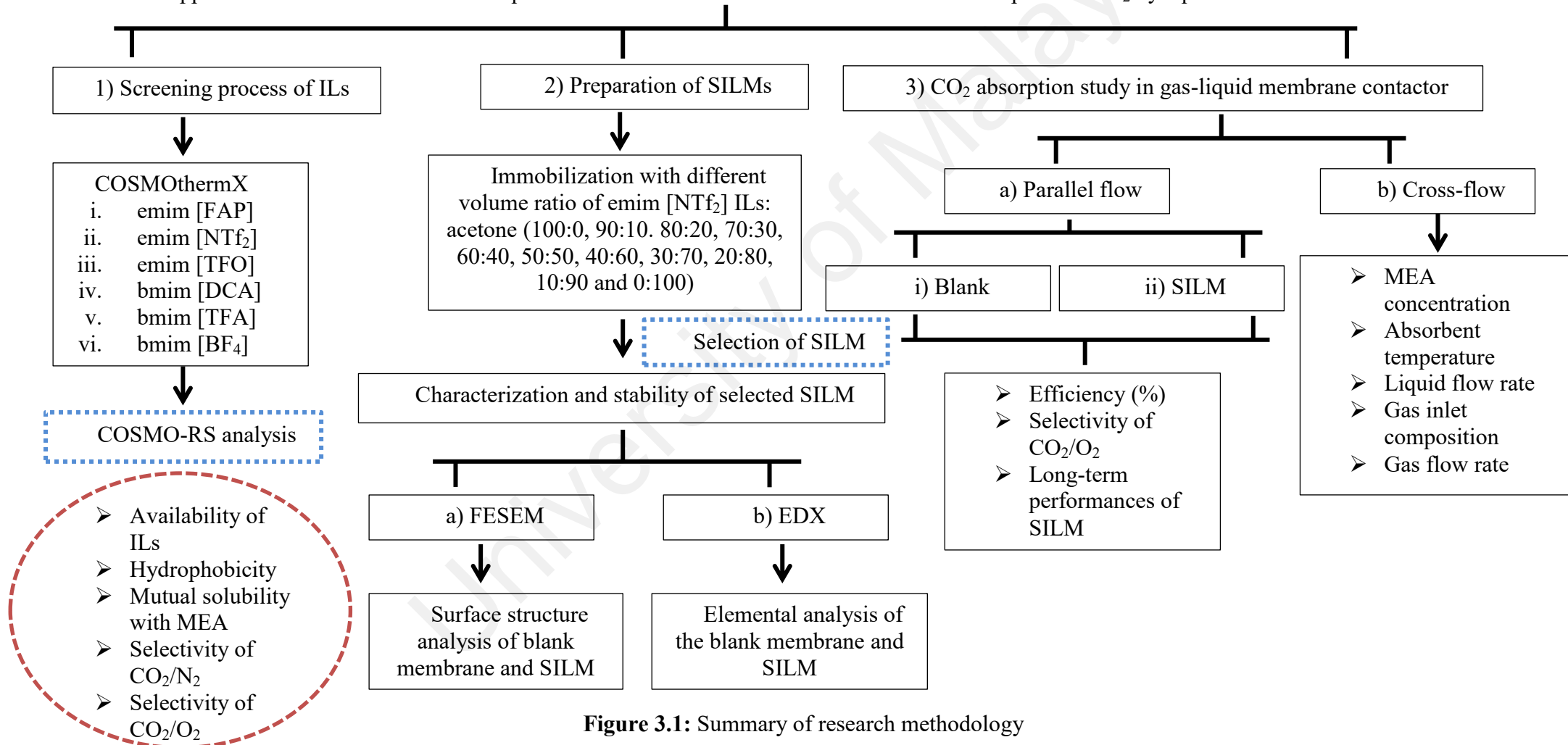
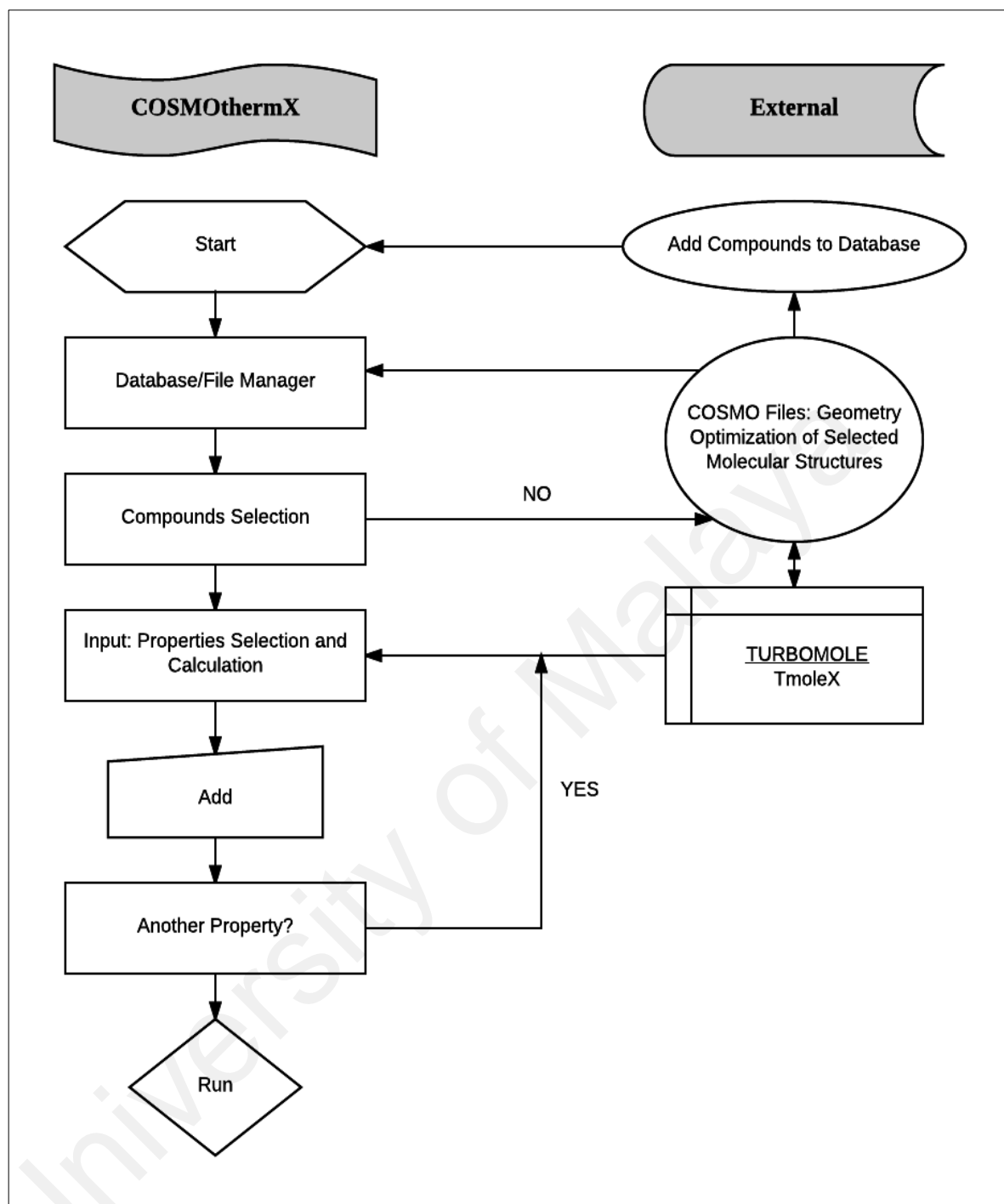


Figure 3.1: Summary of research methodology

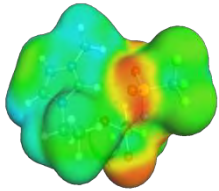
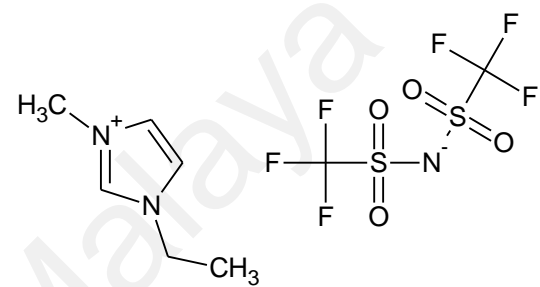
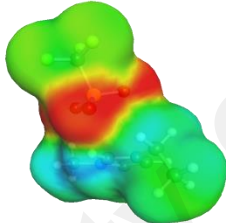
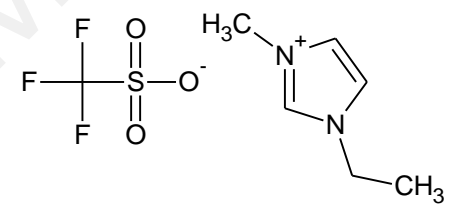
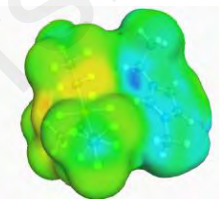
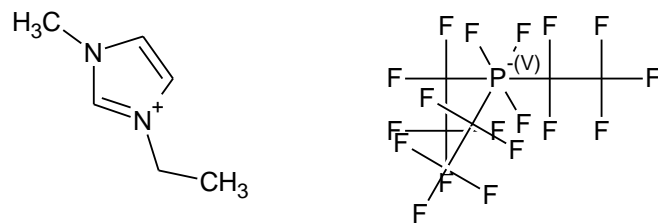
### 3.1 Screening of ionic liquids (ILs) using COSMO-RS analysis

TmoleX software package was used for the drawing and geometry optimization of the cation, anion, water, and monoethanolamine's structure. Hartree-Fock theory was implemented for the geometry optimization with the 6-31G\* elementary set. The use of Hartree-Fock level for geometry optimization calculation produces more precise values, whereas the (\*) denotes the polarization result of the species (Hizaddin et al., 2014). Applying the optimized geometry for specific compounds activates the *.cosmo file* generation through density functional theory (DFT) with the 6-31G\* basic set, which then enables the execution of a single point computation. Then, the *.cosmo file*, along with parameterization file BP\_TZVP\_C30\_1301.ctd, was introduced into the COSMOthermX software package (COSMOthermX, 2013) to attain the Henry's Law, the selectivity of gases pair,  $\sigma$ -potential of the specific elements, and the calculation of activity coefficients of the ILs-water and ILs-MEA binary mixtures. Moreover, a pseudo binary method was implemented into the COSMOthermX software for the estimation of the mixture comprise of ILs-water and ILs-MEA, by which the cation and anion of the ILs were loaded as discrete compounds with similar mole fraction. In this work, 1-ethyl-3-methylimidazolium bis (trifluoromethylsulfonyl) imide [emim] [NTf<sub>2</sub>], 1-ethyl-3-methylimidazolium trifluoromethanesulfonate [emim] [TFO], 1-ethyl-3-methylimidazolium tris(perfluoroethyl)trifluorophosphate [emim] [FAP], 1-butyl-3-methylimidazolium dicyanamide [bmim] [DCA], 1-butyl-3-methyl-imidazolium-trifluoroacetate ionic liquid [bmim] [TFA] and 1-butyl-3-methylimidazolium tetrafluoroborate [bmim] [BF<sub>4</sub>] were selected for the screening process (Table 3.1). The procedure of property calculation using COSMOthermX software was summarized in Figure 3.1.



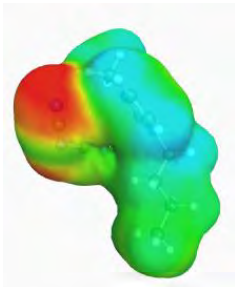
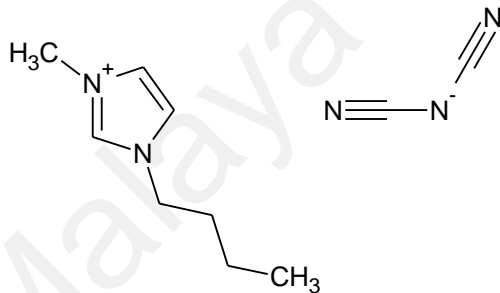
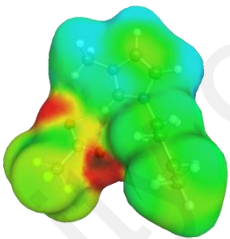
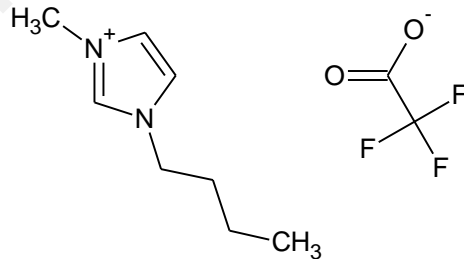
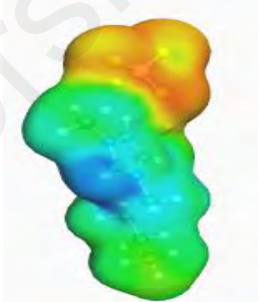
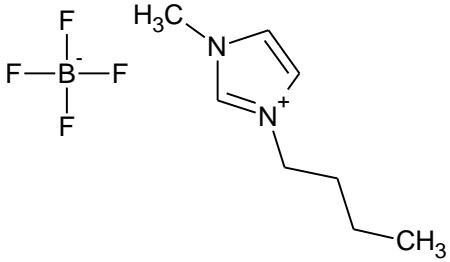
**Figure. 3.2:** Flowchart of property calculation with the COSMOthermX (Adapted from COSMOthermX, 2013)

**Table 3.1:** The sample provenance table for the compounds system

IUPAC name		Molecular structure
1-ethyl-3-methylimidazolium bis (trifluoromethylsulfonyl) imide [emim] [NTf <sub>2</sub> ]  C <sub>8</sub> H <sub>11</sub> F <sub>6</sub> N <sub>3</sub> O <sub>4</sub> S <sub>2</sub>		
1-ethyl-3-methylimidazolium trifluoromethanesulfonate [emim] [TFO]  C <sub>7</sub> H <sub>11</sub> F <sub>3</sub> N <sub>2</sub> O <sub>3</sub> S		
1-ethyl-3-methylimidazolium tris(perfluoroethyl)trifluorophosphate [emim] [FAP]  C <sub>12</sub> H <sub>11</sub> F <sub>18</sub> N <sub>2</sub> P		



**Table 3.1:** The sample provenance table for the compounds system ‘Table 3.1, continued’

IUPAC name		Molecular structure
1-butyl-3-methylimidazolium dicyanamide [bmim] [DCA]  $C_{10}H_{15}N_5$		
1-butyl-3-methyl-imidazolium trifluoroacetate [bmim] [TFA]  $C_{10}H_{15}F_3N_2O_2$		
1-butyl-3-methylimidazolium tetrafluoroborate [bmim] [BF <sub>4</sub> ]  $C_8H_{15}BF_4N_2$		

## 3.2 Preparation of supported ionic liquid membranes (SILMs)

### 3.2.1 Materials

1-ethyl-3-methylimidazolium bis (trifluoromethylsulfonyl) imide [emim] [NTf<sub>2</sub>] IL (hydrophobic) with a molecular weight of 391.31 g/mol, monoethanolamine (MEA) and acetone were purchased and used with the highest purity level available (Merck, Germany). A commercial polypropylene (PP) hollow fiber membrane (Seawell Industrial Limited, China) served as a membrane support in this research. Specifications of the [emim] [NTf<sub>2</sub>] as an ionic liquid supporting phase, hollow fiber membrane and molecular structures of [emim] [NTf<sub>2</sub>], acetone and monoethanolamine are displayed in Table 3.2, Table 3.3 and Figure 3.3, respectively.

**Table 3.2:** Specifications of the [emim] [NTf<sub>2</sub>] IL (hydrophobic)

Purity (High Performance Liquid Chromatography)	≥ 98.0%
Halides (Ion Chromatography)	≤ 0.1%
Water (Karl Fischer)	≥ 1.0%
Melting point (°C)	-15

**Table 3.3:** Characteristics of hydrophobic PP hollow fiber membrane

Parameter	Value
Fiber o.d. $d_o$ (m)	$3 \times 10^{-4}$
Fiber i.d. $d_i$ (m)	$2.4 \times 10^{-4}$
Membrane pore diameter, $d_p$ (μm)	0.03
Porosity (%)	40

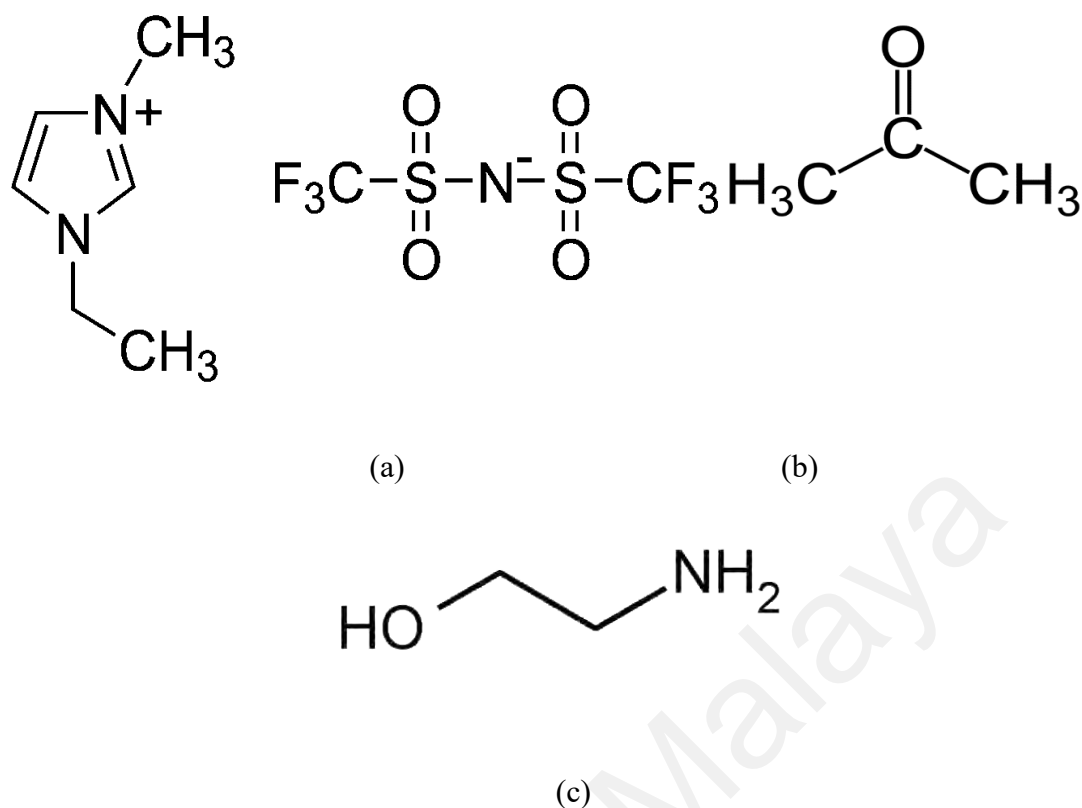


**Figure 3.3:** Molecular structures of [emim] [NTf<sub>2</sub>] IL, acetone, and monoethanolamine (MEA)

### 3.2.2 Supported ionic liquid membranes (SILMs) preparation

Different amount of IL and acetone were blended with different volume ratios of [emim] [NTf<sub>2</sub>] IL: acetone; 100:0 (S1), 90:10 (S2), 80:20 (S3), 70:30 (S4), 60:40 (S5), 50:50 (S6), 40:60 (S7), 30:70 (S8), 20:80 (S9), 10:90 (S10) and 0:100 (S11) at 30°C. Using VT550 rotary viscometer (HAAKE, Germany) and RE50 refractometer (Mettler Toledo, USA), measurements are made on viscosity and refractive index (RI) of binary mixtures respectively. 11 types of SILMs were then prepared via immobilization process of the binary mixtures onto the hollow fiber membranes. The duration of this process was set up to run for 24 hours to provide enough time for the IL's diffusion into the membrane structure, and for it to thoroughly dry over 1-2 days in dry air for acetone removal. The weights of all the membranes prepared were measured before and after impregnation, to measure the loading of immobilized IL in the supporting membrane.

### 3.3 SILMs characterization and stability

The surface structure and elemental analysis of SILMs were determined using a field emission scanning electron microscope (FESEM) AURIGA cross beam workstation (Carl Zeiss, Germany), that was equipped with EDAX (AMETEK, advanced microanalysis solutions) at an accelerating voltage of 1.5 kV. Meanwhile, the measurement of the individual pore diameters was determined from the enlarged micrographs using a computer program called “Gatan: Digital Micrograph”. Furthermore, the EDX analysis was also used to examine the elemental loss, after the membranes were submerged into pure MEA and 2M MEA solutions individually for 14 consecutive days at a temperature of 70°C.

### 3.4 CO<sub>2</sub> absorption study in a gas-liquid membrane contactor system

Figure 3.4 shows the schematic diagram of CO<sub>2</sub> absorption process using a prepared [emim] [NTf<sub>2</sub>]-SILMs gas-liquid membrane contactor (Figure 3.4(a) and (b)) and various composition range of flue gas. In preparation of the aqueous MEA solution, MEA of 99.5% purity level was dissolved in deionized water. The gas and liquid circulated in opposite directions over the module, with the absorbent passing through the shell side, while the gas also circulated countercurrently through the lumen side of the hollow fibers. In the experiments, the introduction of gas mixtures into the process from compressed gas containers and the adjustment of the flow rates using mass flow controller (GFC17, Aalborg, Aalborg Instrument and Control, Inc.) was made, which allows for an accurate control on the gas flow rate. After being channeled through a pressure gauge, the gas mixtures flowed into the membrane module from the lumen side. An analysis of the inlet and outlet gas compositions was analyzed using CO<sub>2</sub> analyzer (Guardian, Edinburgh Instrument Ltd.). A vessel that had been submerged in a

water bath was provided, in order to keep the absorbent solution. The control of the absorbent solution temperature was made by adjusting the temperature of the water bath. Moreover, in order to drive the absorbent into the shell side of the membranes from the absorbent solution vessel with a controlled liquid flow rate, a pump drive (PD5201, Heidolph Instruments GmbH & Co. KG, Germany) was used. Through the application of chemical titration method and the use of oxygen meter, the outlet concentration of CO<sub>2</sub> and O<sub>2</sub> in a liquid absorbent from the membrane contactor were measured respectively.

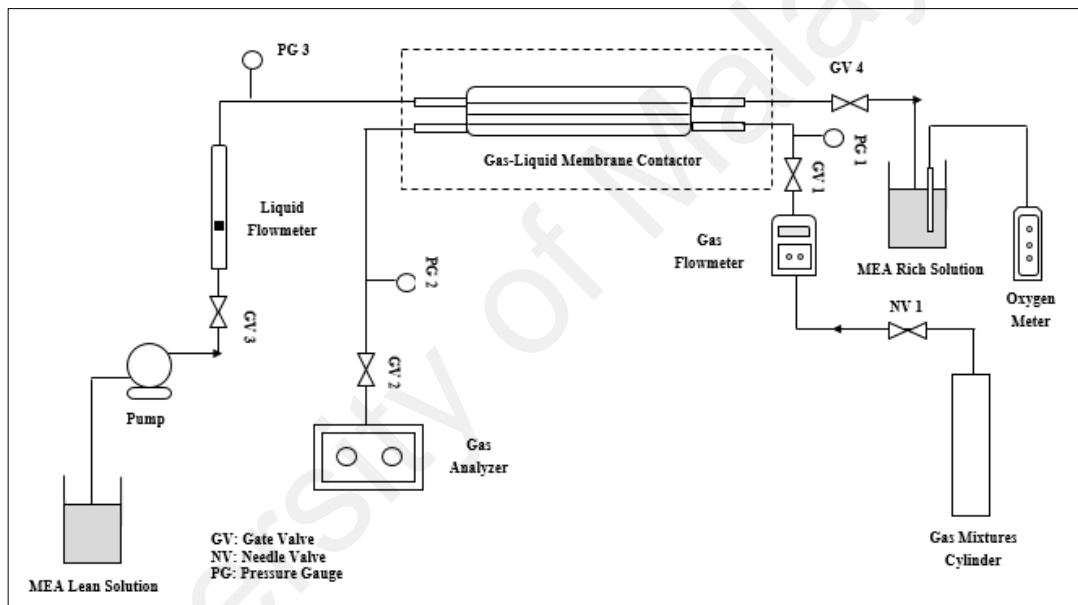


**Figure 3.4:** Experimental setup for CO<sub>2</sub> absorption

### 3.5 Performances and selectivity of CO<sub>2</sub>/O<sub>2</sub> using blank and supported ionic liquid membranes (SILMs) contactor system

CO<sub>2</sub> absorption performances of blank and supported ionic liquid membranes contactor system were performed as per described in section 3.4, using parallel (Figure 3.5(a)) and cross-flow type of Liqui-Cel membrane modules (Figure 3.5(b)). Characteristics of both membrane modules were displayed in Table 3.4. Meanwhile, the ideal selectivity of CO<sub>2</sub>/O<sub>2</sub> for both systems is calculated as the ratio of the outlet concentration of the gases in the absorbent of the membrane modules.

**Table 3.4:** Hollow fiber membrane contactor characteristics for parallel and cross-flow Liqui-Cel type (Hoechst Celanese Corp., Charlotte, NC, USA)

Parameter	Parallel	Cross-flow
Membrane material	Hydrophobic PP	Hydrophobic PP
Fiber o.d. $d_o$ (m)	$3 \times 10^{-4}$	$3 \times 10^{-4}$
Fiber i.d. $d_i$ (m)	$2.4 \times 10^{-4}$	$2.4 \times 10^{-4}$
Fiber length, $L$ (m)	0.115	0.1524
Number of fibers, $n$	2300	10000
Effective inner membrane area, $A$ (m <sup>2</sup> )	0.18	1.4
Membrane thickness, $\delta$ (m)	$0.4 \times 10^{-4}$	$0.4 \times 10^{-4}$
Membrane pore diameter, $d_p$ (μm)	0.03	0.03
Porosity (%)	40	40
Packing factor	0.39	0.39
Tortuosity	2.5	2.5

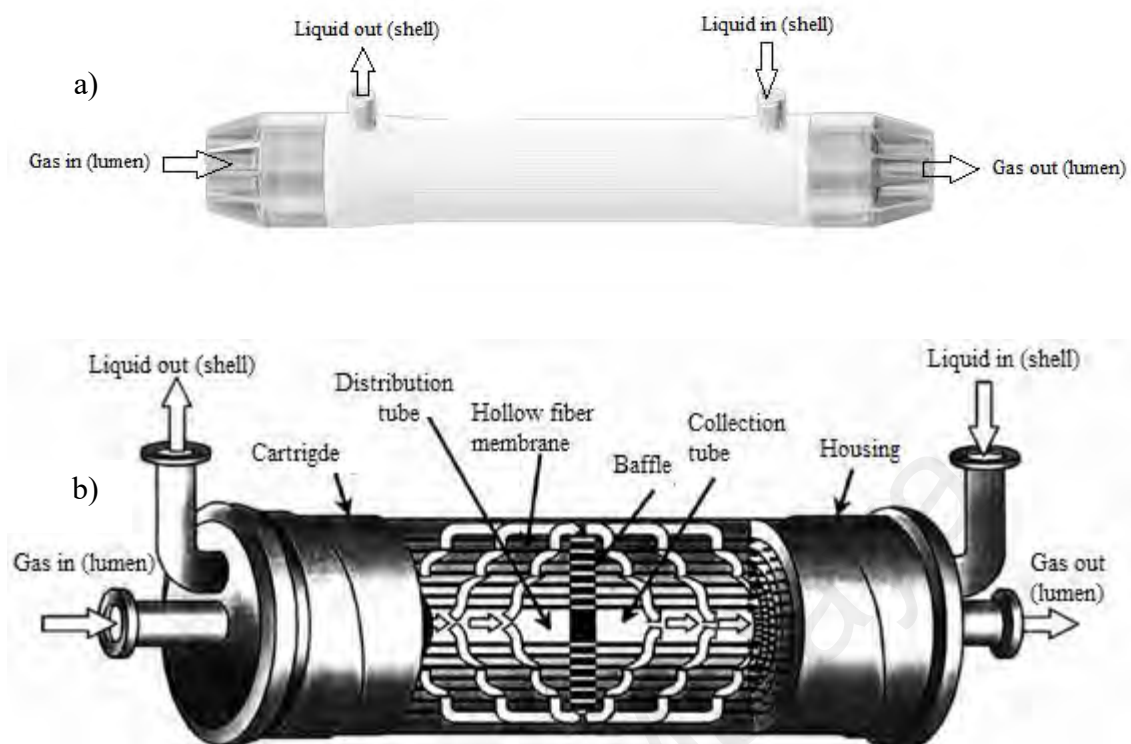


**Figure 3.5:** a) Parallel Liqui-Cel and b) Cross-flow Liqui-Cel gas-liquid membrane contactor

### 3.5.1 Determination of CO<sub>2</sub> loading

For the purpose of obtaining the CO<sub>2</sub> loading of the sample after the reaction, 5 ml sample of the carbonated solution was taken over the sample point. The sample was then mixed with 50 ml solution of 0.5 M BaCl<sub>2</sub> and 50 ml solution of 0.5 M NaOH. In this experiment, NaOH solution was added to convert all the free dissolved gas into non-volatile ionic species, while BaCl<sub>2</sub> solution was used to precipitate all the CO<sub>2</sub> existed in the sample solution. The mixtures were then stirred for 3 hours at 343 K and at atmospheric pressure. The sample was then cooled down to room temperature before filtration and washed thoroughly to eliminate all traces of NaOH.

BaCO<sub>3</sub> was precipitated as a white crystalline solid residue using Glass microfiber filter paper in order to ensure that the whole solid carbonate was collected during this

process. Solid  $\text{BaCO}_3$  was then mixed with 300 ml of distilled water and stirred for 3 hours to ensure complete dissolution of the solid. It was then titrated with a standard solution of 1 M HCl using a computer controlled auto-titrator (Metrohm 716 DMS Titrino). The data obtained were used to calculate the  $\text{CO}_2$  loading. This method of determining  $\text{CO}_2$  loading was verified by conducting a similar experiment on a sample containing a known amount of  $\text{NaHCO}_3$ . The tests were repeated three times for each sample to ensure the accuracy of the data.

The volume of HCl used to neutralize the basic species in the solution is determined from the endpoints using the first derivative of the titration curve. The  $\text{CO}_2$  loading of the solution is defined as total mol of  $\text{CO}_2$  absorbed per mol of MEA and it is calculated by using the following Equation 3.1:

$$\alpha_{\text{CO}_2} = \frac{V_{\text{HCl}} \times M_{\text{HCl}}}{2(M_{\text{MEA}})(V_{\text{Sample}})} \quad (3.1)$$

where;

$\alpha$  =  $\text{CO}_2$  loading in mol of  $\text{CO}_2$  per mol of amine

$V_{\text{HCl}}$  = Volume of HCl needed to neutralized the basic species in ml

$V_{\text{Sample}}$  = Volume of sample taken for analysis in ml

$M_{\text{MEA}}$  = Molarity of the alkanolamine solution in mol per litre



### 3.5.2 Mass transfer calculations

In order to relate the overall mass transfer resistance to the individual mass transfer resistance, the resistance in series approach is used (Equation 3.2).

$$R_{Overall} = R_g + R_{mg} + R_l \quad (3.2)$$

A hollow fiber configuration is selected, with the gas phase flowing through the lumen side and the liquid phase in the shell side. The outer diameters of the tubes are the location where the liquid-gas interface is located. The Equation 3.3 as follows considers the chemical reaction in the liquid side (as expressed by the enhancement factor,  $E_A$ ):

$$\frac{1}{K_{overall}} = \frac{d_o}{k_g d_i} + \frac{d_o}{k_{mg} d_{lm}} + \frac{1}{k_l H_d E_A} \quad (3.3)$$

where  $d_{lm}$ ,  $d_i$  and  $d_o$  are the log mean, inside and outside diameters in (m) of the hollow fiber, with  $H_d$  representing the Henry constant that is dimensionless,  $k_{mg}$ ,  $k_l$ ,  $k_g$ , are the individual mass transfer coefficients for the membrane, liquid phase and gas phase, correspondingly ( $\text{m s}^{-1}$ ) and  $K_{overall}$  is the overall mass transfer coefficient ( $\text{m s}^{-1}$ ). Henry's law constant  $H_d$  which is dimensionless is the important factor in modeling the process of mass transfer. The below equation for Henry constant had been defined in previous researches (Equation 3.4):

$$H_d = \frac{C_{g^*}}{C_l^*} = \frac{y^*}{x_l^*} \frac{P_T}{RT} \quad (3.4)$$

with  $x_l^*$  and  $y^*$  being the molar fractions in the liquid and gas and phases correspondingly and  $P_T$  is the pressure for overall. The mass transfer flux of carbon dioxide is determined as per Equation 3.5:

$$N_{CO_2,g} = \frac{Q_g}{A} (C_{CO_2,in} - C_{CO_2,out}) = K_{overall} \frac{\Delta y_{lm} P_T}{RT} \quad (3.5)$$

Fluxes are equal in the liquid and gas, in the steady state of CO<sub>2</sub>. The overall mass transfer  $K_{overall}$  is able to assess through an experiment from the flux through the concentration gradient and membrane.  $\Delta y_{lm}$  is the logarithmic mean of the driving force that is based on gas phase molar fractions,  $P_T$  is the entire pressure in the gas phase,  $A$  is the membrane area (m<sup>2</sup>) and  $Q_g$  is the gas flow rate (m<sup>3</sup> s<sup>-1</sup>). In view of the carbon dioxide concentration in the outlet ( $y_{CO_2,out}$ ) and the inlet ( $y_{CO_2,in}$ ) of the hollow fiber membrane contactor, it is assumed that CO<sub>2</sub> concentration in the solvent is quite a distance far from the saturation in the experiments, the calculation for  $\Delta y_{lm}$  are as per Equation 3.6:

$$\Delta y_{lm} = \frac{(y_{CO_2,in}) - (y_{CO_2,out})}{\ln ((y_{CO_2,in}) / (y_{CO_2,out}))} \quad (3.6)$$

Quite a few authors have recommended other empirical correlations for the parallel flow in shell-side mass transfer in hollow fiber membrane contactors (Gómez-Coma et al., 2014). Kartohardjono's correlation is being used in this study to estimate  $k_l$ , due to the Reynolds number and packing factor are in a similar range ( $0.029 < \varphi < 0.53$ ;  $Re < 400$ ) (Equation 3.7):

$$Sh = \left( \frac{k_l d_h}{D_{CO_2,l}} \right) = 0.1789 (\varphi^{0.86}) Re^{0.34} Sc^{\frac{1}{3}} \quad (3.7)$$

$$d_h = \frac{d_{cont}^2 - nd_o^2}{nd_o} \quad (3.8)$$

where;

$Re$  = Reynolds number

$Sc$  = Schmidt number

$Sh$  = Sherwood number

$D_{CO_2,l}$  = diffusion coefficient of carbon dioxide in the liquid

$d_h$  = hydraulic diameter (m)

$d_o$  = outside diameter of the fiber (m)

$d_{cont}$  = diameter of the contactor (m)

$n$  = number of fibers

The membrane contactor characteristics and the physical properties of the absorbent determines the mass transfer coefficient in the liquid phase ( $k_l$ ). Morgan et al. (2005) have established a correlation that expresses the liquid viscosity with the dependency of gas diffusivity as per Equation 3.9:

$$D_{CO_2,l} = 2.66 \times 10^{-3} \frac{1}{\mu_{MEA}^{0.66} V_{CO_2}^{1.04}} \quad (2.9)$$

with  $V_{CO_2}$  being the molar volume of carbon dioxide at the normal boiling point (33.3 cm<sup>3</sup> mol<sup>-1</sup>),  $\mu_{MEA}$  being the viscosity of solvent in cP, and the diffusivity found in cm<sup>2</sup> s<sup>-1</sup>. The gas and liquid velocities were also calculated based on Equations 3.10 and 3.11.

$$Q/A = v_{avg} \quad (3.10)$$

where  $Q$  being an inlet volume flow rate to both tube or shell sides of the membranes (ml min<sup>-1</sup>),  $A$  is the inner surface of the hollow fiber membranes (m<sup>2</sup>) and  $v_{avg}$  is the

average velocity ( $\text{m s}^{-1}$ ). Substituting and converting the known values and units produces,

$$v_{avg} = \frac{X (ml/min) (10^{-6} m^3/ml) (1 min/60 s)}{A (m^2)} = Y m s^{-1} \quad (3.11)$$

Prediction of the calculation for this membrane absorption process is basically follows several assumptions such as:

- a) The operating system is under isothermal and steady-state conditions
- b) Consideration of the gas phase as an ideal gas
- c) Incompressible liquid phase and Newtonian-type
- d) Negligible axial diffusion
- e) The Henry's law is appropriate for the gas-liquid surface

## CHAPTER 4: RESULTS AND DISCUSSION

### 4.1 COSMO-RS analysis

#### 4.1.1 Prediction and calculation of Henry's Law constants ( $H$ ) of CO<sub>2</sub>, N<sub>2</sub>, and O<sub>2</sub> were made at different temperatures

To ascertain the perfect gas separation performances for each imidazolium-based ILs under study, the values of Henry's law constants ( $H$ ) for CO<sub>2</sub>, O<sub>2</sub> and N<sub>2</sub> in the ILs (refer Figure 4.1 to Figure 4.3) were estimated at a temperature between 298.15 K and 348.15 K (Sharma et al., 2012; Shimoyama & Ito, 2010; Sumon & Henni, 2011) followed by an estimation of ideal selectivity of the gas pairs. Generally, lower values for Henry's law indicate higher gas solubility and vice-versa. The data showed that [emim] [FAP] displays the highest solubility for CO<sub>2</sub>, due to the decreased  $H$ . For N<sub>2</sub> solubility in ILs the results indicated that [bmim] [BF<sub>4</sub>] displays poorer solubility due to the increased  $H$  in comparison to other ILs. For the ILs solubilities towards O<sub>2</sub>, solubilities increased in the sequence of [emim] [FAP] > [bmim] [DCA] > [bmim] [TFA] > [emim] NTf<sub>2</sub> > [bmim] [BF<sub>4</sub>] and [emim] [TFO]. Data analysis by COSMO-RS method indicated that Henry's law constant was proportionate to the temperature at atmospheric pressure.

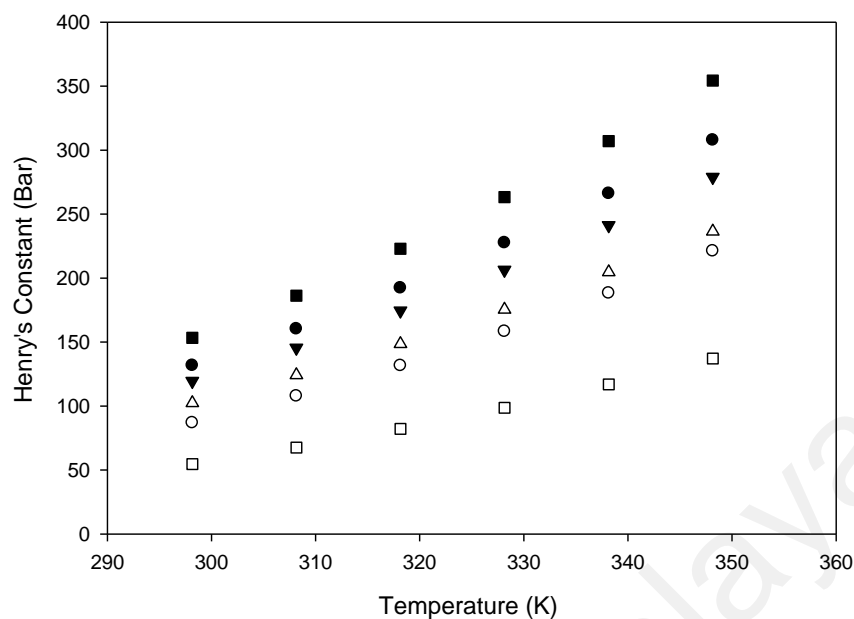


**Figure 4.1:** Henry's law constant for CO<sub>2</sub> in different types of imidazolium-based ILs where (○) [bmim] [DCA], (●) [bmim] [BF<sub>4</sub>], (▼) [bmim] [TFA], (■) [emim] [TFO], (□) [emim] [FAP] and (△) [emim] [NTf<sub>2</sub>]

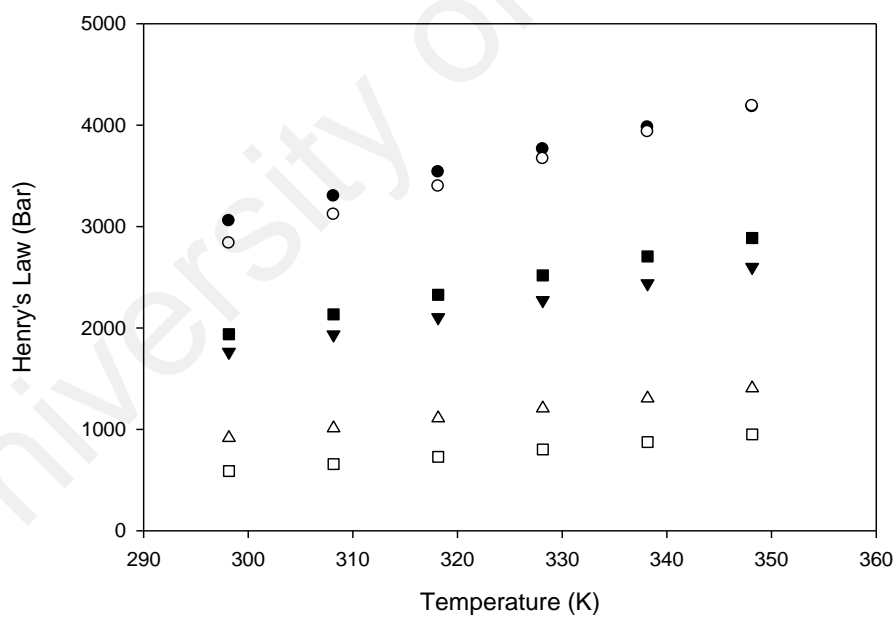


**Figure 4.2:** Henry's law constant for N<sub>2</sub> in different types of imidazolium-based ILs where (○) [bmim] [DCA], (●) [bmim] [BF<sub>4</sub>], (▼) [bmim] [TFA], (■) [emim] [TFO], (□) [emim] [FAP] and (△) [emim] [NTf<sub>2</sub>]

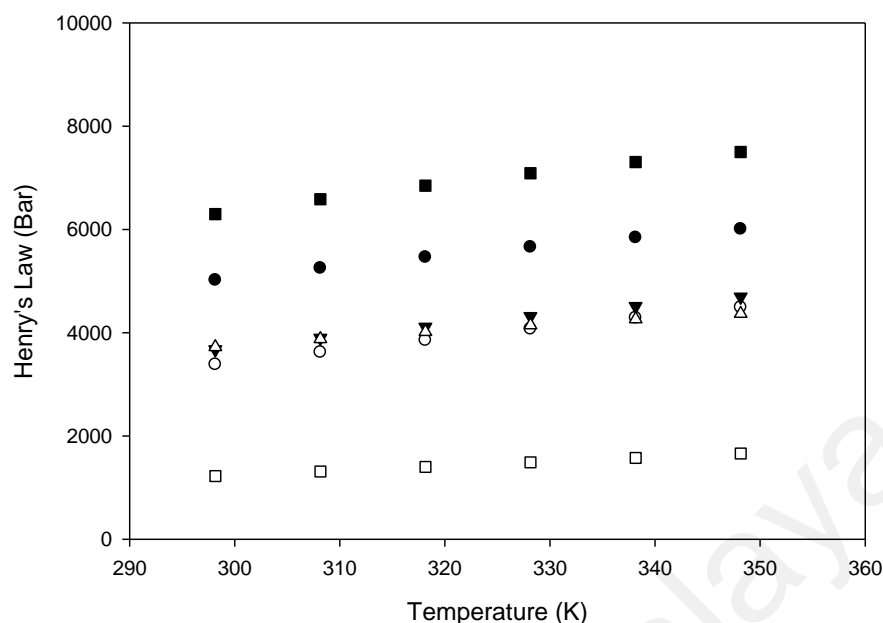


**Figure 4.3:** Henry's law constant for O<sub>2</sub> in different types of imidazolium-based ILs where (○) [bmim] [DCA], (●) [bmim] [BF<sub>4</sub>], (▼) [bmim] [TFA], (■) [emim] [TFO], (□) [emim] [FAP] and (△) [emim] [NTf<sub>2</sub>]

In general, the effects of cation modifications on  $H$  values are quite small subjected to systematic variations in structure, but generally have a greater impact on the solubility of gases. The anions play the main role in CO<sub>2</sub> solubility in ILs, and anions that comprise fluoroalkyl groups were revealed to gain the utmost solubility for CO<sub>2</sub> (Sharma et al., 2012). Prior studies stated that the CO<sub>2</sub> solubility in ILs was predominantly determined by anion-cation interactions, with CO<sub>2</sub>-anion interactions being secondary (Kanakubo et al., 2005; Muldoon et al., 2007). In addition, the link between the cation–anion binding energy and CO<sub>2</sub> solubility suggested that higher CO<sub>2</sub> solubility in ionic liquid could be highly influenced by inadequate cation–anion interaction (Babarao et al., 2011). This conclusion is intuitively valid considering that weaker cation–anion pair interactions mean that the lattice can easily expand, increasing the free volume and allowing more space for CO<sub>2</sub> insertion. In this work, it was found that with similar alkyl chain groups, the anions containing fluoroalkyl groups (FAP,

NTf<sub>2</sub>, TFO and etc.) had higher CO<sub>2</sub> solubility, and that with increasing number of fluoroalkyl groups, the CO<sub>2</sub> solubility was also improved. In NTf<sub>2</sub> anion containing IL, a higher CO<sub>2</sub> absorption capacity can be observed. This is due to the weak NTf<sub>2</sub> anion–cation interaction, attributed to the good charge distribution and irregular shape of the anion, which allows maximum expansion of the lattice. A slightly higher CO<sub>2</sub> absorption capacity could be observed in IL containing DCA anion. This is due to the sufficient amount of charge distribution and its flat shape, which marks to a frail cation–anion interaction. These outcomes and trend are in line with earlier reports (Ahmady et al., 2011; Sharma et al., 2012), which pointed out that the increase of CO<sub>2</sub> solubility in ionic liquids is factored by the decrease of cation–anion interaction strength.

Besides, the absence of charge distribution and symmetrical structure results to an effective cation–anion interaction in IL and the lowest CO<sub>2</sub> absorption capacity. TFO anion comprising IL was found to have low CO<sub>2</sub> absorption capacity attributed to the lower charge distribution and less regular shape of the anion, which results in a stronger TFO anion–cation interactions (Sharma et al., 2012).

Predicted results of CO<sub>2</sub>/N<sub>2</sub> and CO<sub>2</sub>/O<sub>2</sub> selectivities in imidazolium-based ILs are given in Table 4.1, Figure 4.4 and Figure 4.5. As far as the selectivity towards gaseous mixture is concerned, [bmim] [DCA] demonstrates the highest selectivity for CO<sub>2</sub>/N<sub>2</sub>, followed by [bmim] [BF<sub>4</sub>] > [bmim] [TFA] > [emim] [TFO] > [emim] [FAP] > and [emim] [NTf<sub>2</sub>]. For CO<sub>2</sub>/O<sub>2</sub>, [emim] [TFO] has a comparatively higher selectivity. The COSMO-RS data analysis indicated that the selectivity and solubility of this imidazolium-based ILs were proportional to the temperature at atmospheric pressure. Data in this work are compared with those predicted by standard COSMOthermX



process in prior studies (Shimoyama & Ito, 2010; Sumon & Henni, 2011). Significant discrepancies appeared in the estimation of these ILs when compared to these studies. This variation could be due to several aspects such as slight differences in COSMO files, treatment of conformers, and the parameterisations utilised in the COSMOthermX program's various versions (Sumon & Henni, 2011).

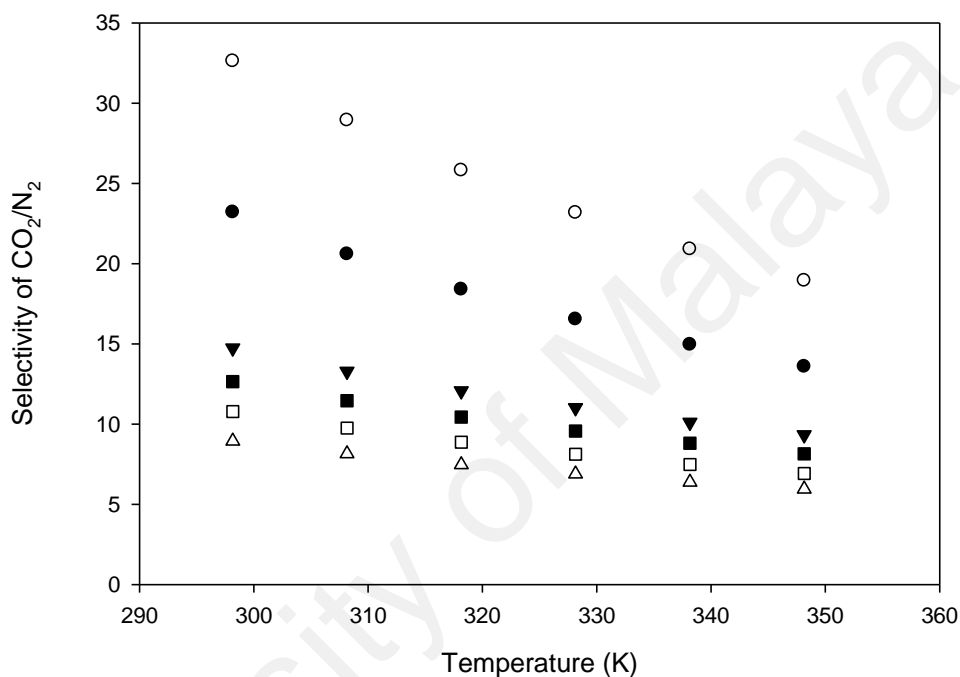


**Figure 4.4:** Selectivity of CO<sub>2</sub>/N<sub>2</sub> in different types of imidazolium-based ILs where (○) [bmim] [DCA], (●) [bmim] [BF<sub>4</sub>], (▼) [bmim] [TFA], (■) [emim] [TFO], (□) [emim] [FAP] and (△) [emim] [NTf<sub>2</sub>]

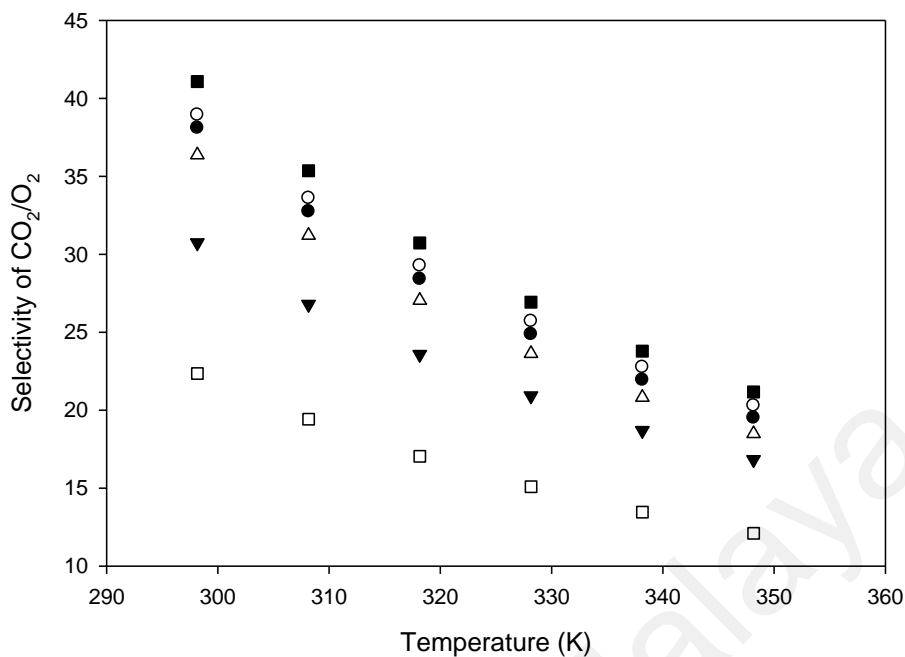


**Figure 4.5:** Selectivity of CO<sub>2</sub>/O<sub>2</sub> in different types of imidazolium-based ILs where (○) [bmim] [DCA], (●) [bmim] [BF<sub>4</sub>], (▼) [bmim] [TFA], (■) [emim] [TFO], (□) [emim] [FAP] and (△) [emim] [NTf<sub>2</sub>]

An important outcome from this work, it has demonstrated the selectivity ranking of ILs that are different for CO<sub>2</sub>/N<sub>2</sub> and CO<sub>2</sub>/O<sub>2</sub>, that justifies the need for a study on the CO<sub>2</sub>/O<sub>2</sub> selectivity.

**Table 4.1:** Predicted results of CO<sub>2</sub>, N<sub>2</sub> and O<sub>2</sub> in imidazolium-based ILs using COSMOthermX program

Ionic Liquids (ILs)	This work (Simulations)		Literatures Data (Simulations)		Literatures Data (Experimental)	
	CO <sub>2</sub> /N <sub>2</sub> (S <sub>12</sub> )	CO <sub>2</sub> /O <sub>2</sub> (S <sub>13</sub> )	CO <sub>2</sub> /N <sub>2</sub> (S <sub>12</sub> )	CO <sub>2</sub> /O <sub>2</sub> (S <sub>13</sub> )	CO <sub>2</sub> /N <sub>2</sub> (S <sub>12</sub> )	CO <sub>2</sub> /O <sub>2</sub> (S <sub>13</sub> )
[emim][FAP]	11	22	Data not available		21 <sup>c</sup> , 2-32.90 <sup>d</sup>	
[emim][NTf <sub>2</sub> ]	9	36	14 <sup>a</sup> (298.15 K)	-		
			25 <sup>b</sup> (298.15 K)			
			25 <sup>b</sup> (313.15 K)		Data not available	
[emim][TFO]	13	41	25 <sup>b</sup> (313.15 K)	-		
[bmim][BF <sub>4</sub> ]	23	38	26 <sup>b</sup> (313.15K)	-		
					52.30 <sup>c</sup> , 86.50 ± 0.10 <sup>f</sup>	
[bmim][DCA]	33	39	Data not available		78.90 ± 0.9 <sup>f</sup>	
[bmim][TFA]	15	31	Data not available			

**Data taken from:** <sup>a</sup> (Sumon & Henni, 2011) – COSMO-RS, <sup>b</sup> (Shimoyama & Ito, 2010) – COSMO-SAC, <sup>c</sup> (Scovazzo et al., 2004a), <sup>d</sup> (Kim et al., 2011), <sup>e</sup> (Cserjési et al., 2010), <sup>f</sup> (Jindaratsamee et al., 2011)

Interactions between these ILs and the gas molecules were further ascertained, in order to examine the discrepancies appeared in the absorption performances relative to the gaseous substances. Particular significant structural properties for N<sub>2</sub>, O<sub>2</sub>, and CO<sub>2</sub>, (i.e. polarizability [ $\alpha$ ], dipole moment [ $\mu$ ] and quadrupole moment [Q]) were displayed in Table 4.2, so a comparison between these gases could be made. These data demonstrated that the quadrupole moment of CO<sub>2</sub> was much prominent compared to the other two gases. Consequently, the hypothesis for this modelling was that the increase of CO<sub>2</sub> solubility in ILs is influenced by the increase of quadrupole moment. In comparison to N<sub>2</sub> and O<sub>2</sub>, the solubility of CO<sub>2</sub> was significantly higher, which indicated the possibility of capturing CO<sub>2</sub> from flue gases.

**Table 4.2:** Polarizability ( $\alpha$ ); dipole moment ( $\mu$ ); and quadrupole moment (Q) for CO<sub>2</sub>, N<sub>2</sub>, and O<sub>2</sub> Copyright 1999, Prentice Hall PTR and Copyright 1966, Taylor and Francis Group (Zhou et al., 2014)

Gas	$\alpha \times 10^{24} (\text{cm}^3)$	$\mu \times 10^{18} (\text{esu} \cdot \text{cm})$	$Q \times 10^{26} (\text{esu} \cdot \text{cm}^2)$
CO <sub>2</sub>	2.64	0	4.3
O <sub>2</sub>	1.60	0	0.39
N <sub>2</sub>	1.74	0	1.5

#### 4.1.2 Sigma profiles/ molecular interaction

Properties of ionic liquids and gases (e.g. sigma profile), which were derived from COSMOthermX, were utilized for a qualitative understanding of the ILs' molecular interactions with CO<sub>2</sub>, N<sub>2</sub>, and O<sub>2</sub>. As the sigma profile of a molecule represented the distribution of charge over its surfaces, a qualitative insight was provided on the molecule's ability for hydrogen bonding or electrostatic interaction with other molecules. Through this modelling, ionic liquid was defined as a cation's and an anion's equimolar mixture. Hence, the mole fraction's average of the cation and anion's sigma profiles was represented by an ILs sigma profile. COSMOthermX was used for the

calculation of the sigma profile, where it only used the ion's lowest energy conformer in the IL-database taken from COSMOlogic. The COSMO scheme has the sigma profile which functions as the descriptor of the molecular surface's local polarity and generator of the interaction energies. This gives more indicators to the polarity of components in a mixture or within itself. The sigma profiles of imidazolium-based ILs with CO<sub>2</sub>, N<sub>2</sub>, and O<sub>2</sub> are displayed in Figure 4.6, Figure 4.7, and Figure 4.8 respectively. In addition, the locations of the cut-off values for the hydrogen bond donor ( $\sigma_{hb} < -0.01 \text{ e}/\text{\AA}^2$ ) and acceptor ( $\sigma_{hb} > 0.01 \text{ e}/\text{\AA}^2$ ) are shown by two vertical straight lines. This cut-off value is important because the profile on the right side of  $\sigma_{hb} = +0.01 \text{ e}/\text{\AA}^2$  will have high hydrogen bond acceptor ability, while the one on the left side will have high hydrogen bond donation level. The inherent positive charge of the atom/molecule results to the profiles within the negative region; meanwhile, the opposite stays within the positive region. Other than that, there were similarities held by all the sigma profiles of cations.

Comparison of the sigma profiles of the ILs and CO<sub>2</sub> is shown in Figure 4.6. Utmost of the molecular surfaces of CO<sub>2</sub> were located adjacent the neutral area. Furthermore, the [emim] and [bmim] cations are the factors of the sigma profiles of ionic liquids, which were within negative sigma region. Although [bmim] [TFA] and [emim] [TFO]'s profiles are nearly similar to CO<sub>2</sub> in the negative sigma region near zero, the [emim] [NTf<sub>2</sub>], [emim] [FAP], and [bmim] [DCA] have more molecular surfaces which functions to provide electrostatic interaction with the CO<sub>2</sub> surfaces within the same region. The sigma profiles of [TFO] and [TFA] anions almost overlap with CO<sub>2</sub>, indicating high immiscibility, which is proof that they are incompatible due to low solubility. One study found that the highest solubility of CO<sub>2</sub> in ILs that contain [FAP] anions was a consequence of the negative sigma potential present within the whole range of CO<sub>2</sub> sigma charge (Sumon & Henni, 2011). The high miscibility of CO<sub>2</sub> with

[FAP] anions can likewise be explained by the complementary nature of the sigma profiles of [emim] [FAP] and CO<sub>2</sub>. Nearly all the surface pieces of CO<sub>2</sub> will locate their opposite surface pieces upon their dissolution in [emim] [FAP] and, therefore, will have low misfit energy. Experimental works by Jalili et al. (2013) likewise supported this finding. Figure 4.7 and 4.8 show that the sigma profiles of all ILs with CO<sub>2</sub> interaction were comparable with those of N<sub>2</sub> and O<sub>2</sub>. Large deviation of [FAP] anion's peaks from those gases peaks indicated its highest solubility characteristic (good miscibility), in contrast to the poor miscibility of [BF<sub>4</sub>] and [TFO] anions.

Each conformer's structures with respect to COSMO energy have been displayed in Figure 4.9. The screening charge density  $\sigma$  as per Figure 4.9 is the conductor response, posing opposing values to the molecular polarity. The anion has yielded primarily positive values (red), whereas the cation has displayed primarily negative screening charge density (blue). Observing non-polar region or neutral region (green) has revealed that [FAP]<sup>-</sup> anion possesses a broader neutral area (green) compared to other anions as it has higher affinity to CO<sub>2</sub>, N<sub>2</sub> and O<sub>2</sub>. In contrast, [BF<sub>4</sub>]<sup>-</sup> anion has displayed the weakest attraction to the gases. Different cations ([emim] and [bmim]) have apparently less significant effects (Sharma et al., 2012) towards the process due to lesser screening charge density of neutral green area compared to anion-gases interactions. Such findings have paralleled prior knowledge regarding CO<sub>2</sub> solubility in ILs being primarily influenced by anion-cation interactions, with CO<sub>2</sub>-anion interactions being secondary (Babarao et al., 2011; Kanakubo et al., 2005; Muldoon et al., 2007). This fact has otherwise confirmed the data shown in Figure 4.6 to 4.8.

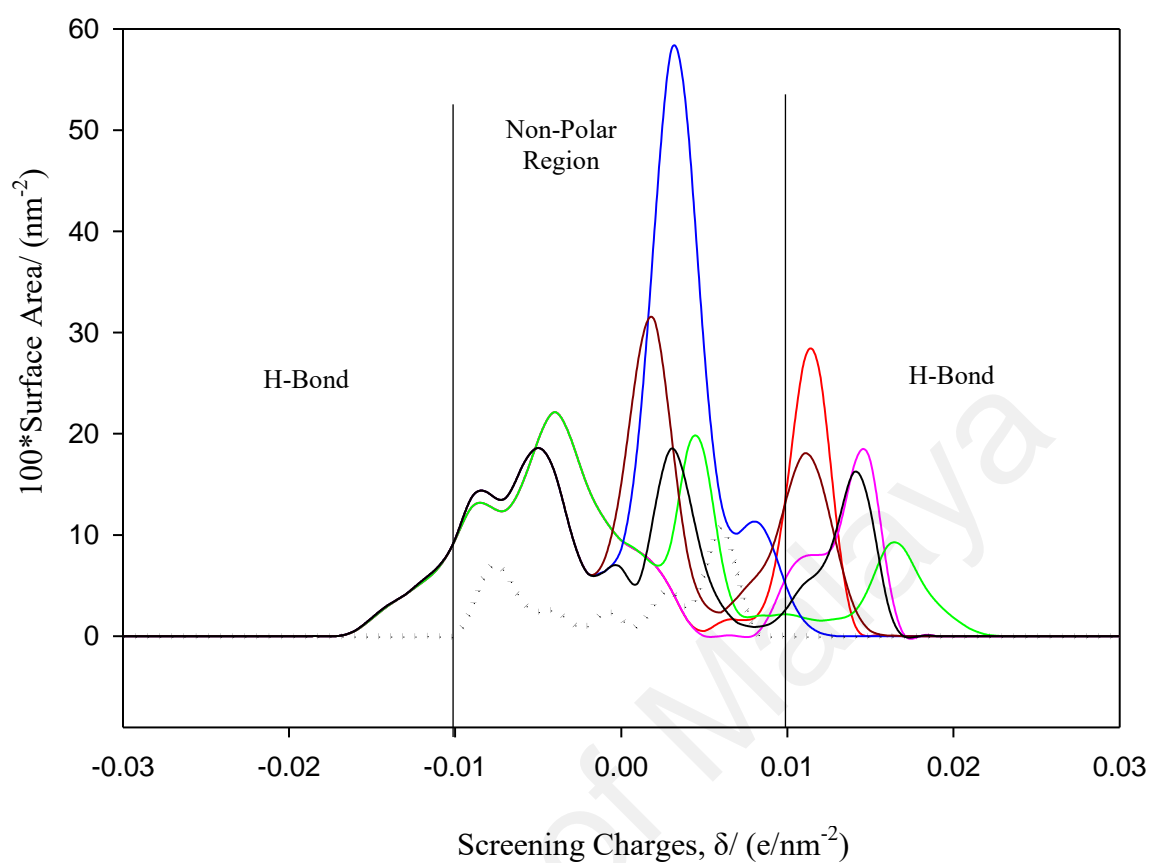


**Figure 4.6:** Sigma profile of several imidazolium-based ILs with a CO<sub>2</sub> where (—) [bmim] [DCA], (—) [bmim] [BF<sub>4</sub>], (—) [bmim] [TFA], (—) [emim] [TFO], (—) [emim] [FAP], (—) [emim] [NTf<sub>2</sub>] and (····) gas

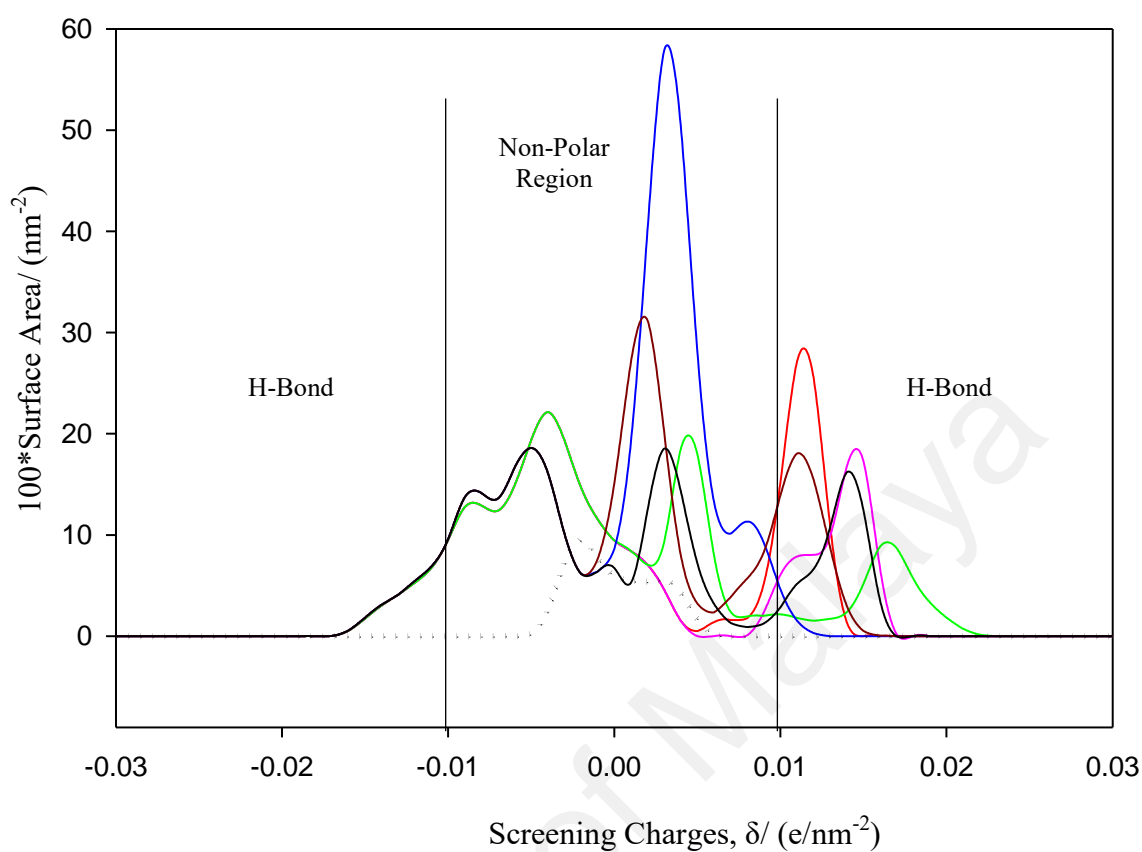


**Figure 4.7:** Sigma profile of several imidazolium-based ILs with  $N_2$  where (—) [bmim] [DCA], (—) [bmim] [BF<sub>4</sub>], (—) [bmim] [TFA], (—) [emim] [TFO], (—) [emim] [FAP], (—) [emim] [NTf<sub>2</sub>] and (····) gas



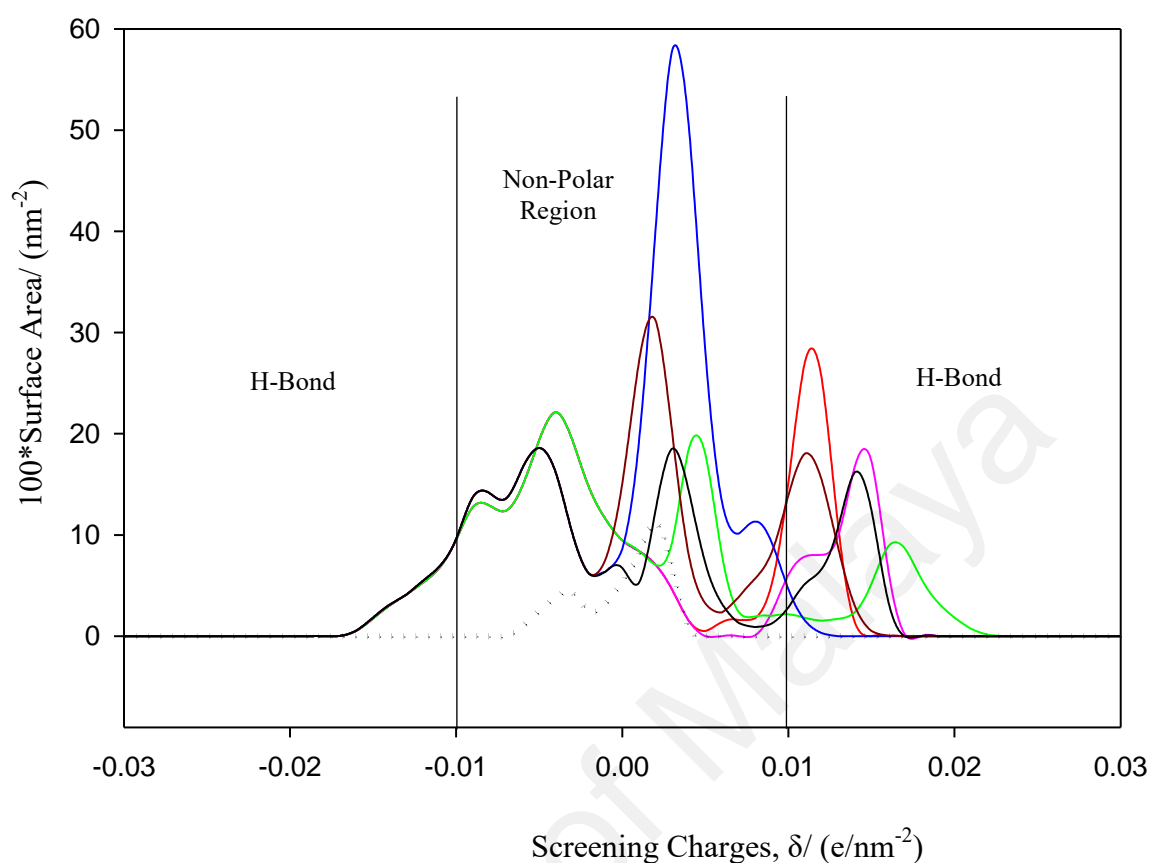


**Figure 4.8:** Sigma profile of several imidazolium-based ILs with O<sub>2</sub> where (---) [bmim] [DCA], (—) [bmim] [BF<sub>4</sub>], (—) [bmim] [TFA], (—) [emim] [TFO], (—) [emim] [FAP], (—) [emim] [NTf<sub>2</sub>] and (...) gas

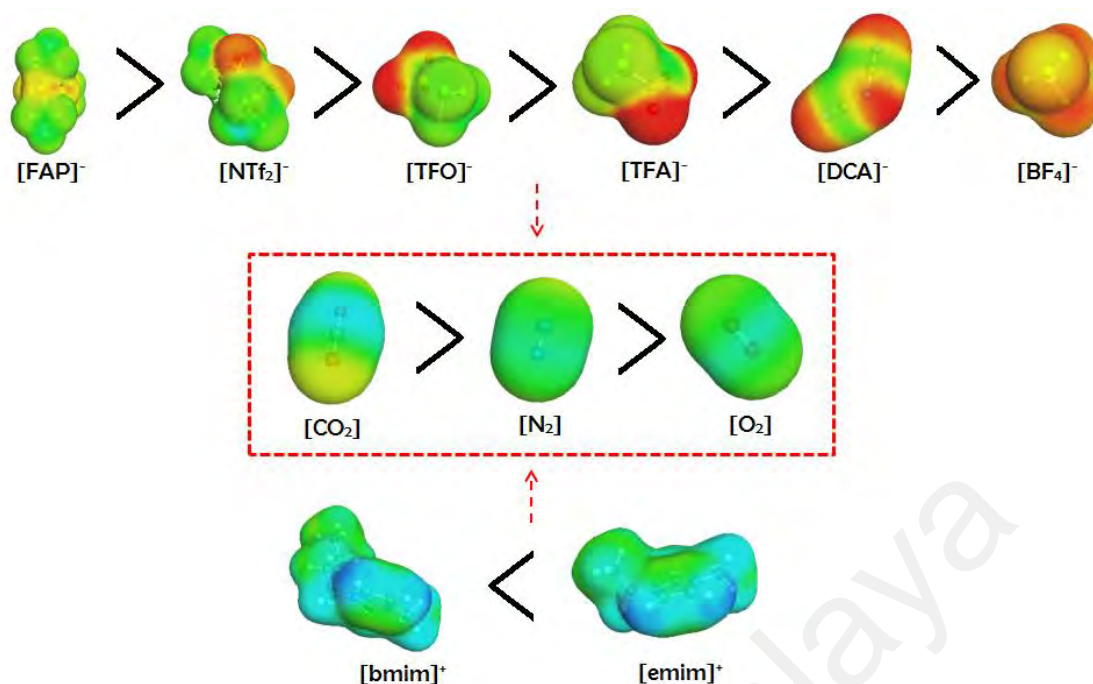


**Figure 4.9:** Screening charge density  $\sigma$  of the conformer of anions, cations,  $\text{CO}_2$ ,  $\text{N}_2$  and  $\text{O}_2$

#### 4.1.3 Activity coefficients at infinite dilution

Furthermore, dealing with the usage of ILs in the modified gas-liquid membrane contactor system, several factors need to be investigated in its selection, despite the selectivity of imidazolium-based ILs towards  $\text{CO}_2/\text{O}_2$  and  $\text{CO}_2/\text{N}_2$  gases. Among the aforementioned factors is the hydrophobicity of ILs, as well as its miscibility with the chosen solvent system (i.e. MEA). COSMO-RS analysis was used to evaluate the activity coefficient of the selected imidazolium-based ILs towards MEA and water. Figures 4.10 and 4.11 present activity coefficients data of water and MEA in imidazolium-based ionic liquids between 298.15 and 348.15 K.

This study considers activity coefficients as helpful quantitative means for studying the mutual solubilities of the ILs-MEA and the ILs- $\text{H}_2\text{O}$  binary system. The activity coefficients of water and MEA in ILs measure the degree of non-ideality of liquid

mixture relative to its pure liquid state. The chemical potential that remains reflects non-ideality caused by energetic interactions was obtained by means of switching off all the compounds' combinatorial contributions. Thus, higher negative  $\ln \gamma$  values have the tendency towards decreasing mutual solubilities.

Figure 4.10 tabulated data of water's activity coefficients in imidazolium-based ionic liquids (ILs) between 298.15 and 348.15 K, where [emim] [FAP] demonstrates the highest activity coefficient with  $H_2O$ , followed by [emim] [NTf<sub>2</sub>] > [bmim] [BF<sub>4</sub>] > [bmim] [DCA] > [emim] [TFO] and [bmim] [TFA]. A negative value of [bmim] [TFA] IL activity coefficient tends to favour its mutual solubility with water, while, highest value obtained from [emim] [FAP] and [emim] [NTf<sub>2</sub>] ILs indicated the increment of a non-ideality degree in the binary system. Data on the activity coefficients likewise illustrate that with temperature increment, the activity coefficients decreased. The miscibility of ILs with water is of particular interest since hydrophobic ILs can be used as the water immiscible polar phase for biphasic processes. The coordinating capability of the ions in an ILs contributed to the major factors in determining the miscibility of water in ILs. [Cl]<sup>-</sup> and [NO<sub>3</sub>]<sup>-</sup> base anions were found to be strongly coordinated with water compared to acidic anions group (i.e. [Al<sub>2</sub>Cl<sub>7</sub>]<sup>-</sup>) and [BF<sub>4</sub>]<sup>-</sup>, [PF<sub>6</sub>]<sup>-</sup>, [NTf<sub>2</sub>]<sup>-</sup> groups which are being classified as non-coordinated and weakly coordinated, respectively. Hydrophobicity characteristic of the ILs would increase the coordinating capability of the anion. On the other hand, the hydrophobicity of the ILs could be controlled by the cations. For example, the rise in the number of alkyl chain lengths such as pyridinium and imidazolium tend to decrease the miscibility of ILs with water. Thus, it can be concluded that both changes have a noteworthy influence on the solubility characteristic of ILs.

In general, ILs can be selected or designed to be miscible or immiscible not only in water but also in all organic solvents depending on their polarities. Liquids with medium to high dielectric constant (liquids consisting of polar molecules) tend to exhibit higher miscibility, while liquids with low dielectric constants are immiscible with solvents.

The data on activity coefficients of MEA in imidazolium-based ILs, at temperature between 298.15 and 348.15 K, are shown in Figure 4.11. Among the selected ILs, hydrophobic [emim] [FAP] IL demonstrated inferior activity coefficients due to the interaction between MEA and ILs. Generally, ILs functions effectively as hydrogen bond donors/acceptors as they are charged. Besides, imidazolium-based ILs is greatly demanded hydrogen bonded substances in most situations, and they pose significant effects on chemical reactions and processes. Meanwhile, the MEA utilized in this study is also an effective hydrogen-bond donor/acceptor (high dielectric constant), albeit ILs having a better performance. Due to stronger interaction between the [FAP] anion and the solvent, a more substantial interaction could be seen for [emim] [FAP] IL with MEA. Therefore, based on this observation, it can be agreed that the mutual solubility of ILs with MEA is enhanced due to the primary impact of [FAP] anion, instead of the impact from cation.

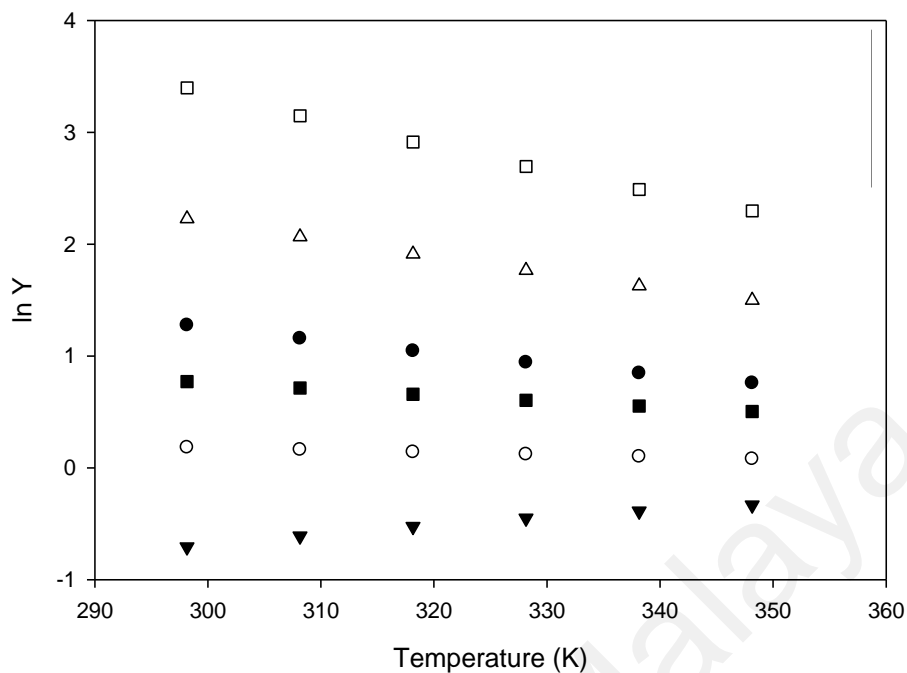


**Figure 4.10:** Activity coefficients data of water in imidazolium-based ionic liquids (ILs) between 298.15 and 348.15 K where (  $\circ$  ) [bmim] [DCA], (  $\bullet$  ) [bmim] [BF<sub>4</sub>], (  $\blacktriangledown$  ) [bmim] [TFA], (  $\blacksquare$  ) [emim] [TFO], (  $\square$  ) [emim] [FAP] and (  $\triangle$  ) [emim] [NTf<sub>2</sub>]

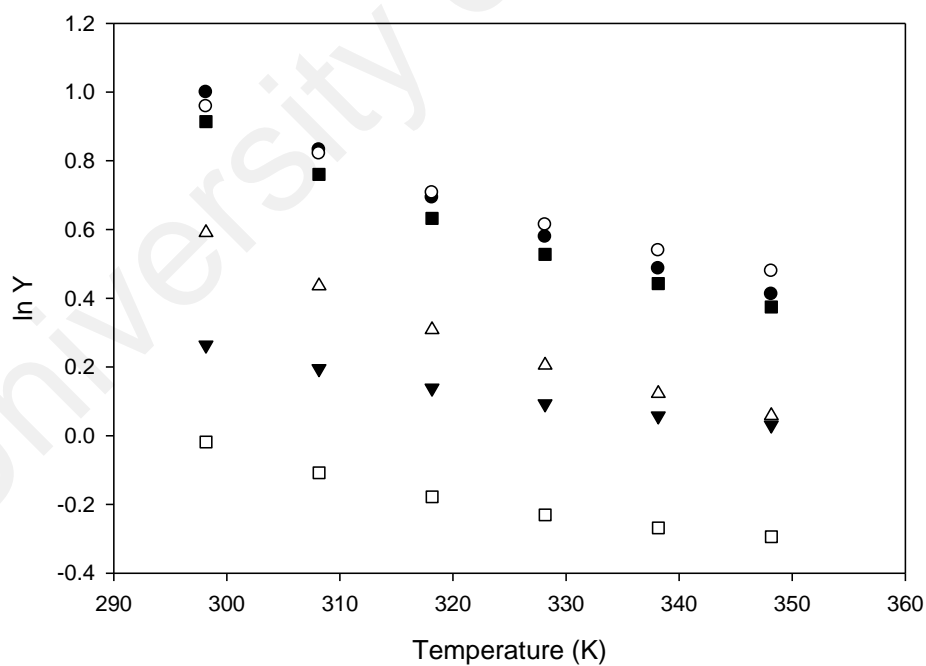


**Figure 4.11:** Activity coefficients data of MEA in imidazolium-based ionic liquids (ILs) at 298.15 to 348.15 K where (  $\circ$  ) [bmim] [DCA], (  $\bullet$  ) [bmim] [BF<sub>4</sub>], (  $\blacktriangledown$  ) [bmim] [TFA], (  $\blacksquare$  ) [emim] [TFO], (  $\square$  ) [emim] [FAP] and (  $\triangle$  ) [emim] [NTf<sub>2</sub>]

#### 4.1.4 Summary (Section 4.1)

Solubilities and selectivities of CO<sub>2</sub>, nitrogen (N<sub>2</sub>), and oxygen (O<sub>2</sub>) gases in imidazolium-based ILs and its activity coefficients in water and monoethanolamine (MEA) were successfully predicted using conductor-like screening model for real solvent (COSMO-RS) method over a wide range of temperature (298.15–348.15 K). Results from the analysis had found that [emim] [NTf<sub>2</sub>] IL is a good candidate for further absorption process, due to its good hydrophobicity and CO<sub>2</sub>/O<sub>2</sub> selectivity characteristics. While their miscibility with pure MEA was somehow higher, utilizing the aqueous phase of MEA would be beneficial in this stage. In conclusion, COSMO-RS has the potential to become a great predictive utility to screen ILs for specific separation applications.

University of Malaya

## 4.2 Preparation of supported ionic liquid membranes (SILMs)

### 4.2.1 Physical properties of binary mixtures

Dynamic viscosities and refractive index ( $\eta_D$ ) of [emim] [NTf<sub>2</sub>] IL and acetone binary mixtures were determined at 30°C. Triplicate determinations were applied for the data reported. The measured parameters of the binary mixtures were presented in Figure 4.12 and Table 4.3. From this study, a significant decrease of viscosities was discovered with a decrease of [emim] [NTf<sub>2</sub>] IL composition, which was from 37 mPa s to 0.57 mPa s. The viscosity values changed significantly at greater volume fraction when compared to lesser volume fractions of [emim] [NTf<sub>2</sub>] IL. This was due to the viscosity of IL, which is higher than the viscosity of acetone. In addition, the results also showed that interactions between the protons of the ring, the methyl and methylene next to the nitrogen of ionic liquids and the carbonyl oxygen of acetone weakened the strong interaction between the cation and anion of the ionic liquid, thus increased the motion and decreased the viscosity of the ionic liquid (Zhai et al., 2006). Similarly, the decrease of the refractive index of mixtures in Figure 4.12 from 1.42 to 1.35 occurs due to the increase of acetone composition in the mixture. Viscosity and refractive index were linearly correlated by the less presence of bigger chains of IL as they have less opportunity to interact to each other and move freely. The decrease of refractive index was due to the existence of highest density of electrons without involving any physical changes.



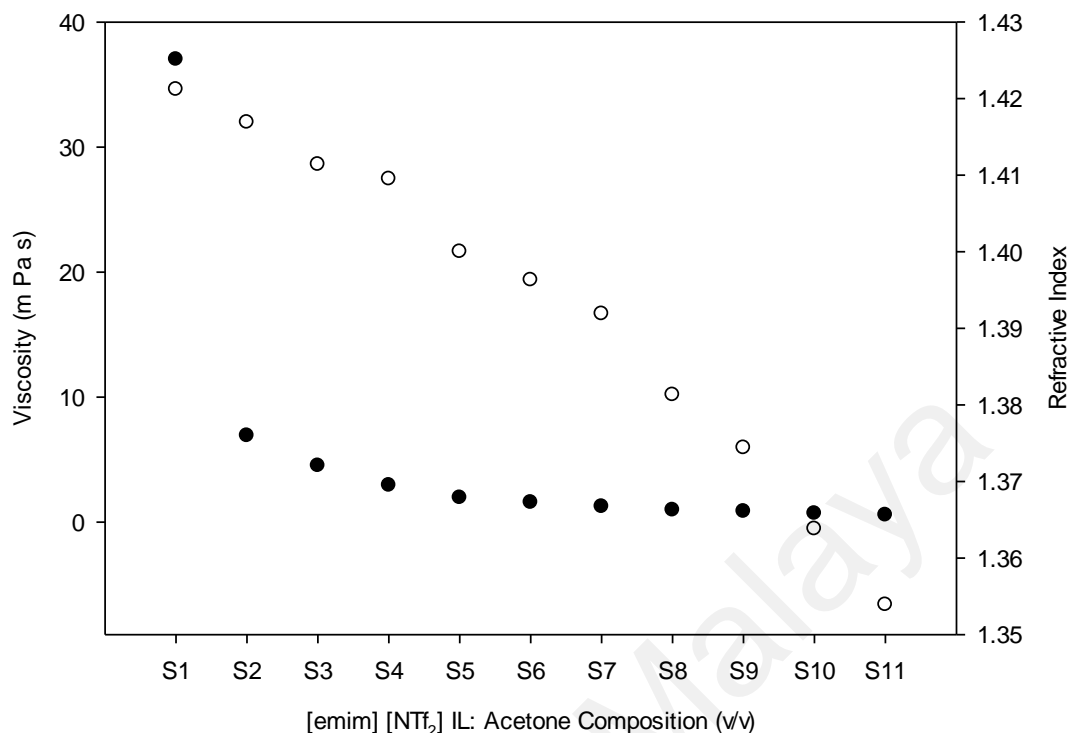


**Figure 4.12:** Viscosity (●) and RI (○) value of binary mixtures at various [emim][NTf<sub>2</sub>] IL: acetone compositions

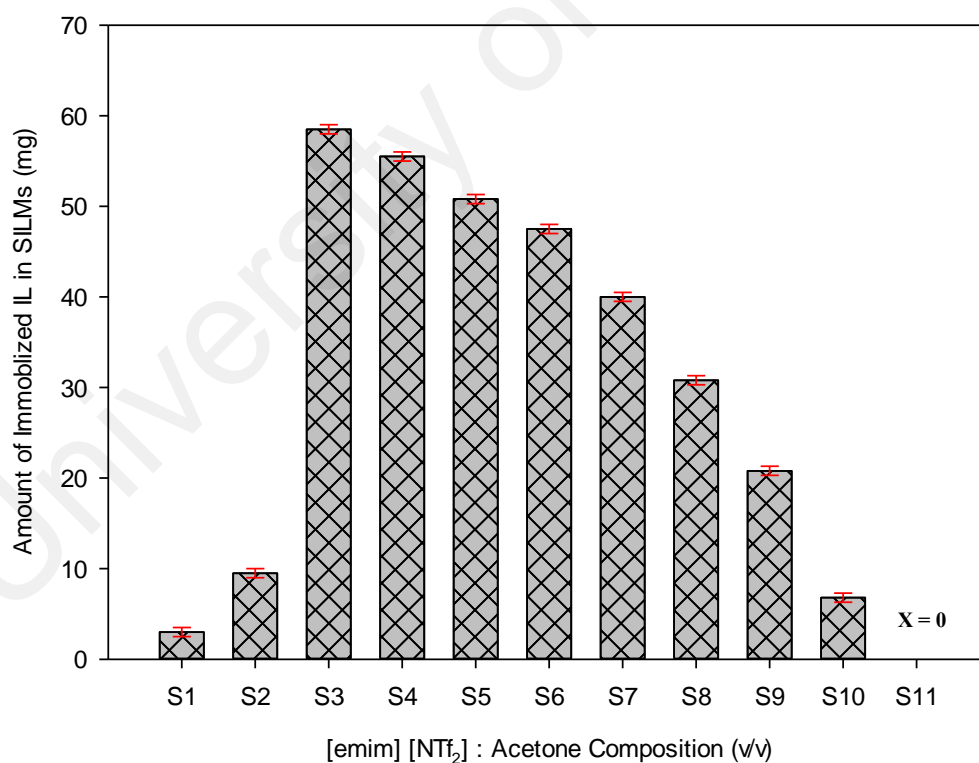
#### 4.2.2 Supported ionic liquid membranes (SILMs)

Figure 4.13 shows the amount of ionic liquid embedded in SILMs as classified by weight differences. Based on the figure, the greatest extent of ionic liquid immobilized was acquired with S3; hence this condition was taken as the optimal composition for SILMs preparation. The liquid membrane phase weight increased from 3 mg (S1) to 58.50 mg (S3) and then dropped continuously to 6.80 mg (S10). The reduction in viscosity of the ionic liquid due to the decline of the capillary force is a basis to elucidate the increase of the amount of immobilized IL on the membranes support of S1 to S3, for which consequently allowing the ionic liquid to penetrate through the porous membrane more efficiently (refer Table 4.3). Nevertheless, it was found that the increase of acetone composition from 30% to 90% in the binary mixtures had caused the

loading of immobilized IL on the S4 to S10 membranes to decrease. This is due to the decreasing IL composition and insufficient amount of IL to be supported in the SILMs.

**Table 4.3:** Viscosity, RI, and the amount of immobilized IL at various [emim] [NTf<sub>2</sub>] IL: acetone composition

SILMs	ILs: Acetone (% v/v)	Viscosity (mPas)	RI	Immobilized ILs (mg)
S1	100:0	37.00	1.4212	3.00
S2	90:10	6.91	1.4169	9.50
S3	80:20	4.50	1.4114	58.50
S4	70:30	2.94	1.4095	55.50
S5	60:40	1.95	1.4000	50.80
S6	50:50	1.57	1.3963	47.50
S7	40:60	1.24	1.3919	40.00
S8	30:70	0.97	1.3813	30.80
S9	20:80	0.85	1.3744	20.80
S10	10:90	0.69	1.3638	6.80
S11	0:100	0.57	1.3539	0.00



**Figure 4.13:** Effect of [emim] [NTf<sub>2</sub>] IL: acetone composition (v/v) on the amount of immobilized IL of SILMs preparation

The microscopic characterization of the surface structures of the membranes was conducted using FESEM. From this observation, it was clearly seen that IL has successfully been immobilized into the external and internal sides of the membranes. Figure 4.14 consists of FESEM micrographs of the PP and SILMs membranes, which were based on (100:0), (80:20) and (10:90) of IL: acetone volume ratio, and prepared via the dipping method. Initial analysis of the structure of the PP polymeric membrane in the FESEM micrographs shows a highly porous material composing of a network of microspores with a mean size of 0.03  $\mu\text{m}$  (refer to Figures 4.14(a) and 4.14(a1)). After the immobilization of the [emim] [NTf<sub>2</sub>] ionic liquid on the blank PP membrane, the SILMs were examined to verify their homogeneity and distribution.

Based on FESEM micrograph analysis presented in Figures 4.14(d) and 4.14(d1), it can be seen that after the impregnation with low [emim] [NTf<sub>2</sub>] IL: acetone composition (10:90); homogenous distribution of the IL on the membrane was not observed and the pores of the membranes were occupied with few IL filling. In addition, the existence of an inadequate amount of ionic liquid on the outer membrane surfaces was apparent in this condition, since the membranes wall was clearly visible in micrograph 4.14(d1). However, the immobilization of 80% of [emim] [NTf<sub>2</sub>] IL: 20% of acetone (v/v) into membrane support appeared to completely fill the membrane pores, and was homogeneously distributed (refer to Figures 4.14(c) and 4.14(c1)).

On the other extreme, Figures 4.14(b) and 4.14(b1) indicate immobilization and poor distribution (overlapping) of the ionic liquid on the outermost layers of the membranes when pure [emim] [NTf<sub>2</sub>] ionic liquid was used. The possible factor to this was the great capillary force associated with the highly viscous liquid, which increased makes it

inconvenient to diffuse into the pores of the membrane. The significance of liquid viscosity on the degree of IL immobilization was validated, provided that there be correlations between these observations and the viscosity of the ionic liquid. Thus, in this study, SILMs based on 80:20 of [emim] [NTf<sub>2</sub>] IL: acetone composition (S3) prepared at optimal composition for SILMs was selected for further investigation. Selection of S3 membranes for the operation was supported by the facts that leakage of ILs outside of the membrane would occurred during the absorption process with the use of pure ILs as a supporting phase, due to an excessive supply of ILs into the membrane and self-cohesiveness of ionic liquid. To resolve the problem, the ILs was diluted with the use of co-solvent (Kim et al., 2011).

Based on Figure 4.15(a), the characteristic peak assigned to C (Carbon) K $\alpha$  line is shown by the EDX spectrum of the PP membrane. The comparative peak height of equivalent elements in a different membrane is associated with their particular concentrations. The existence of these chemical elements corresponds to the predicted chemical formulation of polypropylene. Nonetheless, hydrogen is a lighter chemical element; hence, it could not be detected by EDX. In Figures 4.15(b)-(d), the presence of F (Fluorine), S (Sulphur), O (Oxygen) and N (Nitrogen) elements from [NTf<sub>2</sub>] anion; or peaks spectrum of the SILMs, signified the absorption of IL in the PP membranes. Therefore, the differences in the elemental composition of the SILMs have provided quantitative results, which significantly corroborated FESEM's morphological and EDX spectral results.

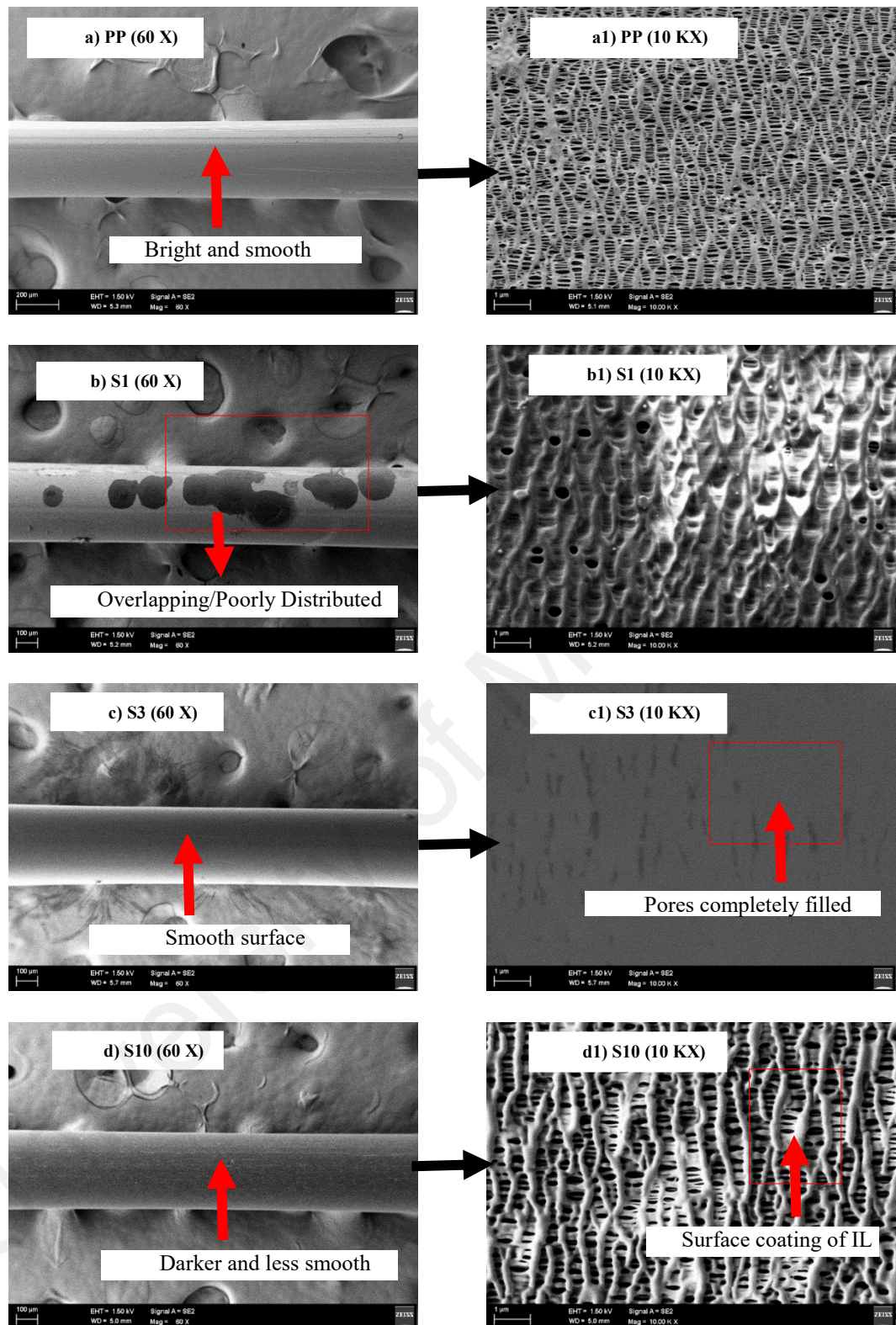


**Figure 4.14:** Micrographs of scanning electron of blank PP and prepared SILMs membranes (outer layer) at different magnifications (Secondary Electron)

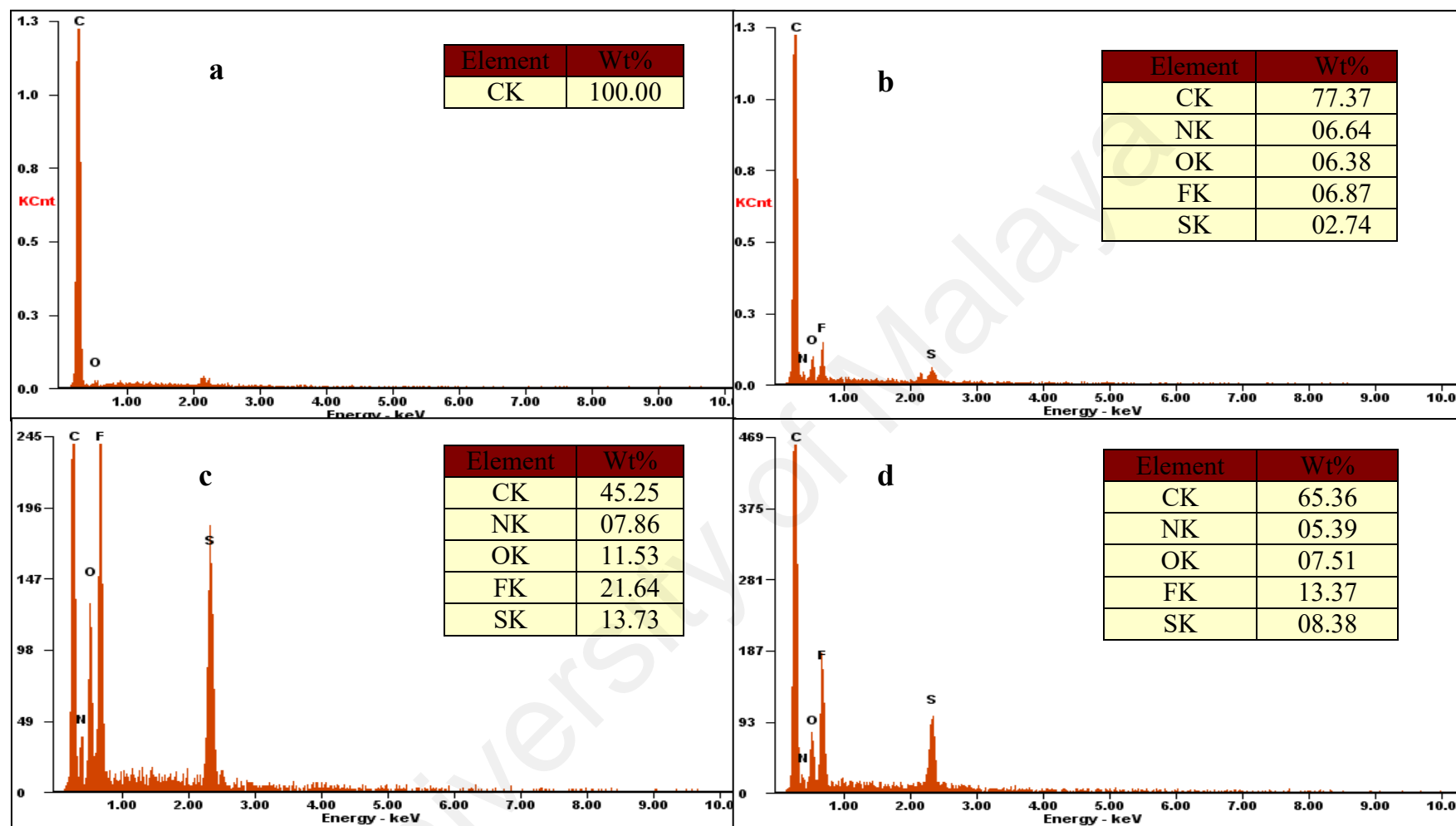
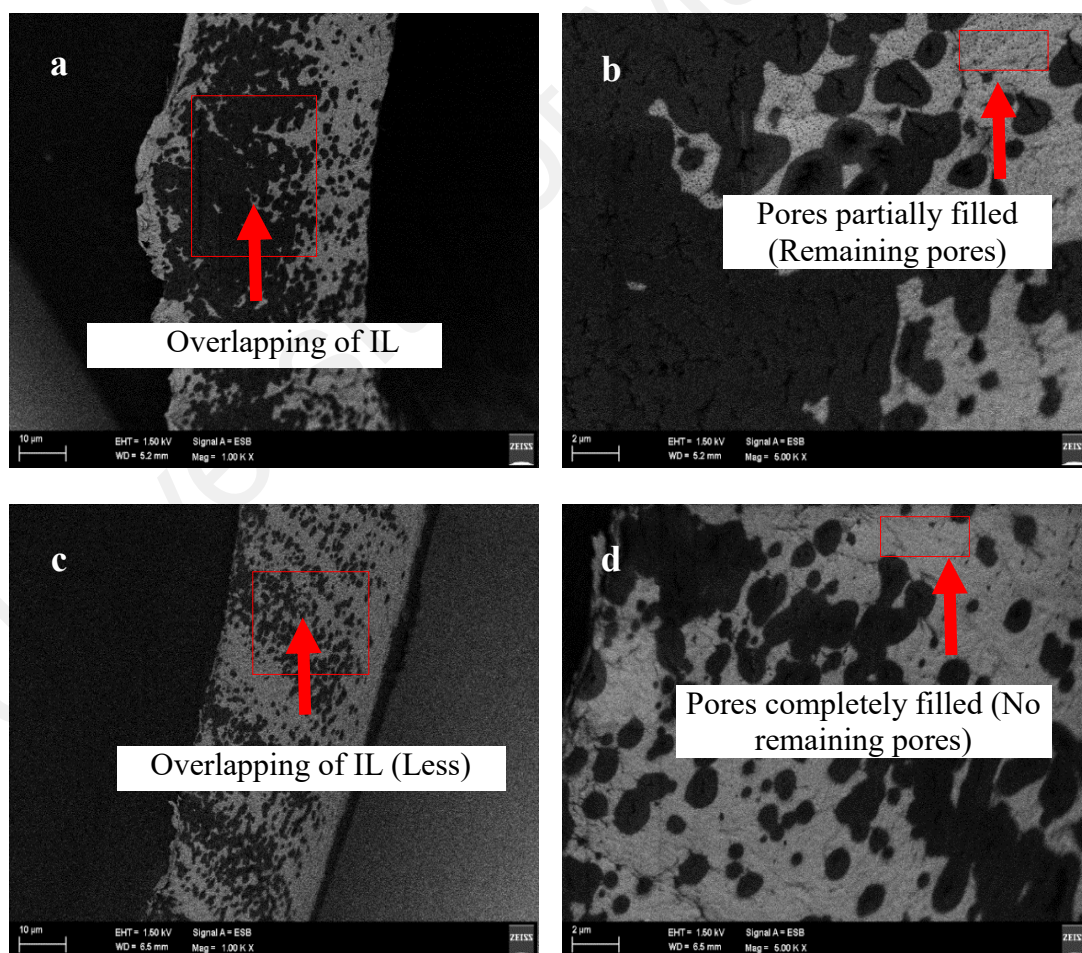


Figure 4.15: EDX spectra of a) PP, b) S1, c) S3 and d) S10 membranes



Based on Figure 4.16, through the use of backscattered electrons (ESB) imaging mode – results have shown that the C, F, S, N and O elements from [emim] [NTf<sub>2</sub>] ionic liquid scattered more effectively; compared to the lighter C element that existed in porous supports. Therefore, the contrast from IL elements should appear brighter than the contrast of the C element in PP membranes. However, the overlapping of the IL amount within the membrane pores (interior) led to the increase of the contrast's darkness; compared to the presence of light elements in the membranes. On the other hand, no remaining pores were observed in the case of (80: 20 – S3) compared to (10: 90 – S10) [emim] [NTf<sub>2</sub>] IL: acetone compositions as noticeably shown in Figures 4.16(d) and 6(b), respectively.



**Figure 4.16:** Micrographs of scanning electron (interior side) of a) S10 at 1000X, b) S10 at 5000X, c) S3 at 1000X and d) S3 membranes at 5000X magnification (Backscattered)

### 4.2.3 SILMs stability

Since CO<sub>2</sub> absorption efficiency in membrane contactors depends on the changes occurring in the pores of membranes, the stability of the SILMs was also examined by submerging the membranes in amine solutions before analyzed using FESEM microscopy. The purpose of this approach was to identify the specific alterations of the membranes structure, the form and dimension of the pores in particular, and potential harms to the cell walls. Figure 4.17 illustrates the FESEM images, which depict the porous structure of PP hollow fiber membranes 14 days before and after submersion in amine solutions (pure MEA and 2M MEA). Prior to the submersion, the cell walls within the neat fiber were fairly identical and small (Figure 4.17(a)). After 14 days in contact with the MEA solutions, enlargement of the membrane pores were observed while the membrane's surface experienced morphological degradation, as illustrated in Figures 4.17(b) and 4.17(c). To support these observations, Table 4.4 describes the data related to the pore enlargement process, with the presence of liquids.

The surface tension of 2M MEA (56.52 mN m<sup>-1</sup>) was greater than that of pure MEA (48.14 mN m<sup>-1</sup>) (Va'zquez et al., 1997); which were consistent with the extent of degradation perceived in the FESEM images. These experimental findings suggest a significant relationship between the structural stability of membrane pores and the surface tension of the surrounding phase (Lv et al., 2010; Wang et al., 2005). The solutions with lesser surface tension could penetrate the pores more efficiently (Mansourizadeh et al., 2010; Zhao et al., 2012). Upon diffusion, the liquid meniscus enforced the pore walls and eliminated them. The FESEM images also portrayed that pure MEA could penetrate into the neat PP membrane pores easily, enlarging the pores and breaking the walls of the membrane pores. All of these observations and findings



were in an agreement with the previous reported studies (Kladkaew et al., 2011; Saiwan et al., 2011).

Membrane stability studies were also conducted to substantiate the potential displacement of ionic liquids from the membrane pores to the surrounding media throughout the operation. Micrographs 4.17(d)-(f) demonstrated the morphological appearance of the PP membrane infused with 80:20 (S3) of [emim] [NTf<sub>2</sub>] ILs: acetone before and after a 14-day cell operation in pure MEA and 2M MEA, respectively. It was also perceived that a minimal amount of [emim] [NTf<sub>2</sub>] ionic liquid remained perpetually on the external surface (bright areas). In addition, some pores of the membrane were partly filled after a long-term operation while aqueous phase of MEA was used as surrounding phase as shown in micrograph 4.17(f).

**Table 4.4:** Mean sizes of membrane pores before and after immersion with MEA solutions for 14 days at 70°C

Types of membranes	Mean sizes of membrane pores (nm)
PP	30.00 ± 2.20
PP-MEA	50.85 ± 3.50
PP-2M MEA	37.55 ± 2.40
S3	0.05 ± 0.01
S3-MEA	6.10 ± 2.70
S3-2M MEA	1.25 ± 0.50

**Table 4.5:** Amount of immobilized IL in S3 membranes before and after immersion in MEA solution for 14 days at 70°C

Types of Membrane	SILMs weight before immersion (mg)	SILMs weight after immersion (mg)	% of IL losses SILMs
S3-MEA	75.50	10.20	86.50
S3-2M MEA	75.50	60.50	19.90

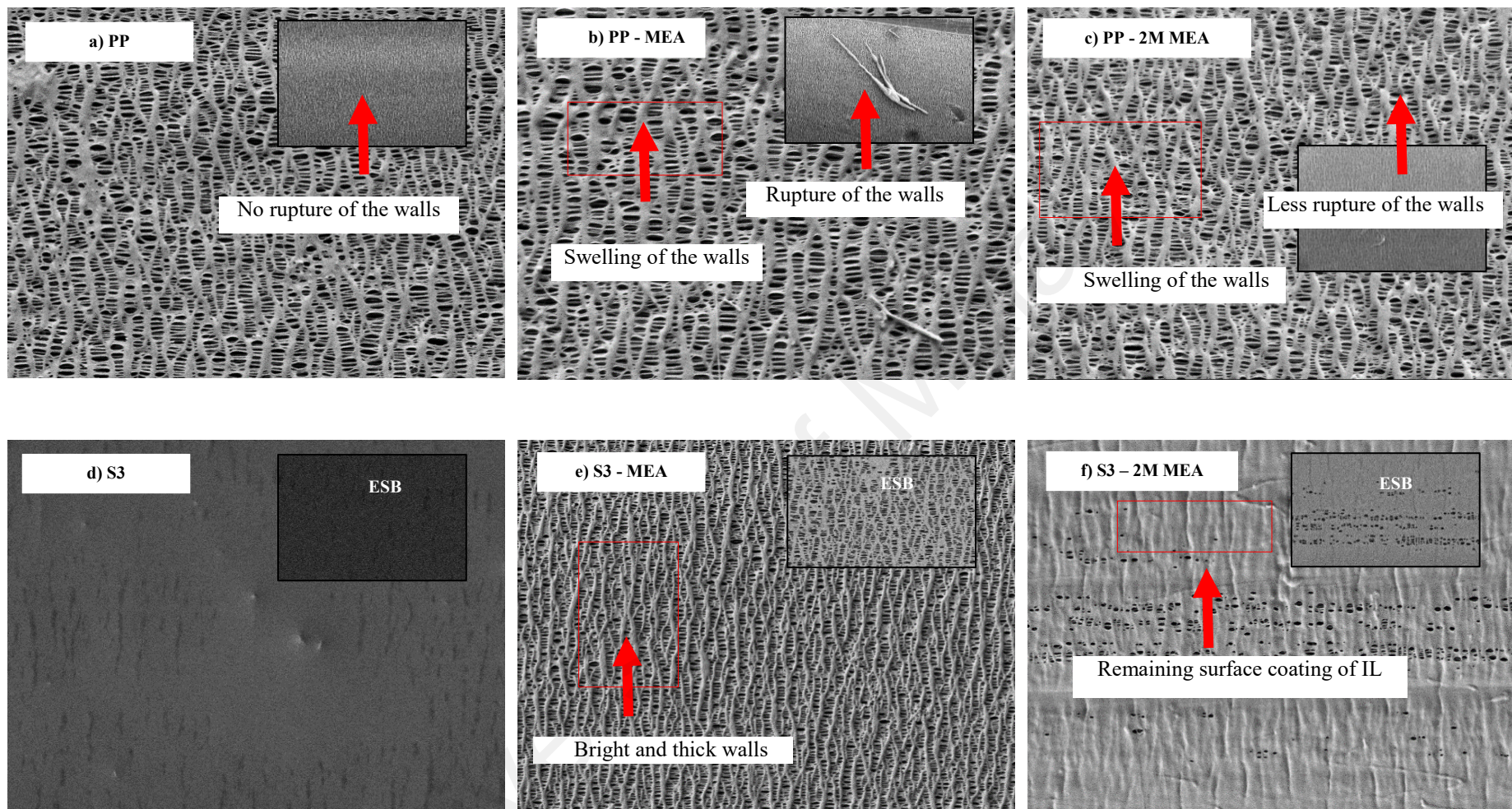


**Figure 4.17:** Micrographs of scanning electron of blank PP and S3 membranes before and after immersion with MEA solution for 14 days at 70°C (10000X magnification)

Figures 4.18 and 4.19 illustrate a comparison of EDX spectra of PP and SILMs based on 80:20 of [emim] [NTf<sub>2</sub>] IL: acetone composition (S3), before and after the immersion in pure and aqueous solutions of MEA for 14 days. For SILMs (see Figure 4.19), it was shown by the results that there were extensive losses of ionic liquid from the membrane after the immersion in pure MEA. In the case of immersion in an aqueous solution of MEA, less substantial losses of IL occurred from this process, which indicated that a large amount of the IL persisted within the pores of the membranes. Accordingly, the membranes could be regarded as more stable in 2M MEA solution. However, the losses of immobilized ionic liquid attained by weight differences can be elucidated by the fact that some of the ionic liquid deposited on the exterior surface of SILMs was mainly miscible with the solvent used; and the immobilized ionic liquid is simply eliminated during the process (Matsumoto et al., 2010; S. Kislik, 2010). The percentages of IL losses are tabulated in Table 4.5. Therefore, the use of [emim] [NTf<sub>2</sub>] IL as supporting phase in SILMs had increased the stability of the PP membrane by reducing solution penetration into the pores and stabilizing the pore structures. In terms of SILMs, the structural degradation has been found to be less significance. Therefore [emim] [NTf<sub>2</sub>] IL also acts as a stabilizer. In addition, SILMs stability and performances studied by Kim and co-workers in 2011 for CO<sub>2</sub>/N<sub>2</sub> separation process verified that SILMs immobilized via dipping method for 24 hours is more effective in comparison with forced immobilization, with good stability under pressure up to 1.5 bars, exhibited high permeability and selectivity as well as good reproducibility (Kim et al., 2011).

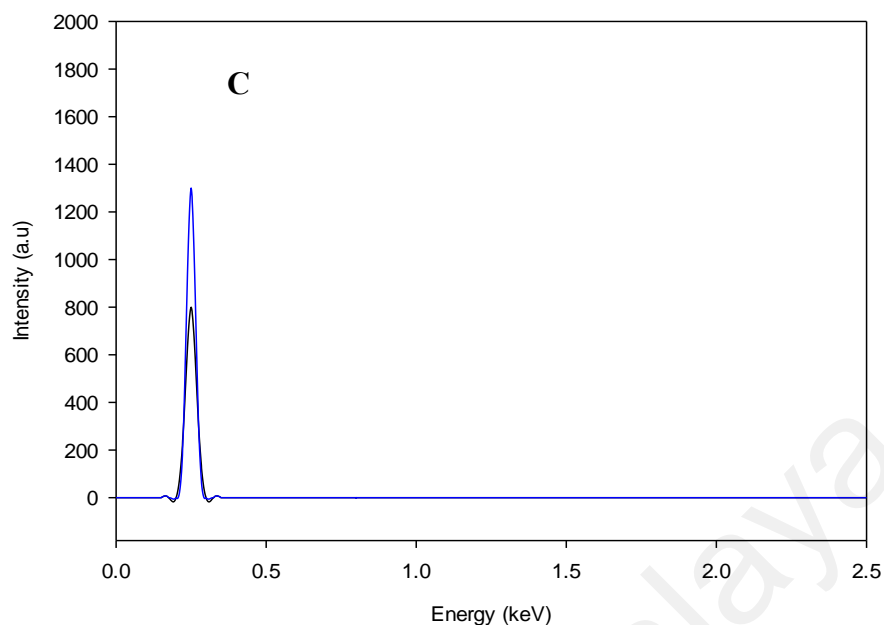


**Figure 4.18:** EDX spectra of PP membranes before and after immersion in MEA solution for 14 days at 70°C where (-) blank PP, (-) PP - pure MEA and (-) PP - 2M MEA

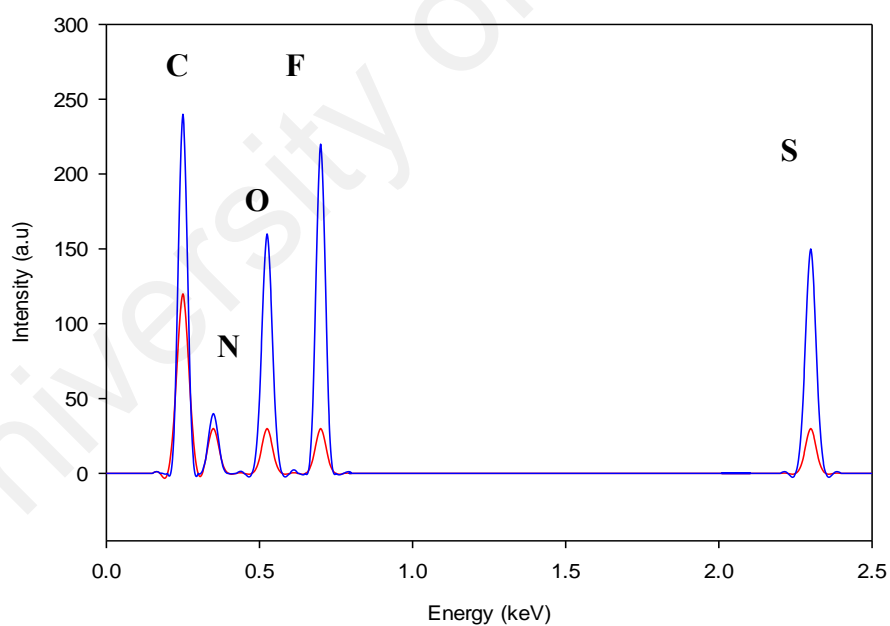


**Figure 4.19:** EDX spectra of S3 membranes before and after immersion in MEA solution for 14 days at 70°C where (-) S3 – 2M MEA, (-) S3 - pure MEA and (-) S3

#### 4.2.4 Summary (Section 4.2)

The highlight of this work is a comparative study on the preparation of hollow fiber supported ionic liquid membranes (SILMs) with the use of various [emim] [NTf<sub>2</sub>] IL: acetone composition under dipping technique. It was carried out in two stages: the impregnation of fresh membranes with IL, and its chemical stability after the immersion in an MEA solution after 14 days. The number of immobilized IL was influenced by the viscosity and RI of the binary mixtures. Additionally, less IL was absorbed into the membranes with the use of pure [emim] [NTf<sub>2</sub>] IL; compared to diluted IL.

A FESEM-EDX study was conducted for PP and SILMs, based on (80:20) of [emim] [NTf<sub>2</sub>] IL: acetone composition (S3) in different surrounding phases. In terms of SILMs, when 2M MEA was used as a surrounding phase, the membranes experienced less substantial IL loss after 14 days of operation. On the contrary, when MEA was used as contacting phases; almost all of the immobilized IL was lost from the membranes. Apart from that, the stability of the resulting SILMs increased when the surface tension of the surrounding phases increased, as demonstrated and confirmed by FESEM-EDX technique. In conclusion, the vital role played by the binary mixture viscosity for the preparation of supported ionic liquid membranes has been highlighted in this study. Besides, data on absorption performances and selectivity of CO<sub>2</sub>/O<sub>2</sub> are hard to find, especially in gas-liquid membrane contactor system. Therefore, considering [emim] [NTf<sub>2</sub>] IL as a supporting material in supported ionic liquid membranes (SILMs), using aqueous phase of MEA as an absorbent would result in a great membrane-solvent combination system in furthering our gas-liquid membrane contactor process.

University of Malaya

### 4.3 CO<sub>2</sub> absorption performance of the SILM contactor in parallel flow mode

To evaluate the process efficiency of both systems at different temperatures and gas velocities, carbon dioxide absorption experiments were carried out in a blank and supported ionic liquid membrane (SILM) contactors. The CO<sub>2</sub> absorption flux of the module can be calculated as per Eqn. 4.1:

$$J_{CO_2} = \frac{(C_{lo} - C_{li})Q_l}{A_i} \quad (4.1)$$

where  $J_{CO_2}$ , is the CO<sub>2</sub> absorption flux (mol m<sup>-2</sup> s<sup>-1</sup>),  $Q_l$  is the liquid flow rate (m<sup>3</sup> s<sup>-1</sup>),  $A_i$  is the inner surface of the hollow fiber membranes (m<sup>2</sup>),  $C_{li}$  and  $C_{lo}$  are the liquid phase CO<sub>2</sub> concentrations (mol m<sup>-3</sup>) at inlet and outlet of the membrane module, respectively. The experimental CO<sub>2</sub> absorption efficiency can be calculated as per Eqn. 4.2:

$$\text{Efficiency, } \eta (\%) = \left(1 - C_{lo}/C_{li}\right) \times 100 \quad (4.2)$$

Figures 4.20 and 4.21 show the experiments of both systems being conducted at different temperatures (303, 318, 333 and 348 K) with a gas velocity of  $4.63 \times 10^{-6}$  m s<sup>-1</sup>. The outlet concentration of carbon dioxide is calculated as  $C_{CO_2,(g),out}/C_{CO_2,(g),in}$ . Meanwhile, Figure 4.22 and 4.23 show the experiment of operating with gas velocity that ranges from  $4.63 \times 10^{-6}$  to  $3.70 \times 10^{-5}$  m s<sup>-1</sup> at 303 K using blank (Figure 4.22) and supported ionic liquid membrane (Figure 4.23) contactor, respectively. The outlet concentration dimensionless of carbon dioxide was calculated for each experiment at pseudo-steady-state, that ranges between a) 0.61 to 0.64 (blank contactor) and 0.19 to 0.21 (supported ionic liquid membrane contactor) at different temperatures and

approximately b) 0.61 to 0.99 (blank contactor) and 0.19 to 0.96 (supported ionic liquid membrane contactor) in the case of different gas velocities.

The CO<sub>2</sub> removal efficiencies were calculated from inlet and outlet CO<sub>2</sub> concentrations of the absorption experiments. In Figure 4.24, the efficiency and mass transfer rate of CO<sub>2</sub> is plotted as a function of absorbent temperature for both membrane contactor systems. The gas and liquid velocities were considered to be constant at  $4.63 \times 10^{-6}$  and  $9.26 \times 10^{-6} \text{ m s}^{-1}$ , respectively. For blank membrane, when absorbent temperature increased from 303 to 348 K; the CO<sub>2</sub> absorption efficiency and mass transfer rate was slightly decreased from 39.13 to 36.23% and from  $2.15 \times 10^{-6}$  to  $1.99 \times 10^{-6} \text{ mol m}^2 \text{ s}$ . Meanwhile for the SILM system, data had shown that the CO<sub>2</sub> absorption efficiency decreases from 80.68 to 79.23%; with the increase of absorbent temperature of 303 to 348 K. By increasing the absorbent temperature, the absorption flux decreases from  $4.43 \times 10^{-6}$  to  $4.36 \times 10^{-6} \text{ mol m}^2 \text{ s}$ . It is known that the increase in temperature favoured reaction rate, according to the Arrhenius expression of reaction rate constant (Dindore et al., 2005; Kumar et al., 2002), and diffusion (Snijder et al., 1993). In addition, the increase in temperature also resulted in a decrease in CO<sub>2</sub> solubility (Song et al., 2003) and an increase in evaporation of absorbent; which are not conducive to absorption (Tan & Chen, 2006). When increasing the temperature of amine solutions, the effects of temperature on reaction rate and diffusion rate are perhaps higher than that on CO<sub>2</sub> solubility (Kim & Yang, 2000). However, the temperature effect is reversed in this study. A more favourable CO<sub>2</sub> removal condition can be seen with a low temperature operation. The reduction of mass transfer rate with an increase in temperature is therefore believed to be more affected by the CO<sub>2</sub> solubility decrease. The results have shown that CO<sub>2</sub> solubility decreases rapidly with an increase in



temperature especially in lower CO<sub>2</sub> loading, and was confirmed by previous works (Song et al., 2006; Tan & Chen, 2006). As discussed above, it should be noted that increasing the absorbent temperature of 2M MEA have been known to reversely influence the efficiency and mass transfer rate of CO<sub>2</sub>. Therefore, a relatively lower value of temperature should be selected for this study.

Furthermore, the impact of gas velocities on the mass transfer rate and absorption efficiency of CO<sub>2</sub> is demonstrated in Figure 4.25. When the gas velocity increases from  $4.63 \times 10^{-6}$  to  $3.70 \times 10^{-5} \text{ m s}^{-1}$ , the residence time of CO<sub>2</sub> in the membrane contactor is reduced significantly. The CO<sub>2</sub> absorption efficiency and flux also dropped continuously and remarkably from 39.13 to 1.45% and from  $2.15 \times 10^{-6}$  to  $8.33 \times 10^{-8} \text{ mol m}^2 \text{ s}$ , respectively. In comparison with similar trends, the efficiency and flux of SILMs respectively measured from 80.68 to 3.86% and from  $4.43 \times 10^{-6}$  to  $2.14 \times 10^{-7} \text{ mol m}^2 \text{ s}$ , were found to be doubled from the blank system. From the results obtained as per Figures 4.20 to 4.25, there were a few remarks that was noted for both systems: (i) the efficiency increases with decreasing gas velocities, (ii) the efficiency decreases with increasing temperatures, (iii) the temperature had a minor influence towards CO<sub>2</sub> absorption process when compared to the dominant impact of gas velocities, and more importantly (iv) the efficiency and residence time in supported ionic liquid membrane was slightly higher as compared to a blank contactor system; which doubles the efficiency values from 303 to 348 K and from  $4.63 \times 10^{-6}$  to  $3.70 \times 10^{-5} \text{ m s}^{-1}$ .

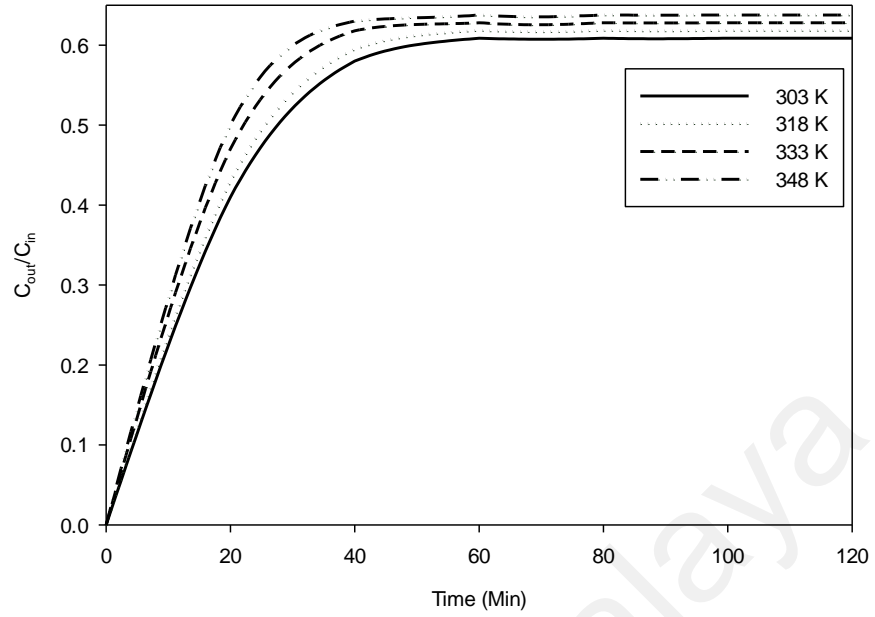


**Figure 4.20:** CO<sub>2</sub> outlet concentration (dimensionless) versus experimental time (time required to achieve steady-state) of blank membrane contactor system at different temperatures (Operating conditions: absorbent concentration = 2M MEA; absorbent temperatures = 303 to 348 K; gas velocity =  $4.63 \times 10^{-6} \text{ m s}^{-1}$ ; liquid velocity =  $9.26 \times 10^{-6} \text{ m s}^{-1}$ ; gas inlet composition (v/v %) = 10% of CO<sub>2</sub>: 10% of O<sub>2</sub> and N<sub>2</sub> balances)

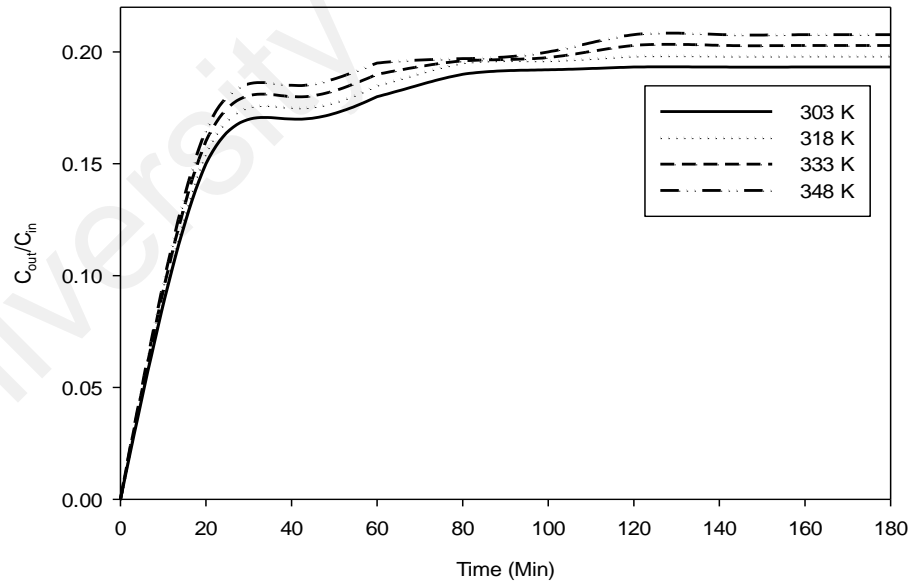


**Figure 4.21:** CO<sub>2</sub> outlet concentration (dimensionless) versus experimental time (time required to achieve steady-state) of supported ionic liquid membrane contactor system at different temperatures (Operating conditions: absorbent concentration = 2M MEA; absorbent temperatures = 303 to 348 K; gas velocity =  $4.63 \times 10^{-6} \text{ m s}^{-1}$ ; liquid velocity =  $9.26 \times 10^{-6} \text{ m s}^{-1}$ ; gas inlet composition (v/v %) = 10% of CO<sub>2</sub>: 10% of O<sub>2</sub> and N<sub>2</sub> balances)

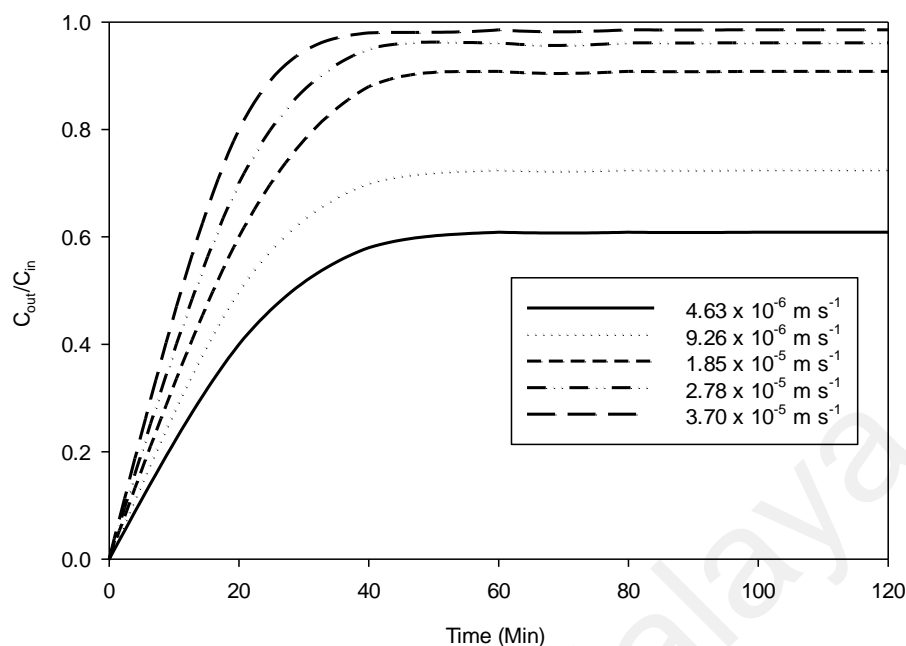


**Figure 4.22:** CO<sub>2</sub> outlet concentration (dimensionless) versus experimental time (time required to achieve steady-state) of blank membrane contactor system at different gas velocities (Operating conditions: absorbent concentration = 2M MEA; absorbent temperature = 303 K; gas velocities =  $4.63 \times 10^{-6}$  to  $3.70 \times 10^{-5} \text{ m s}^{-1}$ ; liquid velocity =  $9.26 \times 10^{-6} \text{ m s}^{-1}$ ; gas inlet composition (v/v %) = 10% of CO<sub>2</sub>: 10% of O<sub>2</sub> and N<sub>2</sub> balances)

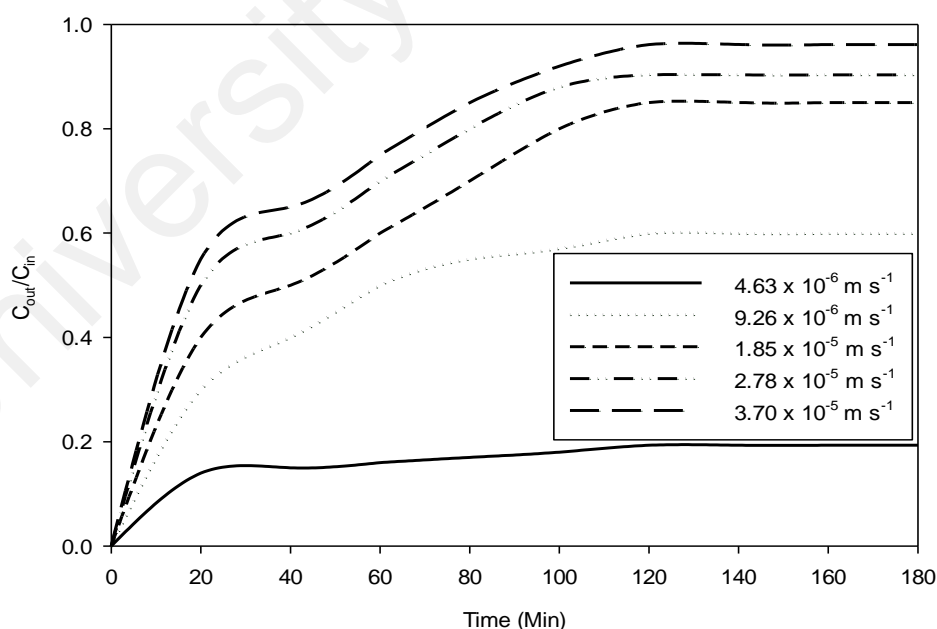


**Figure 4.23:** CO<sub>2</sub> outlet concentration (dimensionless) versus experimental time (time required to achieve steady-state) of supported ionic liquid membrane contactor system at different gas velocities (Operating conditions: absorbent concentration = 2M MEA; absorbent temperature = 303 K; gas velocities =  $4.63 \times 10^{-6}$  to  $3.70 \times 10^{-5} \text{ m s}^{-1}$ ; liquid velocity =  $9.26 \times 10^{-6} \text{ m s}^{-1}$ ; gas inlet composition (v/v %) = 10% of CO<sub>2</sub>: 10% of O<sub>2</sub> and N<sub>2</sub> balances)

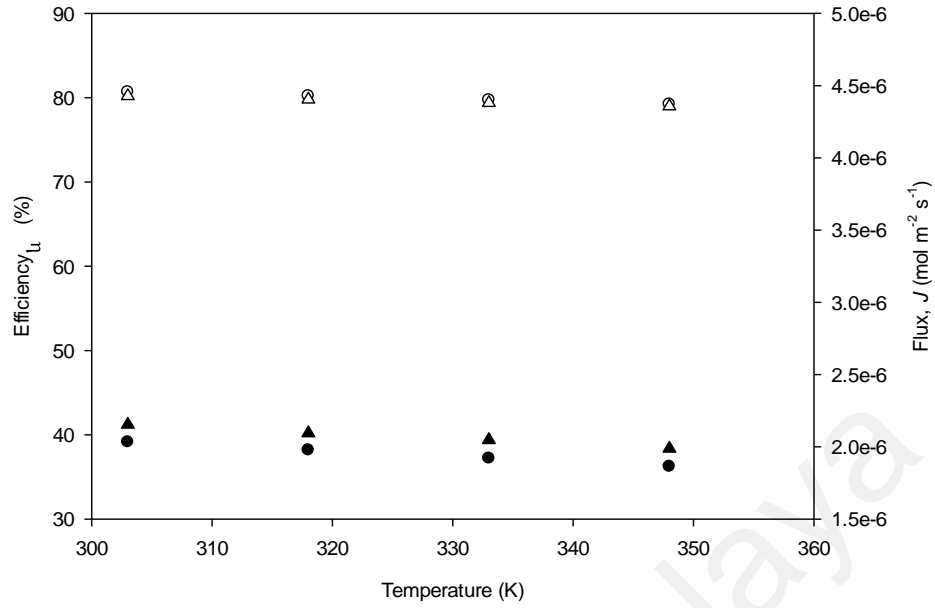


**Figure 4.24:** CO<sub>2</sub> absorption performances of both membrane contactor systems at different temperatures where (●) Efficiency – Blank, (○) Efficiency – SILM, (▲) Flux – Blank and (△) Flux – SILM (Operating conditions: absorbent concentration = 2M MEA; absorbent temperatures = 303 to 348 K; gas velocity =  $4.63 \times 10^{-6} \text{ m s}^{-1}$ ; liquid velocity =  $9.26 \times 10^{-6} \text{ m s}^{-1}$ ; gas inlet composition (v/v %) = 10% of CO<sub>2</sub>: 10% of O<sub>2</sub> and N<sub>2</sub> balances)

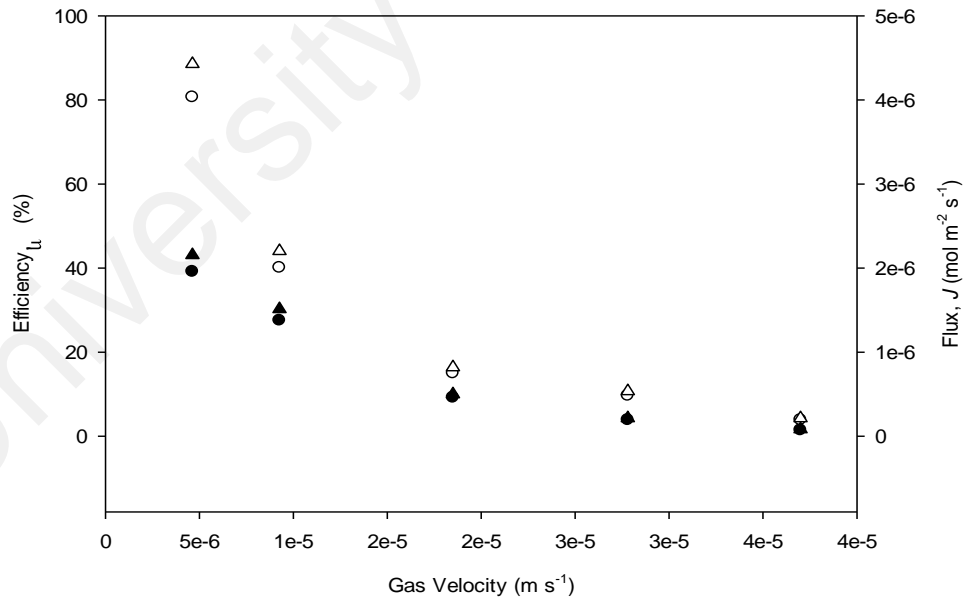


**Figure 4.25:** CO<sub>2</sub> absorption performances of both membrane contactor systems at different gas velocities where (●) Efficiency – Blank, (○) Efficiency – SILM, (▲) Flux – Blank and (△) Flux – SILM (Operating conditions: absorbent concentration = 2M MEA; absorbent temperature = 303 K; gas velocities =  $4.63 \times 10^{-6}$  to  $3.70 \times 10^{-5} \text{ m s}^{-1}$ ; liquid velocity =  $9.26 \times 10^{-6} \text{ m s}^{-1}$ ; gas inlet composition (v/v %) = 10% of CO<sub>2</sub>: 10% of O<sub>2</sub> and N<sub>2</sub> balances)

#### 4.3.1 Selectivity of the SILM contactor in parallel flow mode

It is with high regards, that the information that was obtained from previous COSMO-RS predictions is valuable to identify the selectivity of CO<sub>2</sub>/O<sub>2</sub> in a gas-liquid membrane contactor system for selected ionic liquids. The outcome from the predictions have demonstrated that [emim] [NTf<sub>2</sub>] IL could be a good candidate as supporting material for SILMs, which was attributed to higher CO<sub>2</sub>/O<sub>2</sub> selectivity characteristics as compared to others. For the parallel flow mode system, selectivity data was obtained by plotting the outlet concentration profiles of CO<sub>2</sub> and O<sub>2</sub> for each run at different absorbent temperatures and gas velocities. Typical CO<sub>2</sub> and O<sub>2</sub> loadings at steady state with selectivity data at various operating conditions for the blank and SILM system are provided in Figures 4.26 to 4.29 respectively. To investigate the absorbent temperature effects towards the selectivity of CO<sub>2</sub>/O<sub>2</sub>, a profile of CO<sub>2</sub> and O<sub>2</sub> loading as shown in Figure 4.26 was evaluated. The outlet concentrations of CO<sub>2</sub> and O<sub>2</sub> were calculated for each experiment at pseudo-steady-state that ranged between a) 1.81 to 1.67 mol m<sup>-3</sup> of CO<sub>2</sub> and 0.13 to 0.18 mol m<sup>-3</sup> of O<sub>2</sub> for blank system and b) 3.72 to 3.66 mol m<sup>-3</sup> of CO<sub>2</sub> and 0.05 to 0.09 mol m<sup>-3</sup> of O<sub>2</sub> for SILM system. It is obvious that the loading of CO<sub>2</sub> of the run that was conducted at 303 K was higher than those carried out at the higher temperatures of 318, 333 and 348 K. The loading of O<sub>2</sub> was found to have increased, if the temperature increase was due to the reduction of CO<sub>2</sub> loadings attributed to the low solubility of CO<sub>2</sub> in MEA solution at higher temperatures. Therefore, selectivity of CO<sub>2</sub>/O<sub>2</sub> of the run at 303 K measured at 13.9 was slightly higher than those at 318, 333 and 348 K, respectively, measured at 11.7, 10.8 and 9.3 for blank membrane; and declined from 74.4 to 40.7 for SILM system (Figure 4.27). Based on initial analysis, MEA have shown a tendency to degrade if temperature in the system were increased (Davis & Rochelle, 2009). This is due to the reduction of CO<sub>2</sub> loading that would lead to the enhancement of MEA degradation attributed to the increase of O<sub>2</sub> loading in the

solvent system (Supap et al., 2009). The MEA degradation rate was higher at a lower CO<sub>2</sub> loading, than at a higher CO<sub>2</sub> loading. Then again, the degradation rate in the MEA-CO<sub>2</sub>-O<sub>2</sub> system was found to be 8.3 times higher as that in the MEA-CO<sub>2</sub> system. This shows that MEA is more prone to degradation in the presence of O<sub>2</sub>, as compared to the presence of only CO<sub>2</sub> (Rooney et al., 1998).

Meanwhile, in the case of different gas velocities, the measured loading of CO<sub>2</sub> and O<sub>2</sub> was a) 1.81 to 0.07 mol m<sup>-3</sup> of CO<sub>2</sub> and 0.13 to 0.19 mol m<sup>-3</sup> of O<sub>2</sub> for blank system and b) 3.72 to 0.18 mol m<sup>-3</sup> of CO<sub>2</sub> with 0.05 to 0.09 mol m<sup>-3</sup> of O<sub>2</sub> for SILM system. As a result, the effect of gas velocities on the selectivity of CO<sub>2</sub>/O<sub>2</sub> was evaluated using a similar approach that was used for absorbent temperature. The loadings of CO<sub>2</sub> and O<sub>2</sub> in 2M MEA is shown in Figure 4.28, while selectivity data of CO<sub>2</sub>/O<sub>2</sub> was presented in Figure 4.29. The runs were conducted at 303 K with gas velocities ranging from 4.63 x 10<sup>-6</sup> to 3.70 x 10<sup>-5</sup> m s<sup>-1</sup>. The results have shown that the selectivity for the run with 4.63 x 10<sup>-6</sup> m s<sup>-1</sup> was 37 times higher than that of the run carried out at a gas velocity of 3.70 x 10<sup>-5</sup> m s<sup>-1</sup> for both systems. From the results obtained as shown in Figures 4.26 to 4.29, some remarks are pointed out for both systems: i) the CO<sub>2</sub> loading significantly influences the loading of O<sub>2</sub>, ii) lower O<sub>2</sub> loading attributed to the higher loading of CO<sub>2</sub> in the 2M MEA, due to the fact that the higher CO<sub>2</sub> loading causes a reduction in the solubility of O<sub>2</sub> in the MEA solution and iii) selectivity of CO<sub>2</sub>/O<sub>2</sub> using supported ionic liquid membrane were always higher than that of a blank contactor system with an average selectivity factor of about 5 for both parameters.

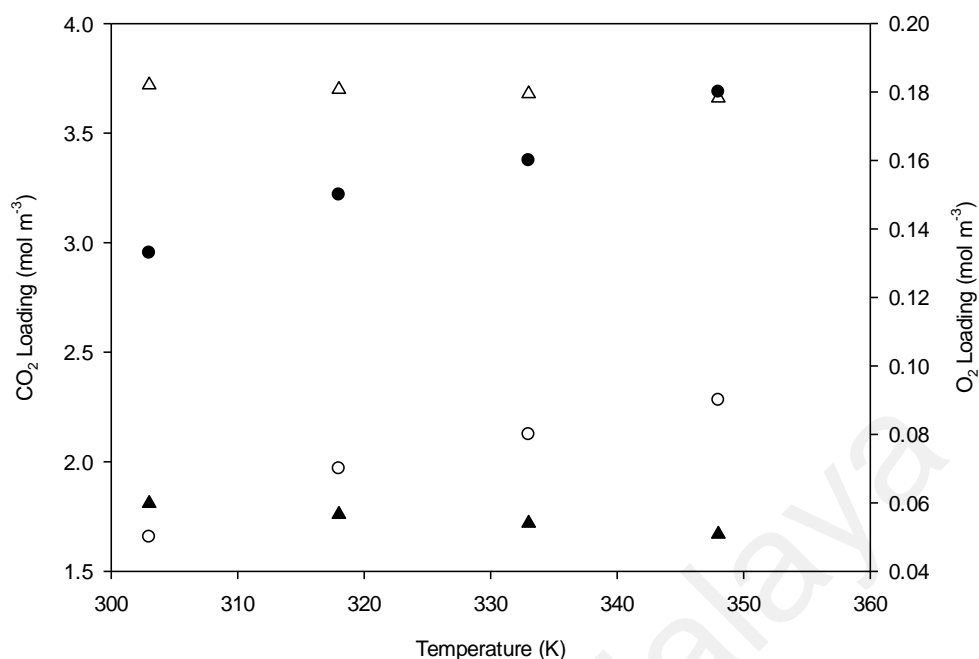


**Figure 4.26:** Loading of CO<sub>2</sub> and O<sub>2</sub> for both membranes contactor systems at different temperatures where (  $\Delta$  ) CO<sub>2</sub> loading – SILM, (  $\blacktriangle$  ) CO<sub>2</sub> loading – PP, (  $\circ$  ) O<sub>2</sub> loading – SILM and (  $\bullet$  ) O<sub>2</sub> loading – PP (Operating conditions: absorbent concentration = 2M MEA; absorbent temperatures = 303 to 348 K; gas velocity =  $4.63 \times 10^{-6} \text{ m s}^{-1}$ ; liquid velocity =  $9.26 \times 10^{-6} \text{ m s}^{-1}$ ; gas inlet composition (v/v %) = 10% of CO<sub>2</sub>: 10% of O<sub>2</sub> and N<sub>2</sub> balances)

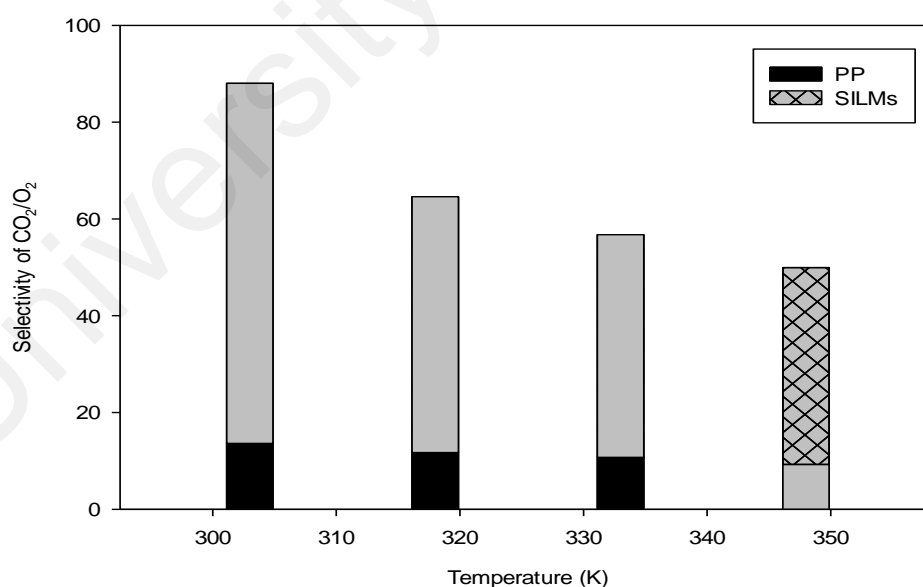


**Figure 4.27:** Selectivity of CO<sub>2</sub>/O<sub>2</sub> for blank and supported ionic liquid membrane contactor systems at different temperatures (Operating conditions: absorbent concentration = 2M MEA; absorbent temperatures = 303 to 348 K; gas velocity =  $4.63 \times 10^{-6} \text{ m s}^{-1}$ ; liquid velocity =  $9.26 \times 10^{-6} \text{ m s}^{-1}$ ; gas inlet composition (v/v %) = 10% of CO<sub>2</sub>: 10% of O<sub>2</sub> and N<sub>2</sub> balances)

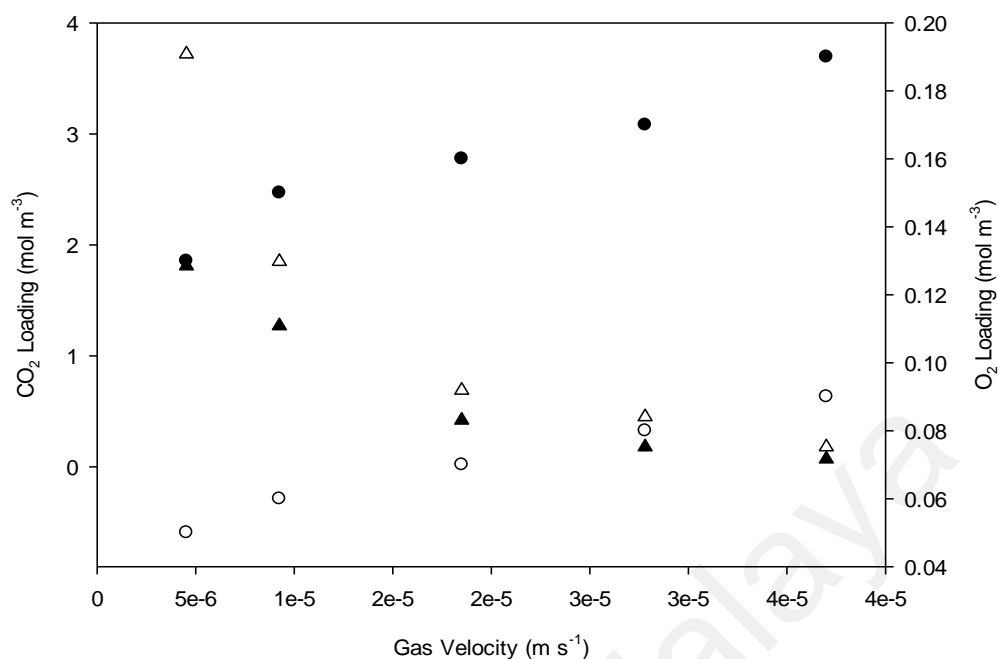


**Figure 4.28:** Loading of CO<sub>2</sub> and O<sub>2</sub> for both membranes contactor systems at different gas velocities where (  $\Delta$  ) CO<sub>2</sub> loading – SILM, (  $\blacktriangle$  ) CO<sub>2</sub> loading – PP, (  $\circ$  ) O<sub>2</sub> loading – SILM and (  $\bullet$  ) O<sub>2</sub> loading – PP (Operating conditions: absorbent concentration = 2M MEA; absorbent temperature = 303 K; gas velocities =  $4.63 \times 10^{-6}$  to  $3.70 \times 10^{-5} \text{ m s}^{-1}$ ; liquid velocity =  $9.26 \times 10^{-6} \text{ m s}^{-1}$ ; gas inlet composition (v/v %) = 10% of CO<sub>2</sub>: 10% of O<sub>2</sub> and N<sub>2</sub> balances)

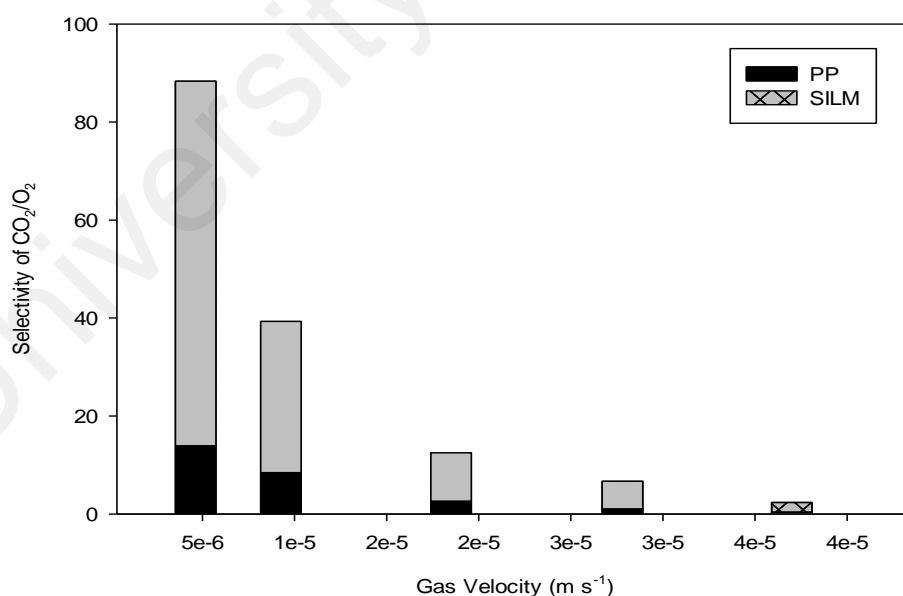


**Figure 4.29:** Selectivity of CO<sub>2</sub>/O<sub>2</sub> for blank and supported ionic liquid membrane contactor systems at different gas velocities (Operating conditions: absorbent concentration = 2M MEA; absorbent temperature = 303 K; gas velocities =  $4.63 \times 10^{-6}$  to  $3.70 \times 10^{-5} \text{ m s}^{-1}$ ; liquid velocity =  $9.26 \times 10^{-6} \text{ m s}^{-1}$ ; gas inlet composition (v/v %) = 10% of CO<sub>2</sub>: 10% of O<sub>2</sub> and N<sub>2</sub> balances)



### 4.3.2 Mass transfer calculations

The overall mass transfer coefficient  $K_{overall}$  is calculated from the experimental results of CO<sub>2</sub> fluxes at different temperatures and gas velocities using Eqn. 4.1. Table 4.6 shows the different trends in the  $K_{overall}$  for both systems. For both contactor systems, the  $K_{overall}$  value remains constant around  $4.60 \times 10^{-6}$  to  $4.17 \times 10^{-6} \text{ m s}^{-1}$  (blank) and  $1.52 \times 10^{-5}$  to  $1.46 \times 10^{-5} \text{ m s}^{-1}$  (supported ionic liquid membrane) for the temperature interval of 303 to 348 K. Despite that, in the case of decreasing gas velocities from  $4.63 \times 10^{-6}$  to  $3.70 \times 10^{-5}$ , the  $K_{overall}$  value increases significantly from  $1.35 \times 10^{-7}$  to  $4.60 \times 10^{-6} \text{ m s}^{-1}$  (blank) and  $3.65 \times 10^{-7} \text{ m s}^{-1}$  to  $1.52 \times 10^{-5}$  (supported ionic liquid membrane) (Wen et al., 2015). Under optimal operating conditions (absorbent concentration = 2M MEA; absorbent temperatures = 303 K; gas velocity =  $4.63 \times 10^{-6} \text{ m s}^{-1}$ ; liquid velocity =  $9.26 \times 10^{-6} \text{ m s}^{-1}$ ; gas inlet composition (v/v %) = 10% of CO<sub>2</sub>: 10% of O<sub>2</sub> and N<sub>2</sub> balances), the mass transfer coefficient using supported ionic liquid membrane contactor is 3.3 times higher as compared to the blank system. This behavior correlates with the presence of [emim] [NTf<sub>2</sub>] ionic liquid as an immobilized liquid in the pores of the membrane and would result in improved process efficiency for CO<sub>2</sub> capture.

**Table 4.6:** Experimental  $K_{overall}$  for a) blank and b) SILM contactor system at different temperatures and gas velocities

Temperature (K)	Gas flow rate ( $\text{m s}^{-1}$ )	$K_{overall}$ ( $\text{m s}^{-1}$ ) (a)	$K_{overall}$ ( $\text{m s}^{-1}$ ) (b)
303	$4.63 \times 10^{-6}$	$4.60 \times 10^{-6}$	$1.52 \times 10^{-5}$
318	$4.63 \times 10^{-6}$	$4.45 \times 10^{-6}$	$1.50 \times 10^{-5}$
333	$4.63 \times 10^{-6}$	$4.30 \times 10^{-6}$	$1.48 \times 10^{-5}$
348	$4.63 \times 10^{-6}$	$4.17 \times 10^{-6}$	$1.46 \times 10^{-5}$
303	$9.26 \times 10^{-6}$	$2.98 \times 10^{-6}$	$4.74 \times 10^{-6}$
303	$1.85 \times 10^{-5}$	$8.91 \times 10^{-7}$	$1.50 \times 10^{-6}$
303	$2.78 \times 10^{-5}$	$3.64 \times 10^{-7}$	$9.41 \times 10^{-7}$
303	$3.70 \times 10^{-5}$	$1.35 \times 10^{-7}$	$3.65 \times 10^{-7}$

### 4.3.3 Long-term performances of SILM contactor in parallel flow mode

The effects of operation time on the CO<sub>2</sub> absorption performances of PP membrane and SILM membrane were investigated by running the system continuously for 72 hours, followed by heating in combination with drying the membranes at 373 K for 24 hours (Yu et al., 2015). This entire process is known as one cycle. For the fresh PP membrane, the CO<sub>2</sub> absorption efficiency and CO<sub>2</sub> mass transfer rate (Figures 4.30 and 4.31) maintained around 39.13% and  $3.76 \times 10^{-6} \text{ mol m}^{-2} \text{ s}^{-1}$ , respectively, within the first 72 hours (Cycle 1). This cycle is illustrated in Figure 4.30. With the increase in the number of cycles, the CO<sub>2</sub> removal efficiency and CO<sub>2</sub> mass transfer rate had obviously decreased. Heating and drying could not recover the performance of the PP membrane. This tendency is attributed to the irreversible changes of the PP membrane surface morphologies, due to swelling caused by long-term exposure of PP fibers to the MEA aqueous solution (Kladkaew et al., 2011; Saiwan et al., 2011). After long-term operations, some slit-like membrane pores in the fresh PP fiber sample shrank longitudinally and became elliptical or even circular. The pore average equivalent diameter had increased with operation time that results in more absorbent liquid being penetrated into the pores (Lv et al., 2010; Mansourizadeh et al., 2010; Wang et al., 2005; Zhao et al., 2012). Therefore, it was found that the PP membrane performance had deteriorated with operation time. For the SILM, the CO<sub>2</sub> absorption efficiency maintained at 80.68% for 72 hours with CO<sub>2</sub> mass transfer rate of  $7.75 \times 10^{-6} \text{ mol m}^{-2} \text{ s}^{-1}$  until the end of the process of Cycle 1 (Figures 4.30 and 4.31). A similar trend was observed for other cycles as well. In this work, the transport mechanism of gases through SILM can be explained by solution-diffusion process principles. After the heating and drying process at 373 K, the membrane's performance was resumed and slightly doubled the performance of PP membrane. This observation suggests that the membrane's surface was not destroyed during the exposure of the membrane to the

MEA aqueous solution. Selectivity of  $\text{CO}_2/\text{O}_2$  for both contactors systems using 2M MEA as a solvent system has been calculated, with the detailed results shown in Figure 4.32. Blank PP membrane has displayed distinct changes in the selectivity values for  $\text{CO}_2/\text{O}_2$  with the membrane process, and the stability of the membrane process was retained until the 3<sup>rd</sup> day of operation. However, in the case of SILM, the selectivity had improved significantly since the  $\text{CO}_2/\text{O}_2$  selectivity of the SILM and is more than 4 times higher than the blank membrane even after the 3<sup>rd</sup> cycle. Meanwhile, the decrease of  $\text{CO}_2/\text{O}_2$  selectivity of SILM after each cycle could be caused by the loss of IL during regeneration process, long-term of operation (Bijani et al., 2009; Cserjesi et al., 2009; Hanioka et al., 2008; Hernandez-Fernandez et al., 2009; Ilconich et al., 2007; Myers et al., 2008) and the IL used was not fully regenerated as there was still  $\text{O}_2$  that remained in this supporting phase ( $\text{O}_2$  loading has been primarily impacted by the  $\text{CO}_2$  loading in the membrane module. This can be explained by the higher  $\text{CO}_2$  loading, which in turn causes a reduction of  $\text{O}_2$  in the MEA solution. In addition, it has been suggested that [emim] [NTf<sub>2</sub>] IL has displayed a higher affinity to  $\text{CO}_2$  (Cserjesi et al., 2009; Hanioka et al., 2008; Scovazzo et al., 2009) as compared to other gases in the gas mixture.

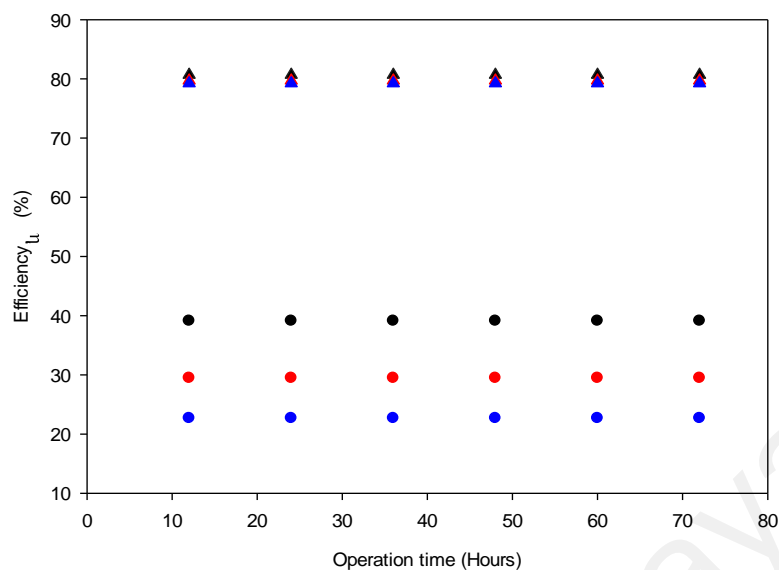


**Figure 4.30:** CO<sub>2</sub> absorption efficiency of both membrane contactor systems for long-term operation where (▲) Efficiency – SILM (Cycle 1), (▲) Efficiency – SILM (Cycle 2), (▲) Efficiency – SILM (Cycle 3), (●) Efficiency – Blank (Cycle 1), (●) Efficiency – Blank (Cycle 2), (●) Efficiency – Blank (Cycle 3) (Operating conditions: absorbent concentration = 2M MEA; absorbent temperature = 303 K; gas velocity =  $4.63 \times 10^{-6} \text{ m s}^{-1}$ ; liquid velocity =  $9.26 \times 10^{-6} \text{ m s}^{-1}$ ; gas inlet composition (v/v %) = 10% of CO<sub>2</sub>: 10% of O<sub>2</sub> and N<sub>2</sub> balances)

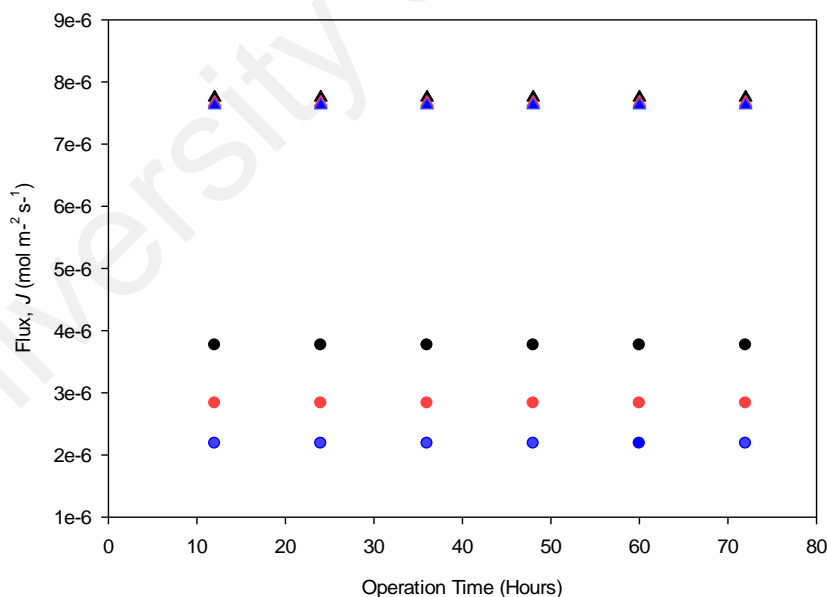


**Figure 4.31:** CO<sub>2</sub> absorption flux of both membrane contactor systems for long-term operation where (▲) Flux – SILM (Cycle 1), (▲) Flux – SILM (Cycle 2), (▲) Flux – SILM (Cycle 3), (●) Flux – Blank (Cycle 1), (●) Flux – Blank (Cycle 2), (●) Flux – Blank (Cycle 3) (Operating conditions: absorbent concentration = 2M MEA; absorbent temperature = 303 K; gas velocity =  $4.63 \times 10^{-6} \text{ m s}^{-1}$ ; liquid velocity =  $9.26 \times 10^{-6} \text{ m s}^{-1}$ ; gas inlet composition (v/v %) = 10% of CO<sub>2</sub>: 10% of O<sub>2</sub> and N<sub>2</sub> balances)

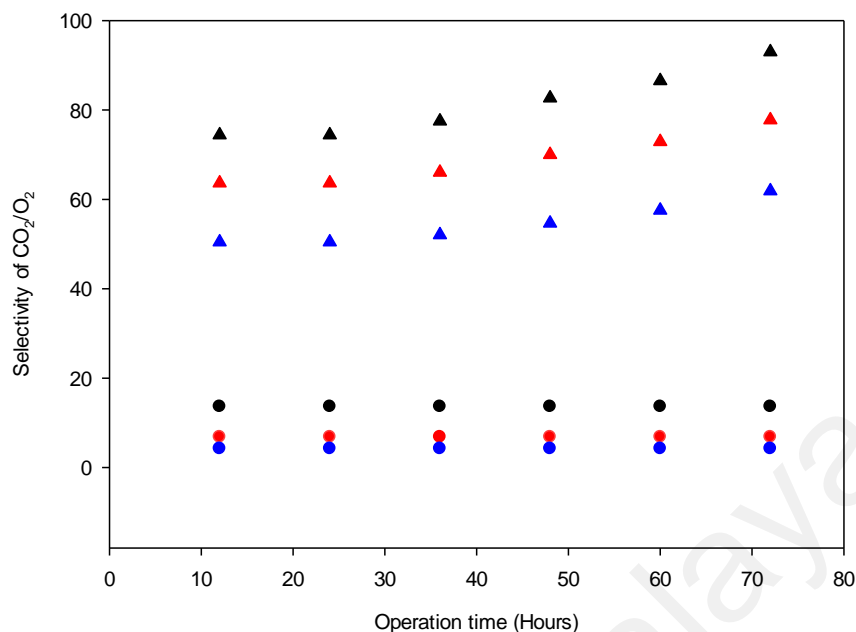


**Figure 4.32:** Selectivity of CO<sub>2</sub>/O<sub>2</sub> for blank and supported ionic liquid membranes contactor systems for long-term operation (▲) Selectivity – SILM (Cycle 1), (▲) Selectivity – SILM (Cycle 2), (▲) Selectivity – SILM (Cycle 3), (●) Selectivity – Blank (Cycle 1), (●) Efficiency – Blank (Cycle 2), (●) Efficiency – Blank (Cycle 3) (Operating conditions: absorbent concentration = 2M MEA; absorbent temperature = 303 K; gas velocity =  $4.63 \times 10^{-6} \text{ m s}^{-1}$ ; liquid velocity =  $9.26 \times 10^{-6} \text{ m s}^{-1}$ ; gas inlet composition (v/v %) = 10% of CO<sub>2</sub>: 10% of O<sub>2</sub> and N<sub>2</sub> balances)

#### 4.3.4 Summary (Section 4.3)

In this study, a modified hydrophobic gas-liquid membrane contactor system was prepared using Liqui-Cel<sup>®</sup> parallel flow module as a membrane support (hydrophobic) and 1-ethyl-3-methylimidazolium bis (trifluoromethylsulfonyl) imide [emim] [NTf<sub>2</sub>] ionic liquid (hydrophobic) as a supporting phase. Further investigation to compare the performances of blank and modified membrane module was implemented at different temperatures (303 to 348K) and gas velocities ( $4.63 \times 10^{-6}$  to  $3.70 \times 10^{-5} \text{ m s}^{-1}$ ). Results revealed that efficiency of the CO<sub>2</sub> absorption process of the modified module was almost doubled with an average selectivity factor of CO<sub>2</sub>/O<sub>2</sub> around 5 times compared to blank contactor system. On the other hand, results indicated that, at optimal operating conditions, the overall mass transfer coefficient,  $K_{overall}$  of modified supported ionic

liquid membranes contactor was 70% higher than that of the blank module. Thus, these results are beneficial for capturing CO<sub>2</sub> with high tendency to prevent oxidative degradation of monoethanolamine (MEA).

University of Malaya

University of Malaya

## 4.4 CO<sub>2</sub> absorption study under different operating conditions in cross-flow mode

### 4.4.1 Effects of MEA concentration

Figure 4.33 illustrated the effects of MEA concentration on the CO<sub>2</sub> absorption performance of the prepared membrane. When the MEA concentration raised from 0.5 to 2M MEA, the CO<sub>2</sub> absorption efficiency and mass transfer rate had increased from 29.70% to 62% and from  $9.88 \times 10^{-6}$  to  $2.07 \times 10^{-5} \text{ mol m}^{-2} \text{ s}^{-1}$ , respectively. It clearly shows that the mass transfer rate generally increases with the absorbent concentration. This is caused by the active component absorbing CO<sub>2</sub> in the liquid boundary layer increases with the absorbent concentration, which in turn results in higher CO<sub>2</sub> solubility (Mansourizadeh et al., 2010). As far as the higher CO<sub>2</sub> absorption efficiency is concerned, it is worthwhile to increase the initial absorbent concentration. However, when the MEA concentration was higher than 2M MEA, it was found that there's a decline in CO<sub>2</sub> flux and absorption efficiency. One possible reason is the decrease in an active gas-liquid contacting area (slightly related to the porosity of membrane) with the increase of the MEA concentration (deMontigny et al., 2005). In the physical absorption, the boundary layer thickness for CO<sub>2</sub> diffusion,  $\delta_L$  is larger than the distance between the adjacent pores,  $L_p$ , and dissolved CO<sub>2</sub> at the pore opening can quickly diffuse along the membrane's surface. This makes the CO<sub>2</sub> concentration of the membrane's surface between the pores is almost equal to that of the pore opening, i.e., liquid at all membrane's surface is saturated with CO<sub>2</sub>. Consequently, CO<sub>2</sub> can diffuse from the total membrane surface towards the bulk liquid; which makes the entire membrane's area effective for absorption. Then again in the case of chemical absorption, the boundary layer for CO<sub>2</sub> diffusion is much thinner than in the physical absorption and smaller than  $L_p$ . In this situation, as dissolved CO<sub>2</sub> at the pore opening



diffuse mainly in the direction perpendicular to the membrane's surface, only the area of pore opening is active for gas absorption. Furthermore, solution viscosity also influences the absorption performance in conjunction of using a high solution concentration. According to deMontigny et al. (2005), absorption performance can decrease with highly concentrated MEA solutions because of the effect caused by viscosity. Therefore, the facilitation effect of high MEA concentration is compensated by the decrease in the effective gas-liquid contacting area and viscosity effects. This leads to the tendency of prepared membrane for CO<sub>2</sub> removal, dropping continuously and remarkably with the MEA concentration from 3 to 4M MEA.

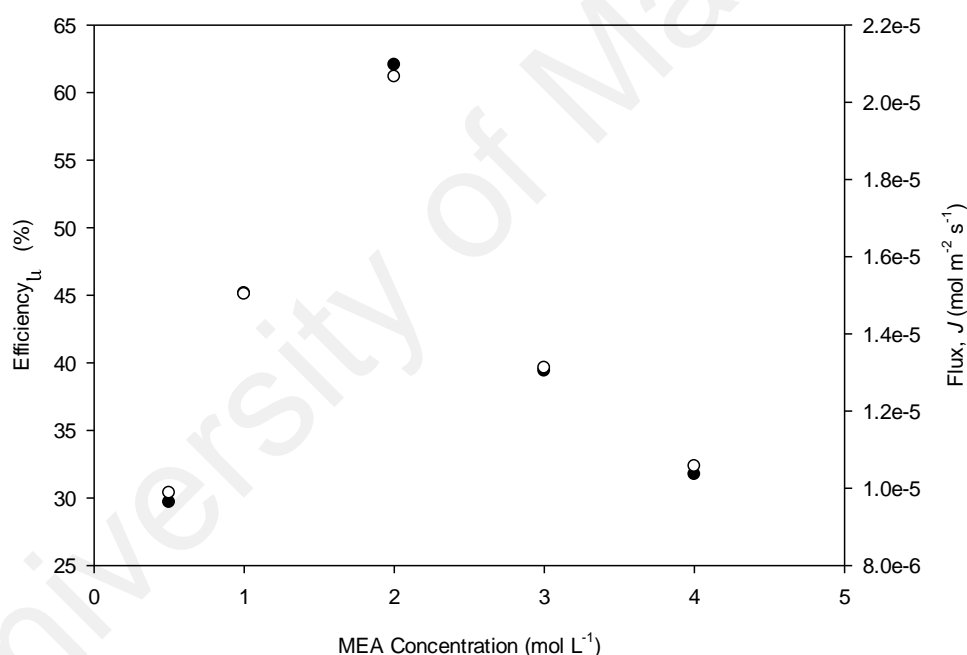


**Figure 4.33:** Effects of MEA concentration on ( ● ) CO<sub>2</sub> absorption efficiency (%) and ( ○ ) flux (Operating conditions: absorbent concentration = 0.5 to 4M MEA; absorbent temperature = 303 K; gas flow rate = 100 ml min<sup>-1</sup>; liquid flow rate = 500 ml min<sup>-1</sup>; gas inlet composition (v/v %) = 30% of CO<sub>2</sub>: 10% of O<sub>2</sub> and N<sub>2</sub> balances)

#### 4.4.2 Effects of absorbent temperature

Figure 4.34 demonstrated the effects of absorbent temperature on the CO<sub>2</sub> absorption's performance. The gas and liquid flow rates were constant at 50 and 500 ml

min<sup>-1</sup>, respectively. When the absorbent's temperature increased from 303 K to 348 K, the CO<sub>2</sub> absorption efficiency and mass transfer rate decreased slightly from 99.84% to 99.36% and from 8.31 x 10<sup>-5</sup> to 8.27 x 10<sup>-5</sup> mol m<sup>-2</sup> s<sup>-1</sup>, respectively. In this study, the data that was obtained had verified that absorbent temperature does not show any significant effect on absorption performance when temperature rises from room temperature to 348 K. It is identified that, the temperature increase preferred a constant reaction rate (Dindore & Versteeg, 2005; Kumar et al., 2002) and diffusion (Snijder et al., 1993). But, the increase in temperature had also resulted in a decrease in CO<sub>2</sub> solubility and an increase evaporation of absorbent that is not conducive to absorption (Song et al., 2006). When increasing the temperature of the absorbent's solution, the effect of temperature on reaction rate and diffusion rate is higher than that in CO<sub>2</sub> solubility. However, in this study, the temperature effect is reversed. It is perceived that a low-temperature process was apparently more promising to the elimination of CO<sub>2</sub>. The reduction of mass transfer rate with increasing temperature is therefore believed to be more affected by the CO<sub>2</sub> decrease in solubility (Ren et al., 2010).

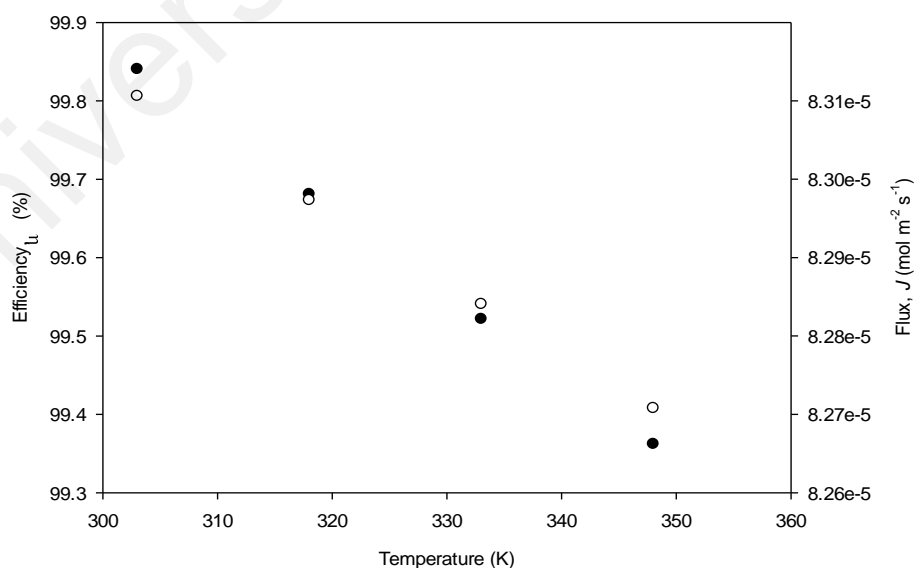


**Figure 4.34:** Effects of absorbent temperature on ( ● ) CO<sub>2</sub> absorption efficiency (%) and ( ○ ) flux (Operating conditions: absorbent concentration = 2M MEA; absorbent temperatures = 303 to 348 K; gas flow rate = 100 ml min<sup>-1</sup>; liquid flow rate = 500 ml min<sup>-1</sup>; gas inlet composition (v/v %) = 30% of CO<sub>2</sub>: 10% of O<sub>2</sub> and N<sub>2</sub> balances)

#### 4.4.3 Effects of liquid flow rate

Liquid flow rate is perhaps the utmost significant operating variable in the membrane gas-liquid membrane contactor (Albo & Irabien, 2012; Albo et al., 2010). This is since in overall, it has an obvious effect on the mass transfer rate of CO<sub>2</sub>. Figure 4.35 shows the absorption performances, expressed as CO<sub>2</sub> absorption efficiency and flux through the membrane as a function of the liquid flow rate. Data was found to show that the CO<sub>2</sub> absorption efficiency increased from 35% to 48% with the increase of liquid flow rate of 100 to 500 ml min<sup>-1</sup>. Meanwhile, the absorption flux had increase from 5.85 x 10<sup>-6</sup> to 4.00 x 10<sup>-5</sup> mol m<sup>-2</sup> s<sup>-1</sup> by increasing the absorbent's flow rate. The absorbent velocity increases by increasing the absorbent flow rate, which results in the increase in liquid phase mass transfer coefficient. This will then cause an increase in the CO<sub>2</sub> absorption flux (Mansourizadeh et al., 2010).

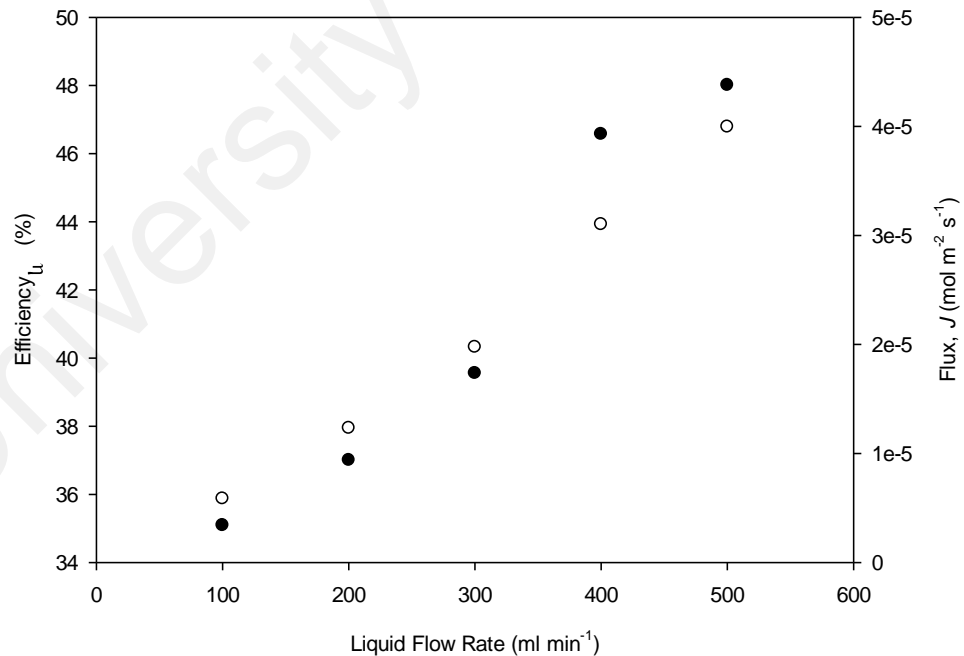


**Figure 4.35:** Effects of liquid flow rate on ( ● ) CO<sub>2</sub> absorption efficiency (%) and ( ○ ) flux (Operating conditions: absorbent concentration = 2M MEA; absorbent temperature = 303 K; gas flow rate = 100 ml min<sup>-1</sup>; liquid flow rates = 100 to 500 ml min<sup>-1</sup>; gas inlet composition (v/v %) = 30% of CO<sub>2</sub>; 10% of O<sub>2</sub> and N<sub>2</sub> balances)

#### 4.4.4 Effects of gas inlet composition

The effects of CO<sub>2</sub> gas inlet composition on the mass transfer rate and CO<sub>2</sub> removal efficiency is illustrated in Figure 4.36. The liquid absorbent passed through the shell side at a constant flow rate of 500 ml min<sup>-1</sup>, while the gas mixtures passed through the lumen side at a constant flow rate of 50 ml min<sup>-1</sup>. A pressure difference of 0.5 x 10<sup>5</sup> Pa was applied onto the liquid stream and gas stream. The absorbent's temperature was kept at 303 K. It is noticeably revealed that the CO<sub>2</sub> gas inlet composition had a substantial outcome on the mass transfer. An increase in CO<sub>2</sub> gas inlet composition shows a rapid increase in the CO<sub>2</sub> absorption efficiency and flux. When the CO<sub>2</sub> volume fraction increases from 11.35% to 31.35%, the mass transfer rate had increased from 2.97 x 10<sup>-5</sup> to 8.31 x 10<sup>-5</sup> mol m<sup>-2</sup> s<sup>-1</sup>, with the efficiency of CO<sub>2</sub> absorption attained was at 99.84%. According to Fick's Law for mass transfer, the molar flux is relative to the concentration gradient. For that reason, the initial CO<sub>2</sub> composition directly effects the CO<sub>2</sub> molecular diffusion through the liquid and gas-filled pores. At greater initial CO<sub>2</sub> loading, both axial and radial diffusion of CO<sub>2</sub> molecules was improved; because of an increase in driving force for mass transfer of CO<sub>2</sub>. Therefore, an increase in initial concentration leads to an increase in absorption flux and efficiency.

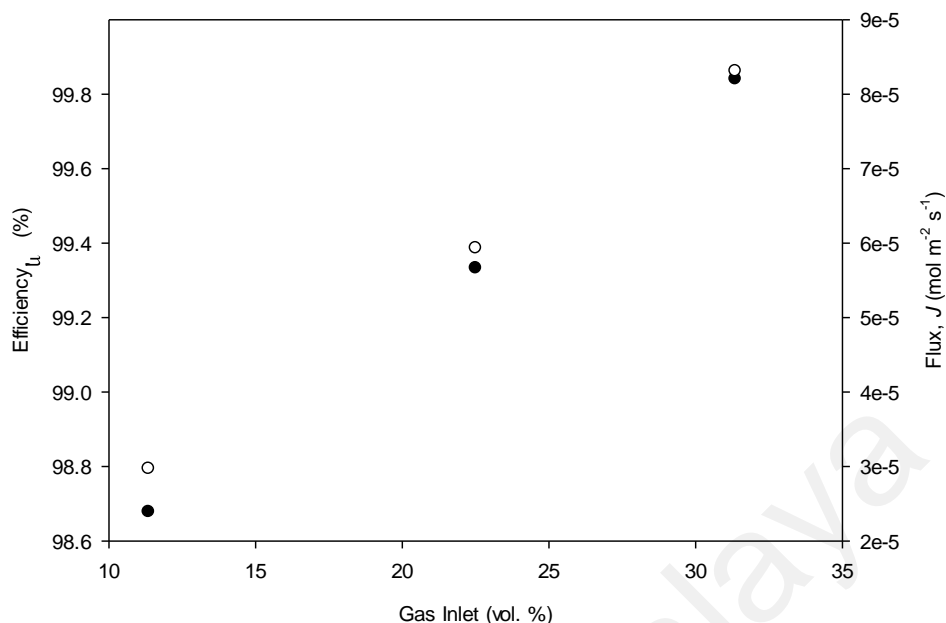


**Figure 4.36:** Effects of gas inlet composition on ( ● ) CO<sub>2</sub> absorption efficiency (%) and ( ○ ) flux (Operating conditions: absorbent concentration = 2M MEA; absorbent temperature = 303 K; gas flow rate = 50 ml min<sup>-1</sup>; liquid flow rate = 500 ml min<sup>-1</sup>; gas inlet compositions (v/v %) = 10 to 30% of CO<sub>2</sub>: 10% of O<sub>2</sub> and N<sub>2</sub> balances)

#### 4.4.5 Effects of gas flow rate

The impact of gas flow rate on the mass transfer rate and absorption efficiency of CO<sub>2</sub> is demonstrated in Figure 4.37. When the gas flow rate increases from 50 to 500 ml min<sup>-1</sup>, the residence time of CO<sub>2</sub> in the membrane contactor was reduced significantly. The CO<sub>2</sub> absorption efficiency and flux was found to have dropped continuously and remarkably from 99.84% to 7.50% and from  $8.31 \times 10^{-5}$  to  $6.24 \times 10^{-6}$  mol m<sup>-2</sup> s<sup>-1</sup>, respectively. Therefore, the increase of gas flow rate is not able to increase the CO<sub>2</sub> mass transfer rate. For a membrane contactor, the feed gas and absorbent liquid flows on the opposite sides of the membrane. CO<sub>2</sub> contained in the gas phase passes through the membrane, whereas absorption commonly occurs on the liquid side. The mass-transfer process consists of the following three consecutive steps: (i) diffusion from bulk gas phase to the outer surface of the membrane; (ii) diffusion through

membrane pores; and (iii) dissolution into the absorption liquid and liquid-phase diffusion/chemical reaction. For gas absorption, the resistance to gas diffusion from the bulk gas to the external membrane surface can be ignored, as compared to other resistances (Rangwala, 1996). It is reported that, in this study, gas flow rate has a very noteworthy influence towards CO<sub>2</sub> removal efficiency and mass transfer resistance.

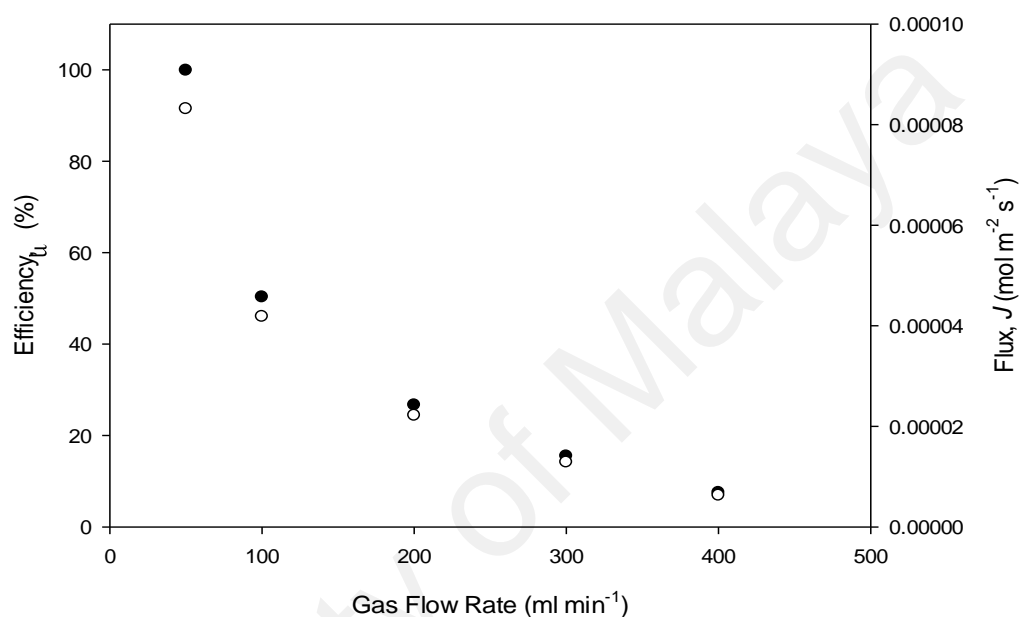


**Figure 4.37:** Effects of gas flow rate on ( ● ) CO<sub>2</sub> absorption efficiency (%) and ( ○ ) flux (Operating conditions: absorbent concentration = 2M MEA; absorbent temperature = 303 K; gas flow rates = 50 to 400 ml min<sup>-1</sup>; liquid flow rate = 500 ml min<sup>-1</sup>; gas inlet composition (v/v %) = 30% of CO<sub>2</sub>: 10% of O<sub>2</sub> and N<sub>2</sub> balances)

#### 4.4.6 Selective absorption of CO<sub>2</sub> by aqueous monoethanolamine (MEA)

For cross-flow mode SILMs, selectivity data was obtained by plotting the outlet concentration profiles of CO<sub>2</sub> and O<sub>2</sub> for each run at different MEA concentrations, absorbent temperatures, liquid flow rates, gas inlet compositions and gas flow rates. Typical CO<sub>2</sub> and O<sub>2</sub> loadings with selectivity profiles at various operating conditions are provided in Figures 4.38 to 4.47. The effects of MEA concentration on the loading of CO<sub>2</sub> and O<sub>2</sub> was evaluated from 0.5 to 4M MEA (Figure 4.38), and the results had shown that the selectivity of CO<sub>2</sub>/O<sub>2</sub> (Figure 4.39) had increased up to 123 with a

concentration of 0.5 to 2M MEA attributed to the highest CO<sub>2</sub> loading in the outlet concentration of liquid phase (low solubility of O<sub>2</sub>). However, when the concentrations of the MEA were decreased from 2 to 4M MEA, the selectivity values tend to reduce to 49.

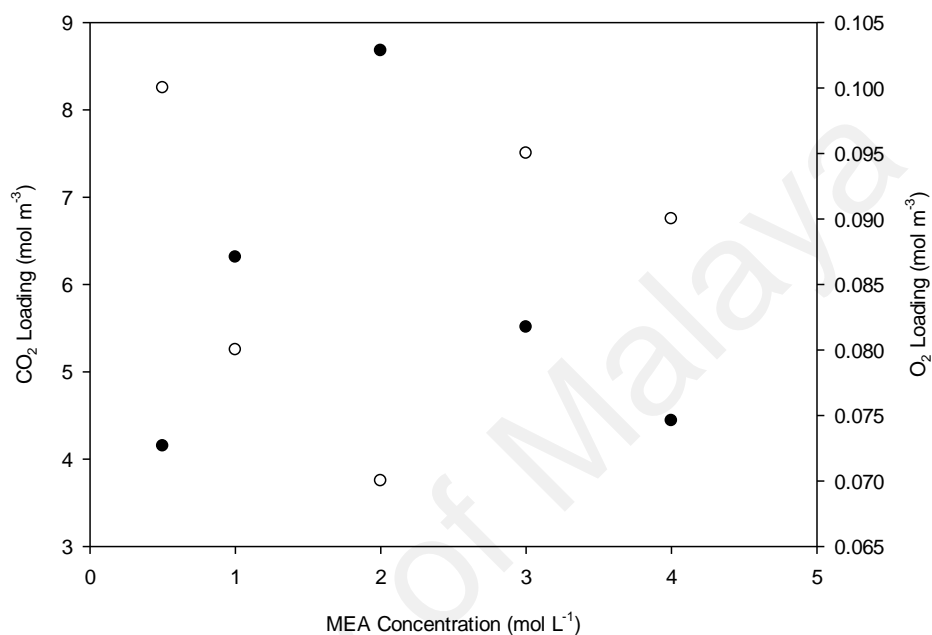


**Figure 4.38:** Loading of CO<sub>2</sub> and O<sub>2</sub> for supported ionic liquid membranes contactor at different MEA concentrations where ( ● ) CO<sub>2</sub> loading and ( ○ ) O<sub>2</sub> loading (Operating conditions: absorbent concentrations = 0.5 to 4M MEA; absorbent temperature = 303 K; gas flow rate = 100 ml min<sup>-1</sup>; liquid flow rate = 500 ml min<sup>-1</sup>; gas inlet composition (v/v %) = 30% of CO<sub>2</sub>: 10% of O<sub>2</sub> and N<sub>2</sub> balances)

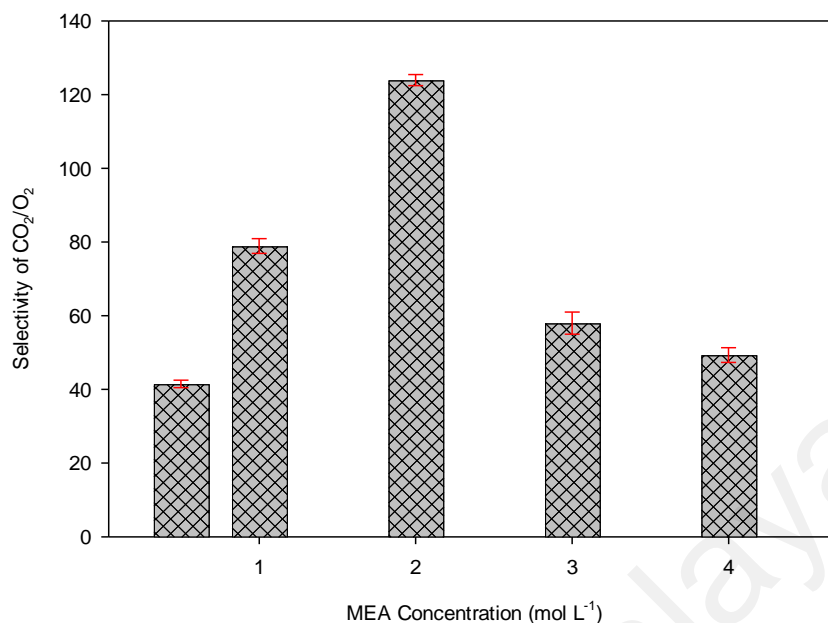


**Figure 4.39:** Selectivity of CO<sub>2</sub>/O<sub>2</sub> for supported ionic liquid membranes contactor system at different MEA concentrations (Operating conditions: absorbent concentrations = 0.5 to 4M MEA; absorbent temperature = 303 K; gas flow rate = 100 ml min<sup>-1</sup>; liquid flow rate = 500 ml min<sup>-1</sup>; gas inlet composition (v/v %) = 30% of CO<sub>2</sub>: 10% of O<sub>2</sub> and N<sub>2</sub> balances)

To evaluate the absorbent temperature effect towards the selectivity of CO<sub>2</sub>/O<sub>2</sub>, a profile of CO<sub>2</sub> and O<sub>2</sub> loading as shown in Figure 4.42 was evaluated. It is clear from Figure 4.40 that the loading of CO<sub>2</sub> of the run conducted at 303 K was higher, than those carried out at the higher temperatures of 318, 333 and 348 K. As a result of this, selectivity of CO<sub>2</sub>/O<sub>2</sub> (Figure 4.41) at the run of 303 K measured at 140 was slightly higher than those at 318, 333 and 348 K, respectively, measured at 116, 107 and 93. The loading of O<sub>2</sub> was found to have increased if the temperature was increased. This is due to the reduction of CO<sub>2</sub> loadings had been attributed to the low solubility of CO<sub>2</sub> in MEA solution at higher temperatures.



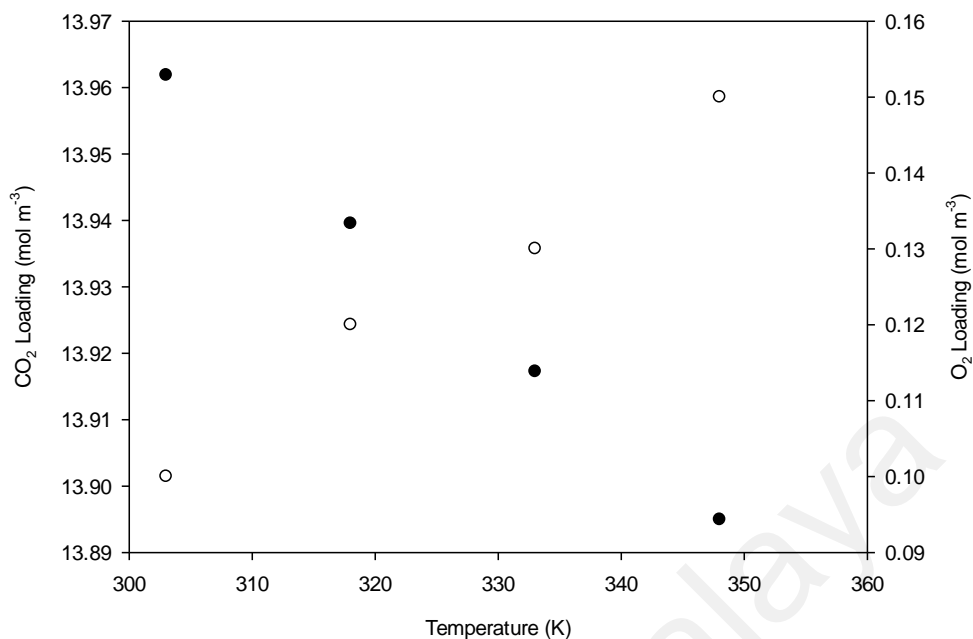


**Figure 4.40:** Loading of CO<sub>2</sub> and O<sub>2</sub> for supported ionic liquid membranes contactor at different temperatures where ( ● ) CO<sub>2</sub> loading and ( ○ ) O<sub>2</sub> loading (Operating conditions: absorbent concentration = 2M MEA; absorbent temperatures = 303 to 348 K; gas flow rate = 100 ml min<sup>-1</sup>; liquid flow rate = 500 ml min<sup>-1</sup>; gas inlet composition (v/v %) = 30% of CO<sub>2</sub>: 10% of O<sub>2</sub> and N<sub>2</sub> balances)

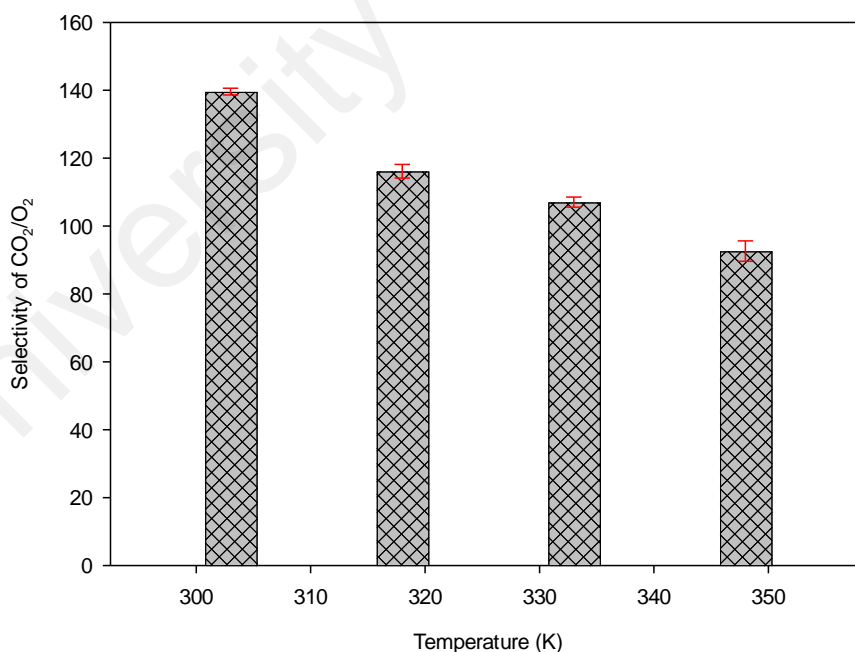


**Figure 4.41:** Selectivity of CO<sub>2</sub>/O<sub>2</sub> for supported ionic liquid membranes contactor system at different temperatures (Operating conditions: absorbent concentration = 2M MEA; absorbent temperature = 303 to 348 K; gas flow rate = 100 ml min<sup>-1</sup>; liquid flow rate = 500 ml min<sup>-1</sup>; gas inlet composition (v/v %) = 30% of CO<sub>2</sub>: 10% of O<sub>2</sub> and N<sub>2</sub> balances)

Figures 4.42 and 4.43 show the effect of liquid flow rates on the selectivity of CO<sub>2</sub>/O<sub>2</sub> runs with different liquid flow rates ranging from 100 to 500 ml m<sup>-1</sup> at a temperature of 303 K. The run conducted with 2M MEA as a solvent system had resulted in selectivity CO<sub>2</sub>/O<sub>2</sub> values of 33 to 67. This is due to the increased in CO<sub>2</sub> outlet concentration from 4.91 to 6.71 mol m<sup>-3</sup> that led to a reduction of O<sub>2</sub> loading from 0.15 to 0.1 mol m<sup>-3</sup>.

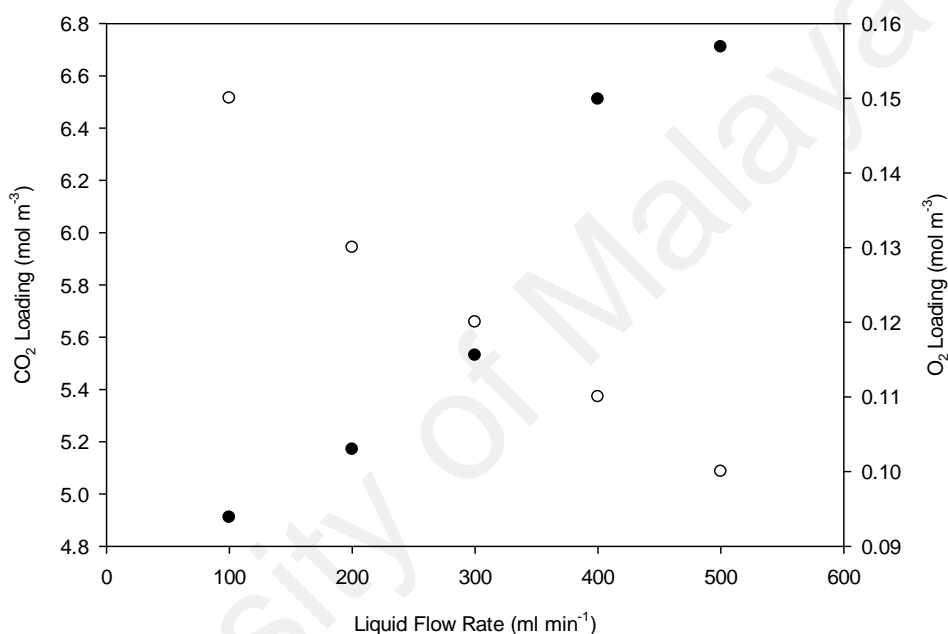


**Figure 4.42:** Loading of CO<sub>2</sub> and O<sub>2</sub> for supported ionic liquid membranes contactor at different liquid flow rates where ( ● ) CO<sub>2</sub> loading and ( ○ ) O<sub>2</sub> loading (Operating conditions: absorbent concentration = 2M MEA; absorbent temperature = 303 K; gas flow rate = 100 ml min<sup>-1</sup>; liquid flow rates = 100 to 500 ml min<sup>-1</sup>; gas inlet composition (v/v %) = 30% of CO<sub>2</sub>: 10% of O<sub>2</sub> and N<sub>2</sub> balances)

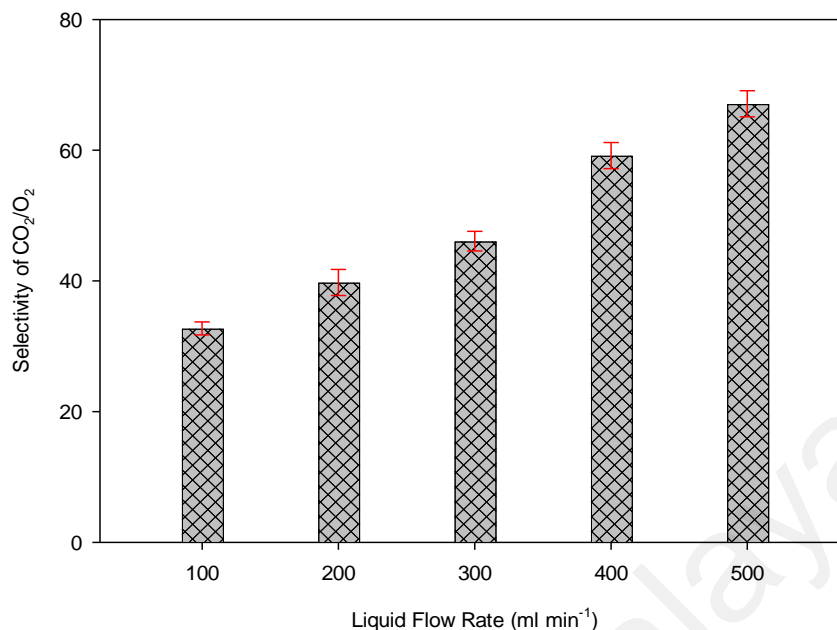


**Figure 4.43:** Selectivity of CO<sub>2</sub>/O<sub>2</sub> for supported ionic liquid membranes contactor system at different liquid flow rates (Operating conditions: absorbent concentration = 2M MEA; absorbent temperature = 303 K; gas flow rate = 100 ml min<sup>-1</sup>; liquid flow rates = 100 to 500 ml min<sup>-1</sup>; gas inlet composition (v/v %) = 30% of CO<sub>2</sub>: 10% of O<sub>2</sub> and N<sub>2</sub> balances)

Then again, the runs involving 11.35% to 31.35% of CO<sub>2</sub> concentration in the simulated flue gas stream and 2M MEA at 303 K; was used to show the effects of CO<sub>2</sub> concentration in the feed gas on the selectivity of CO<sub>2</sub>/O<sub>2</sub>. Figure 4.44 shows that an increase in the initial stage of CO<sub>2</sub> concentration in the gas stream, had resulted in an increase of selectivity values from 42 to 140 (Figure 4.45). Runs conducted with 11.35, 22.50 and 31.35% of initial CO<sub>2</sub> concentration respectively, had resulted in 5 to 13.96% mol m<sup>-3</sup> of CO<sub>2</sub> loadings and 0.12 to 0.10 mol m<sup>-3</sup> of O<sub>2</sub> loadings.

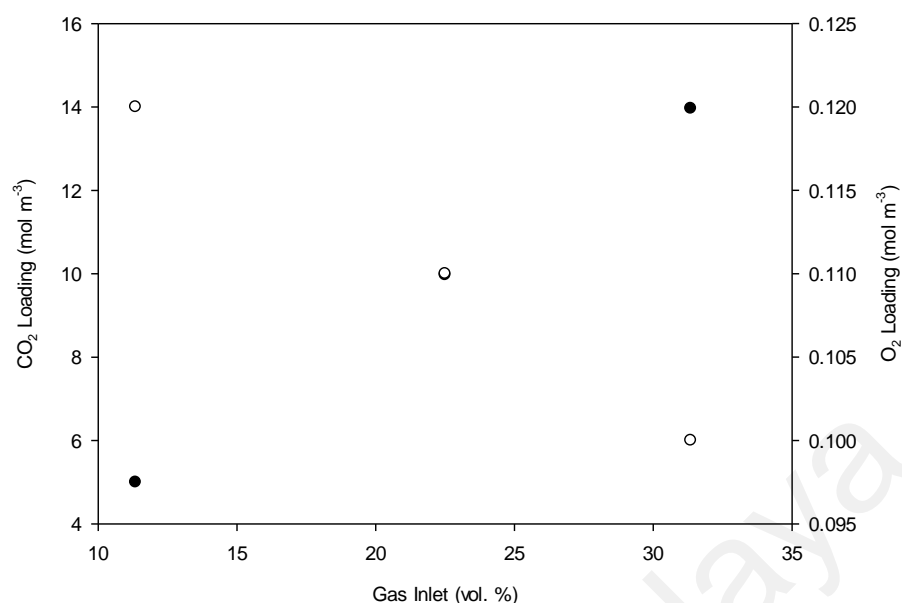


**Figure 4.44:** Loading of CO<sub>2</sub> and O<sub>2</sub> for supported ionic liquid membranes contactor at different gas inlet compositions where ( ● ) CO<sub>2</sub> loading and ( ○ ) O<sub>2</sub> loading (Operating conditions: absorbent concentration = 2M MEA; absorbent temperature = 303 K; gas flow rate = 50 ml min<sup>-1</sup>; liquid flow rate = 500 ml min<sup>-1</sup>; gas inlet compositions (v/v %) = 10 to 30% of CO<sub>2</sub>: 10% of O<sub>2</sub> and N<sub>2</sub> balances)

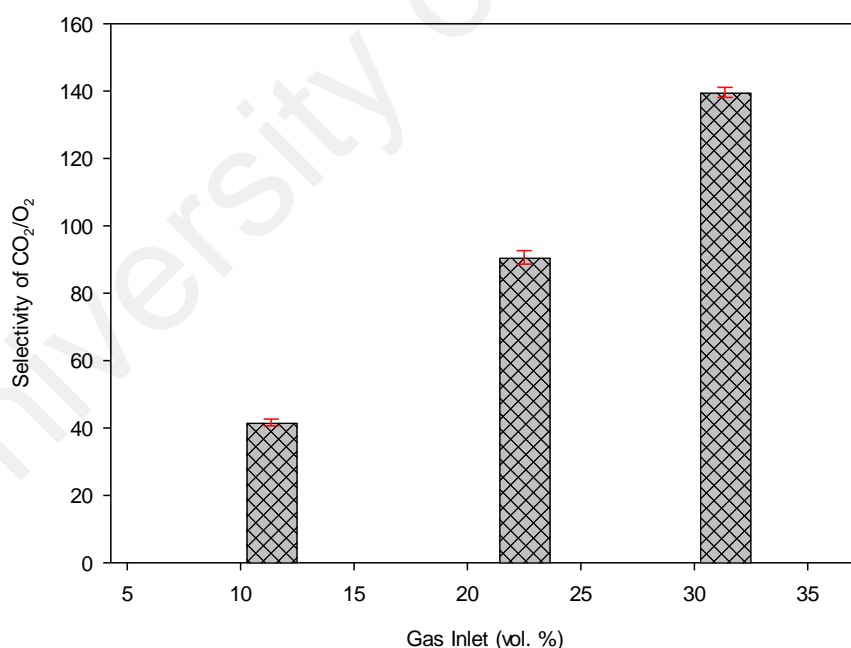


**Figure 4.45:** Selectivity of CO<sub>2</sub>/O<sub>2</sub> for supported ionic liquid membranes contactor system at different gas inlet compositions (Operating conditions: absorbent concentration = 2M MEA; absorbent temperature = 303 K; gas flow rate = 50 ml min<sup>-1</sup>; liquid flow rate = 500 ml min<sup>-1</sup>; gas inlet compositions (v/v %) = 10 to 30% of CO<sub>2</sub>: 10% of O<sub>2</sub> and N<sub>2</sub> balances)

Finally, the effects of gas flow rates on the selectivity of CO<sub>2</sub>/O<sub>2</sub> were evaluated using a similar approach that was used with other operating conditions. The loadings of CO<sub>2</sub> and O<sub>2</sub> in 2M MEA is shown in Figure 4.46, while selectivity profile of CO<sub>2</sub>/O<sub>2</sub> is presented in Figure 4.47. The runs were conducted at 303 K with gas flow rates ranging from 50 to 500 ml min<sup>-1</sup>. The results showed that the selectivity for the run with 50 ml min<sup>-1</sup> measured as 140 was 20 times higher than that of the run that was carried out at gas flow rates of 400 ml min<sup>-1</sup>.

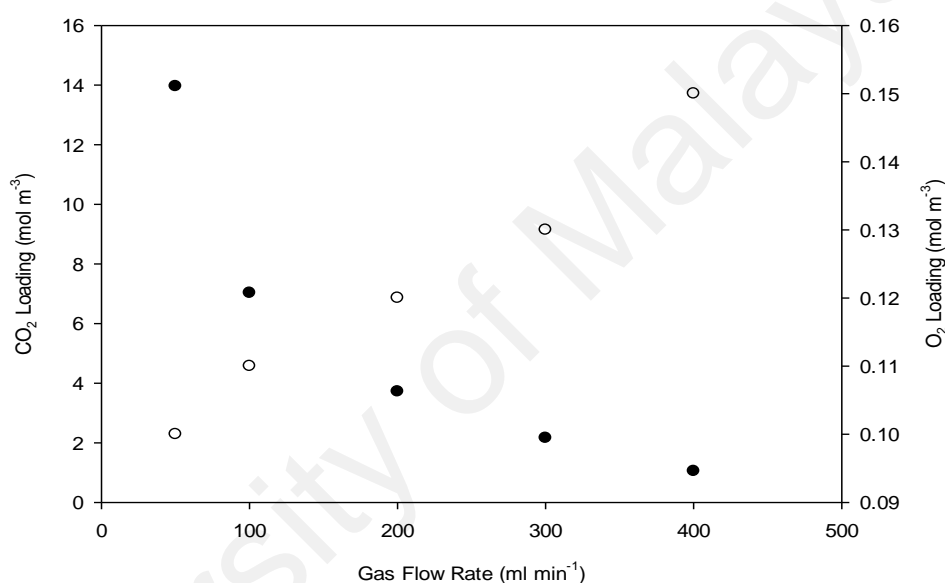


**Figure 4.46:** Loading of CO<sub>2</sub> and O<sub>2</sub> for supported ionic liquid membranes contactor at different gas flow rates where ( ● ) CO<sub>2</sub> loading and ( ○ ) O<sub>2</sub> loading (Operating conditions: absorbent concentration = 2M MEA; absorbent temperature = 303 K; gas flow rate = 50 to 400 ml min<sup>-1</sup>; liquid flow rate = 500 ml min<sup>-1</sup>; gas inlet composition (v/v %) = 30% of CO<sub>2</sub>: 10% of O<sub>2</sub> and N<sub>2</sub> balances)

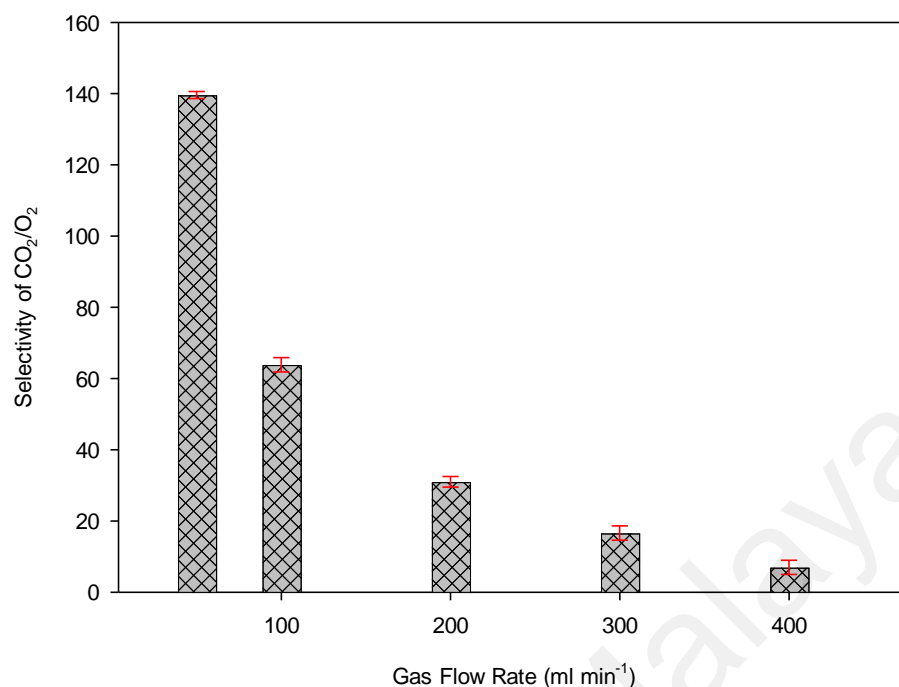


**Figure 4.47:** Selectivity of CO<sub>2</sub>/O<sub>2</sub> for supported ionic liquid membranes contactor system at different gas flow rates (Operating conditions: absorbent concentration = 2M MEA; absorbent temperature = 303 K; gas flow rates = 50 to 400 ml min<sup>-1</sup>; liquid flow rate = 500 ml min<sup>-1</sup>; gas inlet composition (v/v %) = 30% of CO<sub>2</sub>: 10% of O<sub>2</sub> and N<sub>2</sub> balances)

Selectivity data that was obtained from previous works had shown that supported ionic liquids membranes (SILMs) have sufficient selectivity values, that makes it stable enough to be investigated in gas separation performances (Bara et al., 2009b). Furthermore, there are two factors of the imidazolium family's domination over the literature to date, the recent commercial availability of this ILs class, and the perceived convenience of modifying cation structure, which was done by attaching various functional groups for ILs; that are designed particularly for carbon dioxide absorption and separation (Cserjési et al., 2010; Gan et al., 2011a; Ilconich et al., 2007; Jiang et al., 2007; Jindaratsamee et al., 2011; Kim et al., 2011; Luis et al., 2009b; Mahurin et al., 2010; Myers et al., 2008; Neves et al., 2010; Scovazzo et al., 2009; Zhao et al., 2010).

Consequently, in this work, a useful kinetic data was obtained under the conditions that are typical of a CO<sub>2</sub> absorption process i.e., 0.5 to 5M MEA, 303 to 348 K, 100 to 500 ml min<sup>-1</sup> of 2M MEA flow rates, 11.35 to 31.35% of CO<sub>2</sub> inlet compositions and 50 to 400 ml min<sup>-1</sup> of gas flow rates. Based on the initial findings, MEA shows a tendency to degrade if temperature and gas flow rate in the system was increased (Davis & Rochelle, 2009). This is mainly attributed to the reduction of CO<sub>2</sub> loading, which would lead to enhancement of MEA degradation that was caused by the increase of O<sub>2</sub> loading in the solvent system. In addition, it has been proven that the MEA degradation rate was higher at a lower CO<sub>2</sub> loading, than at a higher CO<sub>2</sub> loading (Rooney et al., 1998; Supap et al., 2009). The high temperature and low CO<sub>2</sub> concentration in the solvent section of a gas absorption plant, makes for the exact situations for the degradation of amines. The high temperature will break the chemical bonds of amines and increase the reaction rate of amines reacting with CO<sub>2</sub>, to form high molecular weight degradation products (carbamate polymerization), that in turn will cause loss of amines in the system (Supap et al, 2009; Voice & Rochelle, 2013). The overall mass transfer coefficient from the experimental results of CO<sub>2</sub> fluxes at different operating conditions was then calculated and found to be  $3.83 \times 10^{-5} \text{ m s}^{-1}$  at optimum operating conditions.

#### 4.4.7 Summary (Section 4.4)

Based on experimental data obtained by several effects, by manipulating the gas flow rate from 50 to 500 ml min<sup>-1</sup>; the contribution of overall efficiency of CO<sub>2</sub> absorption and flux were 92.34% and 92.50%, respectively. Major reduction of CO<sub>2</sub> absorption performance was observed in this case, contrary to the results obtained by varying the absorbent temperature from 303 to 348 K. Besides that, gas inlet composition, liquid flow rate and absorbent concentration below 2M had shown an increment of 64.22%,

85.37% and 52.19% from an initial flux. From this observation, it can be concluded that CO<sub>2</sub> absorption performances using SILMs were mainly dependent on the gas inlet composition, liquid flow rate, absorbent concentration and temperature.

University of Malaya



University of Malaya

## CHAPTER 5: CONCLUSIONS AND RECOMMENDATIONS

### 5.1 Conclusions

The main objective of the current project is to evaluate the novel SILM as a contactor for selective absorption of CO<sub>2</sub> by aqueous monoethanolamine (MEA). Consequently, the results that were achieved in the different sections of this study involve the following findings:

1. CO<sub>2</sub> absorption capacity and CO<sub>2</sub>/O<sub>2</sub> selectivity of some selected ILs were successfully predicted using the COSMO-RS molecular modelling system.

- a) The structures of the [bmim]<sup>+</sup> and [emim]<sup>+</sup> cation, [NTf<sub>2</sub>]<sup>-</sup>, [TFO]<sup>-</sup>, [FAP]<sup>-</sup>, [DCA]<sup>-</sup>, [TFA]<sup>-</sup> and [BF<sub>4</sub>]<sup>-</sup> anion, MEA, water, CO<sub>2</sub>, N<sub>2</sub> and O<sub>2</sub> were drawn and geometry optimized using the TmoleX software package at Hartree-Fock theory with 6-31G\* basic set. Subsequently, a *.cosmofile* was created and imported to the COSMOthermX software. Using the COSMOthermX software, a 3D polarized charged distribution ( $\sigma$ , sigma) on the molecular surface of the individual components was generated. Next, activity coefficient of 1-ethyl-3-methylimidazolium bis (trifluoromethylsulfonyl) imide [emim] [NTf<sub>2</sub>], 1-ethyl-3-methylimidazolium trifluoromethanesulfonate [emim] [TFO], 1-ethyl-3-methylimidazolium tris(perfluoroethyl)trifluorophosphate [emim] [FAP], 1-butyl-3-methylimidazolium dicyanamide [bmim] [DCA], 1-butyl-3-methylimidazolium-trifluoroacetate ionic liquid [bmim] [TFA] and 1-butyl-3-methylimidazolium tetrafluoroborate [bmim] [BF<sub>4</sub>] with MEA and water were calculated.  $\sigma$ -profile for all cations and anions shows an H-bond donor and H-bond acceptor, respectively that complemented each of the ion pairs.

- b) It has been proven that [emim] [NTf<sub>2</sub>] IL had significant CO<sub>2</sub> absorption capacity, separation selectivities of CO<sub>2</sub>/O<sub>2</sub> and CO<sub>2</sub>/N<sub>2</sub>, with better activity coefficients in water and monoethanolamine (MEA) as compared to others.
  - c) Therefore, the predicted results were useful to aid the design and operation of novel CO<sub>2</sub> absorption processes employing [emim] [NTf<sub>2</sub>] IL as a supporting phase in a supported ionic liquid membranes (SILMs).
2. The role of viscosity in the preparation of a new supported ionic liquid membrane (SILM) and its chemical stability were successfully investigated.
- a) The number of immobilized IL was influenced by the viscosity and RI of the binary mixtures. In addition, less IL was absorbed into the membranes with the use of pure [emim] [NTf<sub>2</sub>] IL as compared to diluted IL.
  - b) A FESEM-EDX study was conducted for PP and SILMs, based on (80:20) of [emim] [NTf<sub>2</sub>] IL: acetone composition (optimal composition) in different surrounding phases. In terms of SILMs, when 2M MEA was used as a surrounding phase; the membranes experienced a substantially lesser IL loss (19.90%) after 14 days of operation. On the contrary, when MEA was used as contacting phases; almost all (86.50%) of the immobilized IL was lost from the membranes. Apart from that, the stability of the resulting SILMs increased when the surface tension of the surrounding phases also increased; as demonstrated and confirmed by using the FESEM-EDX technique.
  - c) The use of hydrophobic [emim] [NTf<sub>2</sub>] IL could avoid loss of IL and reducing structural degradation of SILMs for long term performances.

3. The CO<sub>2</sub> absorption performance and CO<sub>2</sub>/O<sub>2</sub> selectivity of the supported ionic liquid membrane and its performance with that of the blank membrane were successfully evaluated and compared.

- a) The efficiency of both systems had increased when the gas velocities were reduced and slightly decreased, with the increase in temperature. In addition, the temperature had a minor influence towards the CO<sub>2</sub> absorption process when compared to dominant impact of gas velocities.
- b) The efficiency and residence time in supported ionic liquid membrane were slightly higher as compared to the blank contactor system. The efficiency values had doubled from 303 to 348 K and from  $4.63 \times 10^{-6}$  to  $3.70 \times 10^{-5} \text{ m s}^{-1}$ .
- c) Better capability of CO<sub>2</sub> absorption with a CO<sub>2</sub>/O<sub>2</sub> selectivity factor of 5.
- d)  $K_{overall}$  of SILM contactor was 70% higher than that of blank contactor system.

4. The effect of important operating conditions on CO<sub>2</sub> absorption performance and CO<sub>2</sub>/O<sub>2</sub> selectivity of the supported ionic liquid membrane (SILM) were successfully investigated.

- a) Results have shown that absorbent temperature had a minor influence on the mass transfer resistance and absorption efficiency. This is contrary with the data acquired by exploiting the effects of gas flow rate, gas inlet composition, liquid flow rate and absorbent concentration.
- b) Under optimum operating conditions, the overall mass transfer coefficient of this present work was found to be at  $3.83 \times 10^{-5} \text{ m s}^{-1}$  with a measured CO<sub>2</sub>/O<sub>2</sub> selectivity of 140.

## 5.2 Recommendations for future work

While there have been claims of successful separation of the target components ( $\text{CO}_2$  and  $\text{O}_2$ ) in the laboratory scale, there are still important things that are usually left out in the studies. For future studies, the following are recommended:

- i. The  $\text{SO}_x$  and  $\text{NO}_x$  compounds that may be present in the flue gas and  $\text{CH}_4$  or  $\text{H}_2\text{S}$  present in flue gas may compete with  $\text{CO}_2$  and  $\text{O}_2$ , respectively; during reaction with the active component of the supporting phase and liquid absorbent. Furthermore, these compounds may also interact with the membrane material. The thermal stability of the membranes and the stability of the ILs-based membrane at more realistic operating conditions (i.e., elevated temperatures and mixed-gas feeds) should also be considered.
- ii. Developing great performance polymers that could attain high selectivity without negotiating a lot on selectivity with long-term stability, is extremely required.
- iii. Evaluation work towards the regeneration process of rich monoethanolamine solutions used in this work was beneficial and must be highlighted. This reduces the cost of solvents that are consumed, in line with the use of recycled solvent. It is regarded that prepared SILMs contactor would also be reused for this regeneration system and a study for enhancing its performances are valuable.
- iv. Continued research, development, demonstration, and more studies on the economic feasibility of the process when applied in different industries will aid the growth of the technology for large-scale adoption in the future.

A few works focusing on the development of SILMs for membrane contactor are still under investigation. Success in this area will open the door for widespread application of SILMs technology in  $\text{CO}_2$  absorption applications.

## REFERENCES

- Ab Manan, N., Hardacre, C., Jacquemin, J., Rooney, D. W. & Youngs, T. G. A. (2009). Evaluation of gas solubility prediction in ionic liquids using COSMOthermX. *Journal of Chemical and Engineering Data*, 54, 2005-2022.
- Abdelrahim, M. Y., Martins, C. F., Neves, L. A., Capasso, C., Supuran, C.T., Coelho, I.M., Crespo, J.G. & Barboiu, M. (2017). Supported ionic liquid membranes immobilized with carbonic anhydrases for CO<sub>2</sub> transport at high temperatures. *Journal of Membrane Science*, 528, 225-230.
- Adibi, M., Barghi, S. H. & Rashtchian, D. (2011). Predictive models for permeability and diffusivity of CH<sub>4</sub> through imidazolium-based supported ionic liquid membranes. *Journal of Membrane Science*, 371, 127-133.
- Ahmad, A. L., Sunarti, A. R., Lee, K. T. & Fernando, W. J. N. (2010). CO<sub>2</sub> removal using membrane gas absorption. *International Journal of Greenhouse Gas Control*, 4, 495-498.
- Ahmady, A., Hashim, M. A. & Aroua, M. K. (2011). Absorption of carbon dioxide in the aqueous mixtures of methyldiethanolamine with three types of imidazolium-based ionic liquids. *Fluid Phase Equilibria*, 309, 76-82.
- Al Marzouqi, M. H., Abdulkarim, M. A., Marzouk, S. A., El-Naas, M. H. & Hasanain, H. M. (2005). Facilitated transport of CO<sub>2</sub> through immobilized liquid membrane. *Industrial and Engineering Chemistry Research*, 44, 9273-9278.
- Albo, J. & Irabien, A. (2012). Non-dispersive absorption of CO<sub>2</sub> in parallel and cross-flow membrane modules using EMISE. *Journal of Chemical Technology and Biotechnology*, 87, 1502-1507.
- Albo, J., Luis, P. & Irabien, A. (2010). Carbon dioxide capture from flue gases using a cross-flow membrane contactor and the ionic liquid 1-ethyl-3-methylimidazolium ethylsulfate. *Industrial and Engineering Chemistry Research*, 49, 11045-11051.
- Albo, J., Yoshioka, T. & Tsuru, T. (2014). Porous Al<sub>2</sub>O<sub>3</sub>/TiO<sub>2</sub> tubes in combination with 1-ethyl-3-methylimidazolium acetate ionic liquid for CO<sub>2</sub>/N<sub>2</sub> separation. *Separation and Purification Technology*, 122, 440-448.
- Ansaloni, L. & Deng L. Compatible membrane materials for 3rd generation solvent membrane contactors, ICMAT, Singapore, 2015.
- Arshad, M. W., Svendsen, H. F., Fosbol, P. L., von Solms, N. & Thomsen, K. (2014). Equilibrium total pressure and CO<sub>2</sub> solubility in binary and ternary aqueous solutions of 2-(diethylamino)ethanol (DEEA) and 3-(methylamino)propylamine (MAPA). *Journal of Chemical and Engineering Data*, 59, 764-774.
- Atchariyawut, S., Feng, C., Wang, R., Jiraratananon, R. & Liang, D. T. (2006). Effect of membrane structure on mass-transfer in the membrane gas-liquid contacting

process using microporous PVDF hollow fibers. *Journal of Membrane Science*, 285, 272-281.

- Babarao, R., Dai, S. & Jiang, D. E. (2011). Understanding the high solubility of CO<sub>2</sub> in an ionic liquid with the tetracyanoborate anion. *The Journal of Physical Chemistry B*, 115, 9789-9794.
- Baltus, R. E., Counce, R. M., Culbertson, B. H., Luo, H., DePaoli, D. W., Dai, S. & Duckworth, D. C. (2005). Examination of the potential of ionic liquids for gas separations. *Separation and Science Technology*, 40, 525-541.
- Banu, L. A., Wang, D. & Baltus, R. E. (2013). Effect of ionic liquid confinement on gas separation characteristics. *Energy Fuels*, 27, 4161-4166.
- Bara, J. E. (2012). What chemicals will we need to capture CO<sub>2</sub>? *Greenhouse Gases: Science and Technology*, 2, 162-171.
- Bara, J. E., Camper, D. E., Gin, D. L. & Noble, R. D. (2010). Room-temperature ionic liquids and composite materials: platform technologies for CO<sub>2</sub> capture. *Accounts of Chemical Research*, 43, 152-159.
- Bara, J. E., Carlisle, T. K., Gabriel, C. J., Camper, D., Finotello, A., Gin, D. L. & Noble, R. D. (2009a). Guide to CO<sub>2</sub> separations in imidazolium-based room-temperature ionic liquids. *Industrial and Engineering Chemistry Research*, 48, 2739-2751.
- Bara, J. E., Gabriel, C. J., Carlisle, T. K., Camper, D. E., Finotello, A., Gin, D. L. & Noble, R. D. (2009b). Gas separations in fluoroalkyl-functionalized room-temperature ionic liquids using supported liquid membranes. *Chemical Engineering Journal*, 147, 43-50.
- Bara, J. E., Hatakeyama, E. S., Gin, D. L. & Noble, R. D. (2008). Improving CO<sub>2</sub> permeability in polymerized room-temperature ionic liquid gas separation membranes through the formation of a solid composite with a room-temperature ionic liquid. *Polymers for Advanced Technologies*, 19, 1415-1420.
- Bara, J. E., Noble, R. D. & Gin, D. L. (2009c). Effect of "free" cation substituent on gas separation performance of polymer-room-temperature ionic liquid composite membranes. *Industrial and Engineering Chemistry Research*, 48, 4607-4610.
- Barbe, A. M., Hogan, P. A. & Johnson, R. A. (2000). Surface morphology changes during initial usage of hydrophobic, microporous polypropylene membranes. *Journal of Membrane Science*, 172, 149-156.
- Barghi, S. H., Adibi, M. & Rashtchian, D. (2010). An experimental study on permeability, diffusivity, and selectivity of CO<sub>2</sub> and CH<sub>4</sub> through [bmim][PF<sub>6</sub>] ionic liquid supported on an alumina membrane: Investigation of temperature fluctuations effects. *Journal of Membrane Science*, 362, 346-352.

- Basheer, C., Alnedhary, A. A., Madhava Rao, B. S., Balasubramanian, R. & Lee, H. K. (2008). Ionic liquid supported three-phase liquid-liquid-liquid microextraction as a sample preparation technique for aliphatic and aromatic hydrocarbons prior to gas chromatography-mass spectrometry. *Journal of Chromatography A*, 1210, 19-24.
- Bates, E. D., Mayton, R. D., Ntai, I. & Davis, J. H. (2002). CO<sub>2</sub> capture by a task-specific ionic liquid. *Journal of the American Chemical Society*, 124, 926-927.
- Bhaumik, D., Majumdar, S. & Sirkar, K. K. (1998). Absorption of CO<sub>2</sub> in a transverse flow hollow fiber membrane module having a few wraps of the fiber mat. *Journal of Membrane Science*, 138, 77-82.
- Bijani, S., Fortunato, R., de Yuso, M. V. M., Heredia-Guerrero, F. A., Rodriguez-Castellon, E., Coelho, I., Crespo, J., & Benavente, J. (2009). Physical-chemical and electrical characterizations of membranes modified with room temperature ionic liquids: Age effect, *Vacuum*, 83, 1283-1286.
- Blahušiak, M., Schlosser, Š. & Marták, J. (2011). Extraction of butyric acid by a solvent impregnated resin containing ionic liquid. *Reactive and Functional Polymers*, 71, 736-744.
- Bougie, F., Iliuta, I. & Iliuta, M. C. (2015). Flat sheet membrane contactor (FSMC) for CO<sub>2</sub> separation using aqueous amine solutions. *Chemical Engineering Science*, 123, 255-264.
- Bounaceur, R., Lape, N., Roizard, D., Vallieres, C. & Favre, E. (2006). Membrane processes for post-combustion carbon dioxide capture: A parametric study. *Energy*, 31, 2556-2570.
- Branco, L. C., Crespo, J. G. & Afonso, C. A. M. (2002a). Highly selective transport of organic compounds by using supported liquid membranes based on ionic liquids. *Angewandte Chemie International Edition*, 41, 2771-+.
- Branco, L. C., Crespo, J. G. & Afonso, C. A. M. (2002b). Studies on the selective transport of organic compounds by using ionic liquids as novel supported liquid membranes. *Chemistry-a European Journal*, 8, 3865-3871.
- Brennecke, J. F. & Gurkan, B. E. (2010). Ionic Liquids for CO<sub>2</sub> capture and emission reduction. *The Journal of Physical Chemistry Letters*, 1, 3459-3464.
- Chabanon, E., Belaisaoui, B. & Favre, E. (2014). Gas-liquid separation processes based on physical solvents: opportunities for membranes. *Journal of Membrane Science*, 459, 52-61.
- Chabanon, E., Bounaceur, R., Castel, C., Rode, S., Roizard, D. & Favre, E. (2015). Pushing the limits of intensified CO<sub>2</sub> post-combustion capture by gas-liquid absorption through a membrane contactor. *Chemical Engineering and Processing: Process Intensification*, 91, 7-22.



- Chabanon, E., Roizard, D. & Favre, E. (2011). Membrane contactors for postcombustion carbon dioxide capture: A comparative study of wetting resistance on long time scales. *Industrial and Engineering Chemistry Research*, 50, 8237-8244.
- Chai, S. -H., Fulvio, P. F., Hillesheim, P. C., Qiao, Z. -A., Mahurin S. M. & Dai, S. (2014). "Brick-and-mortar" synthesis of free-standing mesoporous carbon nanocomposite membranes as supports of room temperature ionic liquids for CO<sub>2</sub>/N<sub>2</sub> separation. *Journal of Membrane Science*, 468, 73-80.
- Chanda, M. & S. K. Roy (Eds.), Characteristics of polymers, in: *Plastics Technology Handbook*. Fourth Edition, CRC Press, 2006, pp. 1-128.
- Chau, J., Obuskovic, G., Jie, X. & Sirkar, K. K. (2014). Pressure swing membrane absorption process for shifted syngas separation: Modeling vs. experiments for pure ionic liquid. *Journal of Membrane Science*, 453, 61-70.
- Che, Q., Sun, B. & He, R. (2008). Preparation and characterization of new anhydrous, conducting membranes based on composites of ionic liquid trifluoroacetic propylamine and polymers of sulfonated poly (ether ether) ketone or polyvinylidene fluoride. *Electrochimica Acta*, 53, 4428-4434.
- Chen, H., Kovvali, A. S., Majumdar, S. & Sirkar, K. K. (1999). Selective CO<sub>2</sub> separation from CO<sub>2</sub>/N<sub>2</sub> mixtures by immobilized carbonate-glycerol membranes. *Industrial and Engineering Chemistry Research*, 38, 3489-3498.
- Chen, H., Obuskovic, G., Majumdar, S. & Sirkar, K. K. (2001). Immobilized glycerol-based liquid membranes in hollow fibers for selective CO<sub>2</sub> separation from CO<sub>2</sub>/N<sub>2</sub> mixtures. *Journal of Membrane Science*, 183, 75-88.
- Chiarizia, R. (1991). Stability of supported liquid membrane containing long-chain aliphatic amines as carriers. *Journal of Membrane Science*, 55, 65-77.
- Chun, S., Dzyuba, S. V. & Bartsch, R. A. (2001). Influence of structural variation in room-temperature ionic liquids on the selectivity and efficiency of competitive alkali metal salt extraction by a crown ether. *Analytical Chemistry*, 73, 3737-3741.
- Cichowska-Kopczy, I., Joskowska, M., Debski, B., Luczak, J. & Aranowski, R. (2013). Influence of ionic liquid structure on supported ionic liquid membranes effectiveness in carbon dioxide/methane separation. *Journal of Chemistry*, 10.
- Close, J. J., Farmer, K., Moganty, S. S. & Baltus, R. E. (2012). CO<sub>2</sub>/N<sub>2</sub> separations using nanoporous alumina-supported ionic liquid membranes: Effect of the support on separation performance. *Journal of Membrane Science*, 390, 201-210.
- Coelhoso, I. M., Cardoso, M. M., Viegas, R. M. C. & Crespo, J. P. S. G. (2000). Transport mechanisms and modelling in liquid membrane contactors. *Separation and Purification Technology*, 19, 183-197.

- COSMOthermX, A graphical user interface to the COSMOthermX program user guide; Version C30 1401, COSMOlogic GmbH & Co. KG, Leverkusen, Germany, 2013.
- Cserjési, P., Nemestóthy, N. & Bélafi-Bakó, K. (2010). Gas separation properties of supported liquid membranes prepared with unconventional ionic liquids. *Journal of Membrane Science*, 349, 6-11.
- Cserjesi, P., Nemestothy, N., Vass, A., Csanadi, Z. & Belafi-Bako, K. (2009). Study on gas separation by supported liquid membranes applying novel ionic liquids. *Desalination*, 245, 743-747.
- Cui, Z. & deMontigny, D. (2013). Part 7: A review of CO<sub>2</sub> capture using hollow fiber membrane contactors. *Carbon Management*, 4, 69-89.
- da Silva, E. F., Lepaumier, H., Grimstvedt, A., Vevelstad, S. J., Einbu, A., Vernstad, K., Svendsen, H.F. & Zahlén, K. (2012). Understanding 2-Ethanolamine degradation in post combustion CO<sub>2</sub> capture. *Industrial and Engineering Chemistry Research*, 51, 13329-13338.
- Dai, Z. D., Noble, R. D., Gin, D. L., Zhang, X. P. & Deng, L. Y. (2016). Combination of ionic liquids with membrane technology: A new approach for CO<sub>2</sub> separation. *Journal of Membrane Science*, 497, 1-20.
- Dai, Z., Ansaloni, L., Gin, D. L., Noble, R. D. & Deng, L. (2017). Facile fabrication of CO<sub>2</sub> separation membranes by cross-linking of poly(ethylene glycol) diglycidyl ether with a diamine and a polyamine-based ionic liquid. *Journal of Membrane Science*, 523, 551-560.
- Davis, J. & Rochelle, G. (2009). Thermal degradation of monoethanolamine at stripper conditions, in: Gale, J., Herzog, H., Braitsch, J. (Eds.), *Greenhouse Gas Control Technologies 9*. Elsevier Science Bv, Amsterdam, pp. 327-333.
- Davis, R. A. & Sandall, O. C. (1993). CO<sub>2</sub>/CH<sub>4</sub> separation by facilitated transport in amine polyethylene glycol mixtures. *Aiche Journal*, 39, 1135-1145.
- de los Ríos, A. P., Hernández-Fernández, F. J., Rubio, M., Gómez, D. & Villora, G. (2007). Stabilization of native penicillin G acylase by ionic liquids. *Journal of Chemical Technology and Biotechnology*, 82, 190-195.
- de los Rios, A. P., Hernandez-Fernandez, F. J., Tomas-Alonso, F., Palacios, J. M., Gomez, D., Rubio, M. & Villora, G. (2007). A SEM-EDX study of highly stable supported liquid membranes based on ionic liquids. *Journal of Membrane Science*, 300, 88-94.
- deMontigny, D., Tontiwachwuthikul, P. & Chakma, A. (2005). Comparing the absorption performance of packed columns and membrane contactors. *Industrial and Engineering Chemistry Research*, 44, 5726-5732.
- deMontigny, D., Tontiwachwuthikul, P. & Chakma, A. (2006). Using polypropylene and polytetrafluoroethylene membranes in a membrane contactor for CO<sub>2</sub> absorption. *Journal of Membrane Science*, 277, 99-107.

- Deng, L. Closed cycle continuous membrane ionic liquids absorption/desorption process for CO<sub>2</sub> capture, U.K.P. Application (Ed.), 2015.
- Dindore, V. Y. & Versteeg, G. F. (2005). Gas–liquid mass transfer in a cross-flow hollow fiber module: Analytical model and experimental validation. *International Journal of Heat and Mass Transfer*, 48, 3352-3362.
- Dindore, V. Y., Brilman, D. W. F., Geuzebroek, F. H. & Versteeg, G. F. (2004). Membrane–solvent selection for CO<sub>2</sub> removal using membrane gas–liquid contactors. *Separation and Purification Technology*, 40, 133-145.
- Dlugokencky, E., & Tans, P. (2017). Trends in atmospheric carbon dioxide. Retrieved from [www.esrl.noaa.gov/gmd/ccgg/trends/](http://www.esrl.noaa.gov/gmd/ccgg/trends/)
- Donaldson, T. L. & Nguyen, Y. N. (1980). Carbon dioxide reaction kinetics and transport in aqueous amine membranes. *Industrial and Engineering Chemistry Fundamentals*, 19, 260-266.
- Ebner, A. D. & Ritter, J. A. (2009). State-of-the-art adsorption and membrane separation processes for carbon dioxide production from carbon dioxide emitting industries. *Separation and Science Technology*, 44, 1273-1421.
- Eike, D. M., Brennecke, J. F. & Maginn, E. J. (2004). Predicting infinite-dilution activity coefficients of organic solutes in ionic liquids. *Industrial and Engineering Chemistry Research*, 43, 1039-1048.
- Falk-Pedersen, O., Gronvold, M. S., Nokleby, P., Bjerre, F. & Svendsen, H. F. (2005). CO<sub>2</sub> capture with membrane contactors. *International Journal of Green Energy*, 2, 157-165.
- Favre, E. & Svendsen, H. F. (2012). Membrane contactors for intensified post-combustion carbon dioxide capture by gas–liquid absorption processes. *Journal of Membrane Science*, 407, 1-7.
- Favre, E. (2007). Carbon dioxide recovery from post-combustion processes: Can gas permeation membranes compete with absorption?. *Journal of Membrane Science*, 294, 50-59.
- Favre, E. (2011). Membrane processes and postcombustion carbon dioxide capture: Challenges and prospects. *Chemical Engineering Journal*, 171, 782-793.
- Fehér, E., Illeová, V., Kelemen-Horváth, I., Bélafi-Bakó, K., Polakovič, M. & Gubicza, L. (2008). Enzymatic production of isoamyl acetate in an ionic liquid–alcohol biphasic system. *Journal of Molecular Catalysis B: Enzymatic*, 50, 28-32.
- Fernicola, A., Weise, F. C., Greenbaum, S. G., Kagimoto, J., Scrosati, B. & Soletto, A., (2009). Lithium-ion-conducting electrolytes: From an ionic liquid to the polymer membrane. *Journal of the Electrochemical Society*, 156, A514-A520.

- Feron, P. H. M. & Jansen, A. E. (1995). Capture of carbon dioxide using membrane gas absorption and reuse in the horticultural industry. *Energy Conversion and Management*, 36, 411-414.
- Feron, P. H. M., Jansen, A. E. & Klaassen, R. (1992). Membrane technology in carbon dioxide removal. *Energy Conversion and Management*, 33, 421-428.
- Finotello, A., Bara, J. E., Camper, D. & Noble, R. D. (2008). Room-temperature ionic liquids: Temperature dependence of gas solubility selectivity. *Industrial and Engineering Chemistry Research*, 47, 3453-3459.
- Fontanals, N., Ronka, S., Borrull, F., Trochimczuk, A. W. & Marcé, R. M. (2009). Supported imidazolium ionic liquid phases: A new material for solid-phase extraction. *Talanta*, 80, 250-256.
- Fortunato, R., Afonso, C. A. M., Reis, M. A. M. & Crespo, J. G. (2004). Supported liquid membranes using ionic liquids: study of stability and transport mechanisms. *Journal of Membrane Science*, 242, 197-209.
- Fortunato, R., Gonzalez-Munoz, M. J., Kubasiewicz, M., Luque, S., Alvarez, J. R., Afonso, C. A. M., Coelho, I. M. & Crespo, J. G. (2005a). Liquid membranes using ionic liquids: the influence of water on solute transport. *Journal of Membrane Science*, 249, 153-162.
- Fortunato, R., González-Muñoz, M. J., Kubasiewicz, M., Luque, S., Alvarez, J. R., Afonso, C. A. M., Coelho, I. M. & Crespo, J. G. (2005b). Liquid membranes using ionic liquids: the influence of water on solute transport. *Journal of Membrane Science*, 249, 153-162.
- Francisco, G. J., Chakma, A. & Feng, X. S. (2010). Separation of carbon dioxide from nitrogen using diethanolamine-impregnated poly(vinyl alcohol) membranes. *Separation and Purification Technology*, 71, 205-213.
- Franco, J.A., Kentish, S. E., Perera, J.M. & Stevens, G. W. (2011). Poly(tetrafluoroethylene) sputtered polypropylene membranes for carbon dioxide separation in membrane gas absorption. *Industrial and Engineering Chemistry Research*, 50, 4011-4020.
- Franken, A. C. M., Nolten, J. A. M., Mulder, M. H. V., Bargeman, D. & Smolders, C. A. (1987). Wetting criteria for the applicability of membrane distillation. *Journal of Membrane Science*, 33, 315-328.
- Friess, K., Jansen, J. C., Bazzarelli, F., Izák, P., Jarmarová, V., Kačírková, M., Schauer, J., Clarizia, G. & Bernardo, P. (2012). High ionic liquid content polymeric gel membranes: Correlation of membrane structure with gas and vapour transport properties. *Journal of Membrane Science*, 415, 801-809.
- Gabelman, A. & Hwang, S. -T. (1999). Hollow fiber membrane contactors. *Journal of Membrane Science*, 159, 61-106.

- Gan, Q., Rooney, D., Xue, M., Thompson, G. & Zou, Y. (2006). An experimental study of gas transport and separation properties of ionic liquids supported on nanofiltration membranes. *Journal of Membrane Science*, 280, 948-956.
- Gan, Q., Zou, Y., Rooney, D., Nancarrow, P., Thompson, J., Liang, L. & Lewis, M. (2011a). Theoretical and experimental correlations of gas dissolution, diffusion, and thermodynamic properties in determination of gas permeability and selectivity in supported ionic liquid membranes. *Advances in Colloid and Interface Science*, 164, 45-55.
- Gan, Q., Zou, Y., Rooney, D., Nancarrow, P., Thompson, J., Liang, L. & Lewis, M. (2011). Theoretical and experimental correlations of gas dissolution, diffusion, and thermodynamic properties in determination of gas permeability and selectivity in supported ionic liquid membranes. *Advances in Colloid and Interface Science*, 164, 45-55.
- Gao, Y., Zhang, F., Huang, K., Ma, J. W., Wu, Y. -T., & Zhang, Z. -B. (2013). Absorption of CO<sub>2</sub> in amino acid ionic liquid (AAIL) activated MDEA solutions. *International Journal of Greenhouse Gas Control*, 19, 379-386.
- Goff, G. S. & Rochelle, G. T. (2004). Monoethanolamine degradation: O<sub>2</sub> Mass transfer effect under CO<sub>2</sub> capture conditions. *Industrial and Engineering Chemistry Research*, 43, 6400-6408.
- Gómez-Coma, L., Garea, A. & Irabien, A. (2014). Non-dispersive absorption of CO<sub>2</sub> in [emim][EtSO<sub>4</sub>] and [emim][Ac]: Temperature influence. *Separation and Purification Technology*, 132, 120-125.
- Gómez-Coma, L., Garea, A., Rouch, J. C., Savart, T., Lahitte, J. F., Remigy, J. C. & Irabien, A. (2016). Membrane modules for CO<sub>2</sub> capture based on PVDF hollow fibers with ionic liquids immobilized. *Journal of Membrane Science*, 498, 218-226.
- Gonzalez-Miquel, M., Palomar, J., Omar, S. & Rodriguez, F. (2011). CO<sub>2</sub>/N<sub>2</sub> selectivity prediction in supported ionic liquid membranes (SILMs) by COSMO-RS. *Industrial and Engineering Chemistry Research*, 50, 5739-5748.
- Gorji, A.H. & Kaghazchi, T. (2008). CO<sub>2</sub>/H<sub>2</sub> separation by facilitated transport membranes immobilized with aqueous single and mixed amine solutions: Experimental and modeling study. *Journal of Membrane Science*, 325, 40-49.
- Gupta, K. M., Chen, Y. & Jiang, J. (2013). Ionic liquid membranes supported by hydrophobic and hydrophilic metal-organic frameworks for CO<sub>2</sub> capture. *The Journal of Physical Chemistry, C* 117, 5792-5799.
- Gupta, K. M., Chen, Y., Hu, Z. & Jiang, J. (2012). Metal-organic framework supported ionic liquid membranes for CO<sub>2</sub> capture: anion effects. *Physical Chemistry Chemical Physics*, 14, 5785-5794.
- Gurau, G., Rodriguez, H., Kelley, S. P., Janiczek, P., Kalb, R. S. & Rogers, R. D. (2011). Demonstration of chemisorption of carbon dioxide in 1,3-

Dialkylimidazolium acetate ionic liquids. *Angewandte Chemie International Edition*, 50, 12024-12026.

- Han, D. & Row, K. H. (2010). Recent applications of ionic liquids in separation technology. *Molecules*, pp. 2405-2426.
- Hanioka, S., Maruyama, T., Sotani, T., Teramoto, M., Matsuyama, H., Nakashima, K., Hanaki, M., Kubota, F. & Goto, M. (2008). CO<sub>2</sub> separation facilitated by task-specific ionic liquids using a supported liquid membrane. *Journal of Membrane Science*, 314, 1-4.
- Happel, S., Streng, R., Vater, P. & Ensinger, W. (2003). Sr/Y separation by supported liquid membranes based on nuclear track micro filters. *Radiation Measurements*, 36, 761-766.
- Hasib-ur-Rahman, M., Siaj, M. & Larachi, F. (2012). CO<sub>2</sub> capture in alkanolamine/room-temperature ionic liquid emulsions: A viable approach with carbamate crystallization and curbed corrosion behavior. *International Journal of Greenhouse Gas Control*, 6, 246-252.
- Heitmann, S., Krings, J., Kreis, P., Lennert, A., Pitner, W. R., Górak, A. & Schulte, M. M. (2012). Recovery of n-butanol using ionic liquid-based pervaporation membranes. *Separation and Purification Technology*, 97, 108-114.
- Hernández-Fernández, F. J., de los Ríos, A. P., Rubio, M., Tomás-Alonso, F., Gómez, D. & Villora, G. (2007). A novel application of supported liquid membranes based on ionic liquids to the selective simultaneous separation of the substrates and products of a transesterification reaction. *Journal of Membrane Science*, 293, 73-80.
- Hernandez-Fernandez, F. J., de los Rios, A. P., Tomas-Alonso, F., Palacios, J. M. & Villora, G. (2009). Preparation of supported ionic liquid membranes: Influence of the ionic liquid immobilization method on their operational stability. *Journal of Membrane Science*, 341, 172-177.
- Hernández-Fernández, F. J., de los Ríos, A. P., Tomás-Alonso, F., Gómez, D. & Villora, G. (2009a). Improvement in the separation efficiency of transesterification reaction compounds by the use of supported ionic liquid membranes based on the dicyanamide anion. *Desalination*, 244, 122-129.
- Hizaddin, H. F., Ramalingam, A., Hashim, M. A. & Hadj-Kali, M. K. O. (2014). Evaluating the performance of deep eutectic solvents for use in extractive denitrification of liquid fuels by the Conductor-like Screening Model for Real Solvents. *Journal of Chemical Engineering Data*, 59, 3470-3487.
- Ho, M., W. Allinson, G. & Wiley, D. (2008). Reducing the cost of CO<sub>2</sub> capture from flue gases using pressure swing adsorption. *Industrial and Engineering Chemistry Research*, 47.
- Ho, W. S. W. & Sirkar, K. K. (1992). *Membrane Handbook*, Springer Science + Business Media, New York, US.

- Hoff, kA. Modeling and experimental study of CO<sub>2</sub> absorption in a membrane contactor, Chemical Engineering Department, Norwegian Univerisity and Science and technology, Trondheim, 2003.
- Hojniak, S., Khan, A., Holloczki, O., Kirchner, B., Vankelecom, I., Dehaen, W. & Binnemans, K. (2013). Separation of carbon dioxide from nitrogen or methane by supported ionic liquid membranes (SILMs): Influence of the cation charge of the ionic liquid. *The Journal of Physical Chemistry B*, 117.
- Hojniak, S., Silverwood, I., Khan, A., Vankelecom, I., Dehaen, W., Kazarian, S. & Binnemans, K. (2014). Highly selective separation of carbon dioxide from nitrogen and methane by nitrile/glycol-difunctionalized ionic liquids in supported ionic liquid membranes (SILMs). *The Journal of Physical Chemistry B*, 118, 7440-7449.
- Huang, J., Riisager, A., Wasserscheid, P. & Fehrmann, R. (2006). Reversible physical absorption of SO<sub>2</sub> by ionic liquids. *Chemical Communications*, 4027-4029.
- Huang, K., Zhang, X. -M., Li, Y. -X., Wu, Y. -T. & Hu, X. -B. (2014). Facilitated separation of CO<sub>2</sub> and SO<sub>2</sub> through supported liquid membranes using carboxylate-based ionic liquids. *Journal of Membrane Science*, 471, 227-236.
- Iarikov, D. D., Hacırlıoğlu, P. & Oyama, S. T. (2011). Supported room temperature ionic liquid membranes for CO<sub>2</sub>/CH<sub>4</sub> separation. *Chemical Engineering Journal*, 166, 401-406.
- Iliconich, J., Myers, C., Pennline, H. & Luebke, D. (2007). Experimental investigation of the permeability and selectivity of supported ionic liquid membranes for CO<sub>2</sub>/He separation at temperatures up to 125°C. *Journal of Membrane Science*, 298, 41-47.
- Im, D., Roh, K., Kim, J., Eom, Y. & Lee, J. H. (2015). Economic assessment and optimization of the Selexol process with novel additives. *International Journal of Greenhouse Gas Control*, 42, 109-116.
- Ismail, A. F. & Mansourizadeh, A. (2010). A comparative study on the structure and performance of porous polyvinylidene fluoride and polysulfone hollow fiber membranes for CO<sub>2</sub> absorption. *Journal of Membrane Science*, 365, 319-328.
- Ito, A., Duan, S., Ikenori, Y. & Ohkawa, A. (2001). Permeation of wet CO<sub>2</sub>/CH<sub>4</sub> mixed gas through a liquid membrane supported on surface of a hydrophobic microporous membrane. *Separation and Purification Technology*, 24, 235-242.
- Izák, P., Friess, K., Hynek, V., Ruth, W., Fei, Z., Dyson, J. P. & Kragl, U. (2009). Separation properties of supported ionic liquid–polydimethylsiloxane membrane in pervaporation process. *Desalination*, 241, 182-187.
- Izak, P., Koekerling, A. & Kragl, U. (2006). Solute transport from aqueous mixture through supported ionic liquid membrane by pervaporation. *Desalination*, 199, 96-98.

- Izak, P., Ruth, W., Fei, Z., Dyson, P. J. & Kragl, U. (2008). Selective removal of acetone and butan-1-ol from water with supported ionic liquid-polydimethylsiloxane membrane by pervaporation. *Chemical Engineering Journal*, 139, 318-321.
- Jalili, A. H., Shokouhi, M., Maurer, G. & Hosseini-Jenab, M. (2013). Solubility of CO<sub>2</sub> and H<sub>2</sub>S in the ionic liquid 1-ethyl-3-methylimidazolium tris(pentafluoroethyl)trifluorophosphate. *The Journal of Chemical Thermodynamics*, 67, 55-62.
- Jansen, J. C., Clarizia, G., Bernardo, P., Bazzarelli, F., Friess, K., Randová, A., Schauer, J., Kubicka, D., Kacirková, M. & Izak, P. (2013). Gas transport properties and pervaporation performance of fluoropolymer gel membranes based on pure and mixed ionic liquids. *Separation and Purification Technology*, 109, 87-97.
- Jansen, J. C., Friess, K., Clarizia, G., Schauer, J. & Izák, P. (2011). High ionic liquid content polymeric gel membranes: Preparation and performance. *Macromolecules*, 44, 39-45.
- Jessop, P. G., Stanley, R. R., Brown, R. A., Eckert, C. A., Liotta, C. L., Ngo, T. T. & Pollet, P. (2003). Neoteric solvents for asymmetric hydrogenation: supercritical fluids, ionic liquids, and expanded ionic liquids. *Green Chemistry*, 5, 123-128.
- Jiang, Y. Y., Zhou, Z., Jiao, Z., Li, L., Wu, Y. T. & Zhang, Z. B. (2007). SO<sub>2</sub> gas separation using supported ionic liquid membranes. *The Journal of Physical Chemistry . B*, 111, 5058-5061.
- Jie, X. M., Chau, J., Obuskovic, G. & Sirkar, K. K. (2014). Enhanced pressure swing membrane absorption process for CO<sub>2</sub> removal from shifted syngas with dendrimer-ionic liquid mixtures as absorbent. *Industrial and Engineering Chemistry Research*, 53, 3305-3320.
- Jie, X., Chau, J., Obuskovic, G. & Sirkar, K. K. (2013). Preliminary studies of CO<sub>2</sub> removal from precombustion syngas through pressure swing membrane absorption process with ionic liquid as absorbent. *Industrial and Engineering Chemistry Research*, 52, 8783-8799.
- Jindaratamee, P., Ito, A., Komuro, S. & Shimoyama, Y. (2012). Separation of CO<sub>2</sub> from the CO<sub>2</sub>/N<sub>2</sub> mixed gas through ionic liquid membranes at the high feed concentration. *Journal of Membrane Science*, 423, 27-32.
- Jindaratamee, P., Shimoyama, Y., Morizaki, H. & Ito, A. (2011). Effects of temperature and anion species on CO<sub>2</sub> permeability and CO<sub>2</sub>/N<sub>2</sub> separation coefficient through ionic liquid membranes. *The Journal of Chemical Thermodynamics*, 43, 311-314.
- Jonassen, O., Kim, I. & Svendsen, H. F. (2014). Heat of absorption of carbon dioxide (CO<sub>2</sub>) into aqueous N-methyldiethanolamine (MDEA) and N,N-dimethylmonoethanolamine (DMMEA), in: Dixon, T., Herzog, H., Twinning,



S. (Eds.), 12th International Conference on Greenhouse Gas Control Technologies, Ghgt-12. Elsevier Science Bv, Amsterdam, pp. 1890-1902.

- Kanakubo, M., Umecky, T., Hiejima, Y., Aizawa, T., Nanjo, H. & Kameda, Y. (2005). Solution structures of 1-butyl-3-methylimidazolium hexafluorophosphate ionic liquid saturated with CO<sub>2</sub>: Experimental evidence of specific anion-CO<sub>2</sub> interaction. *The Journal of Physical Chemistry B*, 109, 13847-13850.
- Kasahara, S., Kamio, E., Ishigami, T. & Matsuyama, H. (2012a). Amino acid ionic liquid-based facilitated transport membranes for CO<sub>2</sub> separation. *Chemical Communications*, 48, 6903-6905.
- Kasahara, S., Kamio, E., Ishigami, T. & Matsuyama, H. (2012b). Effect of water in ionic liquids on CO<sub>2</sub> permeability in amino acid ionic liquid-based facilitated transport membranes. *Journal of Membrane Science*, 415, 168-175.
- Kato, T. & Hayase, S. (2007). Quasi-solid dye sensitized solar cell with straight ion paths - Proposal of hybrid electrolytes for ionic liquid-type electrolytes. *Journal of the Electrochemical Society*, 154, B117-B121.
- Kato, T., Kado, T., Tanaka, S., Okazaki, A. & Hayase, S. (2006). Quasi-solid dye-sensitized solar cells containing nanoparticles modified with ionic liquid-type molecules. *Journal of the Electrochemical Society*, 153, A626-A630.
- Kawanami, H., Sasaki, A., Matsui, K. & Ikushima, Y. (2003). A rapid and effective synthesis of propylene carbonate using a supercritical CO<sub>2</sub>-ionic liquid system. *Chemical Communications*, 896-897.
- Kerle, D., Ludwig, R., Geiger, A. & Paschek, D. (2009). Temperature dependence of the solubility of carbon dioxide in imidazolium-based ionic liquids. *The Journal of Physical Chemistry B*, 113, 12727-12735.
- Khaisri, S., Demontigny, D., Tontiwachwuthikul, P. & Jiratananon, R. (2009). Comparing membrane resistance and absorption performance of three different membranes in a gas absorption membrane contactor. *Separation and Purification Technology*, 65, 290-297.
- Kilaru, P.K., Condemarin, P.A. & Scovazzo, P. (2008). Correlations of low-pressure carbon dioxide and hydrocarbon solubilities in imidazolium-, phosphonium-, and ammonium-based room-temperature ionic Liquids. Part 1. Using surface tension. *Industrial and Engineering Chemistry Research*, 47, 900-909.
- Kim, D. -H., Baek, I. -H., Hong, S. -U. & Lee, H. -K. (2011). Study on immobilized liquid membrane using ionic liquid and PVDF hollow fiber as a support for CO<sub>2</sub>/N<sub>2</sub> separation. *Journal of Membrane Science*, 372, 346-354.
- Kim, Y. -S. & Yang, S. M. (2000). Absorption of carbon dioxide through hollow fiber membranes using various aqueous absorbents. *Separation and Purification Technology*, 21, 101-109.

- Kim, Y. S., Choi, W. Y., Jang, J. H., Yoo, K. P. & Lee, C. S. (2005). Solubility measurement and prediction of carbon dioxide in ionic liquids. *Fluid Phase Equilibria*, 228, 439-445.
- Klaassen, R., Feron, P. & Jansen, A. (2008). Membrane contactor applications. *Desalination*, 224, 81-87.
- Kladkaew, N., Idem, R., Tontiwachwuthikul, P. & Saiwan, C. (2011). Studies on corrosion and corrosion inhibitors for amine based solvents for CO<sub>2</sub> absorption from power plant flue gases containing CO<sub>2</sub>, O<sub>2</sub> and SO<sub>2</sub>, in: Gale, J., Hendriks, C., Turkenberg, W. (Eds.), 10th International Conference on Greenhouse Gas Control Technologies. Elsevier Science Bv, Amsterdam, pp. 1761-1768.
- Kocherginsky, N. M., Yang, Q. & Seelam, L. (2007). Recent advances in supported liquid membrane technology. *Separation and Purification Technology*, 53, 171-177.
- Kohl, A. L. & Nielsen, R. B. (1997). Chapter 2 – Alkanolamines for hydrogen sulfide and carbon dioxide removal. In: Kohl, A.L., Nielsen, R.B. (Eds.), Gas Purification. , 5<sup>th</sup> edition. Gulf Professional Publishing, Houston, pp. 40–186
- Kouki, N., Tayeb, R., Zarrougui, R. & Dhahbi, M. (2010). Transport of salicylic acid through supported liquid membrane based on ionic liquids. *Separation and Purification Technology*, 76, 8-14.
- Kreiter, R., Overbeek, J. P., Correia, L. A. & Vente, J. F. (2011). Pressure resistance of thin ionic liquid membranes using tailored ceramic supports. *Journal of Membrane Science*, 370, 175-178.
- Kreulen, H., Smolders, C. A., Versteeg, G. F. & Vanswaaij, W. P. M. (1993). Microporous hollow fiber membrane modules as gas-liquid contactors. 2. Mass transfer with chemical reaction. *Journal of Membrane Science*, 78, 217-238.
- Kroon, M. C., Karakatsani, E. K., Economou, I. G., Witkamp, G. J. & Peters, C. J. (2006). Modeling of the carbon dioxide solubility in imidazolium-based ionic liquids with the tPC-PSAFT equation of state. *The Journal of Physical Chemistry B*, 110, 9262-9269.
- Krull, F. F., Fritzmann, C. & Melin, T. (2008). Liquid membranes for gas/vapor separation. *Journal of Membrane Science*, 325, 509-519.
- Kulkarni, P. S., Neves, L. A., Coelho, I. M., Afonso, C. A. M. & Crespo, J. G. (2012). Supported ionic liquid membranes for removal of dioxins from high-temperature vapor streams. *Environmental Science and Technology*, 46, 462-468.
- Kumar, P. S., Hogendoorn, J. A., Feron, P. H. M. & Versteeg, G. F. (2002). New absorption liquids for the removal of CO<sub>2</sub> from dilute gas streams using membrane contactors. *Chemical Engineering Science*, 57, 1639-1651.

- Labropoulos, A., Romanos, G., Kouvelos, E., Falaras, P., Likodimos, V., Francisco Casal, M. M., Kroon, M. M., Iliev, B., Adamova, G., Schubert, T. (2013). Alkyl-methylimidazolium tricyanomethanide ionic liquids under extreme confinement onto nanoporous ceramic membranes. *The Journal of Physical Chemistry C*, 117, 10114 - null.
- Lee, S. -Y., Ogawa, A., Kanno, M., Nakamoto, H., Yasuda, T. & Watanabe, M. (2010a). Nonhumidified intermediate temperature fuel cells using protic ionic liquids. *Journal of the American Chemical Society*, 132, 9764-9773.
- Lee, S. -Y., Yasuda, T. & Watanabe, M. (2010b). Fabrication of protic ionic liquid/sulfonated polyimide composite membranes for non-humidified fuel cells. *Journal of Power Sources*, 195, 5909-5914.
- Lemus, J., Palomar, J., Gilarranz, M. A. & Rodriguez, J. J. (2011). Characterization of supported ionic liquid phase (SILP) materials prepared from different supports. *Adsorption*, 17, 561-571.
- Lepaumier, H., da Silva, E.F., Einbu, A., Grimstedt, A., Knudsen, J. N., Zahlsen, K. & Svendsen, H. F. (2011). Comparison of MEA degradation in pilot-scale with lab-scale experiments. *Energy Procedia*, 4, 1652-1659.
- Li, J. L. & Chen, B. H. (2005). Review Of CO<sub>2</sub> absorption using chemical solvents in hollow fiber membrane contactors. *Separation and Purification Technology*, 41, 109-122.
- Li, K., Wang, D., Koe, C. C. & Teo, W. K. (1998). Use of asymmetric hollow fibre modules for elimination of H<sub>2</sub>S from gas streams via a membrane absorption method. *Chemical Engineering Science*, 53, 1111-1119.
- Li, M., Pham, P. J., Pittman, C. U. & Li, T. (2009). SBA-15-supported ionic liquid compounds containing silver salts: Novel mesoporous  $\pi$ -complexing sorbents for separating polyunsaturated fatty acid methyl esters. *Microporous and Mesoporous Materials*, 117, 436-443.
- Lin, S. -H., Hsieh, C. -F., Li, M. -H. & Tung, K. -L. (2009a). Determination of mass transfer resistance during absorption of carbon dioxide by mixed absorbents in PVDF and PP membrane contactor. *Desalination*, 249, 647-653.
- Lin, S. -H., Tung, K. -L., Chang, H. -W. & Lee, K. -R. (2009b). Influence of fluorocarbon flat-membrane hydrophobicity on carbon dioxide recovery. *Chemosphere*, 75, 1410-1416.
- Lin, S. T. & Sandler, S. I. (2002). A priori phase equilibrium prediction from a segment contribution solvation model. *Industrial and Engineering Chemistry Research*, 41, 899-913.
- Lin, Y. -F., Ko, C. -C., Chen, C. -H., Tung, K. -L., Chang, K. -S. & Chung, T. -W. (2014). Sol-gel preparation of polymethylsilsesquioxane aerogel membranes for CO<sub>2</sub> absorption fluxes in membrane contactors. *Applied Energy*, 129, 25-31.

- Liu, L., Li, L., Ding, Z., Ma, R. & Yang, Z. (2005a). Mass transfer enhancement in coiled hollow fiber membrane modules. *Journal of Membrane Science*, 264, 113-121.
- Liu, Y., Wang, M., Li, J., Li, Z., He, P., Liu, H. & Li, J. (2005b). Highly active horseradish peroxidase immobilized in 1-butyl-3-methylimidazolium tetrafluoroborate room-temperature ionic liquid based sol-gel host materials. *Chemical Communications*, 1778-1780.
- Lozano, L. J., Godínez, C., de los Ríos, A. P., Hernández-Fernández, F. J., Sánchez-Segado, S. & Alguacil, F. J. (2011). Recent advances in supported ionic liquid membrane technology. *Journal of Membrane Science*, 376, 1-14.
- Lozano, P. (2010). Enzymes in neoteric solvents: From one-phase to multiphase systems. *Green Chemistry*, 12, 555-569.
- Lu, J. G., Wang, L. J., Sun, X. Y., Li, J. S. & Liu, X. D. (2005). Absorption of CO<sub>2</sub> into aqueous solutions of methyldiethanolamine and activated methyldiethanolamine from a gas mixture in a hollow fiber contactor. *Industrial and Engineering Chemistry Research*, 44, 9230-9238.
- Lu, J. -G., Zheng, Y. -F. & Cheng, M. -D. (2008). Wetting mechanism in mass transfer process of hydrophobic membrane gas absorption. *Journal of Membrane Science*, 308, 180-190.
- Luis, P. & Van der Bruggen, B. (2013). The role of membranes in post-combustion CO<sub>2</sub> capture. *Greenhouse Gases*, 3, 318-337.
- Luis, P., Garea, A. & Irabien, A. (2009a). Zero solvent emission process for sulfur dioxide recovery using a membrane contactor and ionic liquids. *Journal of Membrane Science*, 330, 80-89.
- Luis, P., Neves, L. A., Afonso, C. A. M., Coelho, I. M., Crespo, J. G., Garea, A. & Irabien, A. (2009b). Facilitated transport of CO<sub>2</sub> and SO<sub>2</sub> through Supported Ionic Liquid Membranes (SILMs). *Desalination*, 245, 485-493.
- Luis, P., Van Gerven, T. & Van der Bruggen, B. (2012). Recent developments in membrane-based technologies for CO<sub>2</sub> capture. *Progress in Energy and Combustion Science*, 38, 419-448.
- Lv, Y., Yu, X., Jia, J., Tu, S. -T., Yan, J. & Dahlquist, E. (2012). Fabrication and characterization of superhydrophobic polypropylene hollow fiber membranes for carbon dioxide absorption. *Applied Energy*, 90, 167-174.
- Lv, Y., Yu, X., Tu, S.-T., Yan, J. & Dahlquist, E. (2010). Wetting of polypropylene hollow fiber membrane contactors. *Journal of Membrane Science*, 362, 444-452.
- Ma, C., Pietrucci, F. & Andreoni, W. (2015). Capture and release of CO<sub>2</sub> in monoethanolamine aqueous solutions: New insights from first-principles reaction dynamics. *Journal of Chemical Theory and Computation*, 11, 3189-3198.

- Mahurin, S. M., Hillesheim, P. C., Yeary, J. S., Jiang, D. E. & Dai, S. (2012). High CO<sub>2</sub> solubility, permeability and selectivity in ionic liquids with the tetracyanoborate anion. *RSC Advances*, 2, 11813-11819.
- Mahurin, S. M., Lee, J. S., Baker, G. A., Luo, H. & Dai, S. (2010). Performance of nitrile-containing anions in task-specific ionic liquids for improved CO<sub>2</sub>/N<sub>2</sub> separation. *Journal of Membrane Science*, 353, 177-183.
- Maiti, A. (2009). Theoretical screening of ionic liquid solvents for carbon capture. *ChemSusChem*, 2, 628-631.
- Mansourizadeh, A. & Ismail, A. F. (2009). Hollow fiber gas-liquid membrane contactors for acid gas capture: A review. *Journal of Hazardous Materials*, 171, 38-53.
- Mansourizadeh, A., Ismail, A. F. & Matsuura, T. (2010). Effect of operating conditions on the physical and chemical CO<sub>2</sub> absorption through the PVDF hollow fiber membrane contactor. *Journal of Membrane Science*, 353, 192-200.
- Marsh, K. N., Boxall, J. A. & Lichtenthaler, R. (2004). Room temperature ionic liquids and their mixtures—a review. *Fluid Phase Equilibria*, 219, 93-98.
- Marták, J. & Schlosser, S. (2006). Pertraction of organic acids through liquid membranes containing ionic liquids. *Desalination*, 199, 518.
- Matsumiya, N., Teramoto, M., Kitada, S. & Matsuyama, H. (2005). Evaluation of energy consumption for separation of CO<sub>2</sub> in flue gas by hollow fiber facilitated transport membrane module with permeation of amine solution. *Separation and Purification Technology*, 46, 26-32.
- Matsumoto, M., Hasegawa, W., Kondo, K., Shimamura, T. & Tsuji, M. (2010). Application of supported ionic liquid membranes using a flat sheet and hollow fibers to lactic acid recovery. *Desalination and Water Treatment*, 14, 37-46.
- Matsumoto, M., Inomoto, Y. & Kondo, K. (2005). Selective separation of aromatic hydrocarbons through supported liquid membranes based on ionic liquids. *Journal of Membrane Science*, 246, 77-81.
- Matsumoto, M., Ohtani, T. & Kondo, K. (2007). Comparison of solvent extraction and supported liquid membrane permeation using an ionic liquid for concentrating penicillin G. *Journal of Membrane Science*, 289, 92-96.
- Mavroudi, M., Kaldis, S. P. & Sakellaropoulos, G. P. (2003). Reduction of CO<sub>2</sub> emissions by a membrane contacting process. *Fuel*, 82, 2153-2159.
- Mavroudi, M., Kaldis, S. P. & Sakellaropoulos, G. P. (2006). A study of mass transfer resistance in membrane gas-liquid contacting processes. *Journal of Membrane Science*, 272, 103-115.

- McCrellis, C., Rebecca Taylor, S. F., Jacquemin, J. & Hardacre, C. (2016). Effect of the presence of MEA on the CO<sub>2</sub> capture ability of superbase ionic liquids. *Journal of Chemical and Engineering Data*, 61, 1092–1100.
- McGuire, K. S., Lawson, K. W. & Lloyd, D. R. (1995). Pore size distribution determination from liquid permeation through microporous membranes. *Journal of Membrane Science*, 99, 127-137.
- Miller, M. B., Chen, D. -L., Xie, H. -B., Luebke, D. R., Karl Johnson, J. & Enick, R. M. (2009). Solubility of CO<sub>2</sub> in CO<sub>2</sub>-philic oligomers; COSMOtherm predictions and experimental results. *Fluid Phase Equilibria*, 287, 26-32.
- Miyako, E., Maruyama, T., Kamiya, N. & Goto, M. (2003a). Enzyme-facilitated enantioselective transport of (S)-ibuprofen through a supported liquid membrane based on ionic liquids. *Chemical Communications*, 2926-2927.
- Miyako, E., Maruyama, T., Kamiya, N. & Goto, M. (2003b). Use of ionic liquids in a lipase-facilitated supported liquid membrane. *Biotechnology Letters*, 25, 805-808.
- Mosadegh-Sedghi, S., Rodrigue, D., Brisson, J. & Iliuta, M.C. (2014). Wetting phenomenon in membrane contactors – Causes and prevention. *Journal of Membrane Science*, 452, 332-353.
- Mulder, M. (2003). *Basic Principles of Membrane Technology*, 2nd ed., Kluwer Academic Publishers Inc., Netherland.
- Muldoon, M. J., Aki, S., Anderson, J. L., Dixon, J. K. & Brennecke, J. F. (2007). Improving carbon dioxide solubility in ionic liquids. *The Journal of Physical Chemistry B*, 111, 9001-9009.
- Myers, C., Pennline, H., Luebke, D., Ilconich, J., Dixon, J. K., Maginn, E. J. & Brennecke, J. F. (2008). High temperature separation of carbon dioxide/hydrogen mixtures using facilitated supported ionic liquid membranes. *Journal of Membrane Science*, 322, 28-31.
- Néouze, M. -A., Le Bideau, J., Gaveau, P., Bellayer, S. & Vioux, A. (2006). Ionogels, new materials arising from the confinement of ionic liquids within silica-derived networks. *Chemistry of Materials*, 18, 3931-3936.
- Neves, L. A., Crespo, J. G & Coelho, I. M. (2010). Gas permeation studies in supported ionic liquid membranes. *Journal of Membrane Science*, 357, 160-170.
- Neves, L. A., Nemestóthy, N., Alves, V. D., Cserjési, P., Bélafi-Bakó, K. & Coelho, I. M. (2009). Separation of biohydrogen by supported ionic liquid membranes. *Desalination*, 240, 311-315.
- Nosrati, S., Jayakumar, N. S. & Hashim, M. A. (2011). Performance evaluation of supported ionic liquid membrane for removal of phenol. *Journal of Hazardous Materials*, 192, 1283-1290.

- Palomar, J., Gonzalez-Miquel, M., Polo, A. & Rodriguez, F. (2011). Understanding the physical absorption of CO<sub>2</sub> in ionic liquids using the COSMO-RS method. *Industrial and Engineering Chemistry Research.*, 50, 3452-3463.
- Panigrahi, A., Pilli, S.R. & Mohanty, K. (2013). Selective separation of Bisphenol A from aqueous solution using supported ionic liquid membrane. *Separation and Purification Technology*, 107, 70-78.
- Park, H. H., Deshwal, B. R., Kim, I. W. & Lee, H. K. (2008). Absorption of SO<sub>2</sub> from flue gas using PVDF hollow fiber membranes in a gas-liquid contactor. *Journal of Membrane Science*, 319, 29-37.
- Park, S. W., Heo, N. H., Kim, G. W. & Sohn, I. J. (2000). Facilitated transport of carbon dioxide through an immobilized liquid membrane of aqueous carbonate solution with additives. *Separation Science and Technology.*, 35, 2497-2512.
- Park, Y.-I., Kim, B. -S., Byun, Y. -H., Lee, S. -H., Lee, E. -W. & Lee, J. -M. (2009). Preparation of supported ionic liquid membranes (SILMs) for the removal of acidic gases from crude natural gas. *Desalination*, 236, 342-348.
- Peng, J. -F., Liu, J. -F., Hu, X. -L. & Jiang, G. -B. (2007). Direct determination of chlorophenols in environmental water samples by hollow fiber supported ionic liquid membrane extraction coupled with high-performance liquid chromatography. *Journal of Chromatography A*, 1139, 165-170.
- Plechkova, N. V. & Seddon, K. R. (2008). Applications of ionic liquids in the chemical industry. *Chemical Society Reviews*, 37, 123-150.
- Poddar, T. K., Majumdar, S. & Sirkar, K. K. (1996). Membrane-based absorption of VOCs from a gas stream. *Aiche Journal.*, 42, 3267-3282.
- Poliwoda, A., Ilczuk, N. & Wieczorek, P. P. (2007). Transport mechanism of peptides through supported liquid membranes. *Separation and Purification Technology*, 57, 444-449.
- Poole, C. F. & Poole, S. K. (2010). Extraction of organic compounds with room temperature ionic liquids. *Journal of Chromatography A*, 1217, 2268-2286.
- Powell, C. E. & Qiao, G. G. (2006). Polymeric CO<sub>2</sub>/N<sub>2</sub> gas separation membranes for the capture of carbon dioxide from power plant flue gases. *Journal of Membrane Science*, 279, 1-49.
- Raeissi, S. & Peters, C. J. (2009). A potential ionic liquid for CO<sub>2</sub>-separating gas membranes: selection and gas solubility studies. *Green Chemistry*, 11, 185-192.
- Rangwala, H. A. (1996). Absorption of carbon dioxide into aqueous solutions using hollow fiber membrane contactors. *Journal of Membrane Science*, 112, 229-240.

- Rao, A. B. & Rubin, E. S. (2002). A Technical, economic, and environmental assessment of amine-based CO<sub>2</sub> capture technology for power plant greenhouse gas control. *Environmental Science and Technology*, 36, 4467-4475.
- Ren, J., Wu, L. & Li, B. -G. (2012). Preparation and CO<sub>2</sub> sorption/desorption of N-(3-aminopropyl)aminoethyl tributylphosphonium amino acid salt ionic liquids supported into porous silica particles. *Industrial and Engineering Chemistry Research*, 51, 7901-7909.
- Ren, S. H., Hou, Y. C., Wu, W. Z., Liu, Q. Y., Xiao, Y. F. & Chen, X. T. (2010). Properties of ionic liquids absorbing SO<sub>2</sub> and the mechanism of the absorption. *The Journal of Physical Chemistry B*, 114, 2175-2179.
- Rezaei, M., Ismail, A. F., Hashemifard, S. A. & Matsuura, T. (2014). Preparation and characterization of PVDF-montmorillonite mixed matrix hollow fiber membrane for gas-liquid contacting process. *Chemical Engineering Research and Design*, 92, 2449-2460.
- Rooney, P. C., DuPart, M. S. & Bacon, T. R. (1998). Oxygen's role in alkanolamine degradation. *Hydrocarbon Processing*, 77, 109-113.
- Ropel, L., Belveze, L. S., Aki, S. N. V. K., Stadtherr, M. A. & Brennecke, J. F. (2005). Octanol-water partition coefficients of imidazolium-based ionic liquids. *Green Chemistry*, 7, 83-90.
- S. Kislik, V. (2010). Chapter 9 - Progress in liquid membrane science and engineering, liquid membranes. Elsevier, Amsterdam, pp. 401-437.
- Saha, S. & Chakma, A. (1995). Selective CO<sub>2</sub> separation from CO<sub>2</sub>/C<sub>2</sub>H<sub>6</sub> mixtures by immobilized diethanolamine PEG membranes. *Journal of Membrane Science*, 98, 157-171.
- Saiwan, C., Supap, T., Idem, R.O. & Tontiwachwuthikul, P. (2011). Part 3: Corrosion and prevention in post-combustion CO<sub>2</sub> capture systems. *Carbon Management*, 2, 659-675.
- Santos, E., Albo, J. & Irabien, A. (2014a). Acetate based supported ionic liquid membranes (SILMs) for CO<sub>2</sub> separation: Influence of the temperature. *Journal of Membrane Science*, 452, 277-283.
- Santos, E., Albo, J. & Irabien, A. (2014b). Magnetic ionic liquids: synthesis, properties and applications. *RSC Advances*, 4, 40008-40018.
- Santos, E., Albo, J., Rosatella, A., Afonso, C. A. M. & Irabien, A. (2014c). Synthesis and characterization of magnetic ionic liquids (MILs) for CO<sub>2</sub> separation. *Journal of Chemical Technology and Biotechnology*, 89, 866-871.
- Schmidt, C., Glück, T. & Schmidt-Naake, G. (2008). Modification of Nafion membranes by impregnation with ionic liquids. *Chemical Engineering and Technology*, 31, 13-22.



- Scholes, C. A., Qader, A., Stevens, G. W. & Kentish, S. E. (2014). Membrane gas-solvent contactor pilot plant trials of CO<sub>2</sub> absorption from flue gas. *Separation Science and Technology*, 49, 2449-2458.
- Schouten, A. E. & A.K. van der Vegt, A.K. *Plastics*, Spectrum, 1981.
- Scovazzo, P. (2009). Determination of the upper limits, benchmarks, and critical properties for gas separations using stabilized room temperature ionic liquid membranes (SILMs) for the purpose of guiding future research. *Journal of Membrane Science*, 343, 199-211.
- Scovazzo, P., Camper, D., Kieft, J., Poshusta, J., Koval, C. & Noble, R. (2004a). Regular solution theory and CO<sub>2</sub> gas solubility in room-temperature ionic liquids. *Industrial and Engineering Chemistry Research*, 43, 6855-6860.
- Scovazzo, P., Havard, D., McShea, M., Mixon, S. & Morgan, D. (2009). Long-term, continuous mixed-gas dry fed CO<sub>2</sub>/CH<sub>4</sub> and CO<sub>2</sub>/N<sub>2</sub> separation performance and selectivities for room temperature ionic liquid membranes. *Journal of Membrane Science*, 327, 41-48.
- Scovazzo, P., Kieft, J., Finan, D. A., Koval, C., DuBois, D. & Noble, R. (2004b). Gas separations using non-hexafluorophosphate [PF<sub>6</sub>]<sup>-</sup> anion supported ionic liquid membranes. *Journal of Membrane Science*, 238, 57-63.
- Scovazzo, P., Visser, A. E., Davis Jr, J. H., Rogers, R. D., Koval, C. A., DuBois, D. L. & Noble, R. D. (2002). Supported ionic liquid membranes and facilitated ionic liquid membranes. *ACS Symposium Series*, pp. 69-87.
- Seddon, K. R., Stark, A. & Torres, M. J. (2000). Influence of chloride, water, and organic solvents on the physical properties of ionic liquids. *Pure and Applied Chemistry*, 72, 2275-2287.
- Seddon, K. R., Stark, A. & Torres, M. J. (2002). Viscosity and density of 1-alkyl-3-methylimidazolium ionic liquids, in: Abraham, M.A., Moens, L. (Eds.), *Clean Solvents: Alternative Media for Chemical Reactions and Processing*. Amer Chemical Soc, Washington, pp. 34-49.
- Sexton, A. J. & Rochelle, G. T. (2009). Catalysts and inhibitors for oxidative degradation of monoethanolamine. *International Journal of Greenhouse Gas Control*, 3, 704-711.
- Shah, J. K. & Maginn, E. J. (2005). Monte Carlo simulations of gas solubility in the ionic liquid 1-n-butyl-3-methylimidazolium hexafluorophosphate. *The Journal of Physical Chemistry B*, 109, 10395-10405.
- Shahkaramipour, N., Adibi, M., Seifkordi, A. A. & Fazli, Y. (2014). Separation of CO<sub>2</sub>/CH<sub>4</sub> through alumina-supported geminal ionic liquid membranes. *Journal of Membrane Science*, 455, 229-235.
- Sharma, P., Park, S. D., Baek, I. H., Park, K. T., Yoon, Y. I. & Jeong, S. K. (2012). Effects of anions on absorption capacity of carbon dioxide in acid functionalized ionic liquids. *Fuel Processing Technology*, 100, 55-62.

- Shi, W. & Maginn, E. J. (2008). Molecular simulation and regular solution theory modeling of pure and mixed gas absorption in the ionic liquid 1-n-hexyl-3-methylimidazolium bis(trifluoromethylsulfonyl)amide ([hmim] [Tf<sub>2</sub>N]). *The Journal of Physical Chemistry B*, 112, 16710-16720.
- Shi, W. & Sorescu, D. C. (2010). Molecular simulations of CO<sub>2</sub> and H<sub>2</sub> sorption into ionic liquid 1-n-hexyl-3-methylimidazolium bis(trifluoromethylsulfonyl)amide ([hmim] [Tf<sub>2</sub>N]) confined in carbon nanotubes. *The Journal of Physical Chemistry B*, 114, 15029-15041.
- Shiflett, M. B. & Yokozeki, A. (2010). Chemical absorption of sulfur dioxide in room-temperature ionic liquids. *Industrial and Engineering Chemistry Research*, 49, 1370-1377.
- Shimoyama, Y. & Ito, A. (2010). Predictions of cation and anion effects on solubilities, selectivities and permeabilities for CO<sub>2</sub> in ionic liquid using COSMO based activity coefficient model. *Fluid Phase Equilibria*, 297, 178-182.
- Shimoyama, Y., Komuro, S. & Jindaratamee, P. (2014). Permeability of CO<sub>2</sub> through ionic liquid membranes with water vapour at feed and permeate streams. *The Journal of Chemical Thermodynamics*, 69, 179-185.
- Shin, J. H., Henderson, W. A., Appetecchi, G. B., Alessandrini, F. & Passerini, S. (2005). Recent developments in the ENEA lithium metal battery project. *Electrochimica Acta*, 50, 3859-3865.
- Simons, K., Nijmeijer, K., Bara, J. E., Noble, R. D. & Wessling, M. (2010). How do polymerized room-temperature ionic liquid membranes plasticize during high pressure CO<sub>2</sub> permeation?. *Journal of Membrane Science*, 360, 202-209.
- Snijder, E. D., Teriele, M. J. M., Versteeg, G. F. & Vanswaaij, W. P. M. (1993). Diffusion-coefficients of several aqueous alkanolamine solutions. *Journal of Chemical Engineering Data*, 38, 475-480.
- Song, H. J., Lee, S., Maken, S., Park, J. J. & Park, J. W. (2006). Solubilities of carbon dioxide in aqueous solutions of sodium glycinate. *Fluid Phase Equilibria*, 246, 1-5.
- Stéphenne, K. (2014). Start-up of world's first commercial post-combustion coal fired CCS project: Contribution of Shell Cansolv to SaskPower Boundary Dam ICCS Project. *Energy Procedia*, 63, 6106-6110.
- Strazisar, B. R., Anderson R. R. & White, C. M. Degradation pathways for monoethanolamine in a CO<sub>2</sub> capture facility. *Energy and Fuels*, 200, 17, 1034-1039.
- Sumon, K. Z. & Henni, A. (2011). Ionic liquids for CO<sub>2</sub> capture using COSMO-RS: Effect of structure, properties and molecular interactions on solubility and selectivity. *Fluid Phase Equilibria*, 310, 39-55.
- Supap, T., Idem, R., Tontiwachwuthikul, P. & Saiwan, C. (2009). Kinetics of sulfur dioxide- and oxygen-induced degradation of aqueous monoethanolamine

- solution during CO<sub>2</sub> absorption from power plant flue gas streams. *International Journal of Greenhouse Gas Control*, 3, 133-142.
- Takeuchi, H., Takahashi, K. & Goto, W. (1987). Some observations on the stability of supported liquid membranes. *Journal of Membrane Science*, 34, 19-31.
- Tan, C. S. & Chen, J. E. (2006). Absorption of carbon dioxide with piperazine and its mixtures in a rotating packed bed. *Separation and Purification Technology*, 49, 174-180.
- Tan, L., Dong, X., Wang, H. & Yang, Y. (2009). Gels of ionic liquid [C<sub>4</sub>mim] [PF<sub>6</sub>] formed by self-assembly of gelators and their electrochemical properties. *Electrochemistry Communications*, 11, 933-936.
- Teramoto, M., Nakai, K., Ohnishi, N., Huang, Q. F., Watari, T. & Matsuyama, H. (1996). Facilitated transport of carbon dioxide through supported liquid membranes of aqueous amine solutions. *Industrial and Engineering Chemistry Research*, 35, 538-545.
- Teramoto, M., Sakaida, Y., Fu, S. S., Ohnishi, N., Matsuyama, H., Maki, T., Fukui, T. & Arai, K. (2000). An attempt for the stabilization of supported liquid membrane. *Separation and Purification Technology*, 21, 137-144.
- Tome, L. C., Florindo, C., Freire, C. S. R., Rebelo, L. P. N. & Marrucho, I. M. (2014). Playing with ionic liquid mixtures to design engineered CO<sub>2</sub> separation membranes. *Physical Chemistry Chemical Physics*, 16, 17172-17182.
- Tome, L. C., Patinha, D. J. S., Freire, C. S. R., Rebelo, L. P. N. & Marrucho, I. M. (2013). CO<sub>2</sub> separation applying ionic liquid mixtures: the effect of mixing different anions on gas permeation through supported ionic liquid membranes. *RSC Advances*, 3, 12220-12229.
- Toral, A. R., de los Ríos, A. P., Hernández, F. J., Janssen, M. H. A., Schoevaart, R., van Rantwijk, F. & Sheldon, R. A. (2007). Cross-linked Candida antarctica lipase B is active in denaturing ionic liquids. *Enzyme and Microbial Technology*, 40, 1095-1099.
- Vázquez, G., Alvarez, E., Navaza, J. M., Rendo, R. & Romero, E. (1997). Surface tension of binary mixtures of water + monoethanolamine and water + 2-amino 2-methyl-1-propanol and tertiary mixtures of these amines with water from 25°C to 50°C. *Journal of Chemical and Engineering Data*, 42, 7-59.
- Vangeli, O. C., Romanos, G. E., Beltsios, K. G., Fokas, D., Athanasekou, C. P. & Kanellopoulos, N. K. (2010). Development and characterization of chemically stabilized ionic liquid membranes-Part I: Nanoporous ceramic supports. *Journal of Membrane Science*, 365, 366-377.
- Versteeg, G. F., Van Dijck, L. A. J. & Van Swaaij, W. P. M. (1996). On the kinetics between CO<sub>2</sub> and alkanolamines both in aqueous and non-aqueous solutions. An overview. *Chemical Engineering Communications*, 144, 113-158.

- Vevelstad, S. J., Grimstvedt, A., Elnan, J., da Silva, E. F. & Svendsen, H. F. (2013). Oxidative degradation of 2-ethanolamine: The effect of oxygen concentration and temperature on product formation. *International Journal of Greenhouse Gas Control*, 18, 88-100.
- Voice, A. K. & Rochelle, G. T. (2013). Products and process variables in oxidation of monoethanolamine for CO<sub>2</sub> capture. *International Journal of Greenhouse Gas Control*, 12, 472-477.
- Wang, C. M., Luo, H. M., Jiang, D. E., Li, H. R. & Dai, S. (2010a). Carbon dioxide capture by superbase-derived protic ionic liquids. *Angewandte Chemie International Edition*, 49, 5978-5981.
- Wang, J. & Li, Z. (2013). Measurement and modeling of vapor-liquid equilibria for systems containing alcohols, water, and imidazolium-based phosphate ionic liquids. *Journal of Chemical and Engineering Data*, 58, 1641-1649.
- Wang, J., Wang, D., Li, Z. & Zhang, F. (2010b). Vapor pressure measurement and correlation or prediction for water, 1-propanol, 2-propanol, and their binary mixtures with [MMIM] [DMP] ionic liquid. *Journal of Chemical & Engineering Data*, 55, 4872-4877.
- Wang, K. L. & Cussler, E. L. (1993). Baffled membrane modules made with hollow fiber fabric. *Journal of Membrane Science*, 85, 265-278.
- Wang, R., Li, D. F., Zhou, C., Liu, M. & Liang, D. T. (2004). Impact of DEA solutions with and without CO<sub>2</sub> loading on porous polypropylene membranes intended for use as contactors. *Journal of Membrane Science*, 229, 147-157.
- Wang, R., Zhang, H. Y., Feron, P. H. M. & Liang, D. T. (2005). Influence of membrane wetting on CO<sub>2</sub> capture in microporous hollow fiber membrane contactors. *Separation and Purification Technology*, 46, 33-40.
- Wang, X., Chen, H., Zhang, L., Yu, R., Qu, R. & Yang, L. (2014). Effects of coexistent gaseous components and fine particles in the flue gas on CO<sub>2</sub> separation by flat-sheet polysulfone membranes. *Journal of Membrane Science*, 470, 237-245.
- Wei, G. -T., Yang, Z. & Chen, C. -J. (2003). Room temperature ionic liquid as a novel medium for liquid/liquid extraction of metal ions. *Analytica Chimica Acta*, 488, 183-192.
- Wen, L., Liu, H., Rongwong, W., Liang, Z., Fu, K., Idem, R., & Tontiwachwuthikul, P. (2015). Comparison of overall gas-phase mass transfer coefficient for CO<sub>2</sub> absorption between tertiary amines in a randomly packed column. *Chemical Engineering & Technology*, 38(8), 1435-1443.
- Wickramanayake, S., Hopkinson, D., Myers, C., Hong, L., Feng, J., Seol, Y., Plasynski, D., Zeh, M. & Luebke, D. (2014). Mechanically robust hollow fiber supported ionic liquid membranes for CO<sub>2</sub> separation applications. *Journal of Membrane Science*, 470, 52-59.

- Wickramasinghe, S. R., Semmens, M.J. & Cussler, E.L. (1992). Mass transfer in various hollow fiber geometries. *Journal of Membrane Science*, 69, 235-250.
- Wiesler, F. Membrane contactors: an introduction to the technology, *Ultrapure Water*, May 1996, pp. 27–31.
- Yamaguchi, T., Koval, C.A., Noble, R. D. & Bowman, C.N. (1996). Transport mechanism of carbon dioxide through perfluorosulfonate ionomer membranes containing an amine carrier. *Chemical Engineering Science*, 51, 4781-4789.
- Yang, M. C. & Cussler, E. L. (1986). Designing hollow fiber contactors. *Aiche Journal*., 32, 1910-1916.
- Yang, X. -J. & Fane, T. (1997). Effect of membrane preparation on the lifetime of supported liquid membranes. *Journal of Membrane Science*, 133, 269-273.
- Yang, X. J., Fane, A. G. & Soldenhoff, K. (2003). Comparison of liquid membrane processes for metal separations: Permeability, stability, and selectivity. *Industrial and Engineering Chemistry Research*, 42, 392-403.
- Ye, C., Dang, M., Yao, C., Chen & Yuan G. (2013). Process analysis on CO<sub>2</sub> absorption by monoethanolamine solutions in microchannel reactors. *Chemical Engineering Journal*, 225, 120–127.
- Yoo, S., Won, J., Kang, S. W., Kang, Y. S. & Nagase, S. (2010). CO<sub>2</sub> separation membranes using ionic liquids in a Nafion matrix. *Journal of Membrane Science*, 363, 72-79.
- Yu, X., An, L., Yang, J., Tu, S. -T. & Yan, J. (2015). CO<sub>2</sub> capture using a superhydrophobic ceramic membrane contactor. *Journal of Membrane Science*, 496, 1-12.
- Zha, F. F., Fane, A. G. & Fell, C. J. D. (1995). Effect of surface tension gradients on stability of supported liquid membranes. *Journal of Membrane Science*, 107, 75-86.
- Zhai, C. P, Wang, J. J., Zhao, Y., Tang, J. M. & Wang, H. Q. (2006). A NMR study on the interactions of 1-alkyl-3-methylimidazolium ionic liquids with acetone. *International Journal Research Physical Chemistry Chemical Physics*, 220, 775–785.
- Zhang, F., Gao, Y., Wu, X. K., Ma, J. W., Wu, Y. T. & Zhang, Z. B. (2013). Regeneration performance of amino acid ionic liquid (AAIL) activated MDEA solutions for CO<sub>2</sub> capture. *Chemical Engineering Journal*, 223, 371-378.
- Zhang, H. Y., Wang, R., Liang, D. T. & Tay, J. H. (2008a). Theoretical and experimental studies of membrane wetting in the membrane gas-liquid contacting process for CO<sub>2</sub> absorption. *Journal of Membrane Science*, 308, 162-170.

- Zhang, L., Qu, R., Sha, Y., Wang, X. & Yang, L. (2015). Membrane gas absorption for CO<sub>2</sub> capture from flue gas containing fine particles and gaseous contaminants. *International Journal of Greenhouse Gas Control*, 33, 10-17.
- Zhang, Q. & Cussler, E. L. (1985). Microporous hollow fibers for gas absorption. 1. Mass transfer in the liquid. *Journal of Membrane Science*, 23, 321-332.
- Zhang, X. C., Liu, Z. P. & Wang, W. C. (2008b). Screening of ionic liquids to capture CO<sub>2</sub> by COSMO-RS and experiments. *Aiche Journal*, 54, 2717-2728.
- Zhao, H., Xia, S. & Ma, P. (2005). Use of ionic liquids as 'green' solvents for extractions. *Journal of Chemical Technology and Biotechnology*, 80, 1089-1096.
- Zhao, S., Feron, P. H. M., Cao, C., Wardhaugh, L., Yan, S. & Gray, S. (2015). Membrane evaporation of amine solution for energy saving in post-combustion carbon capture: Wetting and condensation. *Separation and Purification Technology*, 146, 60-67.
- Zhao, W., He, G., Nie, F., Zhang, L., Feng, H. & Liu, H. (2012). Membrane liquid loss mechanism of supported ionic liquid membrane for gas separation. *Journal of Membrane Science*, 411, 73-80.
- Zhao, W., He, G., Zhang, L., Ju, J., Dou, H., Nie, F., Li, C. & Liu, H. (2010). Effect of water in ionic liquid on the separation performance of supported ionic liquid membrane for CO<sub>2</sub>/N<sub>2</sub>. *Journal of Membrane Science*, 350, 279-285.
- Zhou, L. Y., Fan, J. & Shang, X. M. (2014). CO<sub>2</sub> capture and separation properties in the ionic liquid 1-n-butyl-3-methylimidazolium nonafluorobutylsulfonate. *Materials*, 7, 3867-3880.

## LIST OF PUBLICATIONS AND PAPERS PRESENTED

### Publications

- N. Ain Ramli, N. Awanis Hashim and M. K. Aroua, Prediction of CO<sub>2</sub>/O<sub>2</sub> absorption selectivity using supported ionic liquid membranes (SILMs) for gas-liquid membrane contactor, *Chemical Engineering Communications*, 2018, 205(3), 295-310.
- N. Ain Ramli, N. Awanis Hashim and M. K. Aroua, Supported ionic liquid membranes (SILMs) as a contactor for the selective absorption of CO<sub>2</sub>/O<sub>2</sub> by aqueous monoethanolamine (MEA), *Separation and Purification Technology*, 2020, 230, 115849.
- N. Ain Ramli, N. Awanis Hashim, M. K. Aroua, M. F. Abdul Patah and A. Shamiri, The effects of 1-ethyl-3-methylimidazolium bis (trifluoromethylsulfonyl) imide [emim] [NTf<sub>2</sub>] IL: acetone compositions on the amount, homogeneity and chemical stability of immobilized IL in hollow fiber supported ionic liquid membranes (SILMs), (*Under revision, Chemical Engineering Communications*).
- N. Ain Ramli, N. Awanis Hashim and M. K. Aroua, Selective absorption of CO<sub>2</sub>/O<sub>2</sub> using cross-flow SILMs membrane contactor (*In progress*).

### Papers presented

- N. Ain Ramli, N. Awanis Hashim and M. K. Aroua. Supported ionic liquid membranes (SILMs) as a contactor for the selective absorption of CO<sub>2</sub>/O<sub>2</sub> by aqueous monoethanolamine (MEA), *1<sup>st</sup> Euro-Asia Conference on CO<sub>2</sub> Capture and Utilisation (EACCO<sub>2</sub>CU 2019)*, Sunway University, 2019.
- N. Ain Ramli, N. Awanis Hashim and M. K. Aroua. The effects of ionic liquids composition on supported ionic liquid membranes (SILMs) preparation and its chemical stability. *Tech-Post conference, University of Malaya*, 2017.
- N. Ain Ramli, N. Awanis Hashim and M. K. Aroua. Potentialities of imidazolium based ionic liquids (ILs) as supporting phase in supported liquids membrane (SLMs) for CO<sub>2</sub> capture: COSMO-RS and FESEM analysis. *Workshop on CO<sub>2</sub> capture and utilization, University of Malaya*, 2017.
- N. Ain Ramli, N. Awanis Hashim and M. K. Aroua. Preventing oxidative degradation of monoethanolamine (MEA) during CO<sub>2</sub> capture by supported ionic liquid membrane. *10<sup>th</sup> conference of Aseanian membrane society (Japan)*, 2016.
- N. Ain Ramli, N. Awanis Hashim and M. K. Aroua. Supported ionic liquids membrane (SILMs) using [emim] [NTf<sub>2</sub>] ILs for CO<sub>2</sub> capture and prevention of MEA oxidation in gas-liquid membrane contactor. *National congress on membrane technology, (NATCOM16), University of Technology Malaysia*, 2016.